Faculteit Farmaceutische, Biomedische en Diergeneeskundige Wetenschappen
Departement Farmaceutische Wetenschappen

Evaluation of newly developed HPMC ophthalmic inserts with sustained release properties as a carrier for thermolabile therapeutics

Evaluatie van nieuw ontwikkelde HPMC oculaire inserten met verlengde afgifte als drager voor thermolabiele geneesmiddelen

Antwerpen - 2017

Proefschrift voorgelegd tot het behalen van de graad van
doctor in de farmaceutische wetenschappen aan de Universiteit van Antwerpen
te verdedigen door

Arnout EVERAERT

Promotoren:
Prof. dr. Wim Weyenberg, Prof. dr. Annick Ludwig en Prof. dr. Filip Kiekens

TABLE OF CONTENTS

Chapter 4: Further development of an ocular insert with slow release properties loaded with lysozyme

Chapter 8: Stability testing of inserts containing lysozyme

Chapter 9: *In vivo* evaluation

Appendix

LIST OF ABBREVIATIONS

AMD	Age-related macular degeneration
Ang	Angiopoietin
ANOVA	Analysis of variance
API	Active pharmaceutical ingredient
BPE	Bovine pituitary extract
CI	Confidence interval
DDS	Drug delivery system
EGF	Epidermal growth factor
EVA	Ethylene-vinyl acetate
FDA	US Food and Drug Administration
FGF	Fibroblast growth factor
FITC	Fluorescein isothiocyanate
Flt	fms-like tyrosine kinase
G’	Storage modulus (elastic modulus)
G”	Loss modulus (viscous modulus)
HEC	Hydroxyethyl cellulose
HPC	Hydroxypropyl cellulose
HPMC	Hydroxypropylmethyl cellulose
IL-1α	Interleukin-1α
KDR	Kinase insert domain-containing receptor
K-SFM	Keratinocyte-Serum-Free Medium
LVER	Linear viscoelastic region
MC	Methyl cellulose
Na CMC	Sodium carboxymethyl cellulose
PBS	Phosphate-buffered saline
PDGF	Platelet-derived growth factor
Ph. Eur.	European Pharmacopoeia
PLGA	Poly-lactic-co-glycolic acid
PlGF	Placental growth factor
PVA	Polyvinyl alcohol
PVC	Polyvinyl chloride
PVD	Posterior vitreous detachment
PVP	Polyvinyl pyrrolidone
RPE	Retinal pigment epithelium
RSD	Relative standard deviation
SAL	Security assurance level
SV40-HCEC	SV40-immortalised human corneal epithelial cells
T_m	Thermal gelation temperature

TNF-α	Tumour necrosis factor-α
TPPV	*Trans pars plana* vitrectomy
USP	US Pharmacopeia
UV	Ultraviolet
VEGF	Vascular endothelial growth factor
VEGFR	Vascular endothelial growth factor receptor
VMT	Vitreomacular traction

INTRODUCTION

Eye drops have been the most popular and best accepted dosage form for ocular delivery of drugs. However, conventional eye drops have well known disadvantages such as low ocular availability due to defence mechanisms of the eye. Frequent instillation is recommended or even required in order to reach therapeutic levels of the drug at the site of action. Many attempts have been made over several decades to increase the ocular availability and hence improve the efficacy of topically applied drugs. This has led to the emergence of new drug delivery devices with common ambitions, including decreasing the instillation frequency, prolonging the residence time of the drug applied and thus improving patient compliance.

The discovery of novel peptides and proteins has led to some breakthroughs in the ophthalmic field. For instance, proteins such as ranibizumab (Lucentis®) and bevacizumab (Avastin®, off-label use) are used to treat age-related macular degeneration, a disease affecting people over the age of 50. It is one of the leading causes of blindness and is characterised by an overgrowth of blood vessels and leakage of blood in the macular region of the retina, which is responsible for visual acuity. There is no permanent cure known for this disease and a monthly or two-monthly injection of an anti-VEGF drug substance in the vitreous of the eye is required to inhibit the growth of blood vessels. Although the efficiency and efficacy of intravitreal injections are difficult to match with topical delivery of the drug, the development of a precorneal insert with slow release properties might be worth considering as this can result in improved patient comfort and a significant reduction in severe side effects associated with intravitreal injections. Furthermore, the burden that such monthly ophthalmic injections pose on both the patient and the ophthalmologist can certainly not be underestimated.

In the present research work, a drug delivery system (DDS) for ophthalmic use was developed to allow thermolabile drugs, such as peptides and proteins, to be incorporated in an ocular insert with slow release properties. Proteins pose specific challenges during formulation, production and storage, for instance denaturation caused by shear forces applied to proteins, stability issues due to elevated temperatures during the production of the DDS, air entrapment potentially causing oxidation, etc.

The main objective of this research project was to develop a method of preparing rod-shaped ocular inserts with slow release properties while maintaining drug stability of thermolabile molecules. This

method brings new opportunities to incorporate thermolabile molecules, which were not suited to be loaded in slow-release formulations earlier. Consequently, this might also allow molecules to be administered topically as most peptides and proteins are currently administered through injection.

As storage time and temperature might have a significant influence on the drug and drug carrier stability, the stability of the inserts was verified by means of activity assay, rheological characterisation and release profiles.
Finally, the *in vivo* behaviour of the inserts was examined in rats with dry eye disease.

The method of developing this DDS might become interesting in the future, as more therapeutic peptides and proteins for ocular use will emerge.

Chapter 1: Biopharmaceutical aspects of ocular drug delivery

1 GENERAL ANATOMY AND STRUCTURES OF THE EYE

1.1 Anatomy of the eye

The human eye is a very complex optical system and of great importance for everyday life. It detects light and converts it into electro-chemical signals which in turn are converted to impulses in neurons, located in the brain. For a better understanding of the complexity of the human eye, the anatomical overview is given in figure 1 [1,2].

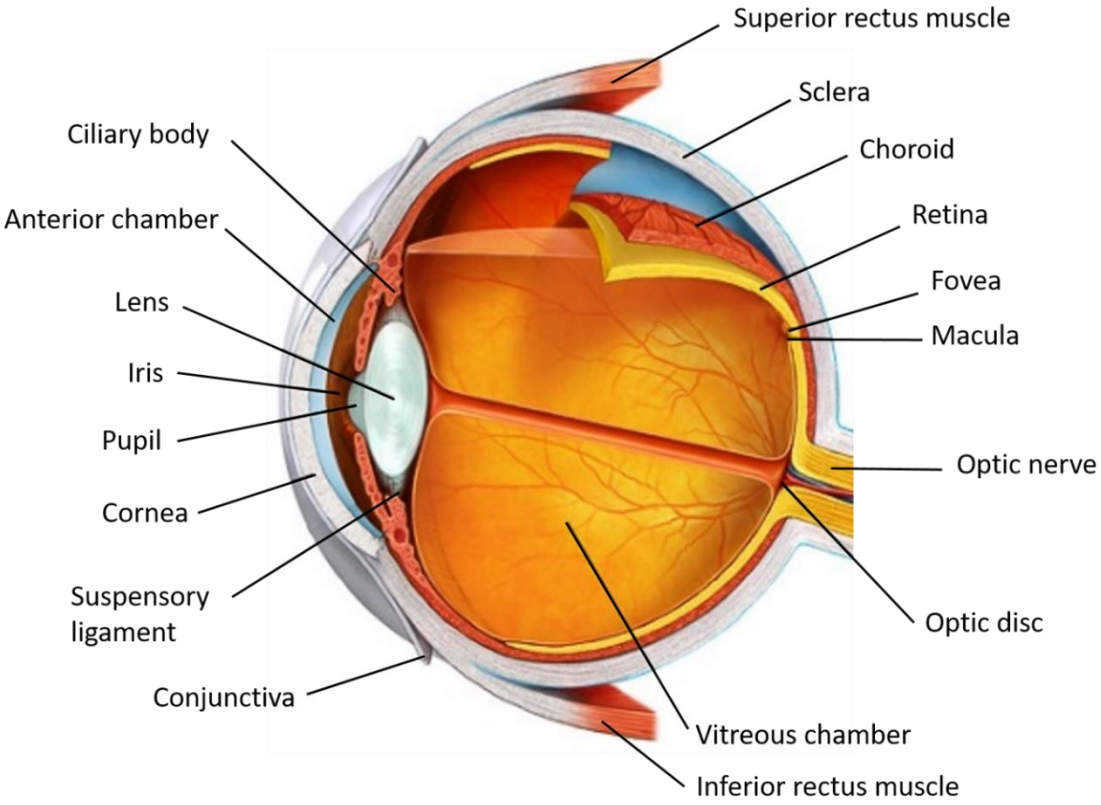

Fig. 1. Anatomy of the human eye. *Figure adapted from myvmc.com* [3].

The wall of the eyeball is made up of three major layers: the outer coat, the uveal coat, which is located underneath, and the retina being the inner layer.

The outer coat is built up from sclera, better known as the white part of the eye. The sclera consists of a connective tissue coat encircling the entire surface of the eye except anteriorly, where it continues in the cornea. The cornea is a transparent tissue which is entirely avascular under normal physiological conditions. It is segmented into three different layers: the outer layer being the epithelium, the stroma making up the largest part of the cornea and the inner layer being the endothelium [4]. The anatomy and function of the cornea will be discussed further in section *1.2.2.1 corneal absorption*.

The sclera provides an anchoring site for the extrinsic eye muscles (superior and inferior rectus muscle) and is almost entirely avascular in healthy humans. It is also responsible for the retention of the shape of the eyeball and protects the internal structures such as the retina and the lens. The sclera and the inner surface of the eyelids are covered by a thin and transparent, but highly vascularised layer, called the conjunctiva. It is composed of a non-keratinised epithelium with goblet cells which lubricate the surface of the eye by secreting mucus. The conjunctiva that lines the inner surface of the eyelids is called palpebral conjunctiva. The conjunctiva that covers the eye itself is referred to as the bulbar conjunctiva; the area where the bulbar and the palpebral conjunctiva meet, is referred to as the fornix or conjunctival sac [5].

The uveal coat is the middle layer of the eye wall and contains the choroid. It is highly vascularised in order to provide nutrition and gases mainly to the iris and ciliary body but also to the lens, retinal layer and sclera. The ciliary body is attached to the lens through suspensory ligaments and is responsible for the shape of the lens. The uveal coat is also very important for the optical properties of the retina. Due to its dark colour, the uveal coat absorbs light that is transmitted through the sclera, improving the contrast of the image that the retina registers [5]. The choroid is situated between the sclera and Bruch's membrane. Bruch's membrane is a thin, acellular membrane between the retinal pigment epithelium (RPE) and the choroid, regulating fluid permeability and nutrient transport [6,7]. The build-up of the eyewall and specifically the macular region is illustrated in more detail in figure 2.

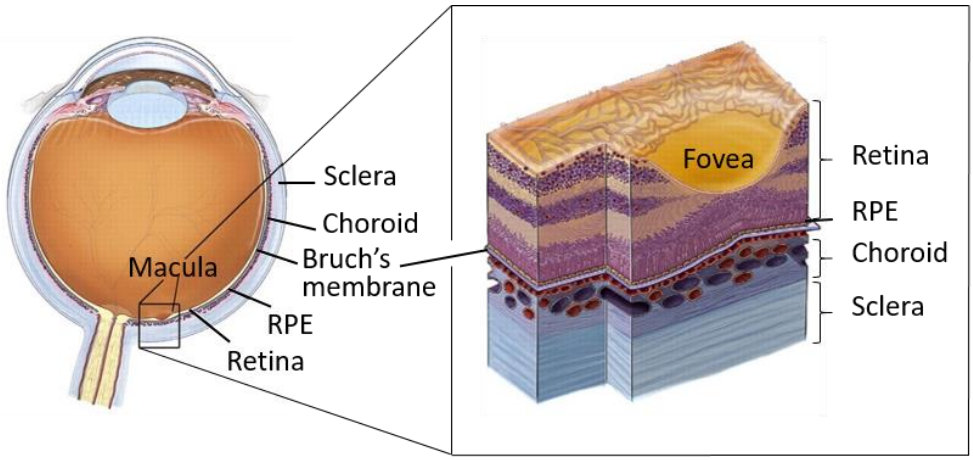

Fig. 2. Cross-section of the eyewall in the macular region. *Figure adapted from Yuan X. et al.* [8].

The third and innermost ocular coat is **the retina**. The retina is the light-sensitive portion of the eye and lines the inner part. The retinal layer is composed with photoreceptor cells. These cells are directly sensitive to light and are mainly of two types: rods and cones. The rods and cones are anchored in the retinal pigment epithelium as illustrated in figure 3. Rods provide black-and-white vision (mainly in dim-light), while cones are associated with high-resolution perception and the perception of colour. Signals are integrated in bipolar and ganglion cells, which are called neurons. Subsequently, these signals leave the retina through the optic disc and the fibres of the optic nerve at the back of the eye [9–12].

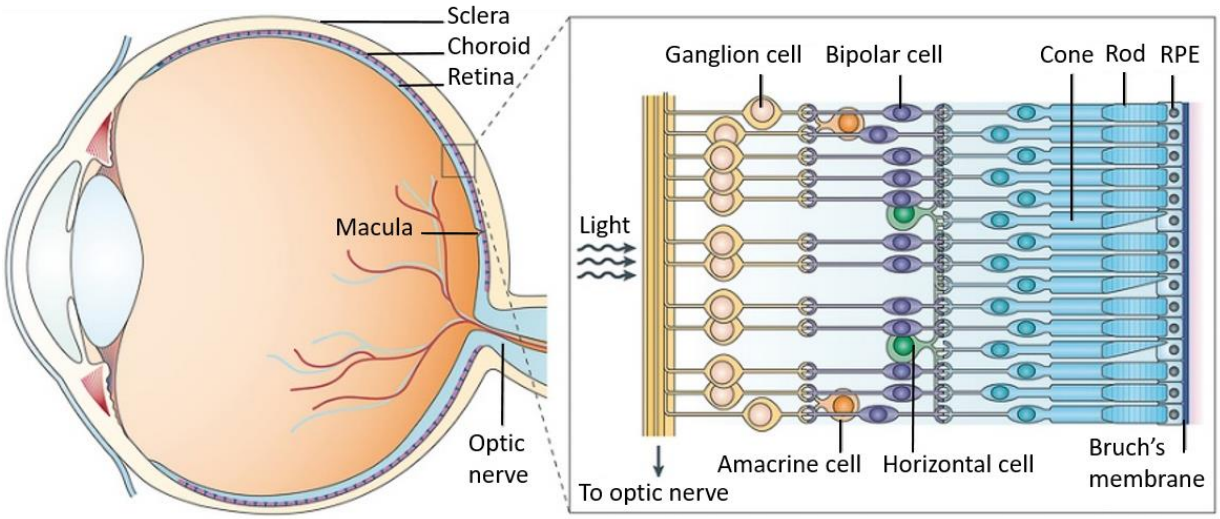

Fig. 3. Structural build-up of the retinal layer. *Figure adapted from Kimbrel E. et al.* [13].

Another important part of the retina is the macula lutea. It is an oval-shaped, pigmented area with a diameter of 5.5 mm near the centre of the retina. The cones located in the centre of the macula lutea are called the fovea. It holds the largest concentration of cone cells, responsible for high-resolution, central vision. In healthy eyes, there are no blood vessels to interfere with vision towards the centre of the macula. In some diseases, such as wet age-related macular degeneration, new blood vessels form underneath the retina and break easily, causing fluid to leak to the surroundings. This interferes with the alignment of the cone cells, compromises the acuity of central vision while peripheral vision is still maintained [10,14,15]. Age-related macular degeneration will be discussed in more detail in section *4.2.2 Age-related macular degeneration.*

The vitreous chamber, which is the large cavity between the lens at the anterior part of the eye and the retina at the posterior part of the eye, is filled with a viscous substance, called vitreous humour.

The external surface of the eye is protected by the eyelids. They lubricate the surface of the eye by spreading tear fluid by blinking. On average, the human eye voluntarily blinks about 10-20 times per minute (periodic blinking) and is highly dependent on the medical condition of the individual. Stimulation of the highly innervated cornea by a foreign substance can elicit a rapid series of repeated and involuntary blinking of the eyelids in order to remove the foreign substance from the eye surface [16]. This process is called corneal reflex or reflex blinking and is often accompanied with tear secretion, draining the foreign substance towards the lachrymal puncti as depicted in figure 4. The puncti are small openings on the inside of the upper and lower eyelids and allow drainage of tear fluid, collected via the lachrymal canaliculi in the lachrymal sac and eventually ending up in the nasal cavity through the nasolachrymal duct. Additionally, the eyelids aid in the regulation of light entering the eye [4,17,18].

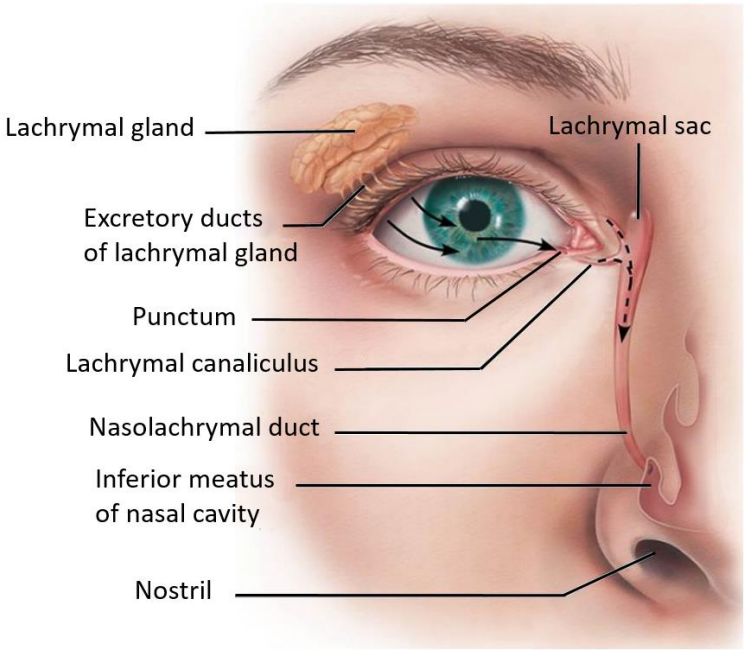

Fig. 4. Overview of the lachrymal drainage system. *Figure adapted from Benjamin Cummings Accessory Structures of the Eye* [19].

Tear glands, found in the upper-outer orbit of each eye, are responsible for the production of lachrymal fluid, the main component of tears. The production of tears is very important for lubrication, cleaning and protection of the ocular surface. Tear fluid serves as a pool for many ions and molecules such as potassium, sodium, glucose, urea, immunoglobulin, lactoferrin, lipocalin, lacritin, lysozyme, mucin and lipids. Therefore, tear fluid and the movement of the eyelids serve as an important barrier against foreign substances [20–25].

1.2 Ocular barriers and availability of topically applied drugs

Topical delivery of drugs through eye drops into the lower fornix (cul-de-sac) is probably the easiest way of administrating drugs to the eye for the treatment of ocular diseases or for diagnostic purposes. Because of its ease of use, eye drops (especially when low viscous) are well accepted by patients causing little to no discomfort when formulated properly [26].

The driving force behind drug absorption is the concentration gradient as described by Fick's first law:

$$J = -D.\frac{dC}{dx} \qquad (mol/m^2s)$$

J = flux of drug molecules

D = diffusion coefficient

dC = change in concentration of drug molecules over the diffusion layers

dx = change in distance that the molecules have to travel through ocular tissues

This means that higher drug absorption levels can be achieved by increasing the drug concentration in the drug solution, but this can potentially cause undesired toxic side effects due to systemic absorption in the nose and can cause cellular damage to the ocular surface [27].

Many factors influence the amount of drug available at the ocular surface and the efficacy by which drugs can be absorbed to exert a pharmacological action. Precorneal drainage, as a result of defence mechanisms of the eye such as eye blinking and tear fluid secretion, are held responsible for reducing the contact time of the drug and the ocular surface. The resulting low ocular availability of topically applied drugs is one of the most important drawbacks of low-viscous eye formulations, such as aqueous eye drops, but which still is a very popular choice of formulation. An instilled dose is drained away within five minutes after instillation in the human eye [28,29]. The drugs used in eye drops are preferably water soluble for easy formulation but emulsions, ointments or oily drops can also be used for molecules with poor hydrophilic properties. An effective delivery of topically administered drugs can be achieved by circumventing the protective barriers of the eye, allowing a better penetration of the molecule into the ocular tissues to treat ophthalmic pathologies [30]. These protective barriers of the eye will be discussed in detail in the following sections.

1.2.1 Precorneal factors

1.2.1.1 Drainage of the drug solution

A tear film covers and protects the ocular surface. It also has multiple purposes such as providing nutrition to the epithelial cells and lubricating the surface of the eye. The tear film has a volume of approximately 7 µl [31,32]. Tear fluid, mainly consisting of water, lipids and mucins, is produced by cooperation of different glands and is distributed during blinking of the eyelids resulting in a thin tear film over the entire ocular surface. The water of the tear film is produced by the main lachrymal gland and the Krause and Wolfring accessory glands as shown in figure 5 [33].

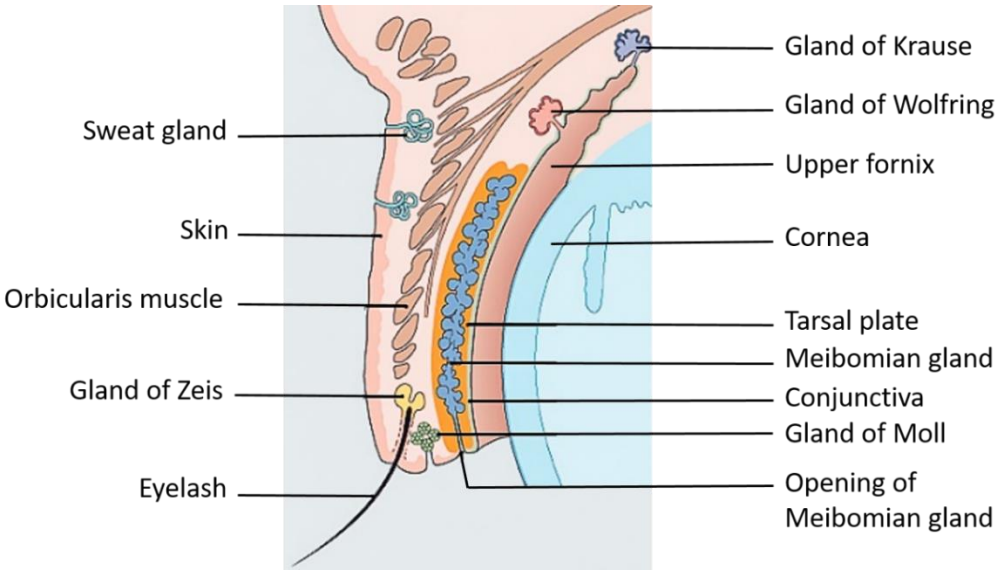

Fig. 5. Overview of various gland and eyelid structures. *Figure adapted from studyblue.com* [34].

A significant part of this layer evaporates (10%), while the remaining solution will be drained through the puncti due to periodic blinking. Since the tear film is relatively unstable, it has to be renewed frequently and continuously and is indicated by the term tear turnover. The basal tear turnover rate is estimated to be at 1.2 µl/minute [35,36]. The basic structure of the tear film is illustrated in figure 6.

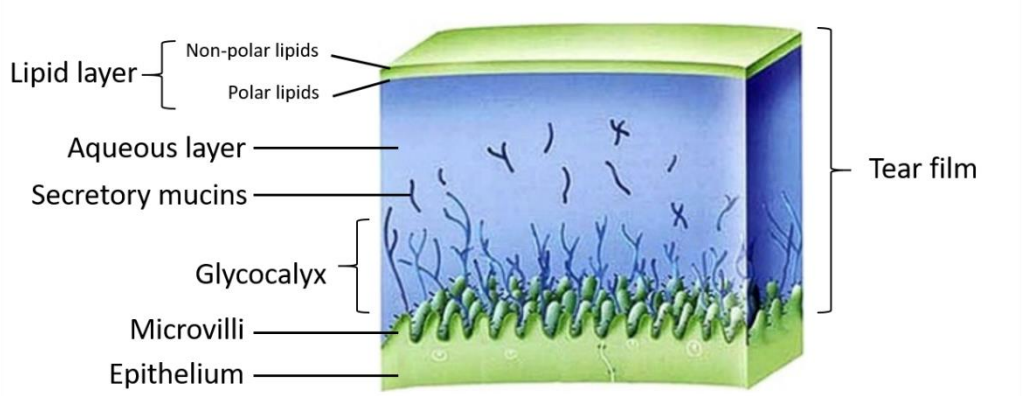

Fig. 6. Structure of the tear film. *Figure adapted from nfburnetthodd.com* [37].

Mucins are large glycoproteins produced by goblet cells. They can be categorised in either transmembrane or secretory mucins. The glycocalyx is a layer of transmembrane mucins which are anchored on the apical surface of the corneal epithelial cells and are secreted by the cornea and the conjunctiva. Secreted mucins play a prominent role as viscosity-enhancers of the tear film. It protects the epithelia from damage, facilitates the movement of the eyelids and spreading of the tear film [38–40]. The tear film does not only protect the ocular surface mechanically, but also through secretion of antimicrobial enzymes by the tear glands, e.g. lysozyme. The presence of certain ocular enzymes, mainly peptidases, limits the absorption of peptides due to their metabolism and clearance. More specifically, endopeptidases, such as plasmin, and collagenase, exopeptidases and aminopeptidases, which reside in the tear film and ocular tissues, form an effective ophthalmic barrier for peptides [41,42].

The outer layer of the tear film is built up from meibum, an oily substance that prevents excessive evaporation of the tear film. Meibum is produced by the Meibomian or tarsal glands, located at the rims of the upper and lower eyelids. There are approximately 50 glands located in the upper and 25 glands in the lower eyelid. Meibomian secretion has a very complex composition. It is mainly composed of various lipids such as sterol esters, wax esters, triacyl glycerol, free sterols, free fatty acids and polar lipids (phospholipids). The lipid layer of the tear film has a biphasic structure. The most hydrophobic, non-polar lipids are found in the superficial region of the lipid layer, while more polar lipids are adjacent to the aqueous layer of the tear film. The non-polar lipids are thought of controlling the evaporation rate of water from the aqueous layer [43–46]. Besides lipids, more than 90 different proteins could be identified, such as lysozyme C precursor, lactotransferrin, lipocalin 1, lacritin precursor, defensin, etc. [23,25,47,48].

1.2.1.2 Mechanical removal of foreign substances

The cornea is strongly innervated with sensory axons of the trigeminal ganglion, making the cornea very sensitive to external stimuli such as cold, touch or nerve stimuli. These sensory nerves are located in the middle and anterior stromal layers and radially spread towards the middle of the cornea. They respond to these stimuli by reflex blinking and inducing lachrymation, which in turn causes administered drugs to be washed out [49,50].

When reflex blinking occurs, the amount of tear flow can vary between 3 to 400 µl/minute triggering the eyelids to blink rapidly [36]. The combination of tear flow and rapid mechanical movement efficiently removes foreign substances from the ocular surface. These mechanisms accelerate the drainage of the instilled eye drop towards the puncti. It enters the nasal cavity through the lachrymal sac and lachrymal duct where it can be absorbed through capillaries, potentially resulting in systemic effects and side effects [51].

1.2.1.3 Conjunctival sac capacity

An aqueous eye drop typically has a volume of about 20-50 µl. But roughly half of it reaches the ocular surface when instilled as the conjunctival sac only has a maximum capacity of 20-30 µl. The conjunctival sac cannot accommodate any excess of fluid when this threshold is surpassed. As a result, the instilled drop will flow over the cheeks and reflex blinking is induced causing a significant amount of drug being lost [31,52].

1.2.1.4 Drug binding

Another precorneal barrier that needs to be considered, is drug metabolism (especially for prodrugs) and proteins in the tear film that have drug binding properties. Examples of such proteins are albumin, globulin and lysozyme. This binding can result in the formation of non-absorbable complexes. These complexes with high molecular weight are unable to cross biological membranes in order to bind to a receptor site [23,28,32,47,53].

1.2.2 Tissue barriers

The remaining part of the instilled eye drop that resides at the ocular surface still needs to penetrate through the biological barriers. Topically applied drugs can reach intraocular tissues through the corneal or through the conjunctival-scleral pathway (transscleral pathway) [54–56]. But precorneally, the ocular drug absorption is mainly limited due to the very tight and selective epithelium of the cornea and the less restricting epithelium of the conjunctiva and sclera [32,57].

1.2.2.1 Corneal absorption

Merely 1-5% of an applied dose will reach the inner eye either through the corneal route or the transscleral pathway where an even smaller portion will be available to exert biological activity. To reach therapeutic levels, eye drops need to be instilled frequently, compromising patient compliance. Consequently, a frequent regime of instillations can also elevate the risk of toxic side effects, due to higher systemic absorption. Frequent instillation also results in pulsed delivery of the drug, meaning that a drug reaches high concentration levels shortly after instillation, followed by underdosage after clearance of the drug as illustrated in figure 7 [5,26].

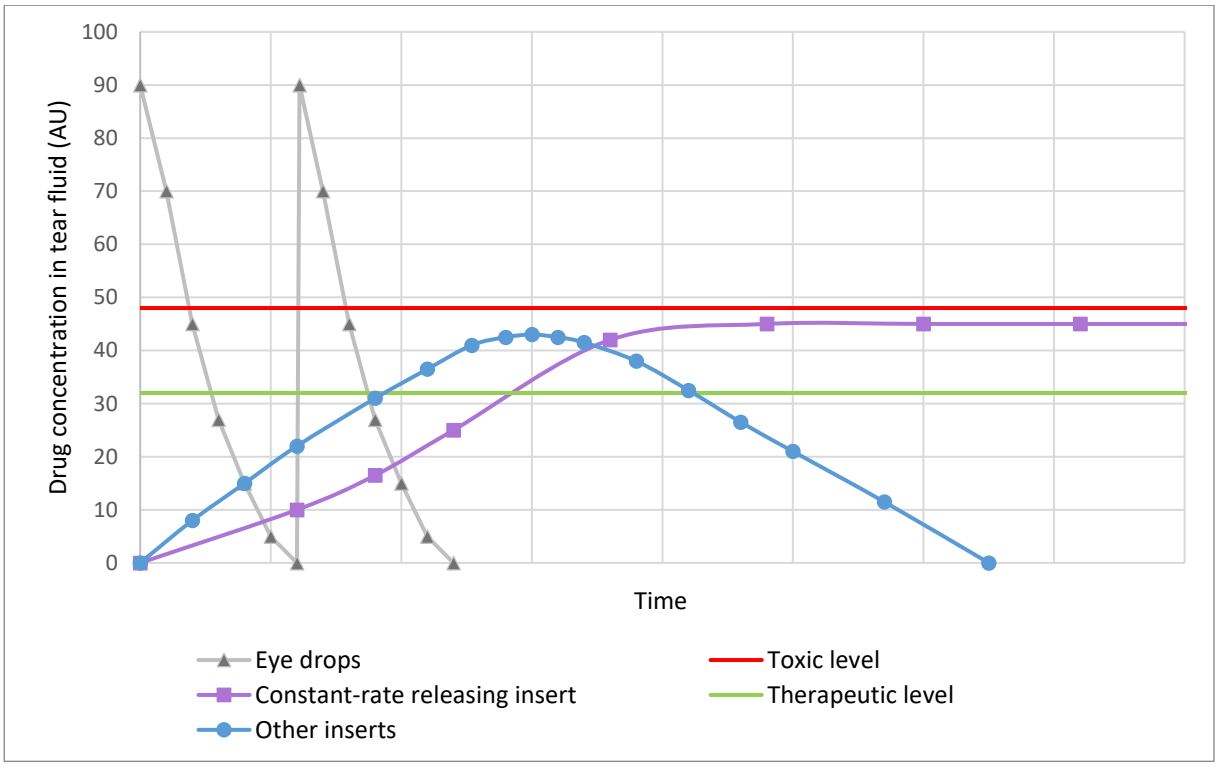

Fig. 7. Profiles of tear film concentrations after instillation. The curve in grey indicates the tear film concentration after eye drop instillation, the curve in purple is indicative for a constant-rate releasing insert and the curve in blue indicates other types of inserts. Therapeutic activity is reached when the dose is higher than the threshold of the therapeutic level (indicated in green), but lower than the toxic level (indicated in red).

Low drug absorption amounts can be attributed to the structure of the cornea. Three major layers can be distinguished, and two sublayers separating these layers: the epithelium, the stroma and the endothelium as depicted in figure 8 [58].

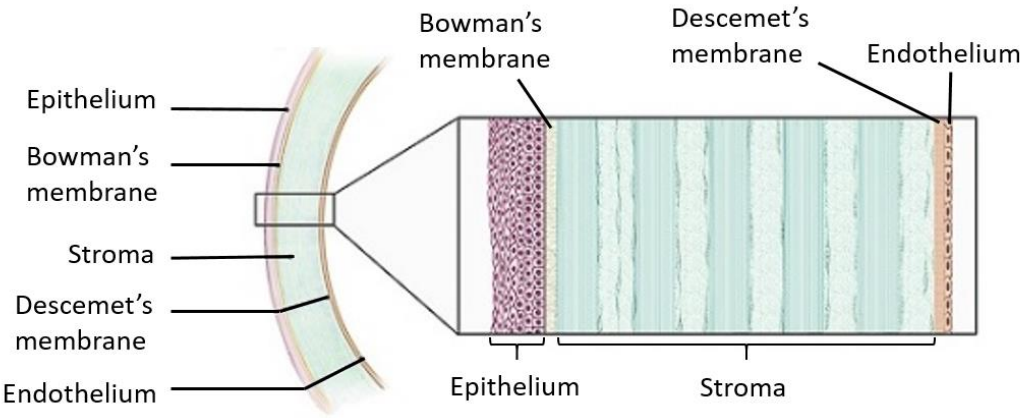

Fig. 8. Cross-section of the structural build-up of the cornea. *Figure adapted from nei.nih.gov* [59].

The epithelium is separated from the stroma by Bowman's membrane while Descemet's membrane separates the stroma and the endothelium. The epithelium is lipophilic by nature, making it impermeable to hydrophilic or polar molecules. This layer is considered rate-limiting for penetration of most drugs because of the tightly packed cell structure [58]. It consists of five or six cell layers: a basal layer of columnar cells, two or three layers of wing cells and one or two layers of squamous, polygonal shaped, flattened cells. The outer layer of cells is closely packed together and forms an effective barrier against microorganisms and other foreign substances [60,61]. The basal layer continuously renews by mitotic division, pushing the cells towards the surface of the eye. These cells differentiate as they are forced towards the epithelial surface resulting in flattened polygonal cells. The shedding of the outer cells possibly prevents the entering of pathogens to the immunologically deficient stromal tissue [48,52,61]. Tight junctions are present between epithelial cells and serve as a selective barrier to small molecules and they are effective in preventing the diffusion of macromolecules through the paracellular route. Furthermore, the epithelium is impermeable for molecules between 60-100 Da [62].

The stroma is the largest part of the cornea (90% in volume) and consists mainly of water, mucopolysaccharides and keratocytes, which are corneal fibroblasts [63]. The collagen fibrils of the stroma hold water and are spaced allowing light signals to pass through the cornea [58,62]. Due to the relatively open structure of the stromal layer, drugs up to a molecular weight of 500 kDa can

penetrate. For highly lipophilic drugs, the hydrophilic stroma represents a rate-limiting barrier for ocular absorption [4,29,58].

The endothelial layer is a single cell layer with a thickness of approximately 4-6 µm. Along the lateral membrane, the endothelial cells exhibit a vast number of active pump sites for transport of ions. The endothelial layer is held responsible for maintaining a normal corneal hydration by actively pumping water out and restraining the influx of water from the aqueous humour of the eye. Adequate water levels to keep the stroma transparent are required: water is actively pumped out of the stroma through sodium-potassium adenosine triphosphate ATPase coupled to a bicarbonate pump while the endothelial cells restrict entry of fluid from the aqueous humour by acting as a tight barrier. These pumps account for 75% of all hydration activity of the cornea. As opposed to the corneal epithelium, the cells of the endothelium are not nearly as closely in contact to each other. This allows the endothelium to be more physiologically leaky for molecules to pass [58,64]. Molecules up to 70 kDa can penetrate through this layer [62].

Permeation of drug molecules through the cornea depends largely on the physicochemical properties of the molecule. Lipophilic drugs penetrate through the transcellular route, while hydrophilic molecules prefer the paracellular pathway. Both pathways involve passive diffusion along the concentration gradient which is the primary mechanism for permeation across the cornea. Due to the particular structural build-up of the cornea, strongly hydrophilic or lipophilic molecules cannot permeate through the cornea as either the lipophilic epithelium or the hydrophilic stroma will effectively block these molecules at a certain stage during penetration [64]. The lipophilic endothelium, being a monolayer of cells, does not have a significant blocking effect on the entry of molecules. The epithelium is the main penetrant barrier of the cornea. It is important to note that these cell layers act as effective barriers only when fully intact [58,65]. In case of disease or in case of instillation of certain chemicals, the structure of the intercellular spaces and tight junctions can be disrupted, causing a higher influx of drug molecules through the cornea. For instance, the use of calcium chelators is well described in literature for disrupting tight junctions. Corneal permeability changes on an epithelial level can also occur with amphiphilic, surface active compounds such as glycosides, fatty acids, preservatives and topical anaesthetics [2,4,65–67].

1.2.2.2 Conjunctival/scleral absorption

While the cornea is avascular, the conjunctiva is highly vascularised. The thin mucous membrane lining the inside of the eyelids and the anterior sclera is known to be very permeable to a variety of molecules. The permeability of the conjunctiva is approximately 20-times higher, compared to the cornea and roughly double compared to the sclera [68]. Also, the relatively large, accessible surface area of the conjunctiva towards an instilled eye drop contributes to the penetration of drugs in the eye. The sclera is a hard, white layer giving the eyeball a tough construction. It is mainly built up from collagen and elastin fibres [69]. The high degree of water content and a low amount of proteolytic enzymes makes the transscleral pathway an interesting route for macromolecules [54,55].

Although the conjunctival and transscleral routes are a possible pathway for the delivery of drugs to the posterior segment of the eye, it is also considered to be an important route for drug loss due to systemic absorption potentially leading to undesired side effects [69]. If an eye drop is instilled in the fornix of the lower eyelid, permeation of the drug occurs for a large part through the conjunctival pathway instead of through the cornea. The conjunctival epithelium also includes tight junctions as an important barrier for drug penetration but the intercellular spaces in the conjunctiva are not as closely packed compared to the tight junctions of the corneal epithelium [64,68,70,71]. For instance in rabbits, the conjunctival permeability for polar solutes was demonstrated to be several times larger than the corneal permeability. Especially for hydrophilic and large molecules, which show poor corneal permeability, the conjunctival/transscleral route is important for delivering drugs to the uveal coat and the vitreous [55,56,72]. Therefore, the transscleral pathway is becoming an important and alternative route for drug delivery of macromolecules, especially with the gaining interest in peptide and protein delivery [54,56,72]. Studies have demonstrated the possibility to deliver high molecular weight molecules up to 150 kDa across rabbit and porcine sclera [54,55].

2 STRATEGIES IMPROVING TOPICAL OCULAR DRUG DELIVERY

As previously mentioned, poor ocular availability due to precorneal barriers and defence mechanisms of the eye hinder topical delivery of drugs. More than 95% of the instilled dose does not even reach the tissues targeted [28,71]. Over the course of decades, many attempts have been made to increase the availability of the drugs administered and lengthen its action, albeit with mixed results. One strategy involves maximising corneal absorption and thereby minimising precorneal drug loss. Another possibility is to use drug delivery systems which provide a prolonged residence time in order to increase drug delivery. An ideal dosage form might be one that is equally easy to use as eye drops, creating little to no problem with vision but with a frequency of application not more than once or twice daily [28]. A schematic overview of possible strategies to increase the ocular availability is given in figure 9 and will be discussed in the following section.

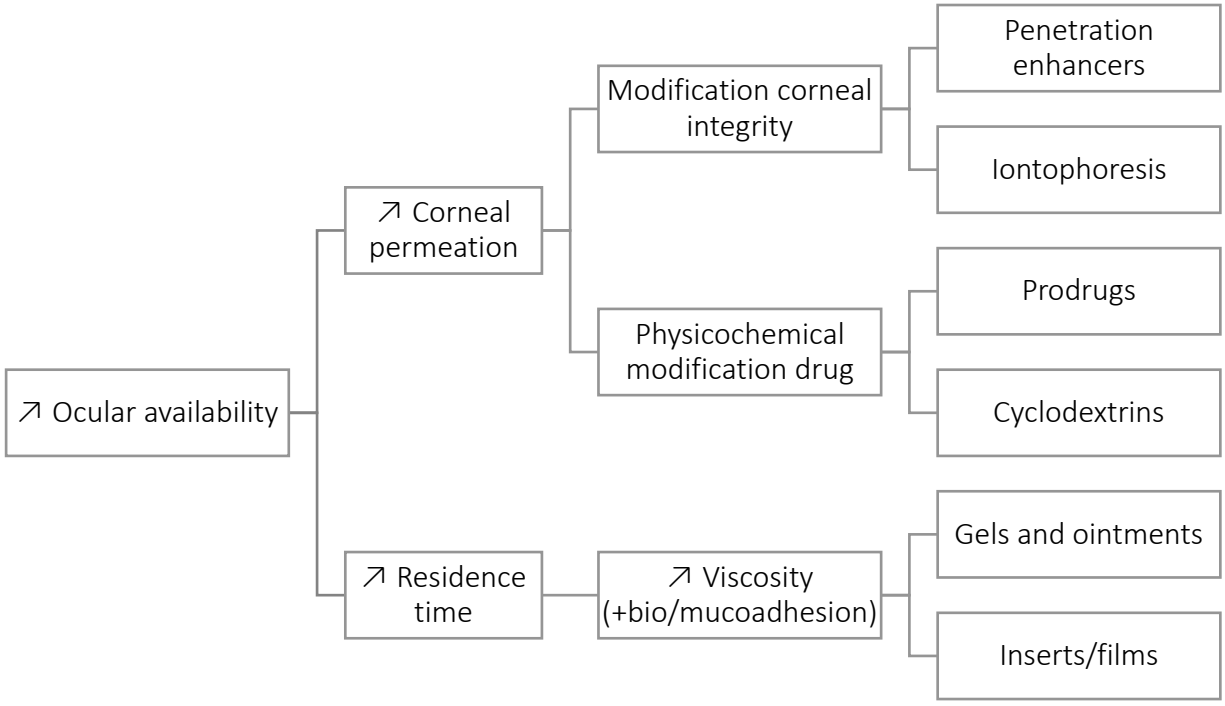

Fig. 9. Overview of the possible strategies to improve the ocular availability.

2.1 Optimisation of ocular availability

2.1.1 Increasing corneal permeation

The first strategy of ocular availability optimisation was set up in order to enhance the absorption of drugs at the ocular surface. By optimising the ocular availability, not only is the retention and penetration of the drug improved, the potentially toxic side effects are minimised. From a theoretical point of view, this can be achieved by disrupting the epithelial barrier of the cornea with chemical substances (penetration enhancers), by decreasing the tear turnover rate or by slowing down drainage of the drug solution, for instance by sealing the puncti of the eyelids with tear duct plugs (punctal plugs) [18,65,66,73]. Except for sealing the puncti, the aforementioned strategies can only be accomplished by compromising the integrity of the protective mechanisms of the eye, thereby increasing the risk of infection which is of course unacceptable for actual use in humans or animals.

2.1.1.1 Modification corneal integrity

Penetration enhancers such as surfactants, fatty acids and some preservatives affect the stability of the phospholipid membranes of the epithelial cells where they induce defects by changing the physical properties of the cell membranes. Paracellular transport can be improved with the use of for example EDTA. As EDTA complexes Ca^{2+} ions, which regulate the tight junctions, the integrity of the tight junctions is compromised [73,74]. Another relatively intrusive technique is iontophoresis. As opposed to the previously mentioned chemical techniques, iontophoresis is a physical method to improve transport of drugs through the epithelial barriers by applying an electric current on the tissues. The major drawback of this method is the use of specially designed electric equipment and the risk of ocular damage that might occur [57,75,76]. This technique is used with success on a limited scale for ocular delivery of large proteins, such as bevacizumab (149 kDa), but the true role of iontophoresis in ophthalmic drug delivery still needs to be identified [77]. The use of peptides and proteins will be discussed in section *4 Ophthalmic delivery of peptides and proteins.*

2.1.1.2 Physicochemical modification drug

Another less intrusive method of enhancing ocular availability is by modification of the physicochemical properties of the drug. Permeation of the transcellular pathway can be promoted by increasing the lipophilic nature of the drug of interest. A drug molecule with a log[octanol/buffer] partition coefficient greater than 1 has good penetrating properties. However, a partition coefficient greater than 2-3 does not further increase its permeability due to the hydrophilic barrier

of the stroma. Drugs can be made more lipophilic by derivatisation creating lipophilic prodrugs. These prodrugs can be absorbed more easily than its active counterpart, to which it is converted chemically or enzymatically after corneal penetration [26,78–80]. Unfortunately, the use of prodrugs in topical ocular delivery is not very common for reasons of stability and solubility. Its inherently lipophilic nature is unsuited for formulation of aqueous eye drops. Furthermore, irritation to the ocular surface has limited its efficacy and clinical acceptability. A possible strategy to diminish the local irritation is by complexation of prodrugs into cyclodextrins [78]. These molecules are a group of homologous cyclic oligosaccharides consisting of six, seven or eight glucose units, more specifically α-, β- and γ-cyclodextrin, which have the unique property of being soluble in water, although having a lipophilic cavity in the centre. With many drugs, cyclodextrin can interact and form complexes, including a lipophilic drug in the central cavity. For ocular administration, hydroxypropyl-β-cyclodextrin is used as it does not have cytotoxic properties [81–84]. The use of cyclodextrins shows great potential for drugs that are poorly water soluble, unstable, irritating or difficult to formulate, but a real breakthrough fails to appear to date.

2.1.2 Improving residence time

2.1.2.1 Viscosity increase

Increasing the viscosity is a very effective approach to increase the drug concentration in the tear film and to improve ocular availability. A higher viscosity of the drug carrier slows down drug elimination from the precorneal site, reducing precorneal drug loss and improving ocular retention and therapeutic efficacy [26,32,84,85].

Except for dermal use, ointments can also be employed for ophthalmic application. The drug availability is influenced by the solubility of the drug in the ointment, the release of the drug and the ability to mix the ointment with tear fluid. The most important inconveniences of ointments are interference with vision associated with visual discomfort and ocular mucosal irritation [86].

The viscosity of an ophthalmic solution can be modified by adding viscosifying agents, either natural, synthetic or semisynthetic. An overview of different polymers used for ophthalmic application is given in table 1.

Table 1. Non-limitative overview of different classes of viscosifying agents for ocular use.

Natural polymers	Synthetic polymers	Semisynthetic polymers
Guar gum, dextran gum, xanthan gum, sodium alginate, carrageenan, chitosan, sodium hyaluronate	Polyvinyl alcohol, polyvinyl pyrrolidone, polyacrylic acid	Hydroxyethyl cellulose, hydroxypropylmethyl cellulose, hydroxypropyl cellulose, methyl cellulose, sodium carboxymethyl cellulose

Natural polymers include botanical polysaccharides (guar gum), microbial polysaccharides (dextran and xanthan gum), algal polysaccharides (sodium alginate, carrageenan) and animal polysaccharides (chitosan, sodium hyaluronate). The most common synthetic polymers are polyvinyl alcohol (PVA), polyvinyl pyrrolidone (PVP) and polyacrylic acid (carbomer). Semisynthetic polymers include cellulose derivatives such as hydroxyethyl cellulose (HEC), hydroxypropylmethyl cellulose (HPMC), hydroxypropyl cellulose (HPC), methyl cellulose (MC) and sodium carboxymethyl cellulose (Na CMC) [87]. Compared to low-viscous eye drops, the commercially available 1% (w/V) suspension of fusidic acid in a viscous aqueous carbomer base has demonstrated a delayed elimination profile from the tear film [88]. In contrast, in 1986, Lee et al. concluded that increasing the viscosity of the ocular solution only has a limited effect on improving the ocular retention and the amount of drug absorbed. Increasing the viscosity can cause discomfort to the patient's eye, resulting in an increase in blinking frequency and drainage rate, which in turn is responsible for faster drug elimination [28]. Viscous solutions based on a gelling agent are commercially used as artificial tears without drug, e.g. Celoftal® eye drops (2% (w/V) HPMC), Lacrisert® (5 mg HPC) and Vidisic® (carbomer 980, 2 mg/g) [1,89–91].

In an attempt to reduce or eliminate the viscosity associated issues, phase transition systems or *in situ* gelling systems were developed. These systems are formulated as aqueous eye drops but shift to a gel or solid phase upon instillation in the lower fornix. The gelling process is triggered by a change in pH, activated by electrolytes present in tear film or by a change in temperature after instillation in the lower fornix. Examples of polymers used for these applications are respectively cellulose acetophtalate, gellan gum (Gelrite®) and poloxamer polymers. For patient compliance, instillation as an eye drop has a major advantage over semisolid or solid devices. After the phase

shift has taken place, the higher viscosity of the *in situ* gelling system results in better ocular retention of the drug and higher ocular availability [4,80,92–99].

Viscous eye drops are relatively easy to formulate, therefore easy to manufacture and provide promising data about availability in animal models. However, a good correlation between human eyes and animal eyes (e.g. rabbit models) is lacking, mainly due to a difference in blinking frequency (3 times/h in rabbits compared to 1000 times/h in humans) and tear film composition (thicker lipid layer in rabbit eyes) between both species [100].

2.1.2.2 Bio- and mucoadhesive dosage forms

When two materials, of which at least one is from biological origin, attach to one another, this can be regarded as bioadhesion. Mucoadhesion in an ocular context is considered to be a property of a formulation which interacts with the mucosal layer of the eye (e.g. the corneal or conjunctival epithelium). It can be considered a type of bioadhesion [101]. The main advantage of mucoadhesion for conventional ocular application is the intimate contact of the dosage form at the site of absorption, thus enhancing the availability of the drugs applied. Another benefit of mucoadhesive dosage forms is the residence time of the drug at the ocular surface being controlled by the rate of mucus turnover instead of tear turnover. This prolongs the residence time of the drug as the mucus turnover rate (once daily) is slower than the tear turnover rate [52,74].

For mucoadhesion to occur, a sufficient hydration or degree of swelling of the polymer is required and is predominantly determined by the contact time between the substrate and the adhesive polymer. When an adhesive polymer is applied to a substrate, interlinking of the polymer chains and the substrate (e.g. mucus layer) will occur over time depending on the hydration degree of the polymer [102–104]. However, water movement from the mucus layer towards the dosage form has a larger impact on adhesion when compared to intermolecular forces between the polymer chains and mucus [105]. Although mucoadhesion is a potentially useful phenomenon for topical drug delivery, its effect is rather unreliable due to a different behaviour of mucoadhesive preparations over a certain pH range, the varying turnover time and composition of mucus, and the disease condition of the eye which might affect the outcome of mucoadhesion.

Furthermore, various researchers have reported differing results concerning mucoadhesion of a given polymer due to different testing methods and individual interpretation [102]. Amongst the most frequently used polymers showing interaction with the mucus layer are polyacrylic acid,

hyaluronic acid, chitosan and thiomers, which are capable of forming disulphide bonds with cysteine structures in the mucosal layer [30,102,106]. Mucoadhesive polymers are generally macromolecular hydrocolloids with a large number of hydrophilic functional groups establishing electrostatic forces and hydrogens bonds in particular between the polymer and the mucus layer [101].

3 INSERTS

Inserts can be described as preparations with a solid or semisolid consistency with a shape and size particularly suited for ophthalmic application, e.g. rods and shields. These devices are interesting for ophthalmic use because the release rate of the drug can be controlled by choosing the excipients thoughtfully. From a therapeutic point of view, the improved accurate dosing and longer residence time leading to less systemic absorption are important benefits of using ocular inserts. However, compared to eye drops, inserts are not very well accepted or tolerated by patients, application is more difficult and a slow release of viscosifying agents can lead to interference with vision [30,106,107]. Different types of inserts can be distinguished based on appearance or based on properties such as solubility behaviour in the fornix of the eye. An overview of the classification of ophthalmic inserts is given in figure 10.

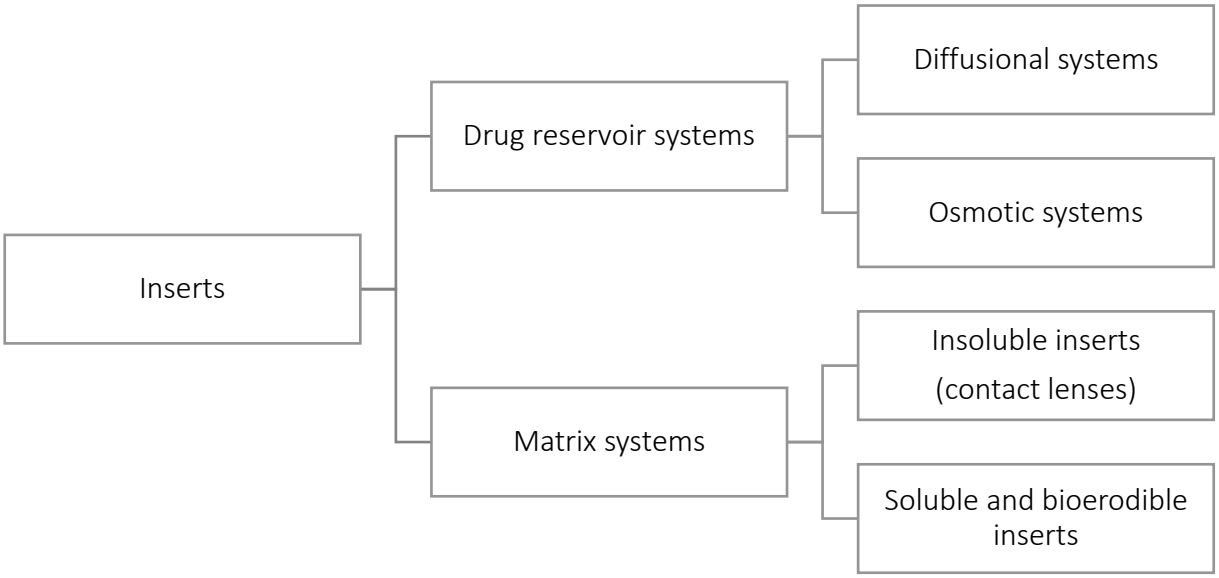

Fig. 10. Classification of ophthalmic inserts.

When the insert is placed in the conjunctival sac, tear fluid will immediately begin to penetrate into the matrix of the insert. Processes of swelling and polymer chain relaxation will occur which in turn will cause drug molecules to diffuse out of the insert and in case of non-crosslinked polymer matrices, dissolution of the matrix will take place [106]. In the following section, a classification of ophthalmic solid dosage forms will be discussed in more detail.

3.1 Classification of ophthalmic solid dosage forms

The composition and solubility of ophthalmic solid dosage forms will be used for the classification of different formulations. Firstly, **drug reservoir systems** such as *diffusional* and *osmotic systems* and secondly, **matrix systems** subdivided into *soluble* and *insoluble systems* will be discussed.

3.1.1 Drug reservoir systems

Drug reservoir systems are devices involving a reservoir comprising the drug of interest and which is in close contact to the inner surface of the rate controlling membrane of the device. This reservoir contains a liquid, gel, colloid, semisolid, solid matrix or a carrier-containing drug dispersed homogeneously or heterogeneously, or dissolved therein.

3.1.1.1 Diffusional systems

Diffusional systems are composed of a central drug reservoir enclosed by semipermeable, transparent membranes which allow the drug to diffuse out of the reservoir compartment at a predetermined rate. The best known ocular device of this type is Ocusert®. This insoluble insert was designed for the treatment of glaucoma. The dimensions of the elliptically shaped Ocusert® dosage form are 13.4 mm x 5.7 mm with a thickness of 0.3 mm. This ocular device consists of a reservoir containing pilocarpine alginate and is limited above and below by a thin, transparent, rate-controlling ethylene-vinyl acetate (EVA) membrane. A ring made of EVA and impregnated with titanium dioxide for visual purposes, encloses the reservoir circumferentially. The build-up of the Ocusert® insert is schematically presented in figure 11.

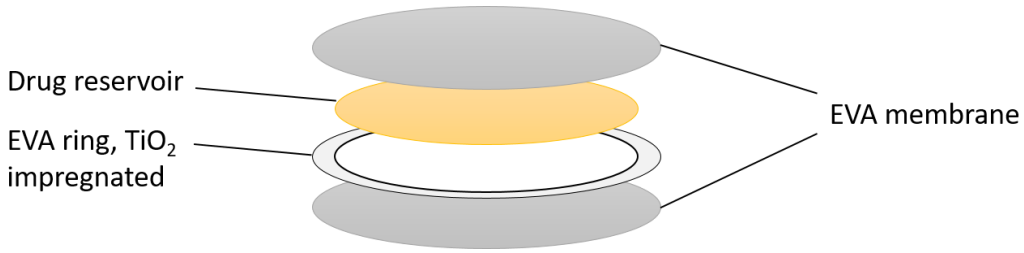

Fig. 11. Schematic overview of the Ocusert® dosage form.

A zero-order release rate is obtained if all variables such as the total surface area, thickness of the insert and concentration gradient remain constant during the diffusional process. Advantages of the device include therapeutic effectiveness and continuous release rate over a period of seven days, less effect on accommodation, less miosis, convenience for the patient and improved compliance for patients who must rely on others for treatment (e.g. children and the elderly). Some

disadvantages that were encountered, were the need for instruction and encouragement of patients; retention difficulties, with some patients being unaware when the device was lost, occasional side effects of a cutting sensation (as when the Ocusert® sometimes doubles over), movement of the insert in the eye, transient blurring of vision and miosis, and high cost. Although from a technological point of view, diffusional systems are very interesting for ophthalmic application, there is a large category of drug molecules that cannot be delivered by these devices because of at least one feature adversely affecting their rate of release from the system or preventing the release of the active agent from the system altogether. For example, many agents cannot be delivered from a diffusion controlled delivery system because their permeation rate through the rate controlling material is too low for a sufficiently high therapeutic effect. Another possible reason is the inability of drug molecules to diffuse through the rate controlling membranes due to their molecular weight or because a suitable membrane material has not been identified yet. Also, chemical characteristics of the drug may prevent a successful diffusion through the membranes, limiting its use. For instance, some salts will not diffuse because of their ionic character through most polymers and polymeric-like materials [30,84,106,108,109].

3.1.1.2 Osmotic systems

Osmotic inserts are the most often described devices in patent literature and can be divided into two major types. The first type consists of a central part which is surrounded by a peripheral part. The central part is generally composed of a single reservoir containing the drug of interest with or without an osmotic solute dispersed through a polymeric matrix. In this case, the drug is surrounded by the polymer as discrete small deposits. In the second case, the drug and the osmotic solutes are placed in two separate compartments. The drug reservoir is surrounded by an elastic impermeable membrane while the osmotic solute reservoir is surrounded by a semipermeable membrane. The peripheral part of these osmotic inserts are comprised of a film covering made of an insoluble semipermeable polymer. As the insert is placed in the lower conjunctival sac, tear fluid starts to diffuse into the peripheral deposits through the semipermeable polymeric membrane causing the deposits to hydrate and inducing dissolution of the drug molecules. The hydrated deposits create a hydrostatic pressure pushing against the polymer matrix, which in turn causes apertures in the structure as the dosage form ruptures. Through these apertures, the drug is released in the conjunctival sac by means of osmosis which is initially characterised by zero order kinetics. As the insert disintegrates over time, the apertures become more interconnected, thereby releasing the drug molecules in a non-constant diffusional manner [30,107,110].

3.1.2 Matrix systems

In a matrix system, the drug is dispersed throughout the entire matrix and released by means of diffusion, erosion or a combination of both.

3.1.2.1 Contact lenses: insoluble ophthalmic drug delivery systems

Contact lenses are drug delivery devices made up of a covalently crosslinked hydrophilic or hydrophobic polymer forming a three-dimensional matrix capable of retaining water, aqueous solutions or solid components. Several studies have demonstrated great potential for topical drug delivery with a particular focus on corneal penetration and availability of topically applied pharmaceutical agents. Generally, contact lenses are loaded by soaking them in a drug solution. After applying the contact lens on the cornea, drug molecules are slowly released through diffusional processes. This results in an initial high release of drug, followed by a slower, long-term release during the next hours of lens wearing. This method of loading the drug into contact lenses is attractive for delivery of antibiotics for severe infections and non-steroidal anti-inflammatory drugs postoperatively. A drawback of this method is the relatively imprecise release rate compared to other non-soluble ophthalmic systems with a rate-limiting membrane. The amount of drug absorbed by the lens is mainly determined by parameters such as the material of the contact lens, the soaking time and the drug concentration of the soaking solution, contributing to and resulting in different release rates [111–116].

Bandage lenses are another type of contact lenses. A topical drug can be applied over the lens while the lens is *in situ* used as a protective device. These lenses take up a certain amount of drug from the tear film and acts as a reservoir in order to slowly release the drug [49,117].

Contact lenses have certain drawbacks, limiting their popularity. Firstly, contact lenses are expensive and require careful manipulation by the patient as cleaning and rinsing procedures can deteriorate contact lenses. Secondly, an issue closely related to the maintenance of these devices is the insufficient exchange of air and other gases with the environment, although the emergence of soft contact lens materials, for once-a-day use, have diminished this issue significantly. Furthermore, covering the cornea might lead to severe eye conditions such as corneal neovascularisation, eye infections such as bacterial or fungal keratitis as well as ‘contact lens induced dry eye’ [25,118–122].

3.1.2.2 Soluble and bioerodible ophthalmic inserts

3.1.2.2.1 Soluble inserts

Soluble inserts for ophthalmic application are made up from one or more hydrophilic polymers that undergo gradual dissolution in the presence of water. Being soluble implies that removal is not necessary which is a major advantage over contact lenses. The release rate mainly depends on the viscosity of the system and releases the drug slowly, lengthening the residence time of the drug at the ocular site. It is important to point out that the terms 'soluble' and 'erodible' correspond to two different chemical processes. If an insert is considered soluble, the main process involves dissolution through polymer swelling in the presence of water, while erodible devices correspond to a hydrolytic process where a chemical or enzymatic hydrolytic reaction leads to solubilisation of the polymer or degradation to smaller water-soluble molecules. These polymers may undergo bulk or surface hydrolysis. If a drug is dispersed in a polymeric matrix, as in case of swelling-controlled devices, the rate of release is mainly determined by polymer swelling, polymer erosion (chemically, physically or enzymatically), drug diffusion through the polymeric network or a combination of these processes [107,123–126]. The process of polymer swelling and erosion is shown in figure 12.

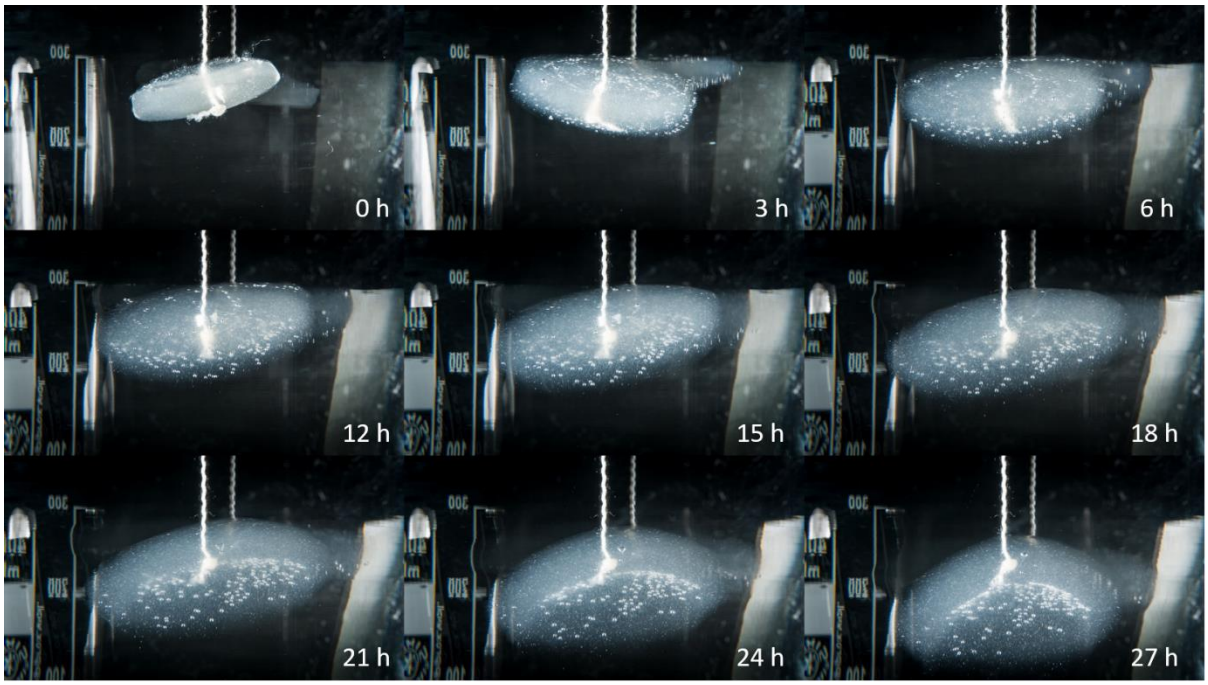

Fig. 12. Swelling and erosion process of an HPMC hydrogel in water. Pictures have been taken every three hours during 27 hours. The hydrogel (20% (w/w)) starts to hydrate and swell upon first contact with water. Parts of the hydrogel that are in a highly swollen state, are not able to absorb more water and start to erode.

As mentioned earlier, after applying a soluble insert in the lower fornix, removal of the insert from the site of application is not required as the insert is entirely soluble and will be drained through the puncti of the eyelids. This is of great importance for patient comfort as inserting these devices is the only manipulation required. Two major categories can be distinguished for soluble inserts, based upon their composition. The first category represent inserts based on natural polymers, the other on (semi)synthetic polymers.

Natural polymers

The best known natural polymers used to produce soluble ophthalmic inserts are collagen, gelatine and chitosan [67,87,127,128]. Collagen was one of the first excipients described in literature for the development of an ophthalmic insert. Bloomfield et al. were credited being the first to develop collagen inserts as delivery systems for the antibiotic gentamicin. Drug loading of collagen inserts occurs by soaking the insert into a drug solution. After placing the insert in the conjunctival sac, the drug is released gradually from the matrix as the collagen dissolves in the aqueous environment of the eye [129,130]. The residence time of drugs such as antibacterial, antiviral and anti-inflammatory agents appeared to be lengthened when compared to traditional eye drops [131].

Another example of soluble inserts are so-called ocular shields. Collagen-based inserts were first developed by Fyodorov et al. as a corneal bandage used after surgical operations and various eye diseases. The collagen corneal bandages in the shape of contact lenses were proposed as an alternative for soft contact lenses to protect the healing corneal epithelium after surgery [106]. Only later, collagen-based shields were also suggested as potential drug carriers for active pharmaceutical ingredients (API) such as amphotericin B, ofloxacin and tobramycin [132–134]. Collagen, as being a natural polymer, is often obtained from porcine (Bio-Cor®, Bausch and Lomb) or bovine (Medilens®, Chiron Ophthalmics) origin. The use of collagen shields has become controversial, as the main problem arising from its use are inflammatory reactions and ulcerations of the cornea in rabbits [106,134].

Another commonly used natural polymer for ophthalmic inserts is gelatine. The first soluble inserts (lamellae) were made of glycerinated gelatine, containing different ophthalmic drugs. However, the use of these inserts ended when more stringent rules for sterility were required [135]. If an ophthalmic inserts based on a gelatine matrix is placed in the conjunctival sac, the lachrymal secretion immediately causes the insert to dissolve. It is possible to convert the soluble gelatine

insert into a non-dissolving insert, if it is chemically or thermally treated to form a crosslinked gelatine hydrogel. Such gelatine hydrogel (Gelfoam®, Pfizer) has been proposed as a carrier in controlled ophthalmic drug delivery. The Gelfoam® device consists of a crosslinked gelatine sponge which is loaded with the active ingredient by soaking the device in a solution containing the active compound. *In vivo* studies have indicated that Gelfoam® is more effective than conventional eye drops for delivery of pilocarpine, phenylephrine and tropicamide [66,67,128].

Synthetic and semisynthetic polymers

Ophthalmic inserts with a matrix based on synthetic (e.g. polyvinyl alcohol) and semisynthetic (e.g. cellulose derivatives) polymers are the most frequently described type of inserts in literature [110,130,136–139]. The preference for (semi)synthetic polymers above natural polymers stems from their advantage of being well adapted for ophthalmic use, as well as their ease of manufacturing by conventional methods including compression, compression moulding or extrusion [137,138,140,141]. The drug release from these systems is characterised by two distinct phases: the first one corresponds to the penetration of tear fluid into the insert that induces a high release rate of drug by diffusion and forms a gel layer around the core of the insert. This external gel formation induces a second phase marked by a decreased release rate of the drug incorporated, but still mainly controlled by diffusional forces. The penetration of aqueous solvent into the matrix followed by matrix swelling, dissolution of drug and the relaxation of the polymer chains inducing erosion of the insert, also contribute to the drug release process. The dissolution of inserts can bring up issues such as blurred vision as a result of the rapid penetration of lachrymal fluid causing the polymer to dissolve, or expulsion of the insert. In order to reduce blurred vision, the hydrophobic polymer ethylcellulose can be incorporated in the ophthalmic formulation to diminish insert deformation [123,136,137,142]. Regarding the expulsion of the insert, this can be addressed by using polymers with bio-adhesive properties such as carbomer, which is well-tolerated in low concentrations [136,137,143,144].

Many attempts have been made by researchers in order to prolong the release of the drug. Cellulose acetate phthalate in combination with gentamicin sulphate has been used in order to reduce the drug solubility resulting in a prolonged drug release [136,137,145,146]. By using the co-polymer of methacrylic acid (Eudragit®) as a coating agent, the release rate can also be decreased [138,141].

Another well-known drug delivery device based on soluble polymers is Lacrisert®, commercialised by Merck Sharp and Dohme in 1981 and still commercially available (although not in Belgium). This ophthalmic device is not loaded with a drug and only consists of hydroxypropyl cellulose (HPC). It weighs 5 mg, measures 1.27 mm in diameter and has a length of 3.5 mm. Lacrisert® has proven to be useful for the treatment of dry eye disease and is placed in the lower fornix of the eye, where it slowly dissolves over a time period of 6-8 hours. The HPC polymer is released in the lachrymal fluid to stabilise and thicken the tear film [1,90,106,126].

3.1.2.2.2 Bioerodible inserts

These inserts mainly consist of bioerodible polymers such as crosslinked gelatine derivatives and polyesters. They are marked by their ability to undergo chemical hydrolysis of chemical bonds and thereby releasing the drug by means of dissolution. They are particularly suited for implants since their use eliminates the step of removing the implant after the drug has been released from the matrix. One of the main advantages of this type of polymer is the ability to modify the rate of erosion by altering the chemical structure of the polymer during synthesis and by addition of cationic or anionic surfactants. Generally, the release rate is increased when anionic surfactants are used (e.g. sulphated derivatives) while cationic surfactants (e.g. alkylammonium derivatives) tend to slow down the erosion rate. These advantages come with potentially severe drawbacks: degradation products and the presence of residual solvents during the preparation of the polymer can initiate inflammatory reactions in patients. Another concern is the significantly variable erosion rates that erodible systems tend to show as a result of individual patient physiology and lachrymation patterns [109,110,139,147–149].

Over several decades, researchers have been trying to develop inserts with various compositions in order to provide a valuable alternative to conventional eye drops. The number of patents and publications over the last few decades have been enormous. However, the number of commercially available inserts is very limited. This can be attributed to the reluctance of clinicians and patients to replace traditional ophthalmic solutions as well as the cost to formulate such ophthalmic inserts. For diseases requiring a frequent instillation of eye drops, inserts can be regarded as a valuable means of drug delivery. But the rather small number of patients benefiting from inserts as a drug delivery device is commercially not interesting for the pharmaceutical industry.

In the future, the use of ophthalmic inserts is likely to increase as a result of the development of new polymers, the emergence of new drugs characterised by short biological half-lives or systemic effects, and also the need to improve the efficacy of ophthalmic treatments by ensuring an effective drug concentration at the site of action over a longer period in time.

4 OPHTHALMIC DELIVERY OF PEPTIDES AND PROTEINS

4.1 Peptides and proteins as biopharmaceuticals in general

Peptides and proteins have emerged as a potentially powerful and interesting group of therapeutics of the future [150–154]. They are estimated to be about 10% of the global market share (sales) of pharmaceuticals. This market is currently growing at a greater pace than the market for small molecules [155]. Peptides and proteins are generally regarded as being highly selective, highly potent, efficacious, have a predictable metabolism while at the same time being relatively safe with excellent tolerability. Especially peptides are truly interesting future therapeutics as they are typically associated with lower production complexity compared to protein biopharmaceuticals, combining the cost and development advantages of small molecules and biopharmaceuticals [153,155,156].

But peptides and proteins have inherent drawbacks: e.g. they are physically and chemically instable as these molecules tend to be prone to oxidation and hydrolysis, have a tendency for aggregation, usually have short half-lives, fast elimination and low membrane permeability, and a significant risk for immunogenicity [150,153,157–159]. A brief overview of possible stability issues of peptides and proteins is given in figure 13.

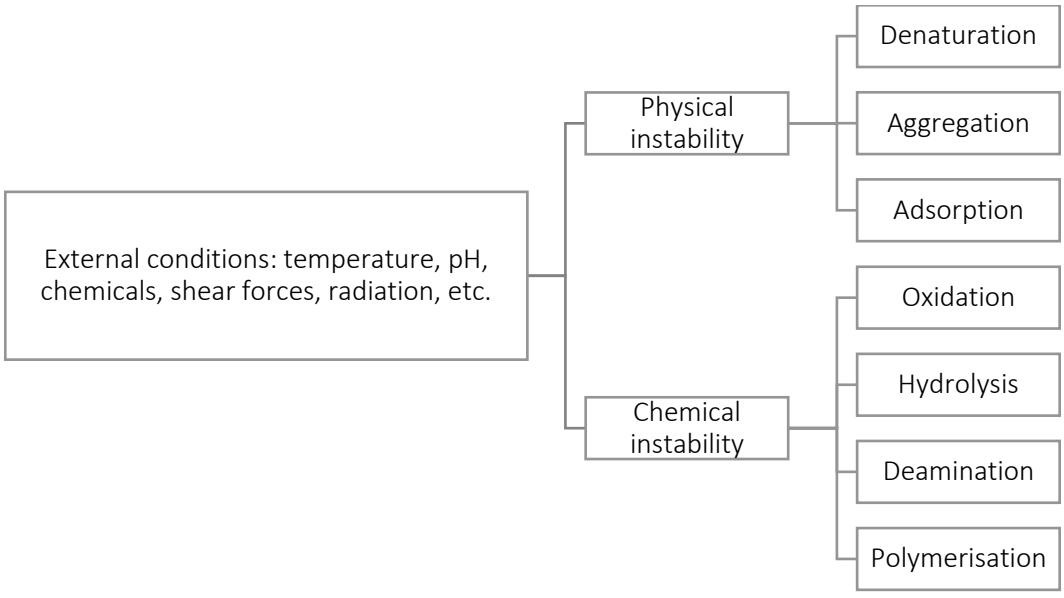

Fig. 13. Overview of possible stability issues associated with peptides and proteins [158,160–166].

The majority of the therapeutic peptides and proteins are delivered through intravenous or subcutaneous injections, to overcome issues of absorption, although not resolving issues related to

low bioavailability due to conformational changes in protein structure, rapid metabolisation or enzymatic degradation [155]. For instance, enzymes such as proteases and aminopeptidases are held responsible for enzymatic degradation of peptides and proteins in the eye [150].

Oncology, neurology and endocrinology are the main driving forces of peptide and protein therapeutics but immunology and infectious diseases are also important fields of discovery [151–153,155]. Table 2 shows a non-limitative list of peptide and protein therapeutics with their major therapeutic indication(s).

Table 2. Non-limitative overview of peptide and protein therapeutics [15,167–170].

Field of application	Product	Therapeutic indication
Oncology		
	Zoladex® (goserelin)	Breast and prostate cancer
	Velcade® (bortezomib)	Multiple myeloma, mantle cell lymphoma
	Lupron®/Enantone®/Eligard® (leuprorelin)	Prostate cancer, endometriosis
	Avastin® (bevacizumab)	Colorectal cancer, non-small-cell lung cancer
Cardiovascular		
	Angiomax® (bivalirudin)	Anticoagulant agent
	Integrilin® (eptifibatide)	Antithrombotic agent
Central Nervous System		
	Copaxone® (glatiramer)	Multiple sclerosis
	Rebif® (interferon β-1a)	Multiple sclerosis
	Plegridy® (peginterferon β-1a)	Multiple sclerosis
Endocrinology		
	Humulin® (insulin)	Diabetes mellitus type II
	Byetta® (exenatide)	Diabetes mellitus type II
	Victoza® (liraglutide)	Diabetes mellitus type II
	Sandostatin® (octreotide)	Acromegaly, metastatic carcinoid tumours

Infection		
	Incivek® (telaprevir)	Hepatitis C
	Victrelis® (boceprevir)	Hepatitis C
	Fuzeon® (enfuvirtide)	HIV
Pneumological Disorders		
	Xolair® (omalizumab)	Persistent allergic asthma and chronic idiopathic Urticaria
Hematological Disorders		
	Firazyr® (icatibant)	Hereditary angioedema
	Kalbitor® (ecallantide)	Hereditary angioedema
	Aranesp® (darbepoetin-α)	Anaemia due to chronic kidney disease
Auto-immune Disorders		
	Cimzia® (certolizumab)	Crohn's disease, rheumatoid arthritis, psoriatic arthritis
	Humira® (adalimumab)	Rheumatoid arthritis, Crohn's disease, ankylosing spondylitis, psoriatic arthritis
	Enbrel® (etanercept)	Rheumatoid arthritis, psoriatic arthritis, ankylosing spondylitis, plaque psoriasis
	Remicade® (infliximab)	Rheumatoid arthritis, Crohn's disease, ankylosing spondylitis, psoriatic arthritis, plaque psoriasis
Gastrointestinal		
	Gattex® (teduglutide)	Short bowel syndrome
	Linzess® (linaclotide)	Irritable bowel syndrome
	Lactaid® (lactase)	Lactose intolerance

Ophthalmology		
	Lucentis® (ranibizumab)	Neovascular age-related macular degeneration (wet-AMD)
	Eylea® (aflibercept)	Wet-AMD
	Macugen® (pegaptanib)	Wet-AMD
	Jetrea® (ocriplasmin)	Vitreomacular traction
	Restasis® (cyclosporin A)	Dry eye disease

Increasing obesity (endocrinology) and a profound desire for replacement of chemotherapeutics (oncology) are linked to the development of these new types of drugs. Other fields of discovery include oral, intranasal and transdermal delivery routes, but to a lesser extent. Unfortunately, ophthalmology does not appear to be a field where a lot of peptide and protein research efforts have gone to so far [153].

4.2 Treatment of eye disorders with peptides and proteins

Even though ophthalmic proteins only represent a very small share of the market, the use of proteins for the treatment of certain eye disorders has been one of great consequence. For ophthalmic application, topical delivery of therapeutic drugs is considered the most favourable option for the treatment of ocular diseases due to patient comfort. As discussed previously, the main challenge of topical drug delivery is to circumvent the ocular barriers which limit the efficacy of the drugs administered to the eye [28]. But a systemic delivery of macromolecules such as peptides and proteins has also been demonstrated for topically applied drugs [171]. Therefore, the loss of peptides and proteins due to nasolachrymal drainage and hence systemic circulation and the resulting side effects also need to be taken into account when designing ocular formulations. This makes ocular injection currently the primary choice for protein delivery in the eye [153,172]. For certain ocular diseases such as uveitis, wound healing or ocular inflammation diseases (e.g. dry eye disease), several peptides and proteins have been investigated and some have been commercially exploited. Other experimental peptides and proteins are still under investigation [173–180].

Proteins are currently being used for the treatment of some major retinal diseases. A description of the most common protein-treated eye diseases is given in the following section.

4.2.1 Vitreomacular traction

The vitreous is the central part of the eyeball and is filled with 98% water and 2% proteins such as collagen fibrils, glycosaminoglycan, opticin and hyaluronic acid, which is held responsible for the gel-like consistency of the vitreous. The vitreous humour is encircled by a collagen membrane, called the vitreous cortex [181,182]. From the age of four, the vitreous starts to liquefy and to contract, which is a common process called synchysis and syneresis respectively. At a certain point, the vitreous humour has contracted to such an extent that separation of the vitreous cortex and retina starts to occur. The separation between the posterior vitreous cortex and the retina is called posterior vitreous detachment (PVD). It is detected in half of subjects at the age of 50 and in almost all of the subjects at the age of 80 and older. Under normal circumstances, PVD is asymptomatic and results in a clean and complete detachment of the collagen fibrils between the macula and the cortical vitreous [183,184]. The progression of PVD with age is shown in figure 14.

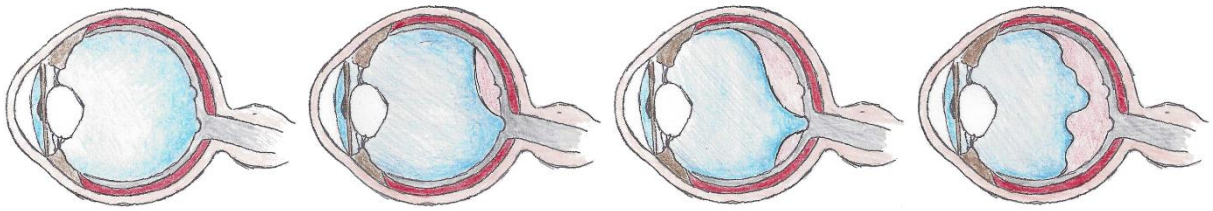

Fig. 14. Progression of posterior vitreous detachment. (L) represents the situation at birth. (R) represents the situation after complete detachment of the vitreous cortex from the retinal layer. *Figure adopted from scottpautlermd.com* [185].

If the vitreous is unable to fully detach from the macular area and continues to liquefy and contract, this creates a traction on the foveal surface which typically results in distorted or reduced vision. This condition is called vitreomacular traction (VMT) and is a sight threatening condition affecting the elderly [181–183]. Until recently, the only viable treatment was *trans pars plana* vitrectomy (TPPV) surgery, where the fibrils were mechanically released. Surgery has the associated risk of hemorrhage, infection, retinal detachment, increased ocular pressure and cataract formation [183].

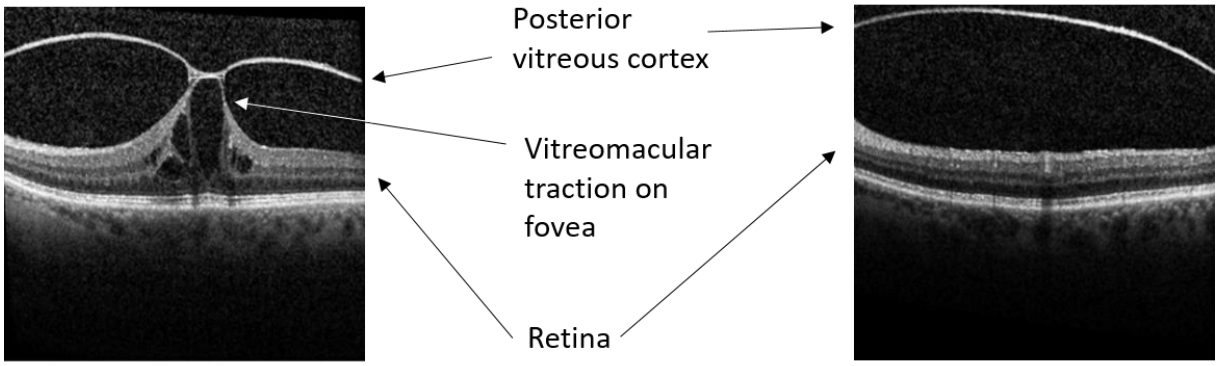

Fig. 14. (L) represents vitreomacular traction where the posterior vitreous cortex did not fully detach from the retina. (R) represents the situation three and a half months after an intravitreal ocriplasmin injection. *Figure adapted from Schumann R. et al.* [186].

The US Food and Drug Administration (FDA) approval of the protein ocriplasmin (Jetrea®, 27.2 kDa) in 2012 led to a breakthrough in VMT treatment. This product was developed by ThromboGenics®, a spin-off company of the University of Leuven, Belgium. Ocriplasmin is the truncated form of the human serine protease plasmin obtained from microplasminogen produced in a *Pichia pastoris* expression system by recombinant DNA technology. It has proteolytic activity against laminin and fibronectin, two major proteins involved in the vitreomacular attachment. This basically means that the vitreous is enzymatically released from the macula, no longer resulting in traction of the fovea. Ocriplasmin is administered through intravitreal injection giving ophthalmologists and patients a valuable alternative to surgery. The effect of ocriplasmin treatment is visualised in figure 14. About one in four patients is successfully treated with ocriplasmin injections [104,181–184,186,187].

Interestingly, topical delivery of ocriplasmin might be possible as some researchers have demonstrated the possibility of repeated topical instillation in rabbits of ranibizumab, a molecule with nearly twice the molecular weight of ocriplasmin [171]. Additionally, topical delivery of ocriplasmin through the transscleral pathway into the vitreous humour could benefit from synchysis, which is at the base of VMT itself [188].

4.2.2 Age-related macular degeneration

Proteins have also changed the treatment of age-related macular degeneration (AMD). AMD is a common eye disease and an important cause of vision loss among people over age 50. It is the leading cause of blindness in industrialised countries and is third worldwide. It is listed among the top ten priority eye diseases by the World Health Organization [9,189–191]. Generally, two

subtypes of AMD are distinguished: a non-neovascular (dry) and a neovascular (wet) AMD type. About 90% of all patients with AMD suffer from the non-neovascular type. Although the neovascular type of AMD is less common, the prognosis of this subtype is much worse [191]. With time, non-neovascular AMD can progress to neovascular AMD. Both types of AMD can be present in the same patient in different eyes. A comparison between a normal macula, dry macular degeneration and wet macular degeneration is given in figure 15.

As age advances, drusen, which are deposits of glycoproteins, lipids, collagen and other debris accumulate extracellularly in the area between the retinal pigment epithelium and Bruch's membrane. A small amount of these drusen are fairly typical, but larger and more numerous drusen can be an indication of AMD. Accumulation of drusen causes deformation of the retinal pigment epithelium and can deprive the RPE from oxygen and nutrients. This can progress into neovascular AMD, characterised by chronic oxidative damage which eventually stimulates the growth and penetration of new blood vessels originating from the choroid into the retina. These vessels leak lipid-rich fluid into the region of the macula, affecting the cells of the retina and resulting in rapid loss of visual acuity. In haemorrhagic forms, blood sometimes leaks from these vessels through the retina into the vitreous [10,11,191–199].

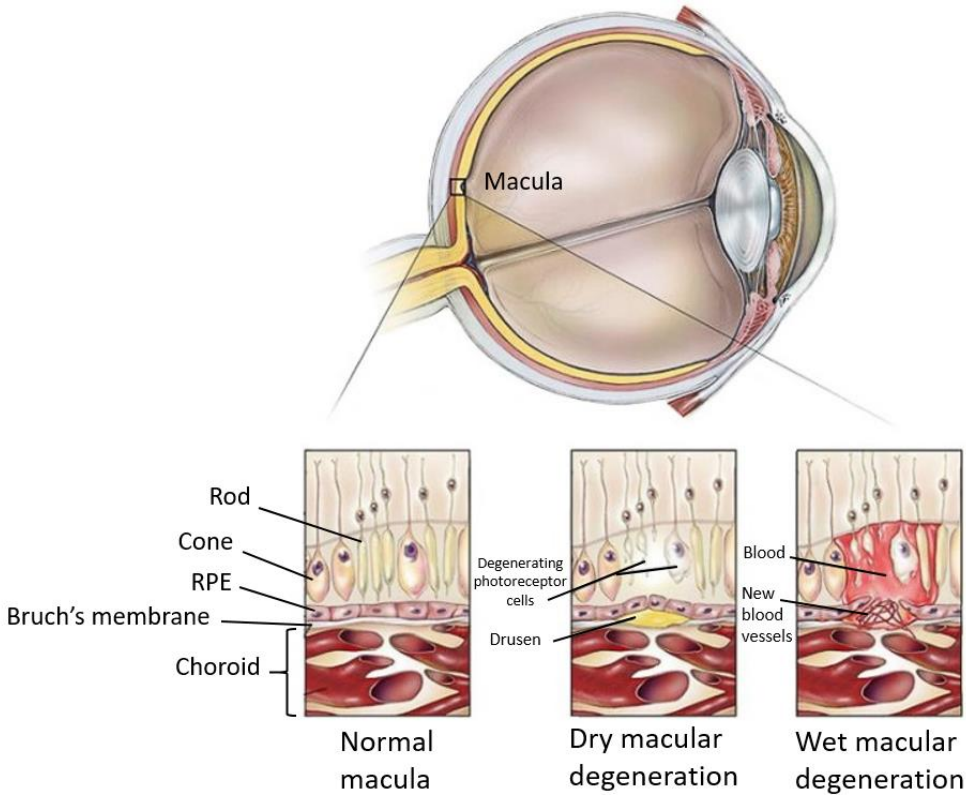

Fig. 15. Comparison between a normal macula, dry macular degeneration and wet macular degeneration. *Figure adapted from brightfocus.org* [200].

For this reason, neovascular age-related macular degeneration is commonly called exudative AMD or wet-AMD [14,201]. The process of growth of blood vessels in AMD appears to be mediated by vascular endothelial growth factor (VEGF), a dimeric glycoprotein (signal protein) promoting angiogenesis. Numerous ligands such as placental growth factor (PlGF), fibroblast growth factor (FGF), angiopoietin-1 and -2 (Ang-1 and -2), platelet-derived growth factor (PDGF) and others play an important role in angiogenesis, but there is a general consensus stating that the hypoxia-inducible cytokine VEGF is the most important angiogenic factor and a crucial rate-determining step in the process of angiogenesis [151,189,191,202–204].

VEGF-A is the first and most important member of the VEGF family that also includes PlGF, VEGF-B, VEGF-C, VEGF-D and VEGF-E [190]. Four different isoforms of VEGF-A have been identified in humans: $VEGF_{121}$, $VEGF_{165}$, $VEGF_{189}$ and $VEGF_{206}$. $VEGF_{165}$ is the predominant isoform in ocular neovascularisation processes. It is generally expressed in hypoxic conditions, where the growth of new blood vessels restore the transport of oxygen molecules [205]. It exerts its action by binding to tyrosine kinase receptors (VEGFR) on the cell surface, which are mainly expressed on endothelial cells [190,199,206,207].

Wet age-related macular degeneration is currently treated with anti-VEGF antibodies such as pegaptanib, bevacizumab, ranibizumab or aflibercept through injection in the vitreous of the eye on a monthly or two-monthly basis [14,15,170,189,191,208–211]. The development of these molecules resulted in a revolution in the management of wet-AMD. Still, after many decades of research, the delivery of macromolecules to the posterior segment of the eye remains one of the toughest challenges in ophthalmology [171,172,212,213]. Although other anti-VEGF molecules such as small interfering RNA and tyrosine kinase inhibitors (lapatinib, sunitinib, sorafenib, axitinib and pazopanib) have been developed, the previously mentioned drugs are the main choice of treatment in the ophthalmic field of wet-AMD. It is important to note that there is no permanent cure to date for this medical condition. An ongoing chronic treatment is therefore required [9,214]. An overview of the anti-VEGF agents that are currently used for the treatment of wet-AMD are given in table 3.

Table 3. Overview of anti-VEGF agents currently used for wet-AMD treatment.

	Pegaptanib	*Bevacizumab*	*Ranibizumab*	*Aflibercept*
Trade name	Macugen®	Avastin®	Lucentis®	Eylea®
Molecule type	28-base ribonucleic acid aptamer covalently linked to 2 branched 20 kDa PEG moieties	Recombinant humanised full-length antibody	Fab fragment derivative from bevacizumab	Recombinant fusion protein
Biological target	VEGF-A isoform 165	VEGF-A all isoforms	VEGF-A all isoforms	VEGF-A all isoforms, VEGF-B, PlGF
Molecular weight	50 kDa	149 kDa	48 kDa	97 kDa
FDA approval date	2004	Not approved for wet-AMD	2006	2011

Pegaptanib (Macugen®, 50 kDa) is a pegylated RNA aptamer targeted against VEGF-A isoform 165. It was approved by the FDA in 2004 and was the first anti-angiogenic therapy for the treatment of wet-AMD [191,215,216]. The molecule is built up from a 28-base ribonucleic acid aptamer covalently linked to two branched 20 kDa polyethylene glycol moieties [198]. It was proven that pegaptanib was able to maintain vision in about 70% of eyes with wet-AMD, but was only able to improve vision in about 10% of patients [191].

Bevacizumab (Avastin®, 149 kDa) is a recombinant humanised monoclonal antibody (full-length antibody, mouse-derived) that was initially developed and FDA approved in 2004 as an angiogenesis inhibitor for certain metastatic colorectal, lung and breast cancers [168,190,192]. The drug substance is not FDA approved for ophthalmic use but nevertheless, starting from 2005-2006, short-term promising results have been described when used off-label with little to no short-term difference compared to ranibizumab. Due to the much lower cost of bevacizumab compared to ranibizumab and aflibercept (roughly 40 times cheaper [210]), bevacizumab is extensively being used for wet-AMD treatment despite the lack of enough clinical evidence supporting its long-term safety and efficacy although comparative studies are continuously being published [191,198,217–220].

Derived from bevacizumab, **ranibizumab** (Lucentis®, 48 kDa) is a recombinant humanised antibody fragment (Fab fragment derivative, developed from the same parent mouse antibody as bevacizumab) and was FDA approved in 2006 for treatment of wet-AMD through intravitreal injection. Not being a full-sized antibody as opposed to bevacizumab, ranibizumab reduces the risk of allergic reactions and can penetrate more easily through the vitreous humour [190,192,221]. It does not only bind to $VEGF_{165}$ but ranibizumab also inhibits all other isoforms of VEGF-A [6,192,196,222]. Monthly intravitreal injections of ranibizumab have become the standard care for patients suffering from this medical condition [212,214].

Aflibercept (Eylea®, 97 kDa) is a recombinant fusion protein acting as a VEGF-antagonist and inhibiting the action of all isoforms of the VEGF-A family, VEGF-B and placental growth factor [14,170,191,198,201,204]. It is the newest member of the anti-VEGF family and was approved by the FDA in 2011 [6,198,204,216,223]. Aflibercept is a potent inhibitor of VEGF mainly due to its strong binding affinity and pharmacokinetic profile potentially leading to prolonged duration of clinical effect when compared to other anti-VEGF agents. As a result, fewer injections (two-monthly) are required [197,201,210,224]. Aflibercept combines the truncated form of the fms-like tyrosine kinase (Flt), the kinase insert domain-containing receptor (KDR), and the Fc portion of human immunoglobulin G [201,223]. This means that aflibercept has two binding domains for VEGF receptors and one for PlGF, enabling stronger binding capacities compared to earlier anti-VEGF agents [204,223].

4.2.3 Corneal neovascularisation

Neovascularisation does not only occur at the back of the eye but the anterior segment is also susceptible. Corneal neovascularisation involves the growth of new blood vessels in the cornea, sprouting from capillaries of the pericorneal plexus [225,226]. Under normal physiological circumstances, the cornea is highly innervated, but clear and avascular [49,204,223,227]. The growth of blood vessels in the cornea can be induced by infectious, degenerative, traumatic, ischemic and inflammatory insults and can cause corneal scarring, inflammation and oedema [223,225,227]. Therefore, contact lens wearers are more prone to developing corneal neovascularisation [225]. As mentioned earlier, VEGF plays an essential role in the formation of new blood vessels and is the main culprit for corneal neovascularisation [204,226,228]. A number of comparative studies have indicated more effective results comparing aflibercept and ranibizumab to bevacizumab after intravitreal injection, but studies comparing topical delivery of different anti-

VEGF agents remain relatively limited [204,218,229,230]. It should also be noted that none of the anti-VEGF molecules used for wet-AMD are FDA approved for corneal neovascularisation.

4.2.4 Dry eye disease

Another well-described ocular disease that can be treated with proteins is dry eye disease. Topical delivery of cyclosporin A for the treatment of dry eye disease has gained a lot of interest in the past decade and the development of formulations based on cyclosporin A have been widely explored and commercialised [175,180,231–236]. Dry eye disease can be classified into two major groups: aqueous tear-deficient dry eye and evaporative dry eye. Aqueous tear-deficient dry eye is marked by an inability to produce or secrete sufficient tear fluid onto the eye surface due to a dysfunction of the lachrymal glands. This can be caused by certain auto-immune diseases such as Sjögren's syndrome dry eye which activates T-cells in the exocrine glands. Evaporative dry eye is caused by an excessive loss of water from the eye by evaporation. The most common cause for this type of dry eye is Meibomian gland dysfunction which is responsible for the secretion of an oily substance in the tear film, limiting the evaporation of water at the surface of the eye. The excessive evaporation can lead to hyperosmolarity of the tear fluid which in turn activates a cascade of inflammatory events. Inflammatory mediators are released at the epithelial surface which results in epithelial damage and apoptosis, a loss of goblet cells and abnormal mucin secretion resulting in tear film instability. Cyclosporin A is a cyclic undecapeptide produced by the fungi *Tolypocladium inflatum* and *Beauveria nevus*. It is well known for its immunomodulatory properties to prevent rejection of transplanted organs after surgery but cyclosporin A is currently also used in ophthalmic applications for its anti-inflammatory properties interrupting the inflammatory cycle of dry eye disease. Contrary to most other proteins, cyclosporin A is lipophilic and therefore formulated as a topical emulsion which allows the patient to apply it as eye drops [234,237–241].

4.3 Formulation considerations for ocular (protein) delivery

Intravitreal aqueous injections are efficient in delivering the drug to the site of action, but they may cause severe adverse side effects including endophthalmitis, retinal detachment, cataract, vitreous haemorrhage, hyphema, uveitis, loss of visual acuity and increased intraocular pressure, especially when chronic treatment is required [115,197,205,214,242,243]. Consequently, to reduce the risk of endophthalmitis, 80% of the ophthalmologists use ophthalmic antibiotics following an intraocular injection [214]. Although these events are relatively rare, the high cost of treatment and severity of these complications cannot be disregarded [54]. Moreover, discomfort and inconvenience associated with repeated and frequent intravitreal injections lead to poor patient acceptance. The recommended volume of injection is merely 100 µl, which stresses the importance of the drug potency required to treat ocular diseases intravitreally [205]. Repeated topical administration of macromolecules would be advantageous as being non-invasive, but these types of formulations are plagued with common issues of low availability especially when peptides and proteins are involved [9,190,205,243]. An aqueous formulation of ranibizumab for the treatment of wet-AMD is unlikely to be an effective therapeutic means as a very high frequency of topical administration is required to reach sufficiently high levels of ranibizumab in the posterior segment of the eye, although some researchers have suggested this possibility [171]. Therefore, current eye research is focussing more towards transscleral pathways for topical delivery of macromolecules to provide a viable alternative to invasive intraocular injections [54,55,77,172,216]. A slow-release formulation might provide a good solution for delivery of macromolecules through the transscleral route.

For the anterior segment of the eye as in the case of corneal neovascularisation, it is anatomically easier to reach the affected tissue through repeated topical delivery, resulting in improved patient comfort, reduced cost and lower complication rates [54,244]. The cornea is an effective barrier for macromolecules under normal physiological circumstances, but a medical condition such as corneal neovascularisation appears to change the structure of the cornea, making it susceptible for topical treatment of proteins such as bevacizumab giving researchers the opportunity to reach tissues which are otherwise impermeable [230].

Alternative vehicles can increase drug permeability to the ocular tissues. Sustained release of peptides and proteins can theoretically be achieved after loading them into a carrier system such as liposomes or biodegradable nanoparticles but a commercial entrance on the market fails to

appear to date [57,84,172,213,245–248]. Another formulation for drug delivery to the posterior segment of the eye are intravitreal implants. After insertion in the vitreous, implants can release a drug substance over a period varying from days to even years [26,249,250]. These implants can deliver molecules when loaded into a reservoir system or when loaded into a matrix system. As mentioned earlier, reservoir systems deliver molecules through zero order kinetics but do not allow biodegradable polymers to be used. This implicates the necessity to remove the implant after drug delivery, making matrix systems the more desirable option, despite non-zero order kinetics [9,205]. Marketed non-biodegradable implants are successfully and routinely being used for molecules such as ganciclovir (Vitrasert®) or fluocinolone acetonide (Retisert® and Iluvien®) with the former being indicated for retinitis and the latter for non-infectious posterior uveitis. Retisert® is said to remain active up to two and a half years after injection while Vitrasert® remains active for over a year [205,243,251–255]. Ozurdex® (dexamethasone) is a commercially available biodegradable implant that is directly injected into the vitreous. It is used to treat macular oedema secondary to retinal vein occlusion and non-infectious posterior and intermediate uveitis. The implant is built up of poly-lactic-co-glycolic acid (PLGA), a biodegradable polymer that is more commonly known for application in nanoparticle technology. The Ozurdex® implant can release the drug up to four months [243,250,254,256,257].

Currently, commercially successful intravitreal implants loaded with peptides or proteins have not been launched due to the nature of these molecules. Their susceptibility to denaturation and degradation as well as their inherently short half-life challenges the formulation process significantly [153,258–260]. But the excipients used for slow-release formulations can be advantageous for protein formulation; excipients such as cellulose-ethers, PLGA, osmolytes and others can stabilise peptides and proteins through surface activity, preferential exclusion, steric hindrance of protein-protein interactions or by increasing viscosity and limiting protein structural movement [258,261–271].

5 STERILISATION METHODS

A very important step in the development of a drug delivery system for ocular use is sterility of the dosage form. Sterility is obviously required in order to prevent the spread of infection. Nevertheless, absolute sterility cannot be verified. For this reason, a statistical definition of sterility is given by the security assurance level (SAL) which is defined as the probability of a single viable microorganism occurring in or on a product after sterilisation. Currently, sterility is regarded as being achieved if the chance of finding a viable organism in or on a medical device is at most 1 in 1 000 000 or a SAL of at most 10^{-6} [272]. Ideally, a sterilisation technique should be fast and safe, efficient, highly reliable and penetrant with a homogeneous distribution within the load. No modifications should occur on both drug molecule or the drug delivery device after sterilisation. Although many sterilisation techniques are currently available, each has its own advantages and disadvantages. If none of the sterilisation methods can be employed, an aseptic preparation method remains a possibility. An overview of the most common sterilisation techniques that will be discussed in this section is given in figure 16.

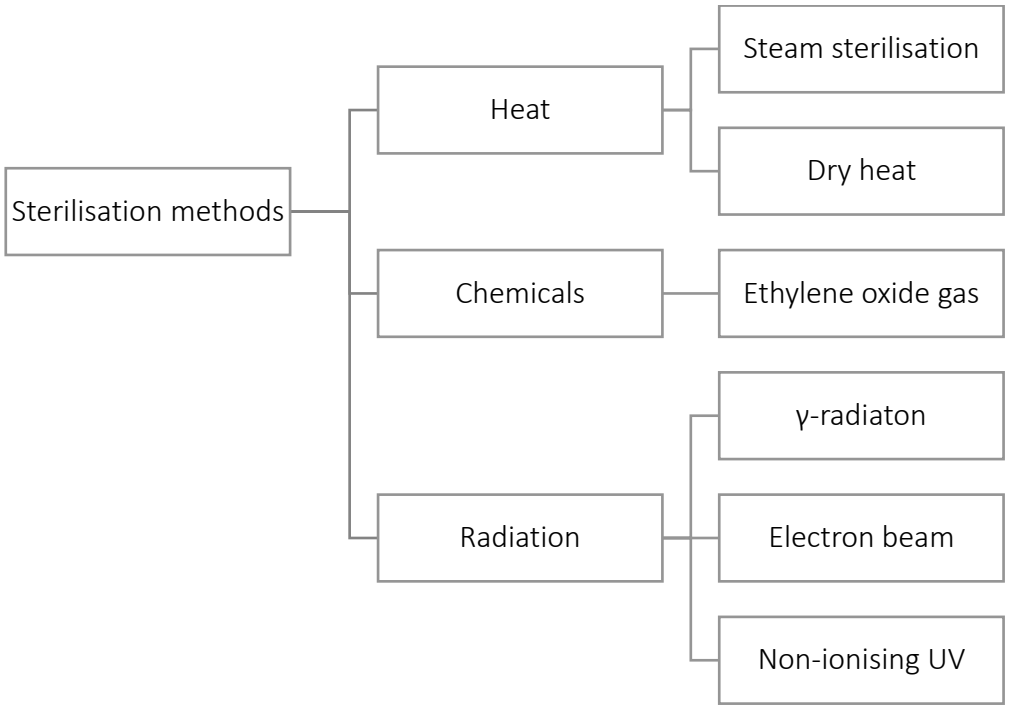

Fig. 16. Overview of common sterilisation techniques [273].

5.1 Heat

5.1.1 Steam sterilisation

Steam or moist heat sterilisation (autoclaving) is one of the most effective and most frequently used sterilisation techniques of medical products. Sterility is obtained by exposing the product directly to saturated steam at a temperature of typically 121 °C and a pressure of 1 bar or 132/134 °C and 2 bar in a pressurised sterilisation chamber during 15 to 30 minutes after all surfaces of the product reach the indicated temperature. Lower temperatures (105-120 °C) can be used to prevent degradation to materials, nutrients, polymers and other substances. Higher temperatures are used for faster, flash sterilisation if the product can withstand these conditions. Sterilisation is based on the thermal damage of metabolic and structural components (denaturation of proteins and nucleic acids) that are essential for the replication of the microorganism [273–278].

Steam sterilisation is easy, safe and efficient with good penetrability. It is also relatively cheap and rapid with no toxic residues. However, this technique has some important limitations: due to its high temperature and moisture, it is incompatible with many products such as most peptides and proteins.

5.1.2 Dry heat

Steam sterilisation is the preferred choice of sterilisation in case of heat-stabile products, but in some cases where moisture is undesirable, such as powders and oils, dry heat can be useful. The latent heat of vaporisation, used in steam sterilisation, transfers at least seven times more heat compared to dry heat at the same temperature. This implicates that sterilisation through dry heat requires much higher temperatures and longer sterilisation times for equivalent sterility levels. Dry heat sterilisation is typically performed at temperatures above 160 °C for several hours (e.g. 160 °C during two hours). Oxidation of cellular components is regarded as being the cause for microbial inactivation [273–276,278].

The high temperatures involved with dry heat sterilisation make this method inapplicable for sterilisation of drug delivery devices loaded with peptides and proteins.

5.2 Chemicals

5.2.1 Ethylene oxide

The class of chemical sterilisation is very broad, but ethylene oxide gas is probably the most popular choice of sterilisation through chemicals. Ethylene oxide sterilisation generally occurs at a temperature of 55 °C, but temperatures between 25-65 °C are possible as well. The gas

concentration levels are set between 400-1500 mg/l during two to five hours. This sterilisation technique has the advantage of having a very broad compatibility with most materials that are non-liquid, contained in gas-permeable packaging and not compatible with heat sterilisation. It is therefore a suitable choice of sterilisation of cellulosic materials such as HPMC. Sterilisation with this gas has serious drawbacks, because it is highly toxic and mutagenic posing safety risks for sterilisation personnel. Aeration is required as toxic ethylene oxide residues and reaction products can occur [273–278].

5.3 Radiation

5.3.1 Gamma radiation

Gamma radiation (γ-radiation) is the primary choice of sterilisation through radiation. The radioisotope cobalt 60 (^{60}Co) is used as the energy source to produce γ-rays. It decays into ^{60}Ni and an electron, emitting γ-rays in the process. These rays ionise cellular components such as nucleic acids, which in turn leads to death of microorganisms. In addition, the formation of hydroxyl radicals, causing DNA damage is responsible for its sterilising action. Gamma radiation has excellent penetrating capabilities, making it a great choice for end-package sterilisation. The amount of dose absorbed is expressed in kilogray (kGy). The radiation dose is approximately between 5-30 kGy with 25 kGy being the most commonly validated dose used for sterilisation of medical products. It also has significant advantages opposed to the other sterilisation methods: it gives better sterility assurance compared to filtration and aseptic processing techniques, it leaves no residues unlike ethylene oxide and it is a low temperature process. However, there are some significant drawbacks of using γ-radiation. Firstly, it is known to alter the structure of some polymers such as HPMC, especially with increasing dose. Secondly, the formation of short-lived but highly reactive hydroxyl radicals as a result of γ-rays interacting with water molecules makes it unsuited for sterilisation of aqueous products, such as hydrogels. Finally, sterilisation through γ-radiation takes several hours to complete [273,274,276–279].

5.3.2 Electron beam

The electron beam (E-beam) technique uses an ionising energy that differs from γ-radiation by its low penetration and high dosage rates. The beam, made up from concentrated, highly energetic electrons, is generated by the acceleration and conversion of electricity. As the product passes the electron beam, energy from the electrons is absorbed. The high dosage rates allow the sterilisation process to complete in seconds to minutes instead of hours as in case of γ-radiation. But the lower penetrability limits the use of E-beams in favour of γ-radiation techniques [273,274,278].

5.3.3 Non-ionising UV radiation

Sterilisation through ultraviolet (UV) radiation is not ionising, which is a major difference compared to the radiation methods mentioned above. The mechanism of sterilisation is based on the formation of dimers (crosslinking) between cytosine and thymine residues, leading to irreversible, stable bonds preventing replication and transcription processes, essential for the survival of microorganisms. The use of UV radiation is limited by its lower energy potential and lower penetrating power than gamma radiation and even electron beams, making it a good choice for small surface sterilisation, but not suitable for dense materials [273,274,278].

It is clear that sterilisation of ocular inserts containing water and thermolabile drugs is not an easy task to perform with the aforementioned sterilisation techniques. The development of novel sterilisation techniques or the use of aseptic preparation methods need to be considered.

References

1. Kuno N, Fujii S. Recent advances in ocular drug delivery systems. Polymers (Basel). 2011;3: 193–221.
2. Achouri D, Alhanout K, Piccerelle P, Andrieu V. Recent advances in ocular drug delivery. Drug Dev Ind Pharm. 2013;39: 1599–1617.
3. The Eye and Vision [Internet]. [cited 3 Feb 2017]. doi:http://www.myvmc.com/anatomy/the-eye-and-vision/
4. Järvinen K, Järvinen T, Urtti A. Ocular absorption following topical delivery. Adv Drug Deliv Rev. 1995;16: 3–19.
5. Sasaki H, Yamamura K, Nishida K, Nakamura J, Ichikawa M. Delivery of drugs to the eye by topical application. Prog Retin Eye Res. 1996;15: 583–620.
6. Sizmaz S, Kucukerdonmez C, Kal A, Pinarci EY, Canan H, Yilmaz G. Retinal and choroidal thickness changes after single anti-vegf injection in neovascular age-related macular degeneration: Ranibizumab vs bevacizumab. Eur J Ophthalmol. 2014;24: 904–910.
7. Chhablani J, Wong IY, Kozak I. Choroidal imaging: A review. Saudi J Ophthalmol. Saudi Ophthalmological Society, King Saud University; 2014;28: 123–128.
8. Yuan X, Gu X, Crabb JS, Yue X, Shadrach K, Hollyfield JG, et al. Quantitative proteomics: comparison of the macular Bruch membrane/choroid complex from age-related macular degeneration and normal eyes. Mol Cell Proteomics. 2010;9: 1031–1046.
9. Thakur SS, Barnett NL, Donaldson MJ, Parekh HS. Intravitreal drug delivery in retinal disease: are we out of our depth? Expert Opin Drug Deliv. 2014;11: 1575–1590.
10. Provis JM, Penfold PL, Cornish EE, Sandercoe TM, Madigan MC. Anatomy and development of the macula: Specialisation and the vulnerability to macular degeneration. Clin Exp Optom. 2005;88: 269–281.
11. Lee SS, Robinson MR. Novel drug delivery systems for retinal diseases: A review. Ophthalmic Res. 2009;41: 124–135.
12. D'amico DJ. Diseases of the Retina. N Engl J Med. 1994;331: 95–106.
13. Kimbrel E a., Lanza R. Current status of pluripotent stem cells: moving the first therapies to the clinic. Nat Rev Drug Discov. Nature Publishing Group; 2015;14: 681–692.
14. Yuzawa M, Fujita K, Wittrup-Jensen KU, Norenberg C, Zeitz O, Adachi K, et al. Improvement in vision-related function with intravitreal aflibercept: Data from phase 3 studies in wet age-related macular degeneration. Ophthalmology. 2015;122: 571–578.
15. Zhu M, Chew JK, Broadhead GK, Luo K, Joachim N, Hong T, et al. Intravitreal Ranibizumab for neovascular Age-related macular degeneration in clinical practice: five-year treatment outcomes. Graefe's Arch Clin Exp Ophthalmol. 2015;253: 1217–1225.
16. Barney NP, Cook EB, Stahl JL. Allergic and Immunologic Diseases of the Eye. Eighth Edi. Middleton's Allergy: Principles and Practice: Eighth Edition. 2013.
17. Capita L, Chalita MR, dos Santos-Neto LL. Prospective evaluation of hypromellose 2% for punctal occlusion in patients with dry eye. Cornea. 2015;34: 188–192.
18. Rabensteiner DF, Boldin I, Klein A, Horwath-Winter J. Collared silicone punctal plugs compared to intracanalicular plugs for the treatment of dry eye. Curr Eye Res. 2013;38: 521–525.
19. Cummings B. Accessory Structures of the Eye Figure 8.2b. Pearson Education; 2006.
20. Aicher SA, Hermes SM, Hegarty DM. Denervation of the lacrimal gland leads to corneal hypoalgesia in a novel

rat model of aqueous dry eye disease. Investig Ophthalmol Vis Sci. 2015;56: 6981–6989.

21. Rolando M, Zierhut M. The ocular surface and tear film and their dysfunction in dry eye disease. Surv Ophthalmol. 2001;45 Suppl 2: S203–S210.
22. Zoukhri D. Effect of inflammation on lacrimal gland function. Exp Eye Res. 2006;82: 885–898.
23. McDermott AM. Antimicrobial compounds in tears. Exp Eye Res. 2013;117: 53–61.
24. Sen DK, Sarin GS. Biological variations of lysozyme concentration in the tear fluids of healthy persons. Br J Ophthalmol. 1986;70: 246–248.
25. Narayanan S, Redfern RL, Miller WL, Nichols KK, Mcdermott AM. Dry eye disease and microbial keratitis: Is there a connection? Ocul Surf. 2013;11: 75–92.
26. Patel A, Cholkar K, Agrahari V, Mitra AK. Ocular drug delivery systems: An overview. World J Pharmacol. 2015;2: 47–64.
27. Himmelstein K. Mathematical models of ocular drug transport and disposition. Mitra AK, editor. New York (USA): Marcel Dekker; 1993.
28. Lee VHL, Robinson JR. Review : Topical Ocular Drug Delivery : Recent Developments and Future Challenges. Ocul Pharmacol. 1986;2: 67–108.
29. Edsman K, Hägerström H. Pharmaceutical applications of mucoadhesion for the non-oral routes. J Pharm Pharmacol. 2005;57: 3–22.
30. Shell J. Ophthalmic Drug Delivery Systems. Surv Ophthalmol. 1984;29: 117–128.
31. Mishima S, Gasset A, Klyce SD. Determination of Tear Volume and Tear Flow. Invest Ophthalmol. 1966;5: 264–276.
32. Cholkar K, Patel SP, Vadlapudi AD, Mitra AK. Novel Strategies for Anterior Segment Ocular Drug Delivery. J Ocul Pharmacol Ther. 2013;29: 106–123.
33. Ludwig A. Study on the administration and physical properties of ophthalmic solutions and the precorneal retention of a tracer. University of Antwerp; 1990.
34. Lachrymal glands [Internet]. [cited 6 Feb 2017]. doi:www.studyblue.com/notes/note/n/des-mgd-blepharitis/
35. Hughes PM, Mitra AK. Overview of ocular drug delivery and iatrogenic ocular cytopathologies. Mitra AK, editor. New York (USA): Marcel Dekker; 1993.
36. Van Ooteghem MM. Factors influencing the retention of ophthalmic solutions on the eye surface. Saettone, M.F., Bucci, M., Speiser P, editor. Padova (Italy): Livinia Press; 1987.
37. Structure of Tear Film [Internet]. [cited 3 Apr 2011]. doi:http://www.nfburnetthodd.com/dryeye.html
38. Ruponen M, Urtti A. Undefined role of mucus as a barrier in ocular drug delivery. Eur J Pharm Biopharm. 2015;96: 442–446.
39. Yoshida Y, Ban Y, Kinoshita S. Tight junction transmembrane protein claudin subtype expression and distribution in human corneal and conjunctival epithelium. Investig Ophthalmol Vis Sci. 2009;50: 2103–2108.
40. Zhang Z, Yang WZ, Zhu ZZ, Hu QQ, Chen YF, He H, et al. Therapeutic effects of topical doxycycline in a benzalkonium chloride-induced mouse dry eye model. Investig Ophthalmol Vis Sci. 2014;55: 2963–2974.
41. Hayasaka S. Lysosomal enzymes in ocular tissues and diseases. Surv Ophthalmol. 1983;27: 245–258.
42. Dartt DA, Willcox MDP. Complexity of the tear film: Importance in homeostasis and dysfunction during disease. Exp Eye Res. 2013;117: 1–3.

43. Nicolaides N, Kaitaranta JK, Rawdah TN, Macy JI, Boswell FM, Smith RE. Meibomian gland studies: comparison of steer and human lipids. Investig Ophthalmol Vis Sci. 1981;20: 522–536.
44. Shine WE, McCulley JP, Pandya AG. Minocycline effect on meibomian gland lipids in meibomianitis patients. Exp Eye Res. 2003;76: 417–420.
45. Butovich IA. The Meibomian Puzzle: Combining pieces together. Prog Retin Eye Res. 2009;28: 483–498.
46. Johnson ME, Murphy PJ. Changes in the tear film and ocular surface from dry eye syndrome. Prog Retin Eye Res. 2004;23: 449–474.
47. Tsai PS, Evans JE, Green KM, Sullivan RM, Schaumberg DA, Richards SM, et al. Proteomic analysis of human meibomian gland secretions. Br J Ophthalmol. 2006;90: 372–377.
48. Evans DJ, Fleiszig SMJ. Why does the healthy cornea resist pseudomonas aeruginosa infection? Am J Ophthalmol. 2013;155: 961–970.
49. Shaheen BS, Bakir M, Jain S. Corneal nerves in health and disease. Surv Ophthalmol. 2014;59: 263–285.
50. Müller LJ, Marfurt CF, Kruse F, Tervo TMT. Corneal nerves: Structure, contents and function. Exp Eye Res. 2003;76: 521–542.
51. Lang JC. Ocular drug delivery conventional ocular formulations. Adv Drug Deliv Rev. 1995;16: 39–43.
52. Greaves JL, Wilson CG. Treatment of diseases of the eye with mucoadhesive delivery systems. Adv Drug Deliv Rev. 1993;11: 349–383.
53. Mann A, Tighe B. Contact lens interactions with the tear film. Exp Eye Res. 2013;117: 88–98.
54. Srikantha N, Mourad F, Suhling K, Elsaid N, Levitt J, Chung PH, et al. Influence of molecular shape, conformability, net surface charge, and tissue interaction on transscleral macromolecular diffusion. Exp Eye Res. 2012;102: 85–92.
55. Miao H, Wu BD, Tao Y, Li XX. Diffusion of macromolecules through sclera. Acta Ophthalmol. 2013;91: 1–6.
56. Tratta E, Pescina S, Padula C, Santi P, Nicoli S. In vitro permeability of a model protein across ocular tissues and effect of iontophoresis on the transscleral delivery. Eur J Pharm Biopharm. 2014;88: 116–122.
57. Souza JG, Dias K, Pereira TA, Bernardi DS, Lopez RF V. Topical delivery of ocular therapeutics: Carrier systems and physical methods. J Pharm Pharmacol. 2014;66: 507–530.
58. Edwards A, Prausnitz MR. Predicted permeability of the cornea to topical drugs. Pharm Res. 2001;18: 1497–1508.
59. Corneal Disease [Internet]. [cited 3 Feb 2017]. doi:https://nei.nih.gov/health/cornealdisease
60. Grass GM, Robinson JR. Mechanisms of corneal drug penetration II: Ultrastructural analysis of potential pathways for drug movement. J Pharm Sci. 1988;77: 15–23.
61. Dua HS, Gomes JA, Singh A. Corneal epithelial wound healing. Br J Ophthalmol. 1994;78: 401–408.
62. Malhotra M, Majumdar DK. Permeation Through Cornea. Indian J Exp Biol. 2001;39: 11–24.
63. Fini ME, Girard MT. Expression of collagenolytic/gelatinolytic metalloproteinases by normal cornea. Investig Ophthalmol Vis Sci. 1990;31: 1779–1788.
64. Huang AJW, Tseng SCG, Kenyon KR. Paracellular permeability of corneal and conjunctival epithelia. Investig Ophthalmol Vis Sci. 1989;30: 684–689.
65. van der Bijl P, van Eyk A, Meyer D. Effects of three penetration enhancers on transcorneal permeation of cyclosporine. Cornea. 2001;20: 505–508.

66. Kaur IP, Kanwar M. Ocular preparations: the formulation approach. Drug Dev Ind Pharm. 2002;28: 473–493.
67. Pahuja P, Arora S, Pawar P. Ocular drug delivery system: a reference to natural polymers. Expert Opin Drug Deliv. 2012;9: 837–861.
68. Hämäläinen KM, Kananen K, Auriola S, Kontturi K, Urtti A. Characterization of Paracellular and Aqueous Penetration Routes in Cornea , Conjunctiva , and Sclera. Invest Ophthalmol Vis Sci. 1997;38: 627–634.
69. Venturoli D. Ficoll and dextran vs. globular proteins as probes for testing glomerular permselectivity: effects of molecular size, shape, charge, and deformability. AJP Ren Physiol. 2004;288: 605–613.
70. Watsky MA, Jablonski MM, Edelhauser HF. Comparison of conjunctival and corneal surface areas in rabbit and human. Curr Eye Res. 1988;7: 483–486.
71. Kaur IP, Garg A, Singla AK, Aggarwal D. Vesicular systems in ocular drug delivery: An overview. Int J Pharm. 2004;269: 1–14.
72. Pescina S, Govoni P, Antopolsky M, Murtomäki L, Padula C, Santi P, et al. Permeation of Proteins, Oligonucleotide and Dextrans Across Ocular Tissues: Experimental Studies and a Literature Update. J Pharm Sci. 2015;104: 2190–2202.
73. Monti D, Chetoni P, Burgalassi S, Najarro M, Saettone MF. Increased corneal hydration induced by potential ocular penetration enhancers: Assessment by differential scanning calorimetry (DSC) and by desiccation. Int J Pharm. 2002;232: 139–147.
74. Kaur IP, Smitha R. Penetration enhancers and ocular bioadhesives: two new avenues for ophthalmic drug delivery. Drug Dev Ind Pharm. 2002;28: 353–369.
75. Eljarrat-Binstock E, Raiskup F, Stepensky D, Domb AJ, Frucht-Pery J. Delivery of gentamicin to the rabbit eye by drug-loaded hydrogel iontophoresis. Investig Ophthalmol Vis Sci. 2004;45: 2543–2548.
76. Colligris B, Crooke A, Huete-Toral F, Pintor J. An update on dry eye disease molecular treatment: advances in drug pipelines. Expert Opin Pharmacother. 2014;15: 1371–1390.
77. Pescina S, Ferrari G, Govoni P, MacAluso C, Padula C, Santi P, et al. In-vitro permeation of bevacizumab through human sclera: Effect of iontophoresis application. J Pharm Pharmacol. 2010;62: 1189–1194.
78. Suhonen P, Järvinen T, Lehmussaari K, Reunamäki T, Urtti A. Ocular Absorption and Irritation of Pilocarpine Prodrug Is Modified with Buffer, Polymer, and Cyclodextrin in the Eyedrop. Pharm Res. 1995;12: 529–533.
79. Tirucherai GS, Dias C, Mitra AK. Corneal permeation of ganciclovir: mechanism of ganciclovir permeation enhancement by acyl ester prodrug design. J Ocul Pharmacol Ther. 2002;18: 535–548.
80. Gaudana R, Jwala J, Boddu SHS, Mitra AK. Recent perspectives in ocular drug delivery. Pharm Res. 2009;26: 1197–1216.
81. Loftssona T, Järvinen T. Cyclodextrins in ophthalmic drug delivery. Adv Drug Deliv Rev. 1999;36: 59–79.
82. Brewster ME, Loftsson T. Cyclodextrins as pharmaceutical solubilizers. Adv Drug Deliv Rev. 2007;59: 645–666.
83. Loftsson T, Stefánsson E. Cyclodextrins in eye drop formulations: enhanced topical delivery of corticosteroids to the eye. Acta Ophthalmol Scand. 2002;80: 144–150.
84. Bourlais CL, Acar L, Zia H, Sado P, Needham T, Leverge R. Ophthalmic drug delivery systems--recent advances. Prog Retin Eye Res. 1998;17: 33–58.
85. Ludwig A, Van Ooteghem M. Influence of viscolysers on the residence of ophthalmic solutions evaluated by slit lamp fluorophotometry. STP pharma Sci. 1992;2: 81–87.

86. Kaur IP, Rana C, Singh H. Development of effective ocular preparations of antifungal agents. J Ocul Pharmacol Ther. 2008;24: 481–493.
87. Sintzel MB, Bernatchez SF, Tabatabay C, Gurny R. Biomaterials in ophthalmic drug delivery. Eur J Pharm Biopharm. 1996;42: 358–374.
88. Van Bijsterveld OP, Andriesse H, Nielsen BH. Fusidic acid in tear fluid: Pharmacokinetic study with fusidic acid viscous eye drops. Eur J Drug Metab Pharmacokinet. 1987;12: 215–218.
89. Thakur RR, Kashiv M. Modern delivery systems for ocular drug formulations: a comparative overview W.R.T conventional dosage form. Int J Res Pharm Biomed Sci. 2011;2: 8–18.
90. Jung HJ, Chauhan A. Extended release of timolol from nanoparticle-loaded fornix insert for glaucoma therapy. J Ocul Pharmacol Ther. 2013;29: 229–235.
91. Nguyen T, Latkany R. Review of hydroxypropyl cellulose ophthalmic inserts for treatment of dry eye. Clin Ophthalmol. 2011;5: 587–591.
92. Deshmukh PK, Gattani SG. In vitro and in vivo consideration of novel environmentally responsive ophthalmic drug delivery system. Pharm Dev Technol. 2013;18: 950–956.
93. Kaur IP, Kakkar S. Newer therapeutic vistas for antiglaucoma medicines. Crit Rev Ther Drug Carrier Syst. 2011;28: 165–202.
94. Zhang M, Djabourov M, Bourgaux C, Bouchemal K. Nanostructured fluids from pluronic® mixtures. Int J Pharm. 2013;454: 599–610.
95. Lin Y-K, Chen K-H, Kuan C-Y. The synthesis and characterization of a thermally responsive hyaluronic acid/ Pluronic copolymer and an evaluation of its potential as an artificial vitreous substitute. J Bioact Compat Polym. 2013;4: 355-367.
96. Gratieri T, Gelfuso GM, De Freitas O, Rocha EM, Lopez RF V. Enhancing and sustaining the topical ocular delivery of fluconazole using chitosan solution and poloxamer/chitosan in situ forming gel. Eur J Pharm Biopharm. 2011;79: 320–327.
97. Desai SD, Blanchard J. In vitro evaluation of pluronic F127-based controlled-release ocular delivery systems for pilocarpine. J Pharm Sci. 1998;87: 226–230.
98. Rozier A, Mazuel C, Grove J, Plazonnet B. Gelrite: A novel, ion-activated, in-situ gelling polymer for ophthalmic vehicles. Effect on bioavailability of timolol. Int J Pharm. 1989;57: 163–168.
99. Sanzgiri YD, Maschi S, Crescenzi V, Callegaro L, Topp EM, Stella VJ. Gellan-based systems for ophthalmic sustained delivery of methylprednisolone. J Control Release. 1993;26: 195–201.
100. Maurice D. The effect of the low blink rate in rabbits on topical drug penetration. J Ocul Pharmacol Ther. 1995;11: 297–304.
101. Smart JD. The basics and underlying mechanisms of mucoadhesion. Adv Drug Deliv Rev. 2005;57: 1556–1568.
102. Grabovac V, Guggi D, Bernkop-Schnürch A. Comparison of the mucoadhesive properties of various polymers. Adv Drug Deliv Rev. 2005;57: 1713–1723.
103. Mikos AG, Peppas NA. Systems for controlled delivery of drugs. V. Bioadhesive Systems. STP pharma Sci. 1986; 705–716.
104. Yellepeddi VK, Palakurthi S. Recent Advances in Topical Ocular Drug Delivery. J Ocul Pharmacol Ther. 2016;32: 67–82.

105. Dumortier G, Zuber M, Chast F, Chaumeil JC. Comparison between a thermoreversible gel and an insert in order to prolong the systemic absorption of morphine after ocular administration. STP pharma Sci. 1992; 111–117.
106. Saettone MF, Salminen L. Ocular inserts for topical delivery. Adv Drug Deliv Rev. 1995;16: 95–106.
107. Sahane NK, Banarjee SK, Gaikwad DD, Jadhav SL, Thorat RM. Ocular Inserts : A Review. Drug Invent Today. 2010;2: 57–64.
108. Molokhia SA, Thomas SC, Garff KJ, Mandell KJ, Wirostko BM. Anterior Eye Segment Drug Delivery Systems: Current Treatments and Future Challenges. J Ocul Pharmacol Ther. 2013;29: 92–105.
109. Sendelbeck L, Moore D, Urquhart J. Comparative distribution of pilocarpine in ocular tissues of the rabbit during administration by eyedrop or by membrane-controlled delivery systems. Am J Ophthalmol. 1975;80: 274–283.
110. Gurtler F, Gurny R. Patent Literature Review of Ophthalmic Inserts. Drug Dev Ind Pharm. 1995;21: 1–18.
111. Xinming L, Yingde C, Lloyd AW, Mikhalovsky S V., Sandeman SR, Howel CA, et al. Polymeric hydrogels for novel contact lens-based ophthalmic drug delivery systems: A review. Contact Lens Anterior Eye. 2008;31: 57–64.
112. Malakooti N, Alexander C, Alvarez-Lorenzo C. Imprinted Contact Lenses for Sustained Release of Polymyxin B and Related Antimicrobial Peptides. J Pharm Sci. 2015;104: 3386–3394.
113. Tieppo A, Boggs AC, Pourjavad P, Byrne ME. Analysis of release kinetics of ocular therapeutics from drug releasing contact lenses: Best methods and practices to advance the field. Contact Lens Anterior Eye. British Contact Lens Association; 2014;37: 305–313.
114. Tieppo A, Pate KM, Byrne ME. In vitro controlled release of an anti-inflammatory from daily disposable therapeutic contact lenses under physiological ocular tear flow. Eur J Pharm Biopharm. 2012;81: 170–177.
115. Tashakori-Sabzevar F, Mohajeri SA. Development of ocular drug delivery systems using molecularly imprinted soft contact lenses. Drug Dev Ind Pharm. 2014;0: 1–11.
116. Bengani LC, Hsu K-H, Gause S, Chauhan A. Contact lenses as a platform for ocular drug delivery. Expert Opin Drug Deliv. 2013;10: 1483–1496.
117. Carreira AS, Ferreira P, Ribeiro MP, Correia TR, Coutinho P, Correia IJ, et al. New drug-eluting lenses to be applied as bandages after keratoprosthesis implantation. Int J Pharm. 2014;477: 218–226.
118. Jain MR. Drug delivery through soft contact lenses. Br J Ophthalmol. 1988;72: 150–154.
119. Gulsen D, Chauhan A. Ophthalmic Drug Delivery through Contact Lenses. Invest Ophthalmol Vis Sci. 2004;45: 2342–2347.
120. Karlgard CCS, Wong NS, Jones LW, Moresoli C. In vitro uptake and release studies of ocular pharmaceutical agents by silicon-containing and p-HEMA hydrogel contact lens materials. Int J Pharm. 2003;257: 141–151.
121. Hehl EM, Beck R, Luthard K, Guthoff R, Drewelow B. Improved penetration of aminoglycosides and fluoroquinolones into the aqueous humour of patients by means of Acuvue contact lenses. Eur J Clin Pharmacol. 1999;55: 317–323.
122. White CJ, McBride MK, Pate KM, Tieppo A, Byrne ME. Extended release of high molecular weight hydroxypropyl methylcellulose from molecularly imprinted, extended wear silicone hydrogel contact lenses. Biomaterials. 2011;32: 5698–5705.
123. Mundada AS, Shrikhande BK. Design and Evaluation of Soluble Ocular Drug Insert for Controlled Release of Ciprofloxacin Hydrochloride Controlled Release of Ciprofloxacin Hydrochloride. Drug Dev Ind Pharm. 2006;32: 443–448.

124. Buwalda SJ, Boere KWM, Dijkstra PJ, Feijen J, Vermonden T, Hennink WE. Hydrogels in a historical perspective: From simple networks to smart materials. J Control Release. 2014;190: 254–273.
125. Kirchhof S, Goepferich AM, Brandl FP. Hydrogels in ophthalmic applications. Eur J Pharm Biopharm. 2015;95: 227–238.
126. Lamberts DW, Langston DP, Chu W. A clinical study of slow-releasing artificial tears. Ophthalmology. American Academy of Ophthalmology, Inc; 1978;85: 794–800.
127. Jain D, Carvalho E, Banthia AK, Banerjee R. Development of polyvinyl alcohol-gelatin membranes for antibiotic delivery in the eye. Drug Dev Ind Pharm. 2011;37: 167–177.
128. Lee YC, Yalkowsky SH. Systemic absorption of insulin from a Gelfoam ocular device. Int J Pharm. 1999;190: 35–40.
129. Bloomfield SE, Dunn MW, Miyata T. Soluble artificial tear inserts. Arch Ophthalmol. 1977;95: 247–250.
130. Bloomfield SE, Miyata T, Dunn MW, Bueser N, Stenzel KH, Rubin AL. Soluble Gentamicin Ophthalmic Inserts as a Drug Delivery System. Arch Ophthalmol. 1978;96: 885–887.
131. Schoenwald RD, Boltralik JJ. A bioavailability comparison in rabbits of two steroids formulated as high-viscosity gels and reference aqueous preparations. Investig Ophthalmol Vis Sci. 1979;18: 61–66.
132. Schwartz SD, Harrison SA, Engstrom Jr. RE, Bawdon RE, Lee DA, Mondino BJ. Collagen shield delivery of amphotericin B. Am J Ophthalmol. 1990;109: 701–704.
133. Taravella MJ, Balentine J, Young D a, Stepp P. Collagen shield delivery of ofloxacin to the human eye. J Cataract Refract Surg. 1999;25: 562–565.
134. Gussler JR, Ashton P, Van Meter WS, Smith TJ. Collagen shield delivery of trifluorothymidine. J Cataract Refract Surg. American Society of Cataract and Refractive Surgery; 1990;16: 719–722.
135. Bisht R, Durgapal S. Potential advantages of novel intracorneal drug delivery system in managemant of fungal keratitis an overview. Int J Pharm Pharm Sci. 2011;3: 12–17.
136. Baeyens V, Kaltsatos V, Boisramé B, Varesio E, Veuthey JL, Fathi M, et al. Optimized release of dexamethasone and gentamicin from a soluble ocular insert for the treatment of external ophthalmic infections. J Control Release. 1998;52: 215–220.
137. Gurtler F, Kaltsatos V, Boisramé B, Gurny R. Long-acting soluble bioadhesive ophthalmic drug insert (BODI) containing gentamicin for veterinary use: optimization and clinical investigation. J Control Release. 1995;33: 231–236.
138. Saettone MF, Torracca MT, Pagano A, Giannaccini B, Rodriguez L, Cini M. Controlled release of pilocarpine from coated polymeric ophthalmic inserts prepared by extrusion. Int J Pharm. 1992;86: 159–166.
139. Urtti A, Salminen L, Miinalainen O. Systemic absorption of ocular pilocarpine is modified by polymer matrices. Int J Pharm. 1985;23: 147–161.
140. Harwood R, Schwartz J. Drug Release from Compression Molded Films: Preliminary Studies with Pilocarpine. Drug Dev Ind Pharm. 1982;8: 663–682.
141. Saettone MF, Chetoni P, Bianchi LM, Giannaccini B, Conte U, Sangalli ME. Controlled release of timolol maleate from coated ophthalmic mini-tablets prepared by compression. Int J Pharm. 1995;126: 79–82.
142. Aburahma MH, Mahmoud AA. Biodegradable ocular inserts for sustained delivery of brimonidine tartarate: preparation and in vitro/in vivo evaluation. AAPS PharmSciTech. 2011;12: 1335–1347.

143. Lee VHL, Li SY, Sasaki H, Saettone MF, Chetoni P. Influence of Drug-Release Rate on Systemic Timolol Absorption From Polymeric Ocular Inserts in the Pigmented Rabbit. J Ocul Pharmacol. 1994;10: 421–429.
144. Tamburic S, Craig DQM. A comparison of different in vitro methods for measuring mucoadhesive performance. Eur J Pharm Biopharm. 1997;44: 159–167.
145. Sundararaj SC, Thomas M V., Dziubla TD, Puleo DA. Bioerodible system for sequential release of multiple drugs. Acta Biomater. 2014;10: 115–125.
146. Deshpande PB, Dandagi P, Udupa N, Gopal S V, Jain SS, Vasanth SG. Controlled release polymeric ocular delivery of acyclovir. Pharm Dev Technol. 2010;15: 369–378.
147. Pavan-Langston D, Langston R, Geary P. Idoxuridine Ocular Insert Therapy. Arch Ophthalmol. 1975;93: 1349–1351.
148. Punch PI, Slatter DH, Costa ND, Edwards ME. Investigation of gelatin as a possible biodegradable matrix for Sustained delivery of gentamicin to the bovine eye. J Vet Pharmacol Ther. 1985; 335–338.
149. Mönkäre J, Pajander J, Hakala RA, Savolainen P, Järveläinen M, Korhonen H, et al. Characterization of internal structure, polymer erosion and drug release mechanisms of biodegradable poly(ester anhydride)s by X-ray microtomography. Eur J Pharm Sci. 2012;47: 170–178.
150. Ibraheem D, Elaissari A, Fessi H. Administration strategies for proteins and peptides. Int J Pharm. 2014;477: 578–589.
151. Kanwar JR, Shankaranarayanan JS, Gurudevan S, Kanwar RK. Aptamer-based therapeutics of the past, present and future: From the perspective of eye-related diseases. Drug Discov Today. 2014;19: 1309–1321.
152. Steckbeck JD, Deslouches B, Montelaro RC. Antimicrobial peptides: new drugs for bad bugs? Expert Opin Biol Ther. 2014;14: 11–14.
153. Fosgerau K, Hoffmann T. Peptide therapeutics: Current status and future directions. Drug Discov Today. 2015;20: 122–128.
154. Kim YC, Chiang B, Wu X, Prausnitz MR. Ocular delivery of macromolecules. J Control Release. 2014;190: 172–181.
155. Bruno BJ, Miller GD, Lim CS. Basics and recent advances in peptide and protein drug delivery. Ther Deliv. 2013;4: 1443–1467.
156. Craik DJ, Fairlie DP, Liras S, Price D. The Future of Peptide-based Drugs. Chem Biol Drug Des. 2013;81: 136–147.
157. Torosantucci R, Schöneich C, Jiskoot W. Oxidation of therapeutic proteins and peptides: Structural and biological consequences. Pharm Res. 2014;31: 541–553.
158. Yang AS, Honig B. On the pH dependence of protein stability. Journal of molecular biology. 1993; 459–474.
159. Manning MC, Chou DK, Murphy BM, Payne RW, Katayama DS. Stability of protein pharmaceuticals: An update. Pharm Res. 2010;27: 544–575.
160. Wang W. Instability, stabilization, and formulation of liquid protein pharmaceuticals. Int J Pharm. 1999;185: 129–188.
161. Kang F, Jiang G, Hinderliter A, Deluca PP, Singh J. Lysozyme stability in primary emulsion for PLGA microsphere preparation: Effect of recovery methods and stabilizing excipients. Pharm Res. 2002;19: 629–633.
162. Wu L, Zhang J, Watanabe W. Physical and chemical stability of drug nanoparticles. Adv Drug Deliv Rev. 2011;63: 456–469.

163. Tamizi E, Jouyban A. Forced degradation studies of biopharmaceuticals: Selection of stress conditions. Eur J Pharm Biopharm. 2016;98: 26–46.
164. Vulic K, Pakulska MM, Sonthalia R, Ramachandran A, Shoichet MS. Mathematical model accurately predicts protein release from an affinity-based delivery system. J Control Release. 2015;197: 69–77.
165. Mozziconacci O, Schöneich C. Chemical degradation of proteins in the solid state with a focus on photochemical reactions. Adv Drug Deliv Rev. 2015;93: 2–13.
166. Chi EY, Krishnan S, Randolph TW, Carpenter JF. Physical stability of proteins in aqueous solution: Mechanism and driving forces in nonnative protein aggregation. Pharm Res. 2003;20: 1325–1336.
167. Aydinoglu-Candan Ö, Araz-Ersan B, Gul A, Badur S, Tugal-Tutkun I. Anti-interferon alpha antibodies and autoantibodies in patients with Behcet's disease uveitis treated with recombinant human interferon alpha-2a. Graefe's Arch Clin Exp Ophthalmol. 2015;253: 457–465.
168. Leader B, Baca QJ, Golan DE. Protein therapeutics: a summary and pharmacological classification. Nat Rev Drug Discov. 2008;7: 21–39.
169. Zhang Y, Yao Z, Kaila N, Kuebler P, Visich J, Maia M, et al. Pharmacokinetics of ranibizumab after intravitreal administration in patients with retinal vein occlusion or diabetic macular edema. Ophthalmology. 2014;121: 2237–2246.
170. Oishi A, Tsujikawa A, Yamashiro K, Ooto S, Tamura H, Nakanishi H, et al. One-year result of aflibercept treatment on age-related macular degeneration and predictive factors for visual outcome. Am J Ophthalmol. 2015;159: 853–860.
171. Chen JJ, Ebmeier SE, Sutherland WM, Ghazi NG. Potential penetration of topical ranibizumab (Lucentis) in the rabbit eye. Eye. Nature Publishing Group; 2011;25: 1504–1511.
172. Davis BM, Normando EM, Guo L, Turner LA, Nizari S, O'Shea P, et al. Topical delivery of avastin to the posterior segment of the eye in vivo using annexin A5-associated liposomes. Small. 2014;10: 1575–1584.
173. El Zaoui I, Touchard E, Berdugo M, Abadie C, Kowalczuk L, Deloche C, et al. Subconjunctival injection of XG-102, a c-Jun N-terminal kinase inhibitor peptide, in the treatment of endotoxin-induced uveitis in rats. J Ocul Pharmacol Ther. 2015;31: 17–24.
174. Zanon C de F, Sonehara NM, Girol AP, Gil CD, Oliani SM. Protective effects of the galectin-1 protein on in vivo and in vitro models of ocular inflammation. Mol Vis. 2015;21: 1036–1050.
175. Di Tommaso C, Torriglia A, Furrer P, Behar-Cohen F, Gurny R, Möller M. Ocular biocompatibility of novel Cyclosporin A formulations based on methoxy poly(ethylene glycol)-hexylsubstituted poly(lactide) micelle carriers. Int J Pharm. 2011;416: 515–524.
176. McClellan SA, Ekanayaka SA, Li C, Jiang X, Barrett RP, Hazlett LD. Thrombomodulin Protects Against Bacterial Keratitis, Is Anti-Inflammatory, but Not Angiogenic. Investig Opthalmology Vis Sci. 2015;56: 8091.
177. Sims JN, Lawler J. Thrombospondin-1-Based Antiangiogenic Therapy. J Ocul Pharmacol Ther. 2015;31: 366–370.
178. Vijmasi T, Chen FYT, Balasubbu S, Gallup M, McKown RL, Laurie GW, et al. Topical administration of lacritin is a novel therapy for aqueous-deficient dry eye disease. Invest Ophthalmol Vis Sci. 2014;55: 5401–5409.
179. Turgut B, Eren K, Akin MM, Bilir Can N, Demir T. Impact of trastuzumab on wound healing in experimental glaucoma surgery. Clin Experiment Ophthalmol. 2014; 67–76.
180. Dogru M, Nakamura M, Shimazaki J, Tsubota K. Changing trends in the treatment of dry-eye disease. Expert

Opin Investig Drugs. 2013;22: 1581–1601.

181. García-Layana A, García-Arumí J, Ruiz-Moreno JM, Arias-Barquet L, Cabrera-López F, Figueroa MS. A review of current management of vitreomacular traction and macular hole. J Ophthalmol. 2015;2015.

182. Levison AL, Kaiser PK. Vitreomacular interface diseases: Diagnosis and management. Taiwan J Ophthalmol. 2014;4: 63–68.

183. Knudsen VM, Kozak I. A retrospective study of a single practice use of ocriplasmin in the treatment of vitreomacular traction. Saudi J Ophthalmol. 2014;28: 139–144.

184. Sharma P, Juhn A, Houston SK, Fineman M, Chiang A, Ho A, et al. Efficacy of intravitreal ocriplasmin on vitreomacular traction and full-thickness macular holes. Am J Ophthalmol. 2015;159: 861–867.

185. Pautler S, Pautler C. Posterior Vitreous Detachment [Internet]. [cited 14 Feb 2017]. doi:http://www.scottpautlermd.com/tag/posterior-vitreous-detachment/

186. Schumann RG, Wolf A, Mayer WJ, Compera D, Hagenau F, Ziada J, et al. Pathology of Internal Limiting Membrane Specimens Following Intravitreal Injection of Ocriplasmin. Am J Ophthalmol. 2015;160: 767–778.

187. Varma R, Haller J a., Kaiser PK. Improvement in Patient-Reported Visual Function After Ocriplasmin for Vitreomacular Adhesion. JAMA Ophthalmol. 2015;133: 997–1004.

188. Mains J, Wilson CG. The Vitreous Humor As a Barrier to Nanoparticle Distribution. J Ocul Pharmacol Ther. 2013;29: 143–150.

189. Barakat MR, Kaiser PK. VEGF inhibitors for the treatment of neovascular age-related macular degeneration. Expert Opin Investig Drugs. 2009;18: 637–646.

190. Hosseini H, Nowroozzadeh MH, Salouti R, Nejabat M. Anti-VEGF therapy with bevacizumab for anterior segment eye disease. Cornea. 2012;31: 322–34.

191. Hashemi S, Faramarzi MA, Ghasemi Falavarjani K, Abdollahi M. Bevacizumab for choroidal neovascularization secondary to age-related macular degeneration and pathological myopia. Expert Opin Biol Ther. 2014;14: 1837–1848.

192. Volz C, Pauly D. Antibody therapies and their challenges in the treatment of age-related macular degeneration. Eur J Pharm Biopharm. 2015;95: 158–172.

193. Klein R, Myers CE, Buitendijk GHS, Rochtchina E, Gao X, De Jong PTVM, et al. Lipids, lipid genes, and incident age-related macular degeneration: The three continent age-related macular degeneration consortium. Am J Ophthalmol. 2014;158: 513–524.

194. Dahlin A, Geier E, Stocker SL, Cropp CD, Grigorenko E, Bloomer M, et al. Gene Expression Profiling of Transporters in the Solute Carrier and ATP-Binding Cassette Superfamilies in Human Eye Substructures. Mol Pharm. 2013;10: 650–663.

195. Channa R, Sophie R, Bagheri S, Shah SM, Wang J, Adeyemo O, et al. Regression of choroidal neovascularization results in macular atrophy in anti-vascular endothelial growth factor-treated eyes. Am J Ophthalmol. 2015;159: 9–19.

196. Yasin MN, Svirskis D, Seyfoddin A, Rupenthal ID. Implants for drug delivery to the posterior segment of the eye: A focus on stimuli-responsive and tunable release systems. J Control Release. 2014;196: 208–221.

197. Hashemi S, Faramarzi MA, Ghasemi Falavarjani K, Abdollahi M. Bevacizumab for choroidal neovascularization secondary to age-related macular degeneration and pathological myopia. Expert Opin Biol Ther. 2014;14: 1837–

1848.

198. Freund KB, Mrejen S, Gallego-Pinazo R. An update on the pharmacotherapy of neovascular age-related macular degeneration. Expert Opin Pharmacother. 2013;14: 1017–1028.

199. Costagliola C, Agnifili L, Arcidiacono B, Duse S, Fasanella V, Mastropasqua R, et al. Systemic thromboembolic adverse events in patients treated with intravitreal anti-VEGF drugs for neovascular age-related macular degeneration. Expert Opin Biol Ther. 2012;12: 1299–1313.

200. Infographic Macula [Internet]. [cited 1 Feb 2017]. doi:http://www.brightfocus.org/macular/infographic/what-macular/

201. Yazdi MH, Faramarzi MA, Nikfar S, Falavarjani KG, Abdollahi M. Ranibizumab and aflibercept for the treatment of wet age-related macular degeneration. Expert Opin Biol Ther. 2015;15: 1349–1358.

202. Lipp M, Bucher F, Parthasarathy A, Hos D, Onderka J, Cursiefen C, et al. Blockade of the VEGF isoforms in inflammatory corneal hemangiogenesis and lymphangiogenesis. Graefe's Arch Clin Exp Ophthalmol. 2014;252: 943–949.

203. Pérez-Santonja JJ, Campos-Mollo E, Lledo-Riquelme M, Javaloy J, Alio JL. Inhibition of corneal neovascularization by topical bevacizumab (Anti-VEGF) and sunitinib (Anti-VEGF and Anti-PDGF) in an animal model. Am J Ophthalmol. 2010;150: 519–528.

204. Hall LB, Zebardast N, Huang JJ, Adelman RA. Aflibercept in the treatment of neovascular age-related macular degeneration in previously treated patients. J Ocul Pharmacol Ther. 2014;30: 346–352.

205. Peyman GA, Lad EM, Moshfeghi DM. Intravitreal injection of therapeutic agents. Retina. 2009;29: 875–912.

206. Chatziralli I, Nicholson L, Sivaprasad S, Hykin P. Intravitreal steroid and anti-vascular endothelial growth agents for the management of retinal vein occlusion: Evidence from randomized trials. Expert Opin Biol Ther. 2015;15: 1685–1697.

207. Kim J-AJ, Kim TE, Kim J-AJ, Yun J-H, Sohn S, Shim SR, et al. Intravitreal Tanibirumab, a Fully Human Monoclonal Antibody Against Vascular Endothelial Growth Factor Receptor 2, Partially Suppresses and Regresses Laser-Induced Choroidal Neovascularization in a Rat Model. J Ocul Pharmacol Ther. 2014;30: 847–853.

208. Grewal DS, Gill MK, Sarezky D, Lyon AT, Mirza RG. Visual and anatomical outcomes following intravitreal aflibercept in eyes with recalcitrant neovascular age-related macular degeneration: 12-month results. Eye. 2014;28: 895–899.

209. Segal O, Mimouni M, Nemet AY, Segev F, Geffen N, Nesher R. The effects of the frequency of the initial treatment with intravitreal bevacizumab on macular volume and visual acuity. J Ocul Pharmacol Ther. 2015;31: 277–281.

210. Hartnett TE, O'Connor AJ, Ladewig K. Cubosomes and other potential ocular drug delivery vehicles for macromolecular therapeutics. Expert Opin Drug Deliv. 2015;12: 1–14.

211. Furuhashi R, Ito Y, Takahashi A, Ishikawa K, Terasaki H. Two-year outcome of intravitreal bevacizumab for myopic choroidal neovascularization. Japanese J Clin Ophthalmol. 2013;67: 1577–1583.

212. El Sanharawi M, Kowalczuk L, Touchard E, Omri S, de Kozak Y, Behar-Cohen F. Protein delivery for retinal diseases: From basic considerations to clinical applications. Prog Retin Eye Res. 2010;29: 443–465.

213. Lajunen T, Hisazumi K, Kanazawa T, Okada H, Seta Y, Yliperttula M, et al. Topical drug delivery to retinal pigment epithelium with microfluidizer produced small liposomes. Eur J Pharm Sci. 2014;62: 23–32.

214. Kim SJ, Toma HS. Ophthalmic antibiotics and antimicrobial resistance: A randomized, controlled study of patients undergoing intravitreal injections. Ophthalmology. 2011;118: 1358–1363.
215. Eugene WM, Shima DT, Calias P, Cunningham ET, Guyer DR, Adamis AP. Pegaptanib, a targeted anti-VEGF aptamer for ocular vascular disease. Nat Rev Drug Discov. 2006;5: 123–132.
216. Schwartz SG, Scott IU, Flynn HW, Stewart MW. Drug delivery techniques for treating age-related macular degeneration. Expert Opin Drug Deliv. 2014;11: 61–68.
217. Berg K, Pedersen TR, Sandvik L, Bragadóttir R. Comparison of ranibizumab and bevacizumab for neovascular age-related macular degeneration according to LUCAS treat-and-extend protocol. Ophthalmology. 2015;122: 146–152.
218. Schmid MK, Bachmann LM, Fäs L, Kessels AG, Job OM, Thiel M a. Efficacy and adverse events of aflibercept, ranibizumab and bevacizumab in age-related macular degeneration: a trade-off analysis. Br J Ophthalmol. 2014; 14–15.
219. Avery RL, Pieramici DJ, Rabena MD, Castellarin AA, Nasir MA, Giust MJ. Intravitreal Bevacizumab (Avastin) for Neovascular Age-Related Macular Degeneration. Ophthalmology. 2006;113: 363–372.
220. Pinheiro-Costa J, Freitas-da-Costa P, Falcao MS, Brandao EM, Falcao-Reis F, Carneiro AM. Switch from intravitreal ranibizumab to bevacizumab for the treatment of neovascular age-related macular degeneration: clinical comparison. Ophthalmologica. 2014;232: 149–155.
221. Altun A, Kurna SA, Olcaysu OO, Sengor T, Aki SF, Atakan TG. Success of ranibizumab in central serous chorioretinopathy resistant to bevacizumab. J Ocul Pharmacol Ther. 2014;30: 842–846.
222. Bashshur ZF, Haddad ZA, Schakal A, Jaafar RF, Saab M, Noureddin BN. Intravitreal Bevacizumab for Treatment of Neovascular Age-related Macular Degeneration: A One-year Prospective Study. Am J Ophthalmol. 2008;145: 249–256.
223. Park Y-R, Chung SK. Inhibitory Effect of Topical Aflibercept on Corneal Neovascularization in Rabbits. Cornea. 2015;34: 1303–1307.
224. Soohoo JR, Seibold LK, Pantcheva MB, Kahook MY. Original Article Aflibercept for the treatment of neovascular glaucoma. 2015; 803–807.
225. Chang J-H, Garg N, Lounde E, Han kyu yeon, Sandeep J, Azar D mitri. Corneal Neovascularisation: An Anti-VEGF Therapy Review. Surv Ophthalmol. 2012;57: 415–429.
226. Menzel-Severing J. Emerging techniques to treat corneal neovascularisation. Eye. Nature Publishing Group; 2012;26: 2–12.
227. Papathanassiou M, Theodoropoulou S, Analitis A, Tzonou A, Theodossiadis PG. Vascular endothelial growth factor inhibitors for treatment of corneal neovascularization: a meta-analysis. Cornea. 2013;32: 435–444.
228. Gonzalez L, Loza RJ, Han K-Y, Sunoqrot S, Cunningham C, Purta P, et al. Nanotechnology in Corneal Neovascularization Therapy—A Review. J Ocul Pharmacol Ther. 2013;29: 124–134.
229. Fassnacht-Riederle H, Becker M, Graf N, Michels S. Effect of aflibercept in insufficient responders to prior anti-VEGF therapy in neovascular AMD. Graefe's Arch Clin Exp Ophthalmol. 2014;252: 1705–1709.
230. Stevenson W, Cheng SF, Dastjerdi MH, Ferrari G, Dana R. Corneal neovascularization and the utility of topical VEGF inhibition: Ranibizumab (Lucentis) Vs bevacizumab (Avastin). Ocul Surf. 2012;10: 67–83.
231. Small DS, Acheampong A, Reis B, Stern K, Stewart W, Berdy G, et al. Blood concentrations of cyclosporin A during

long-term treatment with cyclosporin A ophthalmic emulsions in patients with moderate to severe dry eye disease. J Ocul Pharmacol Ther. 2002;18: 411–418.

232. Turner K, Pflugfelder SC, Ji Z, Feuer WJ, Stern M, Reis BL. Interleukin-6 levels in the conjunctival epithelium of patients with dry eye disease treated with cyclosporine ophthalmic emulsion. Cornea. 2000;19: 492–496.
233. Brignole F, Pisella PJ, De Saint Jean M, Goldschild M, Goguel A, Baudouin C. Flow cytometric analysis of inflammatory markers in KCS: 6-month treatment with topical cyclosporin A. Investig Ophthalmol Vis Sci. 2001;42: 90–95.
234. Pflugfelder SC. Antiinflammatory therapy for dry eye. Am J Ophthalmol. 2004;137: 337–342.
235. Rodriguez-Aller M, Kaufmann B, Guillarme D, Stella C, Furrer P, Rudaz S, et al. In vivo characterisation of a novel water-soluble Cyclosporine A prodrug for the treatment of dry eye disease. Eur J Pharm Biopharm. 2012;80: 544–552.
236. Strong B, Farley W, Stern ME, Pflugfelder SC. Topical cyclosporine inhibits conjunctival epithelial apoptosis in experimental murine keratoconjunctivitis sicca. Cornea. 2005;24: 80–85.
237. Donnenfeld E, Pflugfelder SC. Topical Ophthalmic Cyclosporine: Pharmacology and Clinical Uses. Surv Ophthalmol. 2009;54: 321–338.
238. Kymionis GD, Bouzoukis DI, Diakonis VF, Siganos C. Treatment of chronic dry eye: focus on cyclosporine. Clin Ophthalmol. 2008;2: 829–836.
239. Suzuki T, Schaumberg DA, Sullivan BD, Liu M, Richards SM, Sullivan RM, et al. Do Estrogen and Progesterone Play a Role in the Dry Eye of Sjögren's Syndrome? Ann N Y Acad Sci. 2002;966: 223–225.
240. Latkany R. Dry eyes: etiology and management. Curr Opin Ophthalmol. 2008;19: 287–291.
241. Hermans K, Van Den Plas D, Everaert A, Weyenberg W, Ludwig A. Full factorial design, physicochemical characterisation and biological assessment of cyclosporine A loaded cationic nanoparticles. Eur J Pharm Biopharm. 2012;82: 27–35.
242. Alqawlaq S, Huzil JT, Ivanova M V, Foldvari M. Challenges in neuroprotective nanomedicine development: progress towards noninvasive gene therapy of glaucoma. Nanomedicine. 2012;7: 1067–1083.
243. Delplace V, Payne S, Shoichet M. Delivery strategies for treatment of age-related ocular diseases: From a biological understanding to biomaterial solutions. J Control Release. 2015;219: 652–668.
244. Shell JW. Pharmacokinetics of topically applied ophthalmic drugs. Surv Ophthalmol. 1982;26: 207–218.
245. Jo DH, Kim JH, Lee TG, Kim JH. Nanoparticles in the Treatment of Angiogenesis-Related Blindness. J Ocul Pharmacol Ther. 2013;29: 135–142.
246. Diebold Y, Calonge M. Progress in Retinal and Eye Research Applications of nanoparticles in ophthalmology. Prog Retin Eye Res. 2010;29: 596–609.
247. Kompella UB, Amrite AC, Pacha Ravi R, Durazo SA. Nanomedicines for back of the eye drug delivery, gene delivery, and imaging. Prog Retin Eye Res. 2013;36: 172–198.
248. Kaur IP, Kakkar S. Nanotherapy for posterior eye diseases. J Control Release. 2014;193: 100–112.
249. Cunha-Vaz J, Ashton P, Iezzi R, Campochiaro P, Dugel PU, Holz FG, et al. Sustained delivery fluocinolone acetonide vitreous implants: Long-term benefit in patients with chronic diabetic macular edema. Ophthalmology. 2014;121: 1892–1903.
250. Ali Y, Lehmussaari K, Christie CL, Coelho JF, Ferreira PC, Alves P, et al. Recent advances in ophthalmic drug

delivery. Adv Drug Deliv Rev. 2011;1: 219–263.

251. Jaffe GJ, Martin D, Callanan D, Pearson PA, Levy B, Comstock T. Fluocinolone Acetonide Implant (Retisert) for Noninfectious Posterior Uveitis. Thirty-Four-Week Results of a Multicenter Randomized Clinical Study. Ophthalmology. 2006;113: 1020–1027.

252. Campochiaro PA, Nguyen QD, Hafiz G, Bloom S, Brown DM, Busquets M, et al. Aqueous levels of fluocinolone acetonide after administration of fluocinolone acetonide inserts or fluocinolone acetonide implants. Ophthalmology. 2013;120: 583–587.

253. Edelhauser HF, Rowe-Rendleman CL, Robinson MR, Dawson DG, Chader GJ, Grossniklaus HE, et al. Ophthalmic Drug Delivery Systems for the Treatment of Retinal Diseases: Basic Research to Clinical Applications. Investig Opthalmology Vis Sci. 2010;51: 5403–5420.

254. Perrie Y, Badhan RKS, Kirby DJ, Lowry D, Mohammed AR, Ouyang D. The impact of ageing on the barriers to drug delivery. J Control Release. 2012;161: 389–398.

255. Yasukawa T, Tabata Y, Kimura H, Ogura Y. Recent advances in intraocular drug delivery systems. Recent Pat Drug Deliv Formul. 2011;5: 1–10.

256. Haller JA, Bandello F, Belfort R, Blumenkranz MS, Gillies M, Heier J, et al. Randomized, Sham-Controlled Trial of Dexamethasone Intravitreal Implant in Patients with Macular Edema Due to Retinal Vein Occlusion. Ophthalmology. 2010;117: 1134–1146.

257. Peptu CA, Popa M, Savin C, Popa RF, Ochiuz L. Modern Drug Delivery Systems for Targeting the Posterior Segment of the Eye. 2015; 6055–6069.

258. Agarwal P, Rupenthal ID. Injectable implants for the sustained release of protein and peptide drugs. Drug Discov Today. 2013;18: 337–349.

259. Shmueli RB, Ohnaka M, Miki A, Pandey NB, Lima e Silva R, Koskimaki JE, et al. Long-term suppression of ocular neovascularization by intraocular injection of biodegradable polymeric particles containing aserpin-derived peptide. Biomaterials. 2013;34: 7544–7551.

260. Kirchhof S, Abrami M, Messmann V, Hammer N, Goepferich AM, Grassi M, et al. Diels-Alder Hydrogels for Controlled Antibody Release: Correlation between Mesh Size and Release Rate. Mol Pharm. 2015;12: 3358–3368.

261. Haj-Ahmad RR, Elkordy AA, Chaw CS, Moore A. Compare and contrast the effects of surfactants (Pluronic F-127 and Cremophor EL) and sugars (beta-cyclodextrin and inulin) on properties of spray dried and crystallised lysozyme. Eur J Pharm Sci. 2013;49: 519–534.

262. Avanti C, Saluja V, Van Streun ELP, Frijlink HW, Hinrichs WLJ. Stability of lysozyme in aqueous extremolyte solutions during heat shock and accelerated thermal conditions. PLoS One. 2014;9: 2–7.

263. Varshochian R, Jeddi-Tehrani M, Mahmoudi AR, Khoshayand MR, Atyabi F, Sabzevari A, et al. The protective effect of albumin on bevacizumab activity and stability in PLGA nanoparticles intended for retinal and choroidal neovascularization treatments. Eur J Pharm Sci. 2013;50: 341–352.

264. Wang L, Yang T, Ma G. Microspheres and microcapsules for protein drug delivery. Microspheres Microcapsules Biotechnol Des Prep Appl. 2013; 6340–6352.

265. Edelman R, Kusner I, Kisiliak R, Srebnik S, Livney YD. Sugar stereochemistry effects on water structure and on protein stability: The templating concept. Food Hydrocoll. 2015;48: 27–37.

266. Rawat S, Kohli N, Suri CR, Sahoo DK. Molecular mechanism of improved structural integrity of protein in polymer based microsphere delivery system. Mol Pharm. 2012;9: 2403–2414.
267. Thrimawithana TR, Rupenthal ID, Young SA, Alany RG. Environment-sensitive polymers for ophthalmic drug delivery. J Drug Deliv Sci Technol. 2012;22: 117–124.
268. Vagenende V, Yap MGS, Trout BL. Mechanisms of protein stabilization and prevention of protein aggregation by glycerol. Biochemistry. 2009;48: 11084–11096.
269. Asmus LR, Grimshaw JPA, Richle P, Eicher B, Urech DM, Gurny R, et al. Injectable formulations for an intravitreal sustained-release application of a novel single-chain VEGF antibody fragment. Eur J Pharm Biopharm. 2015;95: 250–260.
270. Cicerone MT, Pikal MJ, Qian KK. Stabilization of proteins in solid form. Adv Drug Deliv Rev. 2015;93: 14–24.
271. Tonnis WF, Mensink MA, De Jager A, Van Der Voort Maarschalk K, Frijlink HW, Hinrichs WLJ. Size and molecular flexibility of sugars determine the storage stability of freeze-dried proteins. Mol Pharm. 2015;12: 684–694.
272. Woedtke T von, Kramer A. The limits of sterility assurance. GMS Krankenhhyg Interdiszip. 2008;3: Doc19.
273. Govindaraj S, Muthuraman MS. Systematic Review on Sterilization Methods of Implants and Medical Devices. Int J ChemTech Res. 2015;8: 897–911.
274. Dai Z, Ronholm J, Tian Y, Sethi B, Cao X. Sterilization techniques for biodegradable scaffolds in tissue engineering applications. J Tissue Eng. 2016;7: 1–13.
275. Rutala W a, Weber DJ. Infection control: the role of disinfection and sterilization. J Hosp Infect. 1999;43 Suppl: S43–S55.
276. Rnjak-Kovacina J, Desrochers TM, Burke KA, Kaplan DL. The effect of sterilization on silk fibroin biomaterial properties. Macromol Biosci. 2015;15: 861–874.
277. Leo WJ, Mcloughlin AJ, Malone DM. Effects of Sterilization Treatments on Some Properties of Alginate Solutions and Gels. Biotechnol Prog. 1990;6: 51–53.
278. Silindir M, Özer AY. Sterilization methods and the comparison of E-beam sterilization with gamma radiation sterilization. Fabad J Pharm Sci. 2009;34: 43–53.
279. Maggi L, Segale L, Machiste EO, Buttafava A, Faucitano A, Conte U. Chemical and physical stability of hydroxypropylmethylcellulose matrices containing diltiazem hydrochloride after gamma irradiation. J Pharm Sci. 2003;92: 131–141.

Chapter 2: Objectives

OBJECTIVES

The most popular ophthalmic route of administering drugs is through topically applied eye drops. However, since the ocular availability of these formulations is very low due to the anatomic structure and protective mechanisms of the eye, the strategy of enhancing the viscosity of the ocular drug delivery systems was followed in the present research work, in order to improve the amount of drug available at the ocular surface. The developed insert is based on hydroxypropylmethyl cellulose as the polymer of choice and is designed to be applied in the lower conjunctival sac of the eyes for once- or twice-a-day application.

The main objective of the present research work was to develop a new drug delivery system that allows thermolabile molecules, such as peptides and proteins, to be incorporated in a gelling system with slow release properties. As these molecules often tend to denaturate when heat or shear forces are applied or in an oxidative environment such as air, a careful approach is required when formulating such molecules in a new drug carrier system. At the same time, the insert should be soft and mouldable to reduce foreign-body sensation and eye irritation and thereby avoiding reflex tears and rapid blinking. The insert should have slow release properties to improve patient compliance by minimising the application frequency to once of twice daily. It should be noted that no particular pathology nor drug substance was targeted in this study.

To achieve this objective, the main strategy was based on preparing the excipients to such an extent, that manipulation of the drug substance is minimised as much as possible. The evolution and progress of developing the inserts is discussed in chapters 3-9.

In chapter 3, a first attempt was performed to load an insert with a small, tracer molecule. Sodium fluorescein was selected as a coloured tracer molecule. The preparation of the inserts involves a loading step of the drug of interest into the blank polymeric device which was carefully prepared to allow drug loading through a passive diffusion process. Exploring the possibilities of the method developed, identifying the influence of various parameters and obtaining slow release kinetics were set as the primary objectives of this chapter.

Following the data obtained in chapter 3, loading of a blank insert with a protein (lysozyme) was undertaken in chapter 4. The higher molecular weight of lysozyme (14.3 kDa) in comparison to sodium fluorescein exposed new challenges, which led to a further improvement of the method.

Subsequently, the method was further optimised in order to improve the preparation characteristics of the inserts.

Analysis of the behaviour of lysozyme loaded inserts led to the development of a significantly altered production method in chapter 5. At this stage, bovine serum albumin (66.4 kDa) was added to the comparison, along with sodium fluorescein and lysozyme in order to assess the next embodiment of the production process.

It was clear from chapter 5 that the physicochemical properties of the drug and polymeric network are the main influencing factors of the drug loading rate and drug release profiles. Therefore, the influence of the molecular weight was determined using FITC labelled dextrans on both the preparation of the inserts as well as on the drug release profiles in chapter 6.

Cytotoxicity and biocompatibility tests were conducted in chapter 7 to assess the potential harm that blank inserts may cause to human corneal epithelial cells. This was evaluated both quantitatively and qualitatively.

Furthermore, good stability is a key requirement for ophthalmic inserts. The stability of the inserts was verified by means of an activity assay, rheological characterisation and release profile analysis. These results are highlighted in chapter 8.

Finally, the objective of chapter 9 was to evaluate the behaviour of dexamethasone loaded inserts *in vivo* in rats with dry eye disease.

Chapter 3: Development of a novel ocular insert with slow release properties loaded with sodium fluorescein

Parts of this chapter have been published in:

Everaert, A., Ludwig, A., Van den Plas, D., Weyenberg, W.

Thermolabile drug release formulation, 2014. Patent: WO/2014/184243

1 INTRODUCTION

In recent years, eye research has been putting more focus and efforts on the administration of proteins for diseases including wet age-related macular degeneration [1,2], uveitis [3,4] and corneal neovascularisation [5,6]. The sensitivity of proteins to elevated temperatures, pH changes, mechanical shear forces and oxidation by air complicates the manufacturing process of ocular drug delivery devices loaded with these molecules [7–9]. For the development of the present drug delivery system, special attention was paid to the development of a method that could potentially minimise the risk of stability issues of thermolabile molecules such as peptides and proteins during preparation to avoid protein unfolding, breakdown and consequently loss of activity. Therefore, shear forces should be minimised and both air entrapment and heating should be avoided. In order to improve eye-comfort, the foreign-body sensation typically associated with ocular inserts in general, should be reduced [10–12]. This can be achieved by making the inserts as small as possible and flexible when pressure is applied by the lower eyelid. The insert should be entirely water dispersible, eliminating the need to remove the insert from its site of application after drug delivery.

Ocular delivery of molecules while maintaining drug stability is already a major challenge, but delivering these drug molecules in a slow release manner complicates matters significantly. To allow slow release, the polymer hydroxypropylmethyl cellulose (HPMC) was used to build up the matrix of the ocular inserts and thereby elevate the viscosity of the matrix to desired levels. HPMC is one of the most frequently used polymers for slow release purposes and has excellent properties for matrix build-up [13–16].

Generally, the homogeneous dispersion of highly viscous polymers in water, such as cellulose ethers, implies the use of hot water to avoid air bubble entrapment and to disperse the polymer molecules homogeneously in the solvent. After being fully wetted and dispersed, a non-thermolabile drug can be added to the mixture at high temperature while stirring continuously. The low-viscous dispersion can be cooled to room temperature or below, promoting the formation of hydrogen bonds and structure build-up. Of course, this procedure cannot be used for peptide or protein molecules as they require a more careful treatment during formulation as a result of their labile physicochemical nature. The developed method was designed to incorporate any molecule with relatively unstable properties, only being limited by its molecular weight and water solubility.

For the initial development of the novel HPMC ophthalmic insert, sodium fluorescein (0.376 kDa) was selected as a tracer molecule because it allows an easy visual assessment of the inserts prepared as well as a good determination of the drug loading capability and release. Sodium fluorescein has excellent water-soluble properties and is stable at physiological pH in the absence of light, making it a good choice for drug carrier development. To enhance the flexibility of the inserts, glycerol was added as a plasticiser. Glycerol is also known to have stabilising effects on proteins, which can be of importance for the development of protein loaded ocular inserts [17–19]. To assess the influence of the subtype of HPMC polymer used, the initial percentage of HPMC polymer, the percentage glycerol and the drying period of the inserts after extrusion, a 2^4 full factorial design was set up.

This chapter describes the proof-of-concept of inserts loaded with sodium fluorescein.

2 MATERIALS AND METHODS

2.1 Materials

Hydroxypropylmethyl cellulose (HPMC) types E4M and E10M CR Premium were obtained from Colorcon (Dartford, UK). By specification, a 2% (w/w) E4M and E10M HPMC solution gives an apparent viscosity of respectively 4.000 and 10.000 mPa.s (20 °C) under the same measuring conditions. Sodium fluorescein and glycerol analytical grade (99.5% (V/V)) were provided by Sigma-Aldrich (Steinheim, Germany). Purified water (18.2 MΩ.cm) was used after being filtered over a 0.2 µm cellulose acetate filter from Sartorius (Vilvoorde, Belgium). Sodium chloride (NaCl), sodium dihydrogen phosphate dihydrate ($NaH_2PO_4.2H_2O$) and disodium hydrogen phosphate dihydrate ($Na_2HPO_4.2H_2O$) of analytical grade were purchased from Merck (Darmstadt, Germany) and were used to prepare phosphate-buffered saline solution (PBS, pH 7.4). PBS is an electrolyte solution composed of 8.2 g/l NaCl, 0.3 g/l $NaH_2PO_4.2H_2O$, 1.54 g/l $Na_2HPO_4.2H_2O$ and purified water.

A Topitec® barrel with a diameter of 36 mm and a height of 60 mm was supplied by ACA Pharma (Waregem, Belgium). A custom made seal was developed and made out of Teflon with an opening of 2 mm through which the inserts were extruded.

2.2 Characterisation of the excipients

2.2.1 Hydroxypropylmethyl cellulose

Hydroxypropylmethyl cellulose (HPMC) or hypromellose is a semisynthetic, non-ionic, hydrophilic polymer based on the polymeric backbone of cellulose. Hypromellose is soluble in cold water and is called a colloidal solution or sol [20,21]. Because of their viscous properties, these colloidal solutions are also called viscous solutions or hydrogels, although the latter is technically spoken reserved for crosslinked gels where polymers are physically or chemically interlinked for instance by means of covalent or ionic bonds [22–24]. These hydrogels are generally obtained after modification by a crosslinking agent (e.g. chemical substance or radiation) and implicate non-dissolving matrices. The gel network consists of a very large branched polymer which spans the entire gel. They can be deformed, but retain their shape like a solid as the crosslinks have a permanent character [25].

However, the term *hydrogel* is also often used to indicate a highly viscous aqueous solution with gel-like structure. Entangled polymer systems are sometimes referred to as pseudo gels as physical entanglements can mimic chemical crosslinks giving them gel-like properties. This is especially true for high molecular weight polymers which can entangle with themselves [25,26]. Therefore, for the

sake of clarity, the term hydrogel will be used in this research work to indicate highly viscous polymer solutions with gel-like structure. Preparing a viscous solution of HPMC results in a non-crosslinked or unlinked polymeric network, where simple entanglement gives strength to the hydrogel structure. Rheological analysis can give a valuable insight in whether a solution is a colloidal solution or a true gel through oscillatory measurements. A sample can be characterised by a storage modulus (G'), which is indicative for elastic behaviour of the sample measured, and a loss modulus (G") which indicates the viscous behaviour. The relationship between G' and G" of a polymeric sample describes the resistance to an externally applied force and hence the relative strength of the intermolecular bonds. This is termed viscoelastic behaviour. In case of a true gel, G' and G" will show a flat spectrum (parallel curves) in an oscillatory measurement with the loss modulus G" being considerably smaller than the elastic component G'. This implicates that the polymer chains are interlinked and the intermolecular bonds are not broken with varying frequencies. In other words, ideal gels have an almost purely elastic response, independent of the frequency applied on the sample [25].

For colloidal solutions with polymeric entanglement, both shear moduli will increase with increasing frequency. The viscous component G" will be higher than the elastic component G' at low oscillatory frequencies, suggesting that the polymer chains have time to disentangle and are unable to store energy. At high frequencies, the polymer will not have sufficient time to rearrange the polymer structure resulting in G' being higher than G". This suggest an elastic and hence more gel-like behaviour [27,28]. The point where G' equals G" is called the crossover point and is defined as the point where the measured sample changes from a viscoelastic liquid to a viscoelastic solid [25].

To determine the viscoelastic behaviour of an HPMC colloidal solution, HPMC E10M aqueous solutions were prepared in three different percentages (5%, 10% and 20% (w/w)). The viscoelastic properties were measured through oscillation on an Anton Paar rheometer (MCR 102, Graz, Austria) at a temperature of 32.0 ± 0.1 °C. Prior to the frequency sweep measurements, an amplitude sweep was performed to determine the linear viscoelastic region (LVER). The LVER determines the amplitudes in which the polymer network is maintained. Setting the amplitude too high will cause a destruction of the polymer network, therefore an amplitude must be chosen within the LVER. In the LVER, the measured moduli G' and G" are independent of the applied strain [25]. After performing an amplitude sweep determining the LVER, the strain was consequently set at 1% amplitude. The following settings were used for all oscillation measurements: parallel plate with a diameter of 8 mm and the gap size set at 1 mm. The angular frequency was varied from 100 to 0.1

rad/s. To prevent evaporation of water from the hydrogel during the measurements, a solvent trap was used to cover the sample.

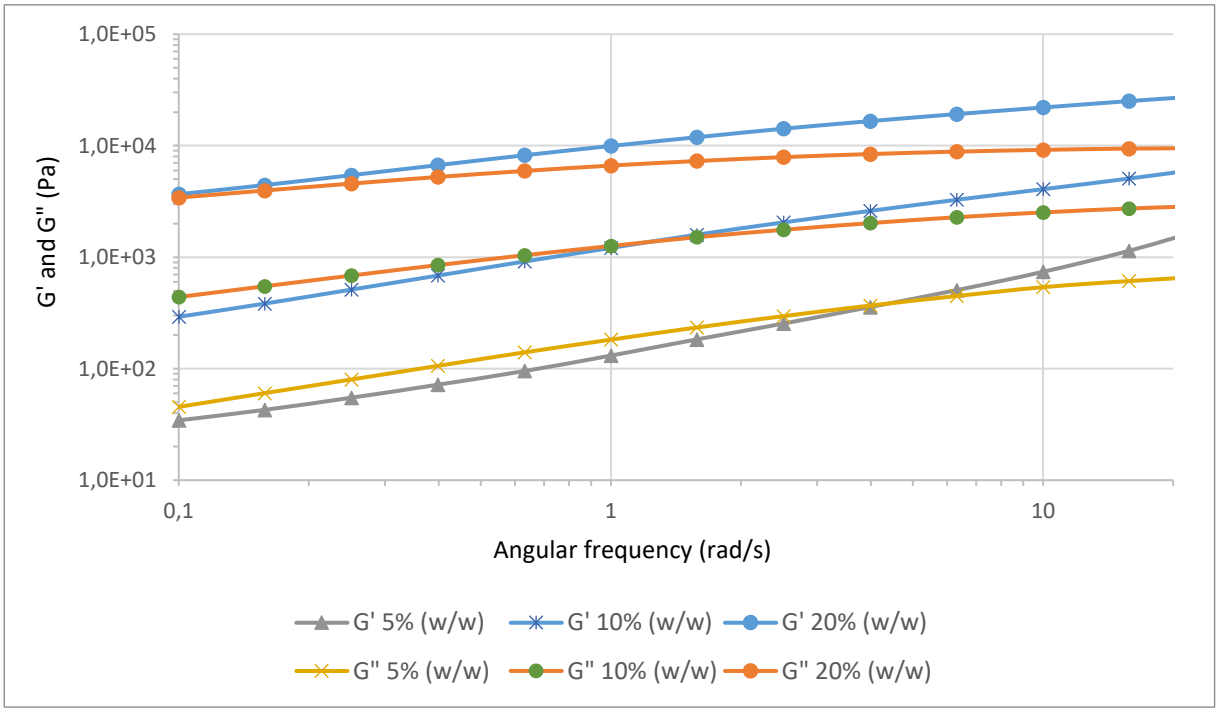

Fig. 1. Overview of the viscoelastic behaviour of three colloidal solutions with an HPMC E10M percentage of 5%, 10% and 20% (w/w). For the sake of clarity, angular frequencies below 20 rad/s are shown.

In figure 1, it can be seen that for every colloidal solution tested, the elastic component G' is higher than the viscous component G" at high oscillatory frequencies, except for a 20% (w/w) HPMC solution. But the opposite is true at low frequencies which is typical for viscoelastic behaviour. The crossover point of the 20% (w/w) HPMC solution has not even been reached at 0.1 rad/s, but in case of a true gel, G' would be much higher than G" which is clearly not the case. Nevertheless, a clear shift of the crossover point towards lower frequencies is noted when increasing the concentration of HPMC with G' still being predominant over G" at the highest percentage HPMC tested. Increasing the percentage polymer in solution increases the likelihood of gel-like behaviour for a colloidal solution as can be noticed for HPMC E10M 20% (w/w).

The polymer HPMC is widely used in the drug and food industry as a stabiliser of emulsions, as an important excipient of slow release matrix tablets, as a viscosifying agent in solid and semisolid formulations, etc. [29,30]. Its stability in the presence of heat, light and air, its excellent biocompatibility, swelling capacity and low toxicity make this polymer a popular choice for various

applications [31–34]. The β-D-glucose (anhydroglucose) units of HPMC are interlinked through β-(1,4)-glycosidic bonds. The basic structure is given in figure 2 [14].

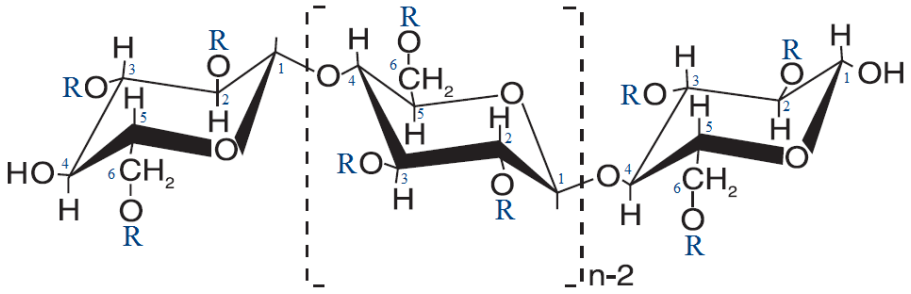

Fig. 2. General structure of hydroxypropylmethyl cellulose with R= -H, or -CH_3, or -$CH_2CH(OH)CH_3$.

During the manufacturing of cellulose ethers, cellulose fibres are treated with a caustic solution (sodium hydroxide), which in turn is treated with methyl chloride and propylene oxide. The fibrous reaction product is purified and ground to a fine powder. Different types of HPMC are classified according to their degree of methoxyl substitution, moles of hydroxypropyl substitution and degree of polymerisation which is indirectly defined by the molecular weight measured as 2% (w/w) solution viscosity [14,33]. The USP 32 describes four different types of HPMC suitable for pharmaceutical use and they are classified according to their methoxy and hydroxypropoxy groups: HPMC 1828, HPMC 2208, HPMC 2906 and HPMC 2910. The first two digits refer to the approximate percentage content of methoxy groups. The second two digits refer to the approximate percentage content of hydroxypropoxy groups, determined after drying at 105 °C for two hours [14,30]. The largest HPMC producing company, the *Dow Chemical Company,* also describes three different types of HPMC Methocel™ based on a letter, followed by a number indicating the viscosity of an aqueous 2% (w/w) solution at 20 °C expressed in mPa.s. For instance, in E10M, the "E" denotes the chemical type of HPMC, while "10M" stands for an apparent viscosity of 10.000 mPa.s for an aqueous solution at 20 °C. The viscosity number is an approximate value and can, in this case, vary between 7.500 and 14.000 mPa.s [35]. An overview of the different HPMC types is given in table 1.

Table 1. Specification for different types of HPMC, classified according to their degree of methoxy and hydroxypropoxy substitution.

Substitution type Ph. Eur. / USP	Methocel™ classification	Methoxy substitution % (w/w)		Hydroxypropoxy substitution % (w/w)	
		Min.	Max.	Min.	Max.
1828	*N/A*	16.5	20.0	23.0	32.0
2208	K	19.0	24.0	4.0	12.0
2906	F	27.0	30.0	4.0	7.5
2910	E	28.0	30.0	7.0	12.0

The methoxy and hydroxypropoxy groups, substituted on β-D-glucose units influence the properties of HPMC of being reversibly insoluble in water at temperatures above the thermal gelation temperature (T_m) [36]. Hypromellose is one of the very few cellulosic polymers that exhibit clear thermal gelation properties. Methyl cellulose (MC) also exhibits these gelation properties, but the limited commercial availability of different subtypes and the lower clarity of MC compared to HPMC makes HPMC a more desirable choice for ophthalmic insert development [29]. At low temperatures, the hydrophobic methyl groups are believed to be shielded by water molecules [37]. If an aqueous solution of HPMC is heated above the T_m, these water molecules are removed and gelation is promoted as intermolecular hydrophobic interactions are being formed [30,37,38]. A schematic representation is given in figure 3.

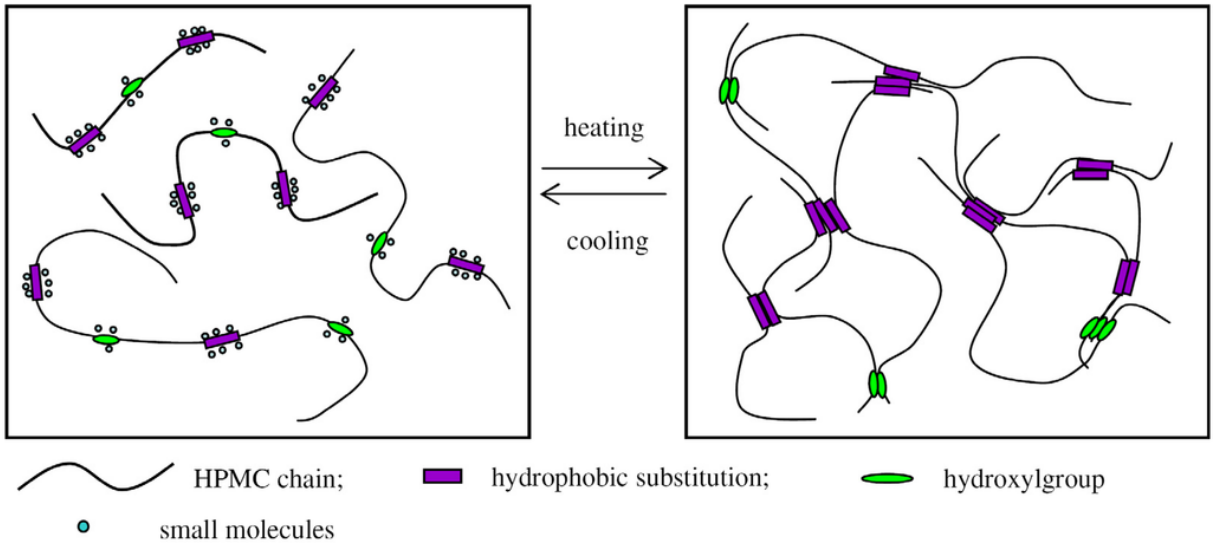

Fig. 3. Sol-gel transition upon heating and cooling. *Figure adopted from Joshi S. et al.* [21].

The thermal gelation temperature is also highly dependent on the percentage HPMC in solution: increasing the polymer concentration will reduce the thermal gelation temperature [39–41]. At temperatures below the thermal gelation temperature, HPMC molecules are hydrated as hydrophilic interactions between hydroxyl groups of HPMC and water molecules are stimulated. There is little polymer-polymer interaction besides physical entanglement. Increasing the temperature reduces the viscosity of the colloidal solution until the thermal gelation temperature is reached. From this point, a polymer-polymer interaction mainly through methoxyl groups will take place, reflected by a sharp rise in viscosity as a gel is formed [30,36,39]. This process is entirely reversible and this property has been cleverly exploited in the development of the ocular inserts.

The thermal gelation temperature of a 20% (w/w) HPMC E10M solution was estimated using an Anton Paar rheometer (MCR 102, Graz, Austria) using a parallel plate geometry of 8 mm diameter. The measurement was performed through oscillation at constant shear with an amplitude of 1% and a frequency of 1 Hz. The temperature was ramped up between 20-90 °C at a heating rate of 1 °C per 0.15 s. The experiment was performed in triplicate and the mean value is shown in figure 4.

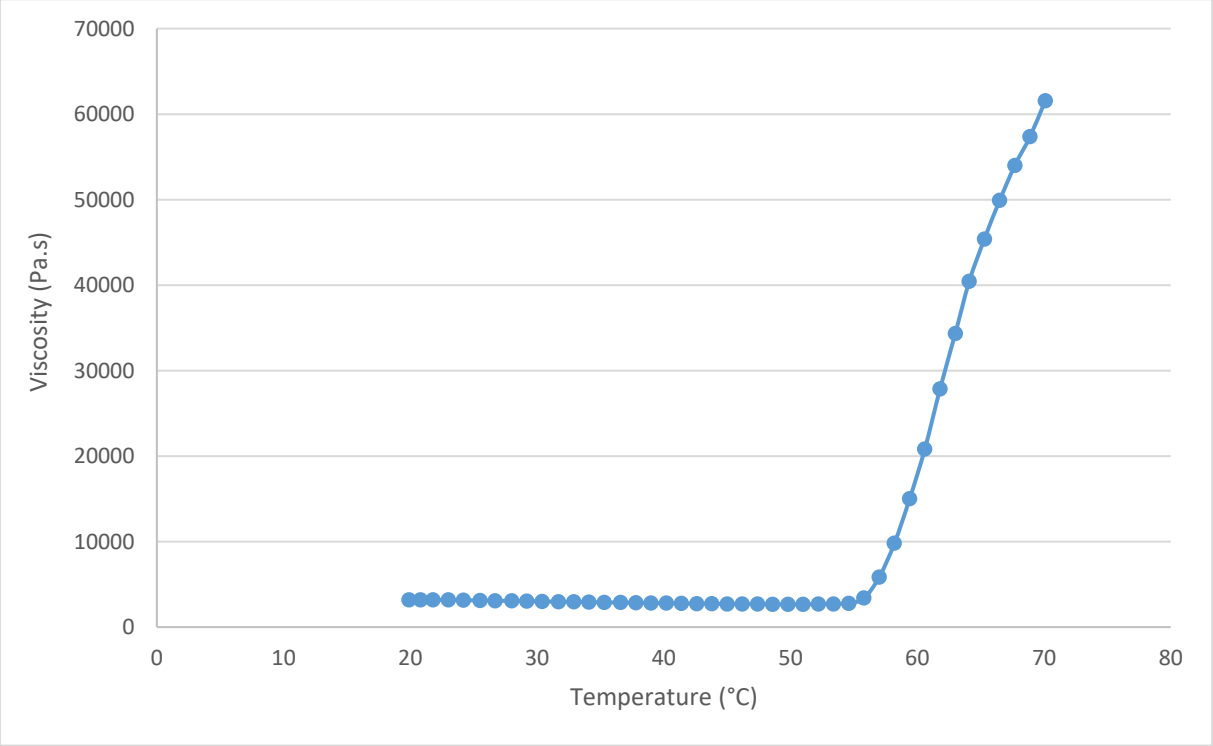

Fig. 4. Viscosity profile of a 20% (w/w) HPMC E10M viscous solution using a temperature ramp between 20-90 °C at a rate of 1 °C/0.15 s. The temperature at which the viscosity starts to rise is considered to be the thermal gelation temperature.

Figure 5 gives the viscosity profile in more detail between 20-53.4 °C for better visual understanding.

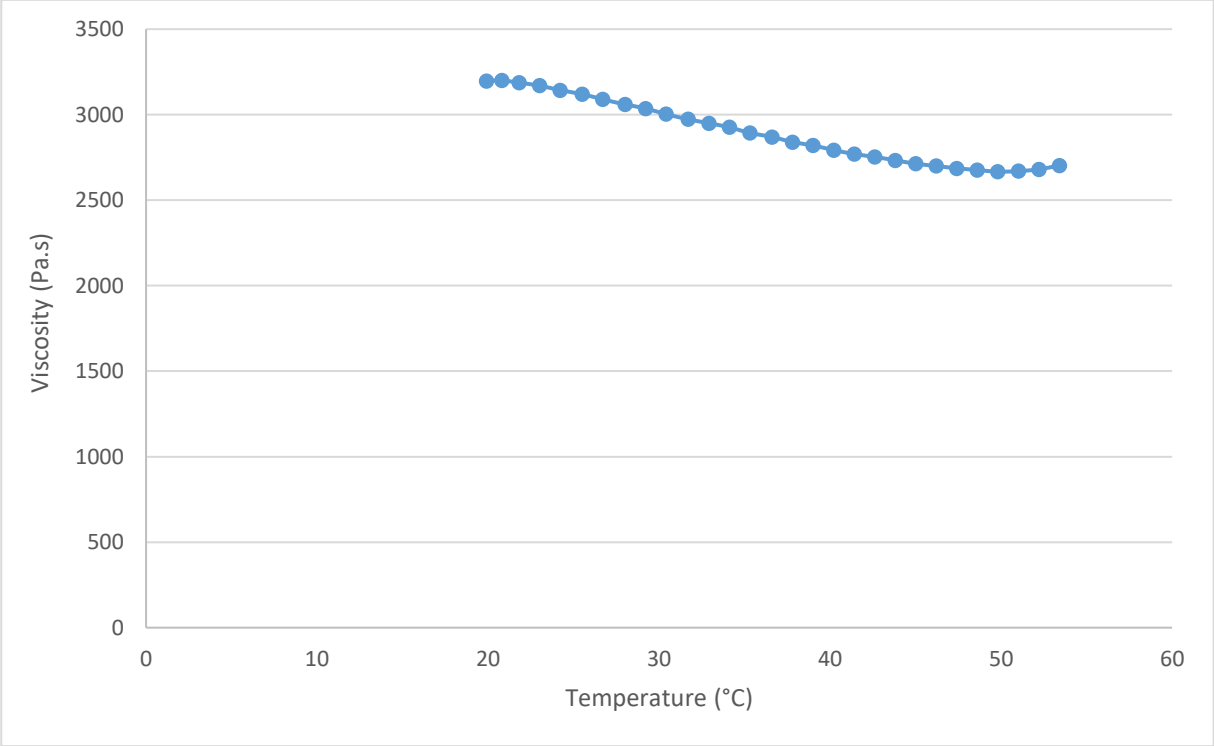

Fig. 5. Enlargement of the viscosity profile shown in figure 4 of a 20% (w/w) HPMC E10M viscous solution using a temperature ramp between 20-53.4 °C.

From 20 °C to 49.8 °C, below the gelation temperature, the viscous solution demonstrates expected behaviour of decreasing viscosity with increasing temperature. Beyond the gelation temperature, viscosity increases as the temperature is increased [29]. At 51 ± 1.2 °C the viscosity increases as polymer-polymer interactions start to appear. This point is considered to be the thermal gelation temperature. A sharp rise in viscosity is seen from 57 ± 1.2 °C in figure 4.

The thermal gelation properties of HPMC, the commercial availability of various subtypes and the pharmaceutical applicability of HPMC have been the main criteria for polymer selection. From preliminary experiments, HPMC E10M seems particularly suited for ophthalmic use. The Methocel™ E-type polymers have higher clarity than K-type polymers, while more commercial grades of E-type polymers are available compared to F-types. However, throughout this research study, E10M and E4M will be studied in the present chapter, while E10M, which is the highest available E-type grade, will be compared to K100M in *chapter 4*. The polymer HPMC K100M is

intrinsically the highest HPMC polymerisation grade available, and was used as a measure of reference despite lower clarity and hence less suited ophthalmic properties.

2.2.2 Glycerol

Glycerol or propane-1,2,3-triol is a clear, viscous solution with hygroscopic properties. Due to its biocompatibility with ocular tissues, it is often added to ocular formulations to enhance the flexibility of the final product [42–45], but glycerol also has excellent protein stabilising properties [17–19]. For these reasons, glycerol was selected as primary choice of plasticiser. The structure of glycerol is given in figure 6.

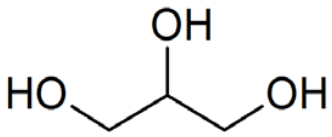

Fig. 6. Structure of glycerol.

2.3 Initial method for the preparation of inserts

Rod-shaped, ocular inserts with different composition were developed and prepared. They are composed of varying initial percentages of HPMC, 0.3% (w/w) sodium fluorescein, a varying amount of glycerol as a plasticiser and purified water as solvent. The choice of HPMC over other polymers was based on its unique gelation properties, commercial availability of pharmaceutical grade HPMC types with different viscosities and suitability for ocular purposes. The final percentage HPMC in the inserts was fixed for all formulations at 15% (w/w). The initial method of preparing this drug delivery system consists of four major phases. A schematic overview of the initial preparation method is given in figure 7.

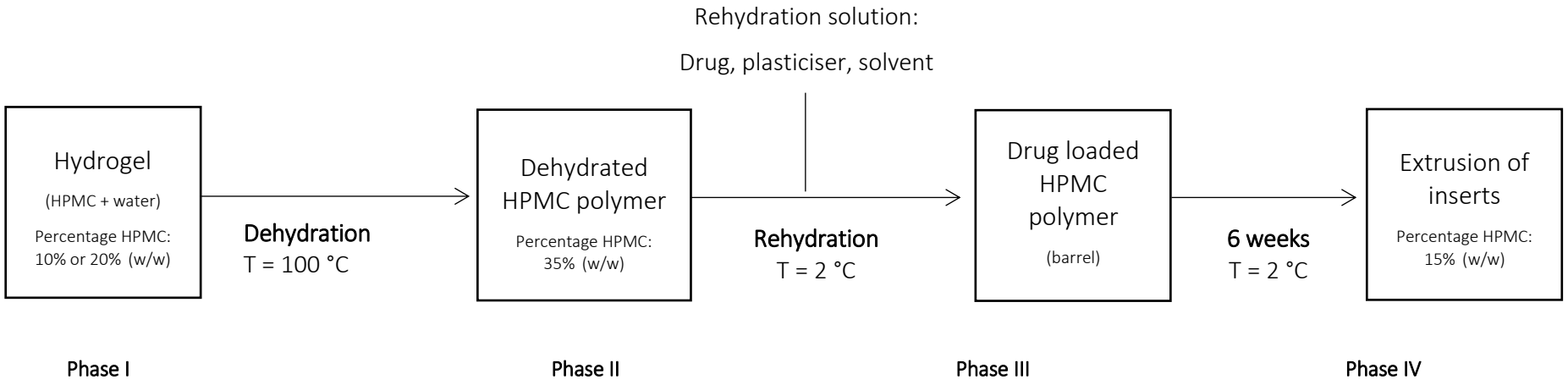

Fig. 7. General overview of the preparation method. A clear hydrogel is prepared while applying heat and stirring, but in the absence of the drug of interest. Dehydration occurs as the hydrogel is placed in a drying oven at a temperature of 100 °C. The endpoint of the dehydration is determined gravimetrically at 35% (w/w) HPMC. The dehydrated matrix is rehydrated with a mixture of drug, plasticiser and solvent. After a rehydration period of six weeks, the rehydrated mass with an HPMC percentage of 15% (w/w) is extruded from the barrel through an opening of 2 mm.

Phase I: Hydrogel-formation

A polymer suspension of E4M or E10M HPMC at a percentage of 10 or 20% (w/w) was prepared by heating purified water up to a temperature of 90-100 °C and adding HPMC as powder to the heated water under continuous stirring (VMS-C7-2, IKA, Staufen, Germany). After homogenisation, the polymer suspension was allowed to cool down to room temperature (22 ± 2 °C) resulting in a highly viscous solution. In addition to this, it was stored at 2 °C overnight in order to obtain full hydration of the polymer chains. For a further understanding of certain effects in the result section, it is important to note that the total mass of the prepared hydrogel was kept constant at 40 g.

Phase II: Dehydration of the polymer solution

The colloidal polymer solution was put in a drying oven (Thermo Scientific Heraeus Function Line T12, Langenselbold, Germany) at a temperature of 100 °C, well above the thermal gelation temperature, in order to dehydrate the HPMC polymer solution [36,37]. At this temperature, the HPMC molecules precipitate rapidly, resulting in the formation of a white polymer core, expelling water from its polymeric network as shown in figure 8. The water expelled from the polymer matrix is clear and removed by pouring it off. The dry percentage of the dehydrated polymer cylinder was set at 35% (w/w) and determined gravimetrically on an analytical balance (Mettler Toledo AB135-S, Greifensee, Switzerland). The drying period took up to several hours for polymer cylinders to partially dehydrate. After dehydration, the HPMC polymer cylinders revert to a clear matrix below the thermal gelation temperature.

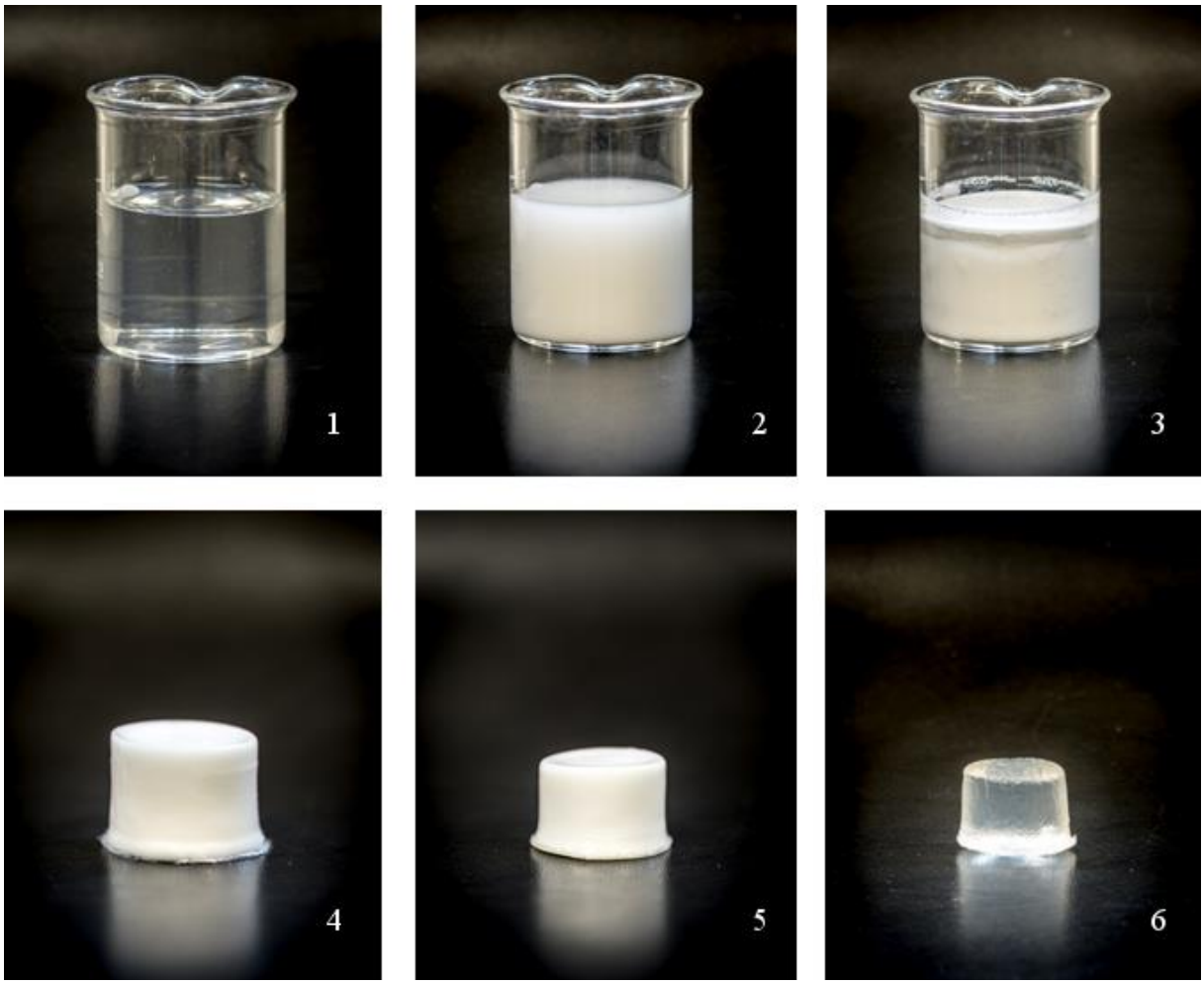

Fig. 8. Representation of the different stages of phase II, starting from a clear, highly viscous HPMC polymer solution (1) (hydrogel, T = 22 °C, 10% (w/w) HPMC) to a dehydrated polymer cylinder (2, 3, 4, and 5) when heated up to 100 °C and reverting to a clear, partially dehydrated polymer matrix (35% (w/w) HPMC) upon cooling to room temperature (6). Pictures 2, 3, 4 and 5 represent different stages during heating, showing that the dehydrated polymer cylinder shrinks as water is expelled from the matrix.

Phase III: Rehydration of the polymer cylinder with drug solution

The partially dehydrated polymer cylinder was rehydrated with drug solution. Prior to adding the drug solution, the partially dehydrated polymer cylinder was perforated centrally to allow the drug solution to reach the centre of the dehydrated polymer cylinder. A larger contact area with the drug solution facilitates the drug diffusion process. The diameter of the central cut was set at 5 mm.

Imbibition of the drug solution into the polymer cylinder occurred, even at temperatures as low as 2 °C. This temperature was chosen in favour of temperature stability of the potential thermolabile molecules to be incorporated. By means of passive diffusion, the drug solution migrates into the polymer cylinder avoiding the use of external forces to obtain a homogeneously loaded matrix.

Figure 9a shows a partially dehydrated HPMC polymer cylinder after placing the bottom part of the polymer cylinder in a sodium fluorescein solution. The polymer cylinder swells where it was submerged in the solution, while the dimensions of the upper half of the polymer cylinder remained more or less unchanged after two hours. This picture was merely taken to demonstrate the effect of swelling and drug solution uptake. In figure 9b, the end result of swelling is shown when a partially dehydrated polymer cylinder was fully submerged in a sodium fluorescein solution. Both components homogenised over the course of six weeks. The polymer cylinder absorbed the coloured solution over time after which it could be extruded. The time required to achieve full hydration and a homogeneous distribution of the drug is highly dependent on the ratio dehydrated polymer mass and drug solution, as well as on the physicochemical properties of the drug.

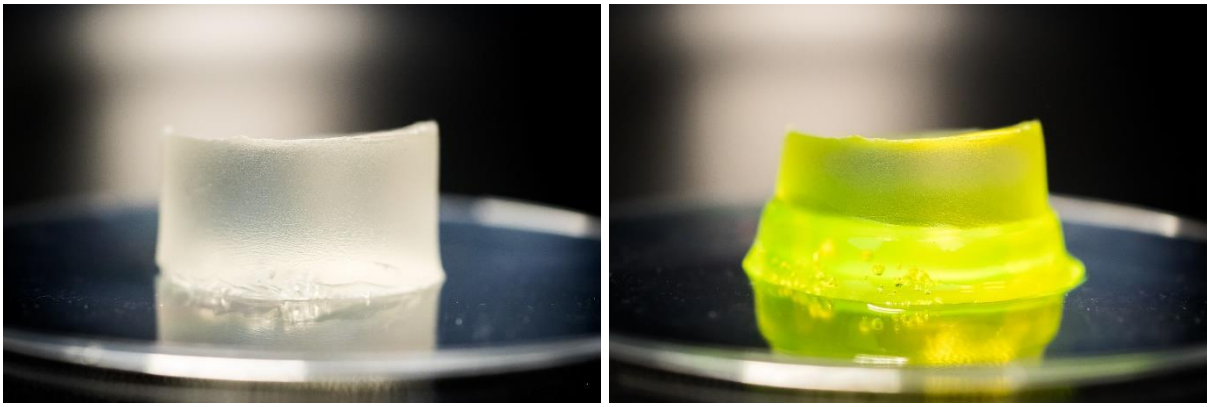

Fig. 9a. Effect of hydration and swelling, situation after two hours. The bottom part of a partially dehydrated HPMC polymer cylinder (L) was submerged in a sodium fluorescein solution, after which the submerged half of the polymer cylinder absorbed the yellow solution (R).

Fig. 9b. End result after a polymer cylinder had been fully submerged in a sodium fluorescein solution over the course of six weeks. Notice how the highly viscous mass does not appear to flow when lying flat on the surface. *Picture taken from above. The samples in these pictures have only been prepared and photographed for demonstrative purposes.*

Due to the inherently low temperature during phase III, the high viscosity of the polymer cylinder and the low diffusional rate lowers the rehydration rate compared to when rehydration would occur at room temperature. For this reason, the rehydration process takes up to several weeks depending on the formulation parameters and the mass produced before extrusion.

Phase IV: Extrusion

After obtaining a semisolid hydrogel in the barrel, the content was manually extruded by means of gentle force where the piston of the barrel extruded the mass through an opening with a diameter of 2 mm after a period of six weeks. A photograph of the insert loaded with sodium fluorescein, with a diameter of 2 mm and a length of 10 mm, is shown in figure 10.

Fig. 10. Extruded insert loaded with sodium fluorescein. The dimensions of the inserts are 2 mm diameter and 10 mm in length.

2.4 Factorial design of experiments

It is clear from the description of the method, that a number of parameters might influence the properties of the inserts obtained. For experiments to be performed efficiently, experimental design allows researchers to obtain a maximum of information about a process while requiring fewer experiments. The influence of four different parameters on the properties of the inserts was evaluated using a 2^4 full factorial design. All formulations were carried out in duplicate to estimate the experimental error. The polymer type, initial percentage HPMC, final percentage glycerol and the drying period of the insert after extrusion were chosen as the factors investigated. All parameters have a certain degree of influence on the viscosity of the inserts extruded. The viscosity of the matrix is regarded as an important release rate determining factor. A total number of 32 experiments was carried out and an overview is presented in table 3. The lower and higher values are represented by (-) or (+) levels, which are given in table 2. The statistical analysis of the data was performed with Statistica® software (Statsoft, Tulsa, USA) using analysis of variance (ANOVA). Effects are considered statistically significant at a level of $p<0.05$.

Table 3. Factorial design of experiments for the preparation of inserts in the initial stage of development.

Formulation	*Polymer type*	*Initial % HPMC*	*Final % glycerol*	*Drying period after extrusion*
1	+	+	+	+
2	+	+	+	-
3	+	+	-	+
4	+	+	-	-
5	+	-	+	+
6	+	-	+	-
7	+	-	-	+
8	+	-	-	-
9	-	+	+	+
10	-	+	+	-
11	-	+	-	+
12	-	+	-	-
13	-	-	+	+
14	-	-	+	-
15	-	-	-	+
16	-	-	-	-

Table 2. The values for the upper (+) level and lower (-) level of the factors investigated in the factorial design.

Fixed parameter		
Final % HPMC	15% (w/w)	
Variable parameters		
	(+) level	***(-) level***
Polymer type	E10M	E4M
Initial % HPMC	20% (w/w)	10% (w/w)
Final % glycerol	10% (w/w)	5% (w/w)
Drying period after extrusion	90 min	45 min

2.5 Characterisation of the extruded inserts

To assess the properties of the inserts after extrusion, several tests were carried out. The uniformity of content determines whether the distribution of the drug molecules complies with the limits set by the Ph. Eur. 7.6 [46]. Furthermore, a characterisation of the drying process, tensile strength and elongation tests, water uptake and drug release studies were performed.

2.5.1 Uniformity of content

As no active forces are applied on the hydrogel mass and the drug solution during the rehydration process, the drug solution is absorbed by the partially dehydrated polymer cylinder merely by means of passive diffusion. To determine the distribution of the sodium fluorescein molecules in the rehydrated mass, ten samples were taken at random after extrusion. Each of the inserts was dissolved in 50 ml of PBS solution while stirring overnight at room temperature on a magnetic stirring device (Variomag poly 15, H+P labortechnik AG, Munich, Germany) at a rate of 650 rpm. After completion of the dissolution process, the absorbance was measured spectrophotometrically at a wavelength of 484 nm.

The Ph. Eur. 7.6, monograph 2.9.6 *Uniformity of content of single-dose preparations (test A)* states that the content of each of ten measured samples should lie within 85 - 115% of the average content. It does not comply with the test if at least one sample fails to fall within the limits stated above. In case of a single sample not meeting the requirement, this sample should lie within 75 -

125% limits. In this case, an additional number of 20 samples should be taken and measured which all should comply with the limits between 85 - 115%.

2.5.2 Characterisation of the drying process

After extrusion, the inserts were dried for either 45 or 90 minutes in a laminar flow cabinet (Safemate 1.8, Euroclone, Pero, Italy) under continuous flow (inflow: 0.54m/s, downflow: 0.39 m/s). The influence of the 'polymer type' and 'final % glycerol' on the drying process was determined. For each formulation, three inserts weighing 150 mg each were taken at random. These samples were weighed carefully before and after the drying process. The amount of evaporated water was calculated with the following formula and expressed as a percentage (W):

$$W = \frac{m_i - m_f}{m_i} .100\%$$

W: percentage water evaporated from the insert

m_i: initial mass of the insert before the drying process

m_f: final mass of the insert after the drying process

Only the results of inserts complying with the test *uniformity of content* as described in section *2.5.1 Uniformity of content* are given and discussed in the results section.

2.5.3 Tensile strength and elongation

Tensile strength is defined as the maximum force a sample can withstand during elongation until it breaks. Elongation is defined as the maximum length of a sample before the sample ruptures. These are useful mechanical properties for a drug delivery device to understand the behaviour of the product when the final product is packaged, handled by the patient or applied in the eye.

To determine the tensile strength of the inserts, three samples of 10 cm each were extruded for every formulation of the experimental design, in duplicate. The extrusion product was dried before measurements, following the drying conditions as described in section *2.5.2 Characterisation of the drying process*. Both ends of the sample were attached to a custom built measuring device with an initial length of the extrusion product of 20 mm. Consequently, increasing weights were attached to exhibit forces on the insert. The length of the extrusion product before rupture was monitored continuously to determine the maximum elongation.

2.5.4 Water uptake of inserts

The swelling properties of the inserts were determined. Swelling affects the drug release from the polymeric matrix as the insert can no longer retain its shape. The water uptake was studied gravimetrically at room temperature (22 ± 2 °C) using a Baumann capillary apparatus. For each experiment, a sample of 150 mg was weighed carefully on an analytical balance and placed on the fritted glass filter of the Baumann apparatus filled with PBS medium. After time intervals of 2, 4 and 24 hours, the mass of the insert was weighed to measure the amount of PBS absorbed by the insert. The measurements were carried out in quadruplicate for each formulation. The amount of water uptake was calculated as follows:

$$W = \frac{m_a - m_d}{m_d} .100\%$$

W: amount of PBS absorbed by the insert expressed as a percentage

m_a: mass of the insert after absorption of medium

m_d: mass of the insert before absorption of medium

2.5.5 Drug release measurement

The amount of sodium fluorescein released from the inserts was determined by cumulative release. For each formulation, samples of 150 mg were taken in duplicate and dried following the method described in section *2.5.2 Characterisation of the drying process* and during 45 or 90 minutes according to the design of experiments. The dried sample was put in a test tube at 2 cm above the bottom of the tube to which 10 g of PBS solution was added. The test tube was placed in a non-oscillating hot water bath (Julabo 20B, Merck-Belgolabo, Overijse, Belgium) at a temperature of 32.0 ± 0.5 °C, corresponding to the lowest temperature of the ocular surface [47]. After sampling intervals of 20, 40, 60, 180 and 300 minutes, 5 g of sample was taken and replaced with fresh PBS medium at 32 °C. The absorbance of the samples was measured spectrophotometrically at a wavelength of 484 nm. After 300 minutes, the insert was dissolved entirely by shaking the test tube to release all of the remaining drug. The drug content was calculated from the total percentage drug present in the insert. Only samples complying with the uniformity of content, as described in section *2.5.1 Uniformity of content,* were plotted.

3 RESULTS AND DISCUSSION

3.1 Uniformity of content

After measuring the content of ten at random taken samples from each formulation (A) and its duplicate (B) (cf. Table 3.), the results are shown in figures 11a and 11b. The average content of all measured inserts is considered 100%. In green, the 85% and 115% limits set by the Ph. Eur. 7.6, monograph 2.9.6 are given. The blue and orange bars represent the lowest and highest value of content of ten measured samples respectively. All formulations of which the lowest and highest content values are calculated within the 85 - 115% limits, comply with the test.

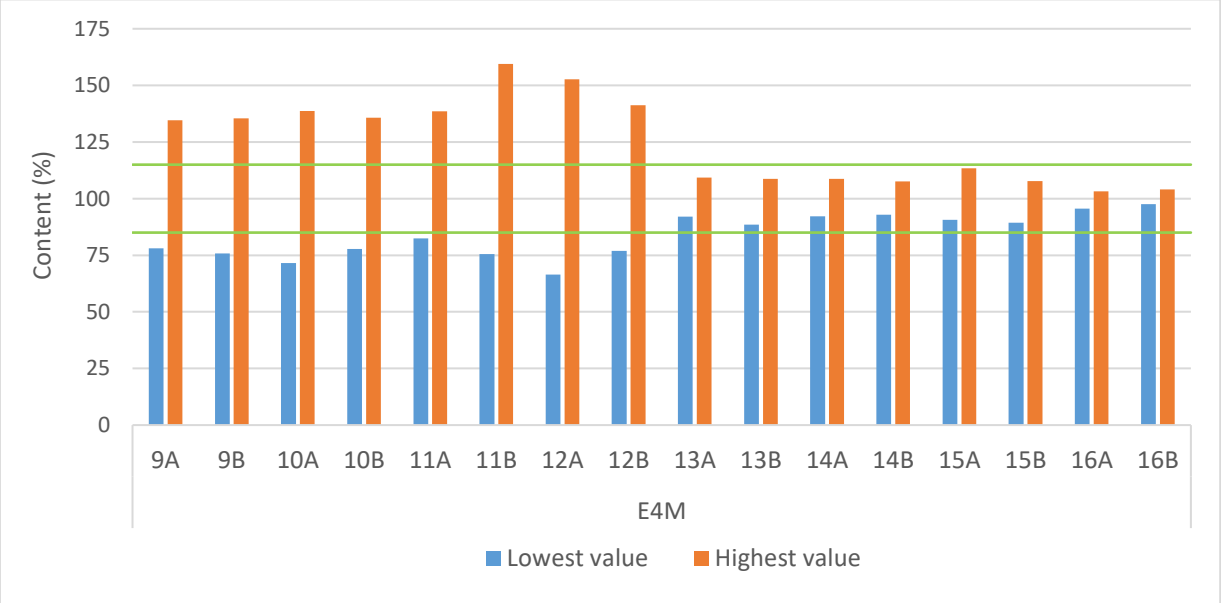

Fig. 11a and 11b. Overview of the sodium fluorescein content in formulations with HPMC E10M and E4M respectively. The 85% and 115% limits are indicated with green lines.

There is not a single formulation prepared with an initial HPMC concentration of 20% (w/w) (F1-4 and F9-12) that complies with the limits of monograph 2.9.6. With exclusion of formulation 6B, two distinct groups can be identified. All inserts prepared with an initial HPMC percentage of 10% (w/w) (F5-8 and F13-16) comply with the test for uniformity of content. Just one of ten extruded inserts from formulation 6B falls short of the 85% limit (84.6%). According to the guidelines of the Ph. Eur. 7.6, an additional number of 20 samples should have been extruded and measured. From a practical point of view, this was not feasible.

The influence of the various parameters on the drug loading was calculated through statistical analysis on the relative standard deviation (RSD) of the drug content of each formulation. The results are given in table 4. A low value for the RSD is indicative for small variations of the individual contents of the inserts compared to the average content of all inserts. The term 'effect' expresses the average value by which a parameter is changed when altering the parameter from the lower level to the upper level.

Table 4. Statistical analysis on RSD of the uniformity of content.

Parameter	Effect (%)	p-value
Polymer type	-2.49	0.054
Initial % HPMC	16.88	0.000
Final % glycerol	-1.48	0.237

Statistical analysis confirms that the initial percentage of HPMC has the largest significant influence ($p = 0.000$) on the homogeneous distribution of sodium fluorescein molecules in the polymer mass upon rehydration. Changing the initial percentage of HPMC from the (-) level (10% (w/w)) to the (+) level (20% (w/w)) increases the RSD with 16.88% on average. This means that samples prepared with an initial HPMC percentage of 10% (w/w) instead of 20% (w/w) yield inserts with the smallest variation on drug content. The type of polymer used (E4M or E10M) also seems to have a modest effect on the RSD, but compared to the initial percentage of HPMC, this effect can be regarded as being minor and strictly spoken, this effect is not considered being statistically significant.

While preparing the inserts, it was clear that the geometry of the dehydrated polymer cylinder was of great importance. The geometry of the dehydrated polymer cylinder is closely linked to the initial percentage HPMC. It is likely one of the most important factors determining the distribution of drug molecules in the polymer cylinder. The experimental design described in this chapter did not allow

to evaluate the effect of geometry directly. The importance of the geometry can be explained by Fick's first law and the Stokes-Einstein law as given below.

Fick's first law

$$J = -D.\frac{dC}{dx} \qquad (mol/m^2s)$$

J = flux of drug molecules

D = diffusion coefficient

dC = change in drug concentration

dx = change in drug diffusion distance

Stokes-Einstein law

$$D = K_b.T.\frac{1}{6\pi\eta r} \qquad (m^2/s)$$

D = diffusion coefficient

K_b = Boltzmann constant

T = absolute temperature of the system

η = viscosity of the polymer cylinder

r = hydrodynamic radius of the migrating particles

However, with drug diffusion occurring in one or more dimensions during drug loading, a change in drug concentration and therefore non-constant mass flux takes place. In this case of non-steady state, Fick's second law is applicable and given as follows:

$$\frac{dC}{dt} = \frac{dJ}{dx} = D.\frac{d^2C}{dx^2}$$

Fick's second law states that the change in concentration with time in a particular region is proportional to the change in the concentration gradient at that point of time.

As the mass prepared during phase I (hydrogel formation) was kept constant at 40 g, this implicates that a hydrogel with an initial percentage of 20% (w/w) has a different volume when it is dehydrated to 35% (w/w) HPMC compared to a hydrogel with an initial percentage of 10% (w/w) dried to the

same level. As an equal mass of hydrogel was prepared for both 10% (w/w) and 20% (w/w) HPMC, the volume of the partially dried polymer cylinder prepared from 20% (w/w) is larger. This means that the surface area for contact between the drug solution and the partially dehydrated polymer cylinder is larger, speeding up the diffusion process. On the other hand, a larger volume also means that the diffusion distance (dx) the molecules have to travel, is longer, slowing down the distribution of drug molecules. In addition, a polymer cylinder with larger dimensions will reach the boundaries of the recipient more quickly upon swelling in comparison to a polymer cylinder of 10% (w/w) HPMC. From that moment on, the swelling can only continue axially. This reduced surface area will slow down the diffusion process. The geometry of the partially dehydrated polymer cylinder in relation to its recipient clearly plays an important role on the diffusion pathway of the drug molecules. Therefore, in the next chapter, the geometry of the polymer matrix will be investigated in more depth.

The data shown in table 4 is visually illustrated in the following surface plot. The effect of the 'initial % HPMC' and 'polymer type' on the RSD is shown figure 12.

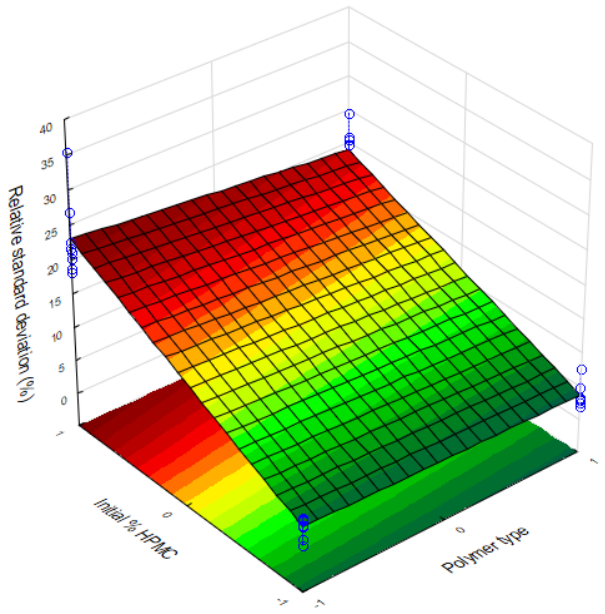

Fig. 12. Influence of the 'initial % HPMC' and 'polymer type' on the RSD of the average sodium fluorescein content in the inserts measured.

The surface plot shows that the initial percentage HPMC can be held responsible for the largest effect on the RSD, while the influence of the type of polymer is very limited.

3.2 Characterisation of the drying process

After extrusion, the inserts were dried following the given time periods in the design of experiments. The parameters 'type polymer' and 'percentage plasticiser' were studied and statistically analysed as they were expected to have a possible influence on the *in vitro* release, water uptake, tensile strength and elongation of inserts. The results of the loss of water during the drying process is given in table 5 while in table 6 the statistical analysis is presented.

Table 5. The average loss of water is given per insert complying with the uniformity of content and expressed as a percentage compared to its initial weight. Inserts marked with (*) were dried during 90 minutes instead of 45 minutes.

Insert	Average loss of water (%)	Standard deviation
5A	45.49	± 3.95
5B	45.61	± 2.83
6A	27.73	± 0.72
6B	35.03	± 3.65
7A	52.54	± 0.95
7B	51.72	± 1.57
8A	24.75	± 1.64
8B	25.17	± 1.81
13A	50.93	± 2.85
13B	48.63	± 4.42
14A	25.63	± 0.56
14B	26.43	± 2.92
15A	45.94	± 1.71
15B	43.94	± 1.20
16A	21.81	± 0.92
16B	21.62	± 0.59

Table 6. Statistical analysis on the loss of water.

Parameter	Effect (%)	p-value
Polymer type	1.32	0.497
Final % glycerol	3.07	0.134
Drying period	21.26	0.000

From table 6, the most influential parameter on the loss of water is unsurprisingly the parameter 'drying period' (p = 0.000). On average, an additional 21.26% (w/w) water is lost when changing the drying period from 45 minutes to 90 minutes. The influence of both 'polymer type' and 'final % glycerol' are not considered statistically significant. These effects are graphically laid out in figures 13a and 13b by means of surface plots.

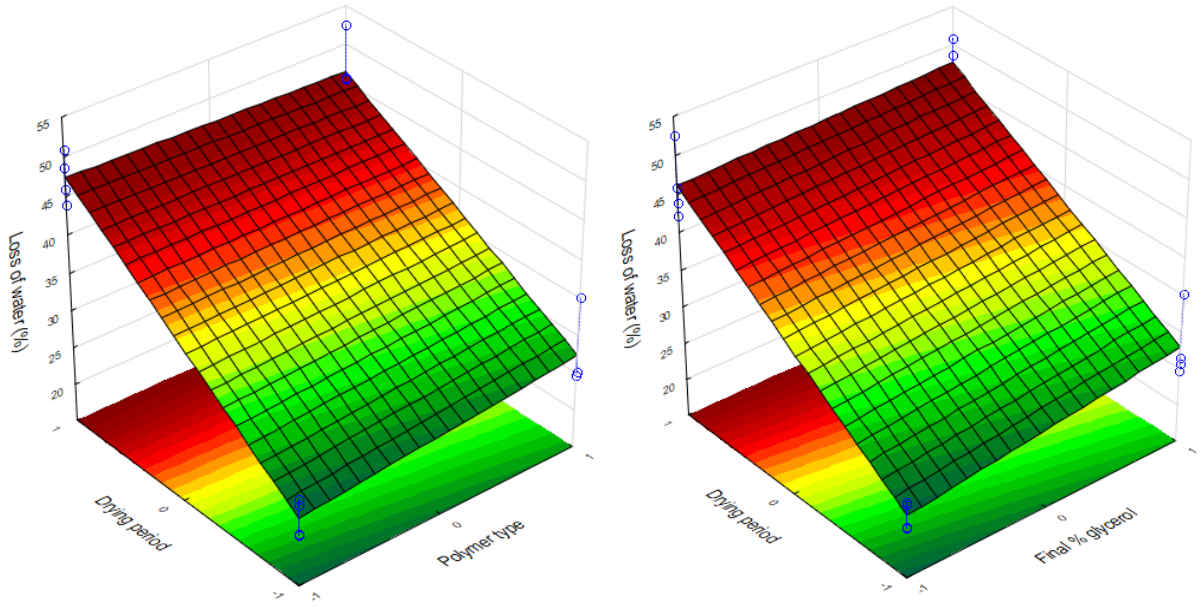

Fig. 13a and 13b. Effect between the 'drying period' and 'polymer type' (a) and the 'drying period' and the 'final % glycerol' (b) on the amount of water lost from the insert.

Figures 13a and 13b indicate that changing the drying period from 45 minutes ((-) level) to 90 minutes ((+) level) increases the amount of water lost from the insert irrespective of the level of the parameters 'final % glycerol' and 'polymer type'. Interestingly, both HPMC and glycerol are known to be hygroscopic compounds and a significant retention of water was expected when increasing the value of these parameters. Statistical analysis reveals that their effect on the amount of water in the insert is small compared to the influence of the drying period and not statistically significant.

3.3 Tensile strength and elongation

The tensile strength of the extruded and dried inserts was measured for all samples complying with the uniformity of content. The results are graphically presented in figure 14a for HPMC type E10M and in figure 14b for HPMC type E4M, the statistical analysis is given in table 7.

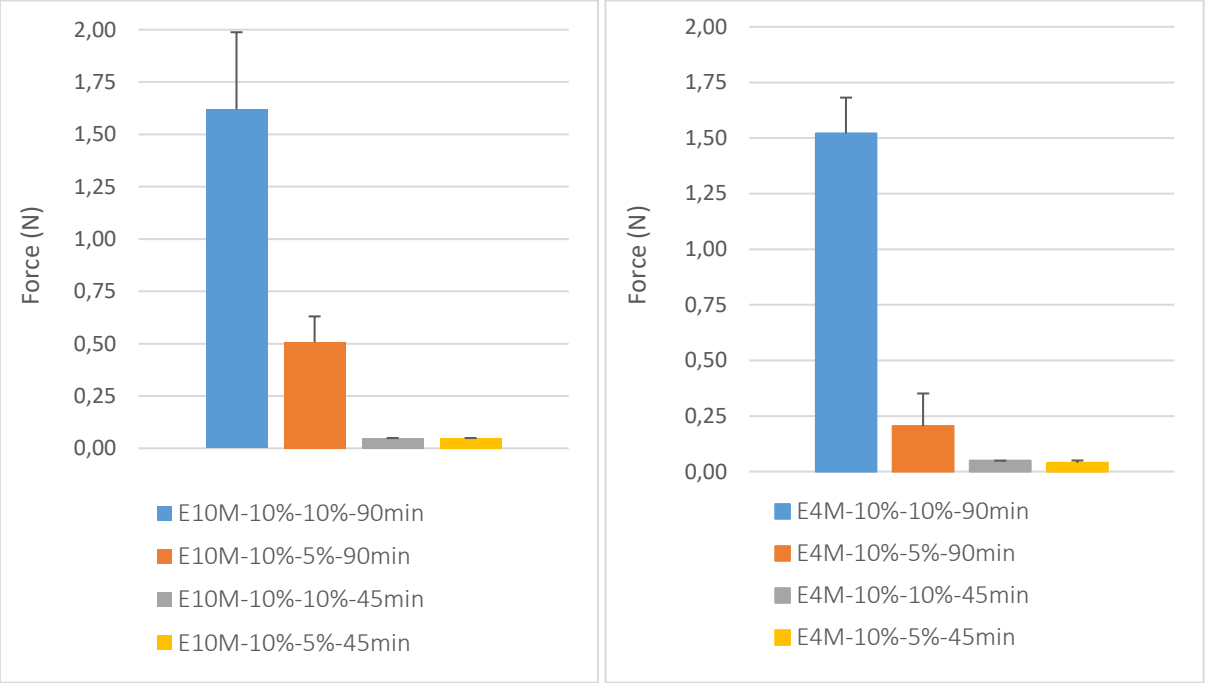

Fig. 14a and 14b. Comparison of the tensile strength between different inserts prepared with HPMC E10M and E4M respectively. Only inserts complying with the uniformity of content are shown. The designation of the legend is as follows: HPMC type – initial % HPMC – final % glycerol – drying time after extrusion.

Table 7. Statistical analysis on the tensile strength.

Parameter	Effect (N)	p-value
Polymer type	0.10	0.069
Final % glycerol	0.61	0.000
Drying period	0.92	0.000
Interaction effect polymer type – final % glycerol	-0.05	0.309
Interaction effect polymer type – drying period	0.10	0.081
Interaction effect final % glycerol – drying period	0.61	0.000

Firstly, the main effects of the measured parameter are given, followed by the interaction effects. Interaction effects represent the combined effects of factors on the dependent measure. When an

interaction effect is observed, the impact of one factor depends on the level of the other factor. Therefore, in case of statistically significant interaction effects, interpretation of the main effects is incomplete or misleading. Part of the power of ANOVA is the ability to estimate and test interaction effects [48].

The results from table 7 show a statistically significant effect for the 'final % glycerol' and the 'drying period'. The parameter 'polymer type' was expected to have a significant influence on the tensile strength, but falls short of the threshold value of statistical significance. A more accurate measuring device might have changed the outcome of the results obtained. The largest effect can be seen for the drying period, which means that drying the inserts for 90 minutes will yield inserts with higher HPMC percentages and therefore higher tensile strengths. But the effect of the drying period appears to be linked to the amount of glycerol in the insert (interaction effect) as shown in figure 15. Inserts prepared with 10% (w/w) glycerol can withstand higher forces than inserts prepared with 5% (w/w) glycerol, particularly after 90 minutes of drying as opposed to 45 minutes where the influence of the percentage glycerol is minimal. This is a clear example stressing the importance of interpreting the interaction effect (p = 0.000) between the 'final % glycerol' and the 'drying period'.

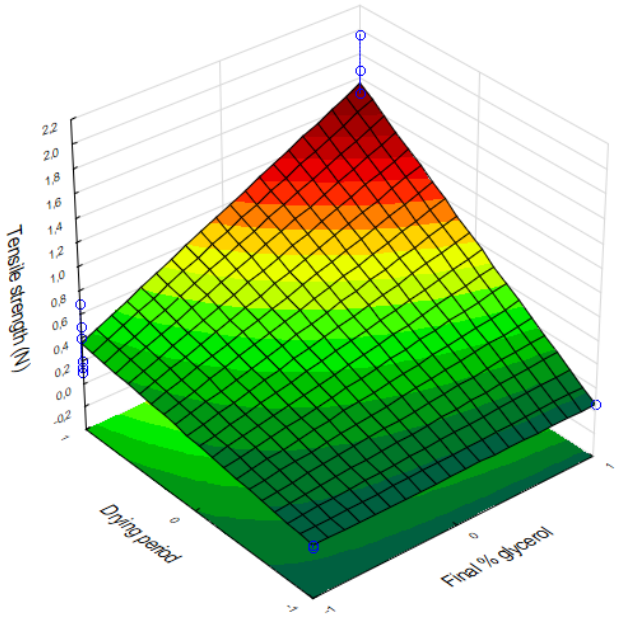

Fig. 15. Interaction effect and influence of the 'drying period' and 'final % glycerol' on the tensile strength of the inserts.

A possible explanation why the influence of glycerol is higher for the tensile strength after 90 minutes of drying, can be given when the ratio plasticiser/water is considered. Water basically acts

as a plasticiser, therefore, drying for an extended period of time reduces water levels in the insert and increases the relative amount of glycerol in the insert. This makes the effect of glycerol on the tensile strength more pronounced after 90 minutes of drying. When more water is present in the insert, the relative impact of glycerol as a plasticiser is reduced and mobility of the polymer chains is increased, lowering the tensile strength.

The elongation of the insert is expressed as the ratio between the final length of the insert before it breaks, compared to the initial length of the insert and is expressed as a percentage. The results of elongation of the measured inserts is given in the following figures 16a and 16b. Statistical analysis is presented in table 8.

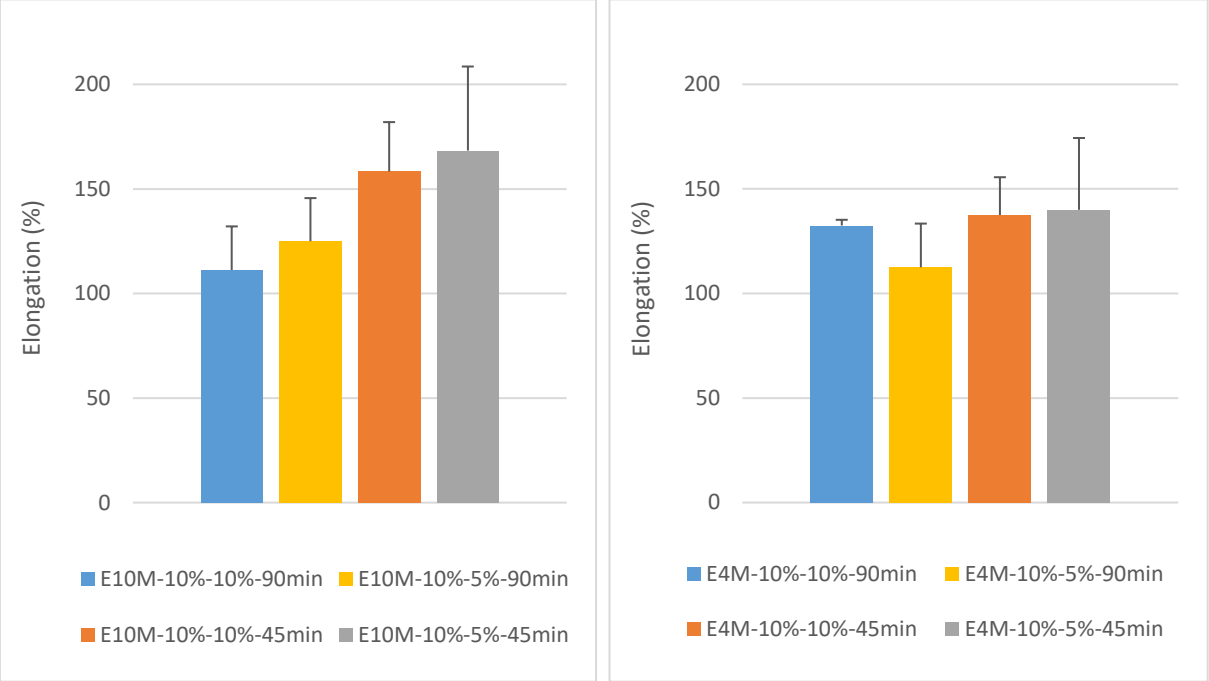

Fig. 16a and 16b. Comparison of the elongation between different inserts prepared with HPMC E10M and E4M. Only inserts complying with the uniformity of content are shown. The designation of the legend is as follows: HPMC type – initial % HPMC – final % glycerol – drying time after extrusion.

Table 8. Statistical analysis on the elongation of inserts.

Parameter	Effect (%)	p-value
Polymer type	10.10	0.254
Final % glycerol	-1.56	0.855
Drying period	-30.73	0.005

As expected, drying the inserts for a longer period of time (90 minutes instead of 45 minutes) reduces elongation by 30.73%. The 'drying period' was found to be the only statistically significant parameter (p = 0.005) on the elongation of the inserts. A graphical representation of the influence of the 'drying period' compared to 'polymer type' and 'final % glycerol' is given in figure 17a and 17b.

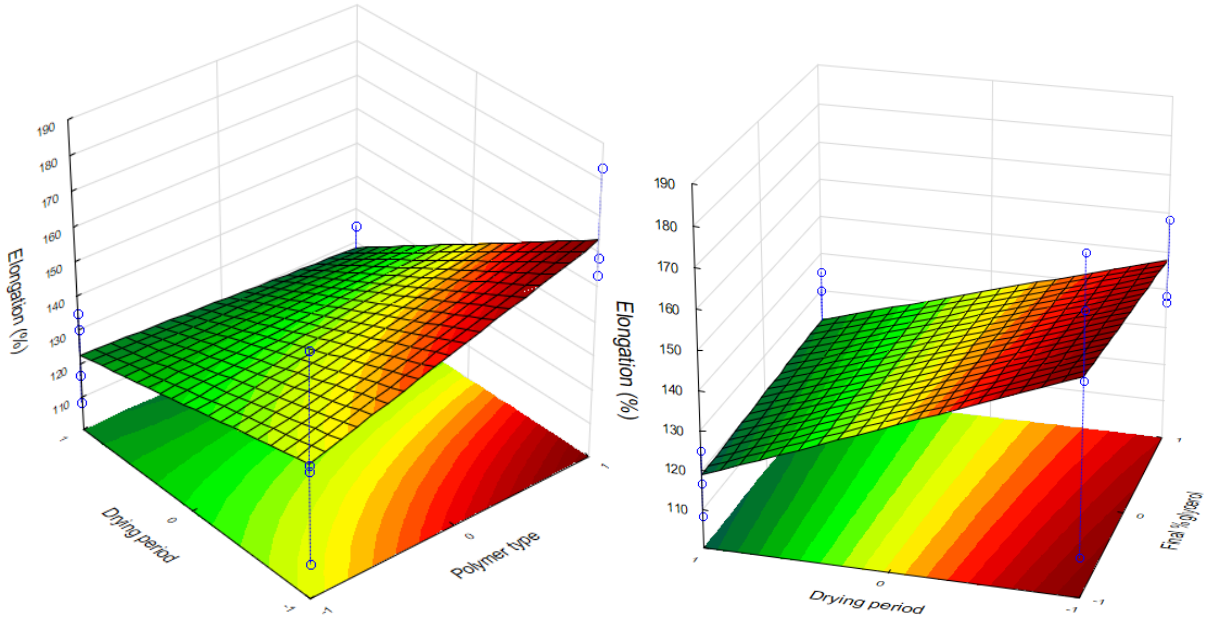

Fig. 17a and 17b. Effect between the 'drying period' and the 'polymer type' (a) and the 'drying period' and the 'final % glycerol' (b) on the elongation of the insert.

The influence of the 'polymer type' and 'final % glycerol' is relatively small and not statistically significant compared to the effect of the 'drying period' on the elongation.

3.4 Water uptake of inserts

The degree of hydration and the time required for the inserts to lose their shape was measured. The results for water uptake are given in figures 18a and 18b. Statistical analysis was carried out on every measured time point (2, 4 and 24 hours) and a summary is given in table 9.

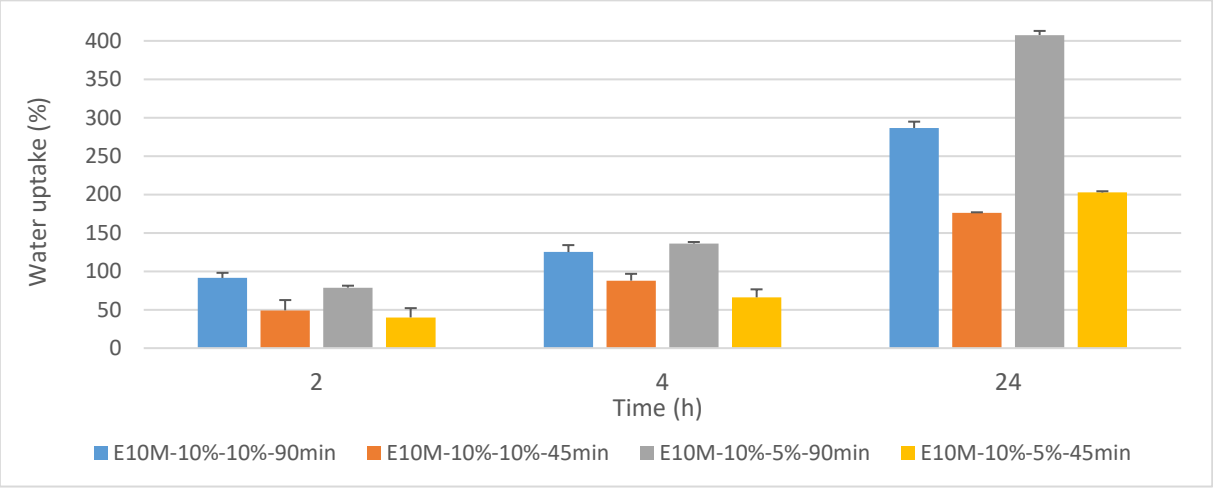

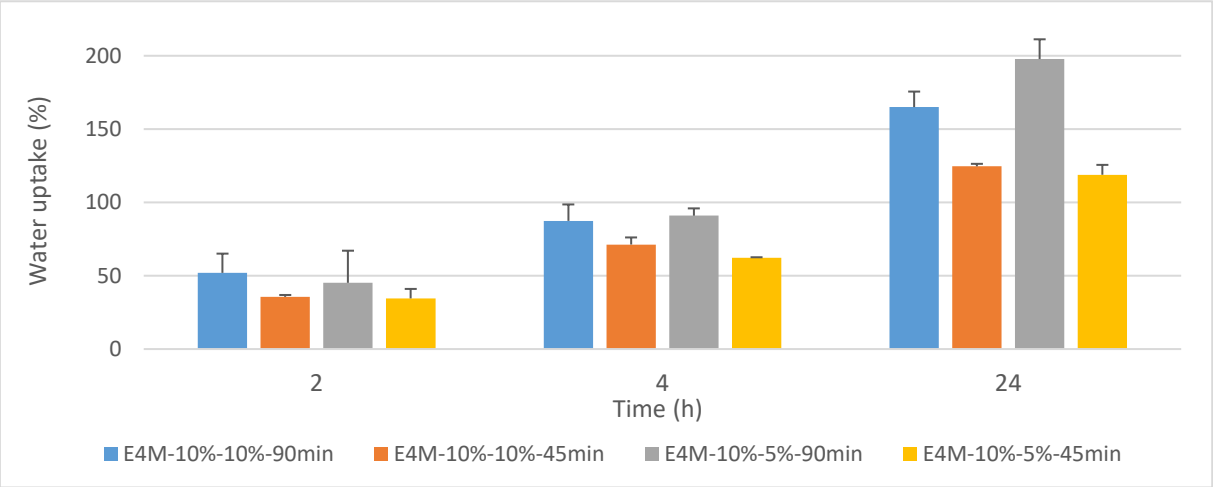

Fig. 18a and 18b. Comparison of the water uptake between different inserts prepared with HPMC E10M and E4M respectively and complying with the uniformity of content. The designation of the legend is as follows: HPMC type – initial % HPMC – final % glycerol – drying time after extrusion.

From figure 18a and 18b, a distinct difference in water uptake can be observed between the polymer types HPMC E10M and E4M. Particularly after 24 hours, HPMC E10M approximately doubled the amount of water taken up compared to HPMC E4M. This can be attributed to the larger hydrodynamic volume occupied by higher molecular weight chains when hydrated. As the polymer chains become more hydrated, disentanglement of polymer chains will occur. Polymers with a higher polymerisation degree, such as HPMC E10M in this case, are able to absorb more water before disentanglement will take place [49,50].

Table 9. Statistical analysis on the water uptake of inserts.

Parameter	Effect (%) 2 h	p-value	Effect (%) 4 h	p-value	Effect (%) 24 h	p-value
Polymer type	23.04	0.000	25.85	0.000	116.78	0.000
Final % glycerol	7.41	0.022	4.01	0.299	-43.59	0.001
Drying period	26.99	0.000	38.01	0.000	108.58	0.000
Interaction effect polymer type – final % glycerol	3.50	0.224	1.30	0.728	-30.12	0.009
Interaction effect polymer type – drying period	13.48	0.001	15.62	0.002	48.95	0.000
Interaction effect final % glycerol – drying period	2.28	0.417	-11.35	0.012	-33.24	0.005

The largest effect on the water uptake is observed for the 'polymer type' and 'drying period' from the initial measuring point after two hours up till 24 hours. By dehydrating the inserts for a longer period, the inserts are able to absorb larger quantities of water. Even though the overall effect is smaller, after two hours, the amount of water absorbed by the insert is also higher when 10% (w/w) glycerol is used ($p = 0.022$) likely due to the hygroscopic effect of glycerol.

The interaction effect between the 'polymer type' and the 'drying period' results in the highest water uptake when HPMC E10M is used and even more pronounced when the drying period is increased ($p = 0.000$). An additional interaction effect is also seen between the 'final % glycerol' and the 'drying period' after four hours ($p = 0.012$) and between the 'polymer type' and the 'final % glycerol' after 24 hours ($p = 0.009$). At first glance, it might seem strange that adding a higher percentage of glycerol has a negative impact on the water absorbing properties of the inserts by 11.35% (w/w), but this could be indicative for competition between glycerol and HPMC. During preliminary studies, glycerol in a percentage up to 50% (w/w) of the drug solution was added to the dehydrated polymer cylinder, in order to see the effect of high amounts of plasticiser on the rehydration process. It was noticed that rehydration of the polymer cylinder did not occur at all in the presence of high amounts of glycerol. Even five years after preparing the sample, both phases (dehydrated polymer cylinder and the drug solution containing glycerol) are still present.

Figures 19a and 19b show the interaction effects of 'drying period', 'polymer type' and 'final % glycerol' on the water uptake after 24 hours.

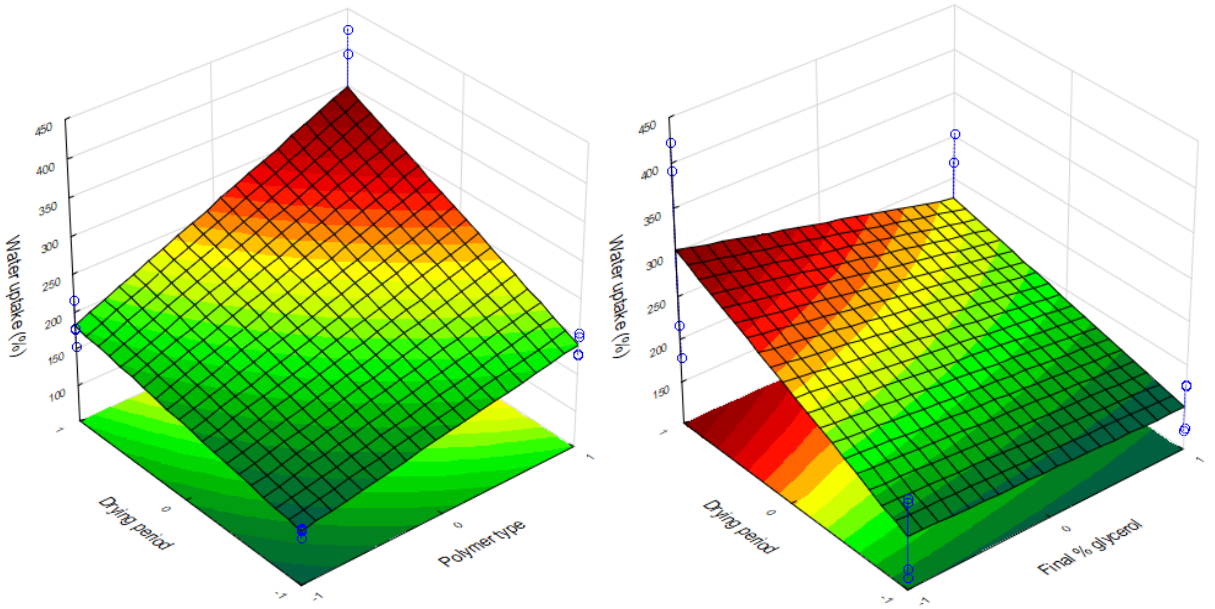

Fig. 19a and 19b. Effect between the 'drying period' and the 'polymer type' (a) and the 'drying period' and the 'final % glycerol' (b) on the water uptake capacity of the inserts after 24 hours.

In figure 19a, it can be seen that changing the polymer type from E4M ((-) level) to E10M ((+) level) gives an additional effect on the water uptake when the drying period is set to 90 minutes ((+) level) compared to 45 minutes ((-) level). A similar effect was found for the 'final % glycerol', where using a percentage of glycerol of 5% (w/w) ((-) level) instead of 10% (w/w) ((+) level) resulted in an additional effect on the water uptake when drying the inserts for 90 minutes after extrusion.

3.5 Drug release measurement

The sodium fluorescein release curves from the extruded inserts are drawn in figure 20 for inserts prepared from HPMC E10M and HPMC E4M.

At this stage of the development, the main goal was to investigate whether slow release profiles could be obtained. For both HPMC types, sodium fluorescein was released in a slow release manner by means of diffusion or, most likely to a lesser extent, erosion with no appreciable lag time. Solvent absorption into the matrix causes polymer chain relaxation and volume expansion which in turn facilitates the drug diffusion into the surrounding medium [51]. About 50% of the total amount of sodium fluorescein was released between 120-180 minutes, while 70-80% of sodium fluorescein is

released after 300 minutes. The chosen parameters of the insert do not have a significant impact on the release rate of sodium fluorescein, most likely due to its low molecular weight (0.376 kDa).

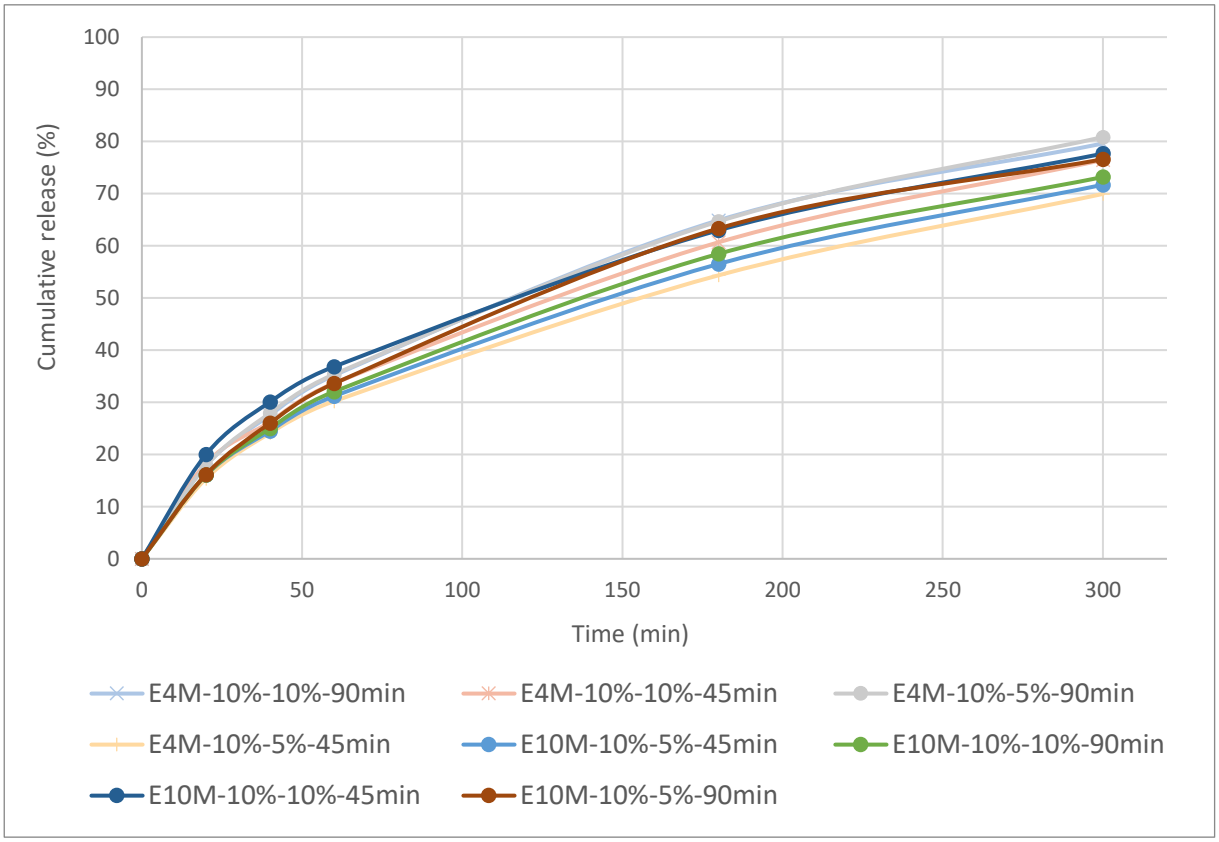

Fig. 20. Comparison of release profiles from inserts developed with HPMC E4M and E10M. The designation of the legend is as follows: HPMC type – initial % HPMC – final % glycerol – drying time after extrusion (n=4).

From visual observation, an immediate release of yellow-coloured sodium fluorescein was seen from the surface of the insert. Generally, the release process of the HPMC molecules of the inserts can be described as a combination of a two-stage process [52]. Firstly, the HPMC matrix absorbs water from the release medium after which the insert hydrates and the rate of diffusion of drug molecules accelerates. In the second stage, swelling of the unlinked polymer matrix causes disentanglement and hence inserts to erode, releasing the drug molecules further. In case of small, highly water-soluble molecules, drug diffusion will occur before polymer erosion takes place [13,14,16,52]. The chosen formulation parameters might have a significant impact on the release rate and kinetics of larger molecules, as will be investigated in more depth in the following chapters.

4 CONCLUSION

In this chapter, a first proof of concept was demonstrated. The method developed showed it is possible to formulate inserts loaded with a tracer molecule such as sodium fluorescein with slow release properties but without the need for shear forces, heat or air entrapment. The inserts were flexible in order to reduce foreign-body sensation and hence circumvent the defence mechanisms of the eye. The initial percentage HPMC was the main influencing factor for a homogeneous distribution of sodium fluorescein molecules during rehydration, not necessarily due to the percentage chosen, but due to the geometry of the partially dehydrated polymer cylinder as a result of the initial percentage HPMC. As expected, the drying percentage of HPMC had the largest influence on the tensile strength and elongation. The HPMC type E10M appeared to have greater water uptake capacity compared to E4M most likely caused by its longer polymer chains which allow more hydration before disentanglement starts to occur. The amount of plasticiser has an important influence on the behaviour of the water uptake. Changing the chosen parameters had a limited influence on the drug release amounts of sodium fluorescein over time, caused by the relatively small size of sodium fluorescein, but the goal of obtaining slow release profiles was achieved.

The most interesting observation was the impact of the initial HPMC percentage, or indirectly the geometry of the polymer cylinder as a result of the chosen HPMC percentage, on the drug loading process. Therefore, in the next chapter, a new experimental design was set up starting with HPMC E10M in order to investigate the effect of geometry on the drug loading characteristics in closer detail. In order to estimate the relative influence of the viscosity of the insert, HPMC K100M with an intrinsically higher viscosity grade was added to the comparison, despite less favourable ophthalmic characteristics as mentioned earlier. Furthermore, a globular model protein (lysozyme) was loaded in inserts, using the basic principles of the method developed with further improvements to accelerate the drug loading rate.

References

1. Barakat MR, Kaiser PK. VEGF inhibitors for the treatment of neovascular age-related macular degeneration. Expert Opin Investig Drugs. 2009;18: 637–646.
2. Yazdi MH, Faramarzi MA, Nikfar S, Falavarjani KG, Abdollahi M. Ranibizumab and aflibercept for the treatment of wet age-related macular degeneration. Expert Opin Biol Ther. 2015;15: 1349–1358.
3. Pleyer U, Stübiger N. New pharmacotherapy options for noninfectious posterior uveitis. Expert Opin Biol Ther. 2014;14: 1783–1799.
4. Mesquida M, Molins B, Llorenç V, Sainz De La Maza M, Adán A. Long-term effects of tocilizumab therapy for refractory uveitis-related macular edema. Ophthalmology. 2014;121: 2380–2386.
5. Chang J-H, Garg N, Lounde E, Han kyu yeon, Sandeep J, Azar D. Corneal Neovascularisation: An Anti-VEGF Therapy Review. Surv Ophthalmol. 2012;57: 415–429.
6. Liarakos VS, Papaconstantinou D, Vergados I, Douvali M, Theodossiadis PG. The effect of subconjunctival ranibizumab on corneal and anterior segment neovascularization: Study on an animal model. Eur J Ophthalmol. 2013;24: 299–308.
7. Vogt W. Oxidation of methionyl residues in proteins: Tools, targets, and reversal. Free Radic Biol Med. 1995;18: 93–105.
8. Di Stasio E, De Cristofaro R. The effect of shear stress on protein conformation: Physical forces operating on biochemical systems: The case of von Willebrand factor. Biophys Chem. 2010;153: 1–8.
9. Torosantucci R, Schöneich C, Jiskoot W. Oxidation of therapeutic proteins and peptides: Structural and biological consequences. Pharm Res. 2014;31: 541–553.
10. Nguyen T, Latkany R. Review of hydroxypropyl cellulose ophthalmic inserts for treatment of dry eye. Clin Ophthalmol. 2011;5: 587–591.
11. Le Bourlais C, Acar L, Zia H, Sado P, Needham T, Leverge R. Ophthalmic Drug Delivery Systems - Recent Advances. Prog Retin Eye Res. 1998;17: 33–58.
12. Saettone MF, Salminen L. Ocular inserts for topical delivery. Adv Drug Deliv Rev. 1995;16: 95–106.
13. Bettini R, Catellani PL, Santi P, Massimo G, Peppas NA, Colombo P. Translocation of drug particles in HPMC matrix gel layer: Effect of drug solubility and influence on release rate. J Control Release. 2001;70: 383–391.
14. Siepmann J, Peppas NA. Modeling of drug release from delivery systems based on hydroxypropyl methylcellulose (HPMC). Adv Drug Deliv Rev. 2001;48: 139–157.
15. Barba AA, d'Amore M, Chirico S, Lamberti G, Titomanlio G. Swelling of cellulose derivative (HPMC) matrix systems for drug delivery. Carbohydr Polym. 2009;78: 469–474.
16. Siepmann J, Kranz H, Bodmeier R, Peppas NA. HPMC-matrices for controlled drug delivery: A new model combining diffusion, swelling, and dissolution mechanisms and predicting the release kinetics. Pharmaceutical Research. 1999; 1748–1756.
17. Sedgwick H, Cameron JE, Poon WCK, Egelhaaf SU. Protein phase behavior and crystallization: Effect of glycerol. J Chem Phys. 2007;127: 1–6.

18. Esposito A, Comez L, Cinelli S, Scarponi F, Onori G. Influence of glycerol on the structure and thermal stability of lysozyme: a dynamic light scattering and circular dichroism study. J Phys Chem B. 2009;113: 16420–16424.
19. Vagenende V, Yap MGS, Trout BL. Mechanisms of protein stabilization and prevention of protein aggregation by glycerol. Biochemistry. 2009;48: 11084–11096.
20. Bajwa GS, Sammon C, Timmins P, Melia CD. Molecular and mechanical properties of hydroxypropyl methylcellulose solutions during the sol:gel transition. Polymer. 2009;50: 4571–4576.
21. Joshi SC. Sol-gel behavior of hydroxypropyl methylcellulose (HPMC) in ionic media including drug release. Materials. 2011;4: 1861–1905.
22. Peppas NA, Bures P, Leobandung W, Ichikawa H. Hydrogels in pharmaceutical formulations. Eur J Pharm Biopharm. 2000;50: 27–46.
23. Sannino A, Demitri C, Madaghiele M. Biodegradable cellulose-based hydrogels: Design and applications. Materials. 2009;2: 353–373.
24. Sannino A, Pappadà S, Madaghiele M, Maffezzoli A, Ambrosio L, Nicolais L. Crosslinking of cellulose derivatives and hyaluronic acid with water-soluble carbodiimide. Polymer. 2005;46: 11206–11212.
25. Grillet AM, Wyatt NB, Gloe LM. Polymer Gel Rheology and Adhesion. Rheology. 2012; 59–81.
26. Patel SK, Malone S, Cohen C, Gillmor JR, Colby RH. Elastic modulus and equilibrium swelling of poly (dimethylsiloxane) networks. Macromolecules. 1992;25: 5241–5251.
27. Ferry JD. Viscoelastic properties of polymer solutions. J Res Natl Bur Stand. 1948;41: 53–62.
28. Ceulemans J, Vermeire A, Adriaens E, Remon JP, Ludwig A. Evaluation of a mucoadhesive tablet for ocular use. J Control Release. 2001;77: 333–344.
29. Rowe R, Sheskey P, Quinn M. Handbook of Pharmaceutical Excipients. Handbook of pharmaceutical excipients, Sixth edition. 2009.
30. Silva SMC, Pinto F V., Antunes FE, Miguel MG, Sousa JJS, Pais AACC. Aggregation and gelation in hydroxypropylmethyl cellulose aqueous solutions. J Colloid Interface Sci. 2008;327: 333–340.
31. Zhou D, Law D, Reynolds J, Davis L, Smith C, Torres JL, et al. Understanding and managing the impact of HPMC variability on drug release from controlled release formulations. J Pharm Sci. 2014;103: 1664–1672.
32. Asare-Addo K, Conway BR, Larhrib H, Levina M, Rajabi-Siahboomi AR, Tetteh J, et al. The effect of pH and ionic strength of dissolution media on in-vitro release of two model drugs of different solubilities from HPMC matrices. Colloids Surfaces B Biointerfaces. 2013;111: 384–391.
33. Burdock GA. Safety assessment of hydroxypropyl methylcellulose as a food ingredient. Food Chem Toxicol. 2007;45: 2341–2351.
34. Li CL, Martini LG, Ford JL, Roberts M. The use of hypromellose in oral drug delivery. J Pharm Pharmacol. 2005;57: 533–546.
35. Dow. METHOCEL Cellulose Ethers Technical Handbook. Journal of the National Cancer Institute. 2012.
36. Ford JL. Thermal analysis of hydroxypropylmethylcellulose and methylcellulose: Powders, gels and matrix tablets. Int J Pharm. 1999;179: 209–228.
37. Hussain S, Keary C, Craig DQM. A thermorheological investigation into the gelation and phase separation

of hydroxypropyl methylcellulose aqueous systems. Polymer. 2002;43: 5623–5628.

38. Almeida N, Rakesh L, Zhao J. Monovalent and divalent salt effects on thermogelation of aqueous hypromellose solutions. Food Hydrocoll. 2014;36: 323–331.
39. Bain MK, Maity D, Bhowmick B, Mondal D, Mollick MMR, Sarkar G, et al. Effect of PEG-salt mixture on the gelation temperature and morphology of MC gel for sustained delivery of drug. Carbohydr Polym. 2013;91: 529–536.
40. Dewan M, Bhowmick B, Sarkar G, Rana D, Bain MK, Bhowmik M, et al. Effect of methyl cellulose on gelation behavior and drug release from poloxamer based ophthalmic formulations. Int J Biol Macromol. 2015;72: 706–710.
41. Bain MK, Bhowmick B, Maity D, Mondal D, Mollick MMR, Paul BK, et al. Effect of PVA on the gel temperature of MC and release kinetics of KT from MC based ophthalmic formulations. Int J Biol Macromol. 2012;50: 565–572.
42. Kurek M, Brachais CH, Nguimjeu CM, Bonnotte A, Voilley A, Galić K, et al. Structure and thermal properties of a chitosan coated polyethylene bilayer film. Polym Degrad Stab. 2012;97: 1232–1240.
43. Fajardo P, Balaguer MP, Gomez-Estaca J, Gavara R, Hernandez-Munoz P. Chemically modified gliadins as sustained release systems for lysozyme. Food Hydrocoll. 2014;41: 53–59.
44. Cissé M, Montet D, Loiseau G, Ducamp-Collin MN. Influence of the Concentrations of Chitosan and Glycerol on Edible Film Properties Showed by Response Surface Methodology. J Polym Environ. 2012;20: 830–837.
45. Silva CL, Pereira JC, Ramalho A, Pais AACC, Sousa JJS. Films based on chitosan polyelectrolyte complexes for skin drug delivery: Development and characterization. J Memb Sci. 2008;320: 268–279.
46. European Pharmacopoeia Online. In: European Pharmacopoeia 7.6 [Internet]. [cited 1 May 2012]. doi:http://online.edqm.eu/EN/entry.htm#
47. Purslow C, Wolffsohn JS. Ocular Surface Temperature. Eye Contact Lens Sci Clin Pract. 2005;31: 117–123.
48. Stevens. Interaction Effects in ANOVA. In: UOregon [Internet]. 1999; 1–36. doi:http://eprints.utas.edu.au/4774/
49. Akbari J, Enayatifard R, Saeedi M, Saghafi M. Influence of hydroxypropyl methylcellulose molecular weight grade on water uptake, erosion and drug release properties of diclofenac sodium matrix tablets. Trop J Pharm Res. 2011;10: 535–541.
50. Abrahamsson B, Alpsten M, Bake B, Larsson A, Sjögren J. In vitro and in vivo erosion of two different hydrophilic gel matrix tablets. Eur J Pharm Biopharm. 1998;46: 69–75.
51. Siepmann J, Siepmann F. Modeling of diffusion controlled drug delivery. J Control Release. 2012;161: 351–362.
52. Ghori MU, Ginting G, Smith AM, Conway BR. Simultaneous quantification of drug release and erosion from hypromellose hydrophilic matrices. Int J Pharm. 2014;465: 406–412.

Chapter 4: Further development of an ocular insert with slow release properties loaded with lysozyme

Parts of this chapter have been published in:

Everaert A, Broeckx G, Fransen E, Ludwig A, Kiekens F, Weyenberg W. Evaluation of a newly developed HPMC ophthalmic insert with sustained release properties as a carrier for thermolabile therapeutics. Int J Pharm. 2015;481: 37–46.

1 INTRODUCTION

The primary objective of the present chapter was to further develop and evaluate the method of preparing ocular HPMC inserts while avoiding production steps that might have a negative impact on drug stability. Instead of a small molecule such as sodium fluorescein, the much larger molecule lysozyme was chosen as a globular model protein [1,2]. Lysozyme or muramidase is a ubiquitous enzyme present in various body fluids, such as human serum, urine, tears, seminal fluid and milk. Lysozyme hydrolyses ß-(1-4)-glycosidic linkages between *N*-acetylmuramic acid and *N*-acetyl-D-glucosamine residues present in the mucopolysaccharide cell wall of a variety of microorganisms [3–6]. Despite a visibly lower opacity of K100M polymers, HPMC K100M was selected and compared to HPMC E10M. From the manufacturer's technical handbook, K100M has an intrinsically higher viscosity which might influence the outcome of drug loading and release [7]. Preliminary studies showed that increasing the glycerol percentage negatively influences the diffusion process of the drug solution in the partially dehydrated polymer cylinder. Therefore, in this chapter, the amount of glycerol was set to 5% (w/w) instead of 10% (w/w).

Peptides and proteins require specific attention during the development and processing of ophthalmic inserts as described in the following parts. Firstly, proteins containing thiol groups, such as methionine and cysteine residues, are particularly susceptible to oxidation [8,9]. Therefore, air bubble entrapment in the viscous polymer dispersion should be avoided. Solvent casting is a commonly used method for the preparation of ocular inserts (e.g. ocular films) [10–18]. This method does not require heat in order to disperse the drug molecules homogeneously. A low-viscous solution is formed by mixing the various components and is poured into an appropriate mould. The solution is dried over an extended period of time at room temperature or above. The exposure of the drug molecules to air and the suboptimal temperatures at which solvent casting is performed, may cause proteins to denaturate. Oxidation can be avoided by performing the dehydration step in an inert atmosphere and at low temperatures for drug stability reasons. However, inherent to low temperatures, the time required to dry the dispersion will extend and is therefore undesirable. In addition, the very thin shape and low moisture content of polymer based ocular films can make these formulations extract tear fluid from the eye, hereby elevating the risk of eye irritation [19].

Secondly, denaturation of peptides and proteins can also occur by applying mechanical stress such as shear forces [20–24]. Mechanical agitation such as high shear homogenisers and comparable

blending devices can change the conformation of peptides and proteins, potentially causing loss of activity.

Thirdly, the most common way of preparing a homogeneous gel is blending the different excipients and active pharmaceutical ingredient (API) together in the same vessel under high shear forces [25]. Due to the desired properties of the gel (high viscosity), the aforementioned method of preparing homogeneous gels is not appropriate as lumping of the hydrogel cannot be avoided easily at low temperatures. Additionally, high shear mixing enhances the entrapment of air bubbles.

In the previous chapter, sodium fluorescein was used as a tracer molecule to assess the early development of the new preparation method for ocular inserts. The incorporation of lysozyme as model protein is described in this chapter. The higher molecular weight of lysozyme (14.3 kDa) as opposed to the molecular weight of sodium fluorescein (0.376 kDa) brings new challenges along. The early method described the loading process of sodium fluorescein in a period of six weeks. In the present chapter, the aim was to keep the loading process at six weeks, while homogeneously incorporating a protein with a higher molecular weight.

2 MATERIALS AND METHODS

2.1 Materials

Hydroxypropylmethyl cellulose types E10M CR Premium and K100M Premium were obtained from Colorcon (Dartford, UK). By specification, a 2% (w/w) E10M HPMC solution gives an apparent viscosity of 10.000 mPa.s (20 °C) while a 2% (w/w) solution of K100M HPMC has an apparent viscosity of 100.000 mPa.s under the same measuring conditions. Glycerol analytical grade and lysozyme from chicken egg white were provided by Sigma-Aldrich (Steinheim, Germany). Purified water (18.2 MΩ.cm) was used after being filtered over a 0.2 µm cellulose acetate filter from Sartorius (Vilvoorde, Belgium). Sodium chloride (NaCl), sodium dihydrogen phosphate dihydrate ($NaH_2PO_4.2H_2O$) and disodium hydrogen phosphate dihydrate ($Na_2HPO_4.2H_2O$) of analytical grade were purchased from Merck (Darmstadt, Germany) and were used to prepare phosphate-buffered saline solution (PBS, pH 7.4). PBS is an electrolyte solution composed of 8.2 g/l NaCl, 0.3 g/l $NaH_2PO_4.2H_2O$, 1.54 g/l $Na_2HPO_4.2H_2O$ and purified water.

The barrels are syringes of 20 ml and 30 ml with the outer cylinder consisting of polypropylene. The piston is made of polypropylene and polyethylene. The joint of the piston is made of synthetic isoprene with silicone as lubricant (BD Plastipak, Drogheda, Ireland).

2.2 Preparation of ocular inserts

The different rod-shaped, ocular inserts consist of varying percentages of HPMC, 3% (w/w) lysozyme, 5% (w/w) glycerol as a plasticiser and water as solvent. The preparation of this drug delivery system consists of four major phases which have been described in *chapter 3* under *2.3 Initial method for the preparation of inserts*. A schematic overview of the preparation method is summarised in figure 1 and the differences with the early method are marked with an asterisk (*) throughout this section.

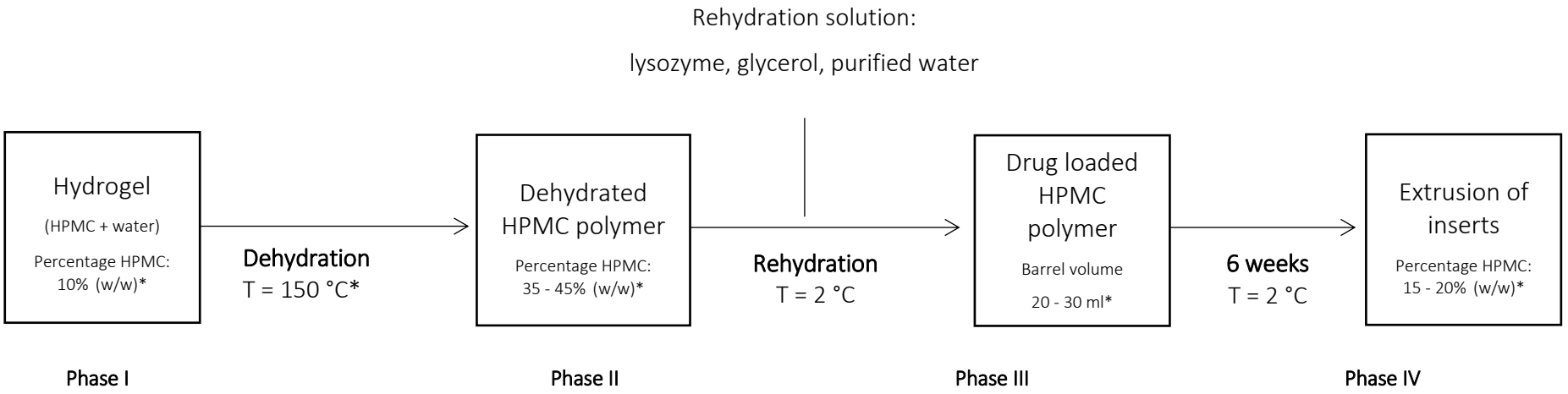

Fig. 1. General overview of the preparation method. A clear hydrogel is prepared while applying heat, but in the absence of lysozyme. Dehydration occurs as the hydrogel is placed in a drying oven at a higher temperature (150 °C) compared to the early method (100 °C), to allow better dehydration of the HPMC polymer K100M. The endpoint of the dehydration is determined gravimetrically at 35% (w/w) or 45% (w/w) depending on the design of experiments. The dehydrated matrix is rehydrated with a solution of lysozyme, glycerol and purified water. After a rehydration period of six weeks, the mass is extruded from the barrel through an opening of 2 mm.

Contrary to other often used preparation methods such as solvent casting methods, a drying step at room temperature is not necessary, thus minimising air contact time and potential oxidation of the protein. The entrapment of air bubbles was avoided by preparing the HPMC solution in hot purified water (>90 °C) which allows air bubbles to escape due to the initially low viscosity of the polymer dispersion upon cooling. Temperature stability of the drug was ensured by working conditions below room temperature and storing conditions at 2 °C. With the exception of gentle extrusion, no external shear forces were applied on the formulations, thereby avoiding alleged conformational modifications of the drug.

Phase I: Hydrogel-formation

A polymer solution of E10M or K100M* 10% (w/w)* was prepared by heating purified water up to a temperature of 90-100 °C and adding HPMC to the water under continuous agitation. The HPMC dispersion was steadily stirred (VMS-C7-2, IKA, Staufen, Germany) and was cooled down to room temperature (22 ± 2 °C) resulting in a highly viscous polymer solution. In addition to this, it was stored at 2 °C overnight in order to obtain full hydration of the polymer chains.

Phase II: Dehydration of the polymer solution

The viscous polymer solution was put in a drying oven (Thermo Scientific Heraeus Function Line T12, Langenselbold, Germany) at a temperature of 150 °C* in order to dehydrate the HPMC polymer solution. The higher temperature was required to allow dehydration of the polymer HPMC K100M which did not adequately precipitate and expel water at 100 °C as initially chosen. The dry percentage of the dehydrated polymer cylinder was determined gravimetrically on an analytical balance (Mettler Toledo AB135-S, Greifensee, Switzerland). To avoid a strongly dehydrated outer layer and a relatively more hydrated core, a glass beaker was reversely put over the polymer cylinder to create a saturated atmosphere of vapour around the polymer cylinder during dehydration. The drying time took up to three hours for polymer cylinders dried up to 45% HPMC (w/w)* and about two hours for polymer cylinders dried up to 35% HPMC (w/w).

Phase III: Rehydration of the polymer cylinder formed

In the previous, early method, only a central perforation was punched in the polymer matrix for a better and easier distribution of the drug solution. For this series of experiments, the polymer cylinder was cut into a hashtag geometry* viewed from above to reduce the diffusion path of the drug solution and was put in a closed barrel with a volume of 20 ml or 30 ml. These barrels have an inner diameter of 20 mm and 25 mm respectively. The diameter of the central cut was set to 5 mm.

On each side, a rectangular shape was cut measuring 3 mm in each direction over the entire height of the dehydrated polymer cylinder. A schematic drawing of the hashtag geometry is illustrated in figure 2.

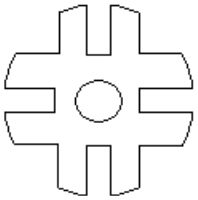

Fig. 2. Hashtag shaped cuts made in the polymer cylinder. View from above.

The volume of the barrels was chosen accordingly, in order to allow the dehydrated polymer cylinder to be fully submerged in the drug solution but also changing the distribution of the solution around the dehydrated polymer. This means that a polymer cylinder with certain dimensions (H = 17 mm, Ø = 20 mm for both K100M and E10M dehydrated polymer cylinders (35% (w/w) HPMC) and H = 15 mm, Ø = 18 mm in case of both K100M and E10M dehydrated polymer cylinders (45% (w/w) HPMC)) is exposed to a different distribution of the drug solution depending on the chosen barrel. For example, a barrel with a larger diameter will have relatively less drug solution on top of the polymer cylinder, but more drug solution will be available radially around the polymer cylinder. Figure 3 represents schematically two examples of how the distribution of drug solution around the polymer cylinder depends on the dimensions of the polymer cylinder.

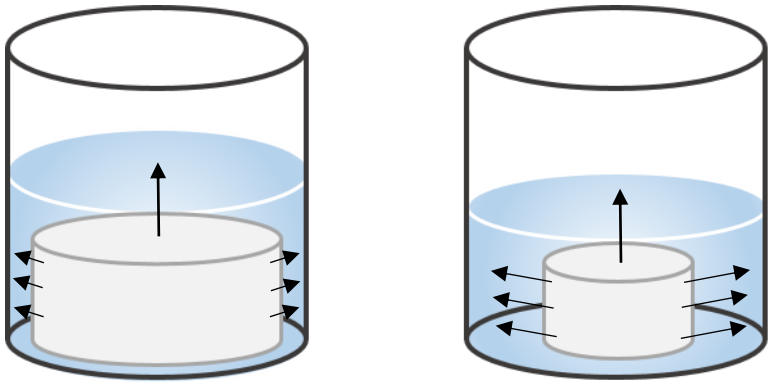

Fig. 3. Examples of two polymer cylinders dehydrated to different HPMC degrees. The size of the barrel, shown in black, is equal in both situations. The left polymer cylinder is dehydrated to a lesser extent and contains higher water levels than the one on the right. Therefore, less drug solution is required for rehydration of the left polymer cylinder. The amount of drug solution added (blue), depends on the dehydration degree of the polymer cylinder (grey) in case of the same final HPMC concentrations. The left picture shows a less dehydrated polymer cylinder, implicating less

drug solution being available radially of the polymer cylinder compared to the situation on the right. This means that swelling is mainly limited in the axial direction for the picture on the left, while swelling in all directions will occur for the polymer cylinder on the right. These examples show the influence of the polymer cylinder dimensions on the distribution of the drug solution added.

An aqueous solution of lysozyme and glycerol was prepared and added to the barrel after finalising the dehydration step. As all calculations have been performed by mass, the composition of the drug solution added can be given by means of mass. The exact composition of the drug solution depended on the exact composition and cut of every dehydrated polymer cylinder prepared. Table 1 gives an overview of the composition of the different formulations merely as an example.

Table 1. Overview of the different formulations and their composition.

Dry percentage HPMC % (w/w)	End percentage HPMC % (w/w)	Mass glycerol added (g)	Mass purified water added (g)	Mass lysozyme added (g)*
35	20	0.31	2.195	0.189
35	15	0.42	4.127	0.252
45	20	0.30	2.890	0.182
45	15	0.41	4.753	0.243

**The amount of lysozyme added to the solution was calculated as 3% (w/w) of the total mass.*

The rehydration process is performed at 2 °C to ensure drug stability of the potentially thermolabile proteins or molecules incorporated in the insert. Even at temperatures as low as 2 °C, the drug solution migrates by means of passive diffusion into the polymer matrix avoiding the use of mixing forces to obtain a homogeneously loaded matrix. Due to the low temperature used during this phase, the high viscosity of the polymer cylinder and the low diffusional rate slow down the rehydration process in comparison to the same process at room temperature. After a homogenisation period of six weeks, the inserts were extruded from the barrel. The period of rehydration was kept equal to the previously introduced method, keeping in mind that lysozyme is a much larger molecule than sodium fluorescein.

Phase IV: Extrusion

After obtaining a semisolid hydrogel in the barrel, the content of the syringe was manually extruded through an opening of 2 mm by applying mild extrusion forces. The extruded samples were packaged in a sealed container and stored in a refrigerator at a temperature of 2 °C.

2.3 Factorial design and statistical analysis

A 2^4 full factorial design, performed in duplicate resulting in 2 x 16 different formulations, was set up to determine the influence of the chosen parameters yielding inserts with suitable characteristics. Furthermore, their influence on the release profile and water uptake was investigated by means of statistical analysis with an ANOVA-test using the statistical software package R®, version 2.13.1 (R Foundation for Statistical Computing, Vienna, Austria). An overview of the levels of the parameters is given in table 2 and an overview of the experiments is summarised in table 3.

Table 3. Overview of the different experiments and selected variables. Each formulation was prepared and measured in duplicate.

Formulation	*Polymer type*	*Dry % HPMC*	*Final % HPMC*	*Volume barrel*
1	+	+	+	+
2	+	+	-	+
3	+	-	+	+
4	+	-	-	+
5	-	+	+	-
6	-	+	-	-
7	-	-	+	+
8	-	-	-	+
9	+	+	+	-
10	+	+	-	-
11	+	-	+	-
12	+	-	-	-
13	-	+	+	+
14	-	+	-	+
15	-	-	+	-
16	-	-	-	-

Table 2. Overview of the upper (+) levels and lower (-) levels of the chosen parameters in the factorial design. Dry and end percentages of HPMC were calculated by gravimetric analysis.

Fixed parameter		
Final % glycerol	5% (w/w)	
Variable parameters		
	(+) level	*(-) level*
Polymer type	E10M	K100M
Dry % HPMC	45% (w/w)	35% (w/w)
Final % HPMC	20% (w/w)	15% (w/w)
Volume barrel	30 ml	20 ml

The different levels for the parameters chosen were based on experience from previously conducted research.

The influence of the parameters 'polymer type' (E10M or K100M), 'dry % HPMC' (35% (w/w) or 45% (w/w)), 'final % HPMC' (15% (w/w) or 20% (w/w)) and 'volume barrel' (20 ml or 30 ml) on the release profiles of lysozyme at time point 480 minutes, was tested using ANOVA. During the development and manufacturing of the inserts, the dry and final percentages of HPMC were calculated by gravimetric analysis.

2.4 Visual appearance and texture

The extruded inserts were visually evaluated for translucency and texture.

2.5 Uniformity of drug content

Uniformity of drug content is required to obtain the same amount of drug in each extruded insert according to the limits set by the European Pharmacopoeia (Ph. Eur. 7.6, monograph 2.9.6. *Uniformity of content of single-dose preparations*). A series of ten inserts from each batch with a mass of 250 mg were individually dissolved in 250 ml of PBS solution. The drug content of each insert was analysed spectrophotometrically (Genesys 10 UV, Thermo Electron Corporation, Madison, USA) by measuring the absorbance of lysozyme at a wavelength of 280 nm. The average drug content and standard deviation values were calculated. The uniformity of drug content

measurement was performed in duplicate on each formulation. Validation of the method was assessed prior to the measurements and given in *Appendix*.

2.6 Water uptake

Water uptake was studied gravimetrically using a Baumann apparatus with PBS as medium. A small amount of sample (± 120 mg) was put on a molecular porous membrane (Spectra/Por® MWCO: 12000 – 14000, Spectrum, Breda, The Netherlands) which was placed on the fritted glass plate of the Baumann capillary apparatus and covered to prevent evaporation of the medium. The amount of water absorption was calculated after the sample had been weighed at 60, 120, 240 and 360 minutes. The following formula was used to determine the amount of water uptake (W) at a given time:

$$W = \frac{m_a - m_d}{m_d} .100\%$$

W: amount of PBS absorbed by the insert expressed as a percentage

m_a: mass of the insert after absorption of medium

m_d: mass of the insert before absorption of medium

2.7 Viscosity measurements

In order to correlate the drug release profiles to the viscosity of the lysozyme loaded inserts, viscosity measurements were carried out. Samples of HPMC K100M and E10M, both in 20% (w/w) and 15% (w/w) final HPMC percentages with 5% (w/w) glycerol, were prepared. The viscosity was measured through oscillation on an Anton Paar rheometer (MCR 102, Graz, Austria) at a temperature of 32.0 ± 0.1 °C. Prior to the frequency sweep measurements, a maximum amplitude measurement was performed to determine the linear viscoelastic region. The strain was consequently set at an amplitude of 1%. The following settings were used for all oscillation measurements: parallel plate with a diameter of 8 mm and the gap size set at 1 mm. The angular frequency was varied from 100 to 0.1 rad/s. To prevent evaporation of water from the hydrogel during the measurements, a solvent trap was used to cover the sample.

2.8 *In vitro* drug release studies

The release patterns of the different formulations were determined. Two inserts weighing 150 mg each (Ø = 2 mm, L = 10 ± 1 mm) were extruded at random from a single barrel and put into separate

test tubes containing 5 g PBS. The test tubes were placed in a non-oscillating water bath (Julabo 20B, Merck-Belgolabo, Overijse, Belgium) at a temperature of 32.0 ± 0.5 °C. After intervals of 30, 60, 90, 120, 180, 240, 360, 420 and 480 minutes, samples of 1 g were withdrawn from the release medium after gentle homogenisation and replaced with an equal mass of fresh PBS solution at 32 °C. The drug content at each time interval was measured spectrophotometrically at a maximum wavelength of 280 nm. After 480 minutes, the insert was intensively vortexed to release all of the remaining drug from the insert. The drug content was calculated from the total percentage drug present in the insert.

2.9 Drug release analysis

The *in vitro* release patterns were analysed for zero order, first order or mixed order kinetics. The Korsmeyer-Peppas equation, also referred to as the so-called power law, is a semi-empirical equation to describe drug release from a polymeric system. The power law is given as follows:

$$\frac{\mathrm{M}_t}{\mathrm{M}} = \mathrm{K}t^n$$

M_t: amount of drug released at time t

M: total amount of drug in the dosage form

K: kinetic constant

n: release exponent indicating the drug release mechanism

This equation is applicable in swellable systems when the system only swells to a moderate equilibrium degree [26]. For cylindrically shaped dosage forms, a release exponent of $n \leq 0.45$ indicates Fickian diffusion or first order kinetics. If $n \geq 0.89$, the drug release rate is independent of time, corresponding to case-II transport or zero order kinetics. Values of n between 0.45 and 0.89 can be seen as mixed zero and first order kinetics, also referred to as anomalous diffusion or non-Fickian diffusion [27].

3 RESULTS AND DISCUSSION

3.1 Visual appearance and texture

The extruded ocular inserts were rod shaped and appeared translucent with a smooth texture. All inserts were flexible and had no sharp edges which is beneficial for pre-corneal use. However, when large volumes of hydrogels were prepared with HPMC K100M, some turbidity was noticed, even in percentages as low as 2% (w/w). Hydrogels prepared with HPMC E10M always showed excellent clarity, regardless of the volume prepared or the percentage of HPMC used. Whether this turbidity influences the vision in human eyes in case of very small inserts, remains to be investigated.

3.2 Uniformity of drug content

For the different experiments, uniformity of content revealed that four out of sixteen duplicate experiments complied with the limits set by the Ph. Eur. 7.6, monograph 2.9.6 *Uniformity of single-dose preparations.* Content measurements of formulations 2, 4, 13 and 14 exhibited a homogeneous distribution of lysozyme for both duplicates. The results are graphically shown in figure 4a and 4b.

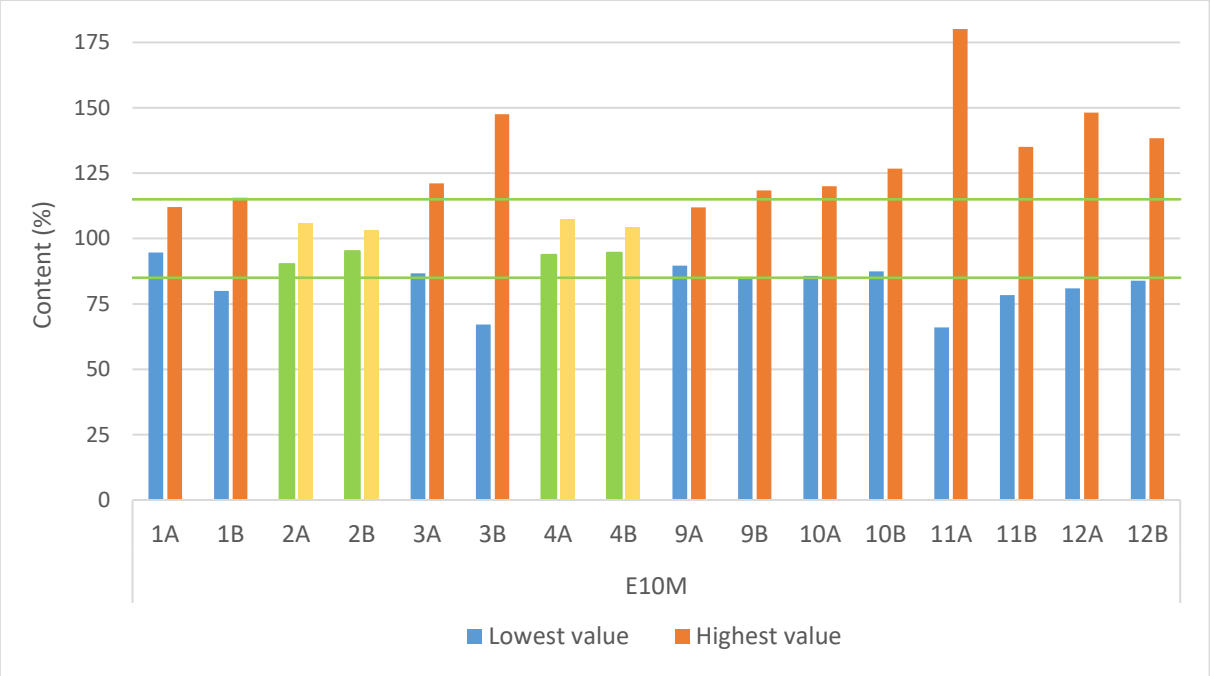

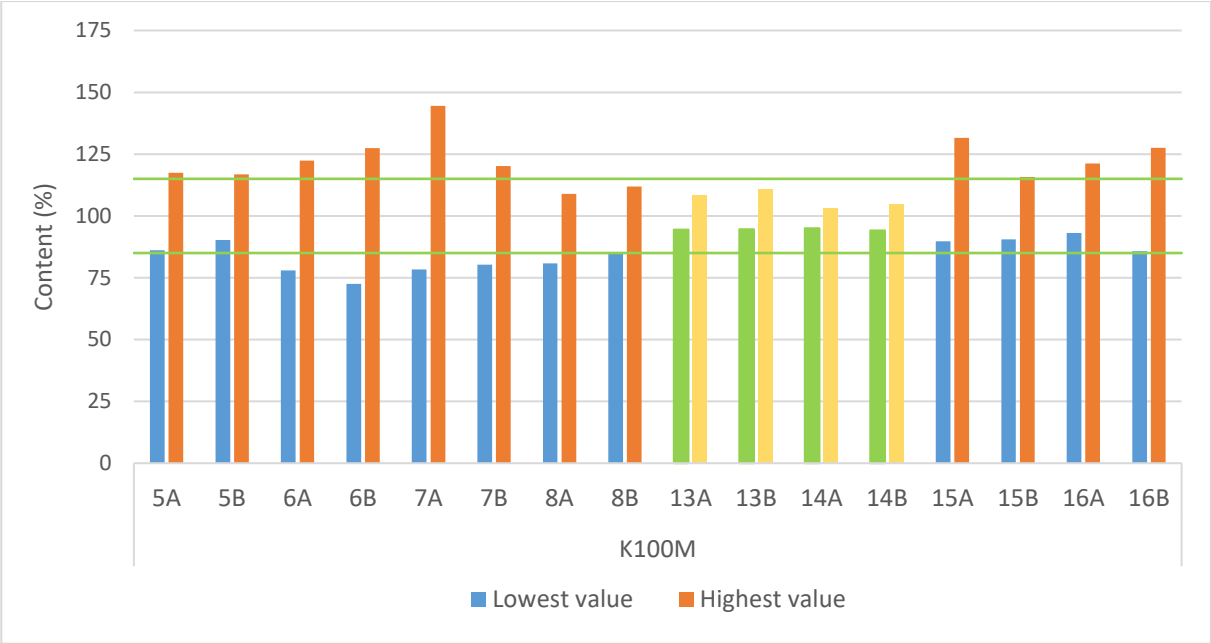

Fig. 4a and 4b. Overview of the content lysozyme in formulations with HPMC E10M and K100M respectively. The average content of all measured inserts is considered 100%. Indicated with green lines, the 85% and 115% limits set by the Ph. Eur. 7.6, monograph 2.9.6 are given. The blue and orange bars represent the lowest and highest value of content of ten measured samples respectively. All formulations of which the lowest and highest values are within the 85 - 115% limits, comply with the test and are shown in green/yellow bars.

Although the formulations 2, 4, 13 and 14 comply with the monograph 2.9.6 in duplicate, the average drug content was also calculated and expressed in function of the theoretical drug content. The results for these experiments are shown in table 3.

Table 3. Results of the average drug content of ten inserts extruded from a single barrel. For each formulation, two replicates A and B were prepared and analysed.

Formulation	Average drug content	Standard deviation
2A	86,58%	4,38
2B	89,65%	1,79
4A	81,83%	3,32
4B	79,01%	3,19
13A	84,61%	5,80
13B	85,17%	6,58
14A	91,40%	2,96
14B	90,71%	4,19

The average drug content of all formulations is about 10 - 20% lower than the theoretical value. This lower average drug content can be attributed to loss during the production process. Due to the capillary shape at the opening of the barrel (the capillary was filled with drug solution to avoid air entrapment in the barrel), a small amount of drug solution remained unabsorbed from the polymer cylinder and was removed before analysis. This could explain the lower drug content as reported in table 3.

3.3 Water uptake

Hydrophilic polymeric systems swell upon contact with water due to hydration of the polymer chains. Additionally, as a result of steep water concentration gradients, the uptake of water into the polymer network of the insert is promoted causing the polymer chains to relax, which in turn enhances the mobility of the polymer molecules. A more densely packed polymer network, such as high molecular weight HPMC polymers, resists a rapid penetration of water molecules but can absorb higher amounts of solvent [28,29]. The results for the water uptake from different formulation are shown in figures 5a and 5b. The resulting graphs for water uptake are constructed by combining all formulations into categories, based on the end percentage HPMC and the type of HPMC used.

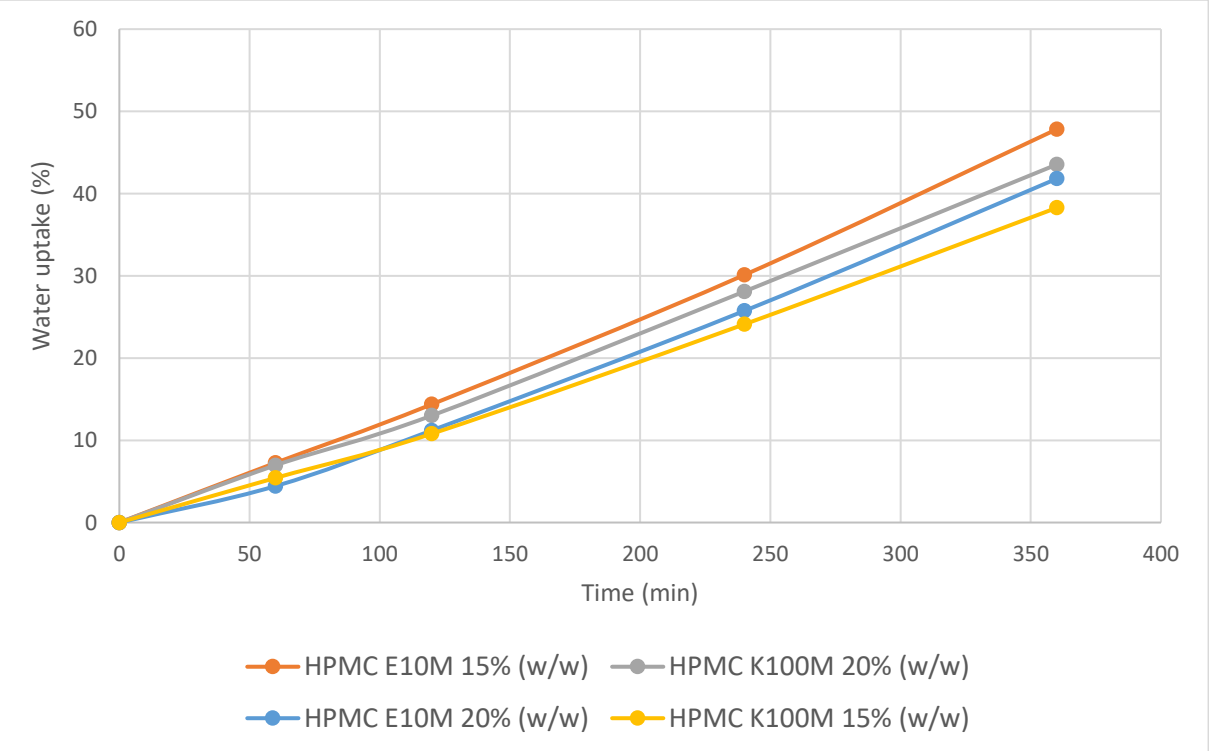

Fig. 5a. Water uptake profile for E10M and K100M HPMC inserts loaded with lysozyme (n=16).

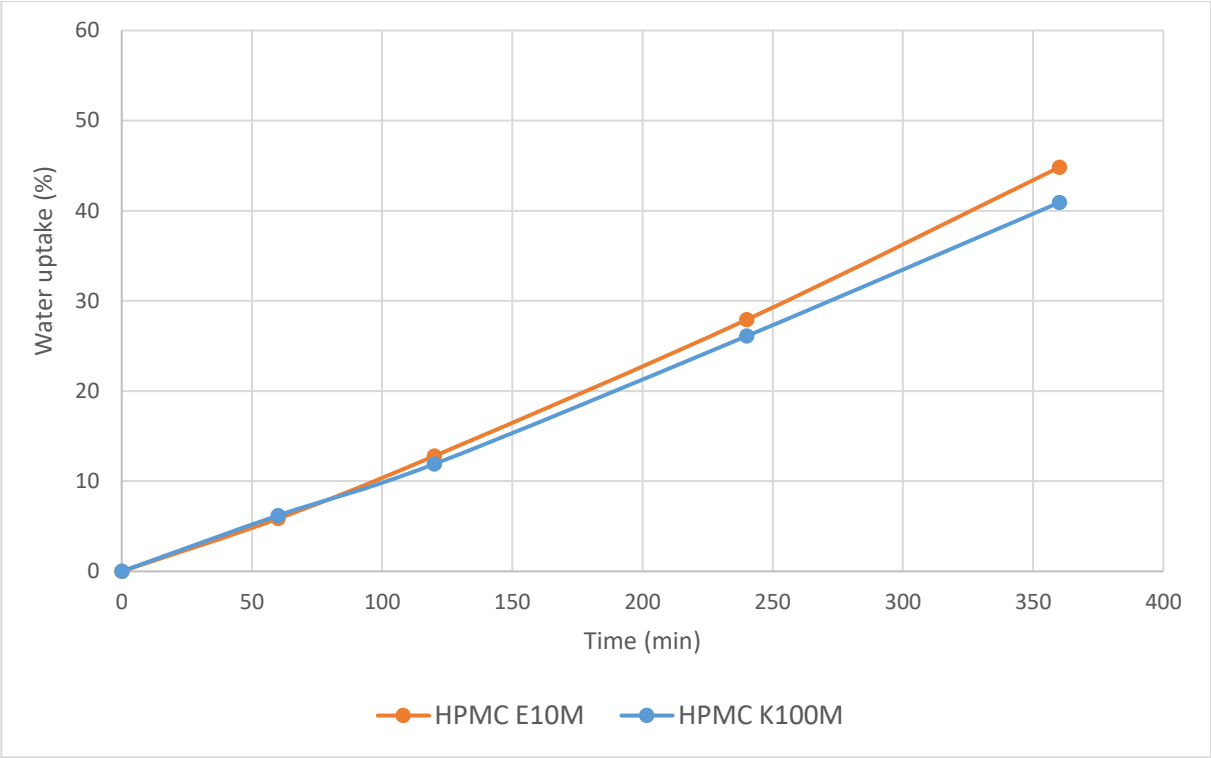

Fig. 5b. Water uptake profile for HPMC inserts E10M and K100M loaded with lysozyme (n=16).

Graphical analysis showed that the increase in water uptake over time was almost linear. However, the large gap between the last measuring point at 1440 minutes and the previous measuring point (360 minutes) makes the last measurement significantly influential in a regression analysis. Therefore, regression analysis was carried out excluding the measurements at 1440 minutes and they are therefore not shown. A first regression analysis was carried out on the results of time point 360 minutes. The influence of 'polymer type', 'dry % HPMC', 'final % HPMC' and 'volume barrel' was assessed using stepwise backward regression, starting from a model with these four variables and their pairwise interactions. No significant effect of any of these factors could be found ($p>0.05$).

Next, the effect of time on the water uptake was examined by a longitudinal analysis on all measurements between the start of the experiment and time point 360 minutes. The influence of the parameters 'polymer type', 'end percentage' and 'volume barrel' on the water uptake was investigated. Since the evolution of water uptake over time appeared linear, the parameter 'time' was included as a continuous variable. On each formulation, several repeated measurements over time were carried out. To account for the dependence between different samples within one formulation, a random intercept term for the formulation type was added to the regression model.

Starting from a model with the parameters 'time', 'polymer type', 'volume barrel' and 'final % HPMC' including their pairwise interactions, a stepwise backward model building was used. The final model revealed a significant interaction between 'polymer type' and 'time' ($p = 0.010$) indicating that the slope of the curve versus time is different for E10M and K100M HPMC samples.

Although from figure 5a, it could have been expected that the percentage of polymer had a significant influence on the water uptake, no statistical difference between 15% (w/w) and 20% (w/w) HPMC on the water uptake behaviour was observed. In contrast, the type of polymer used had a statistically significant effect on the water uptake as demonstrated in figure 5b. In conclusion, the polymer HPMC E10M appears to have a higher water uptake capacity than HPMC K100M for the given time period, albeit the overall effect is relatively small.

3.4 Viscosity measurements

The viscosity was plotted in function of angular frequency, as shown in figure 6.

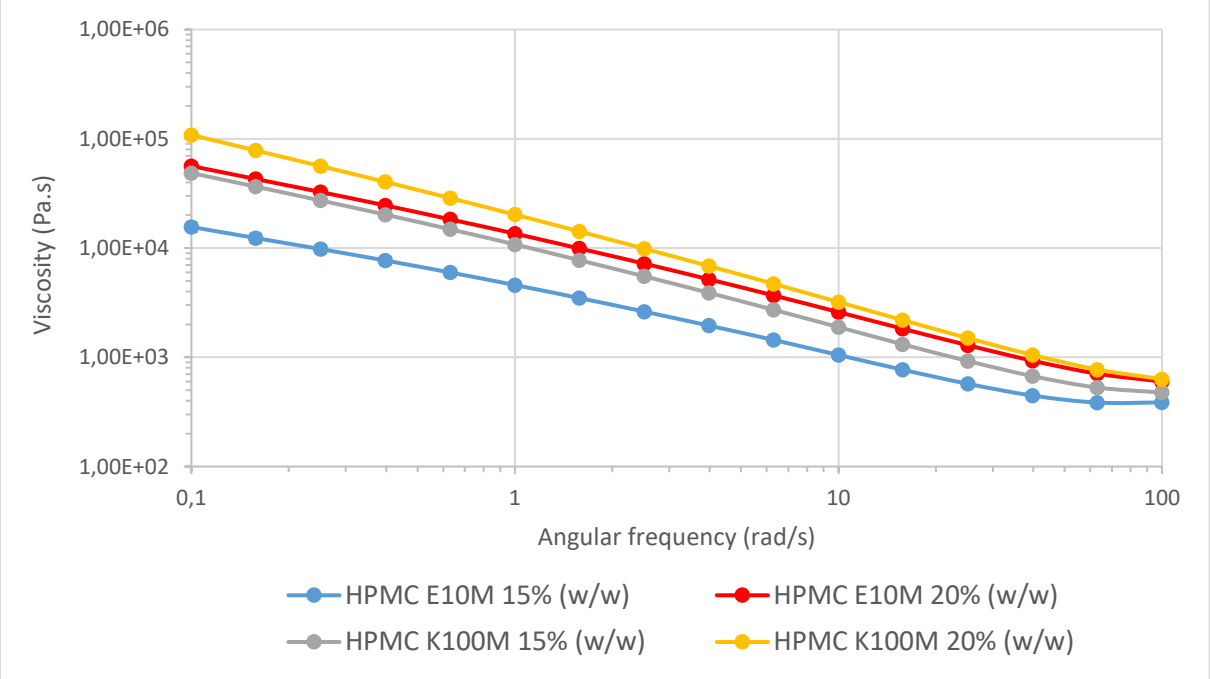

Fig. 6. Viscosity profiles for inserts loaded with lysozyme with both types of HPMC (E10M and K100M) and two different HPMC percentages (15% (w/w) and 20% (w/w)).

The viscosity of all measured samples increased with decreasing angular frequencies. As expected, K-type HPMC has a higher viscosity than E-type HPMC for corresponding polymer percentages measured. The highest viscosity values were obtained in case of HPMC K100M 20% (w/w) while the lowest viscosity values were measured for HPMC E10M 15% (w/w). HPMC E10M 20% (w/w) showed

higher viscosity values than K100M 15% (w/w), although the viscosities of both samples were comparable at the lowest angular frequencies.

3.5 Release profile

The initial release rate of drug molecules is mainly driven by diffusional forces. As the prepared inserts already contain a certain amount of water, drug molecules can readily be released by means of passive diffusion from the unlinked polymer matrix. Additionally, as the polymer chains become hydrated, the hydrodynamic dimensions of the polymeric matrix will increase as a result from swelling of the insert. This swelling dilutes the polymeric network causing disentanglement, and thereby releasing the drug by means of erosion until equilibrium is reached [30,31]. Polymers with high molecular weight such as HPMC K100M have a more closely packed polymeric network and a higher intrinsic viscosity, slowing down the release rate of the drug molecules incorporated [17,31–33]. This effect is more pronounced for larger drug molecules.

The amount of lysozyme released from the HPMC inserts is given in the cumulative release plots in figures 7a and 7b for inserts prepared in 20 ml and 30 ml barrels respectively.

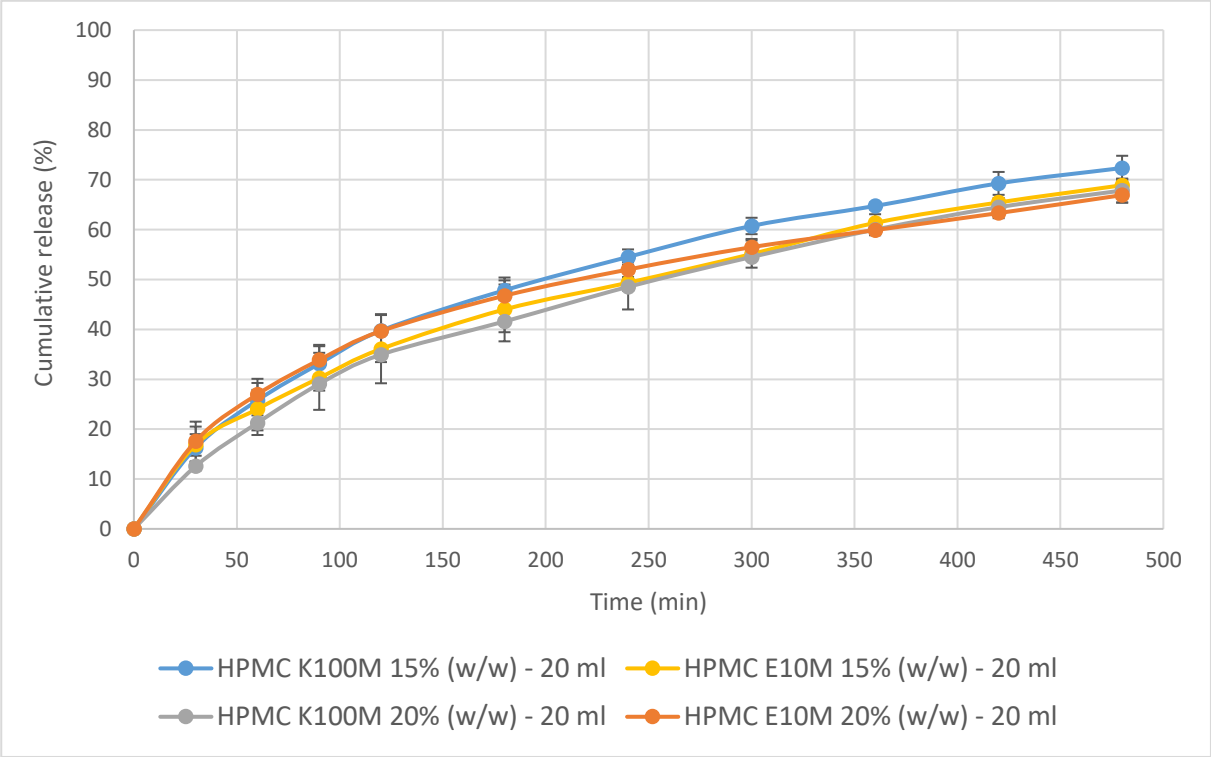

Fig. 7a. Cumulative release profiles of lysozyme loaded inserts prepared in 20 ml barrels (n=8).

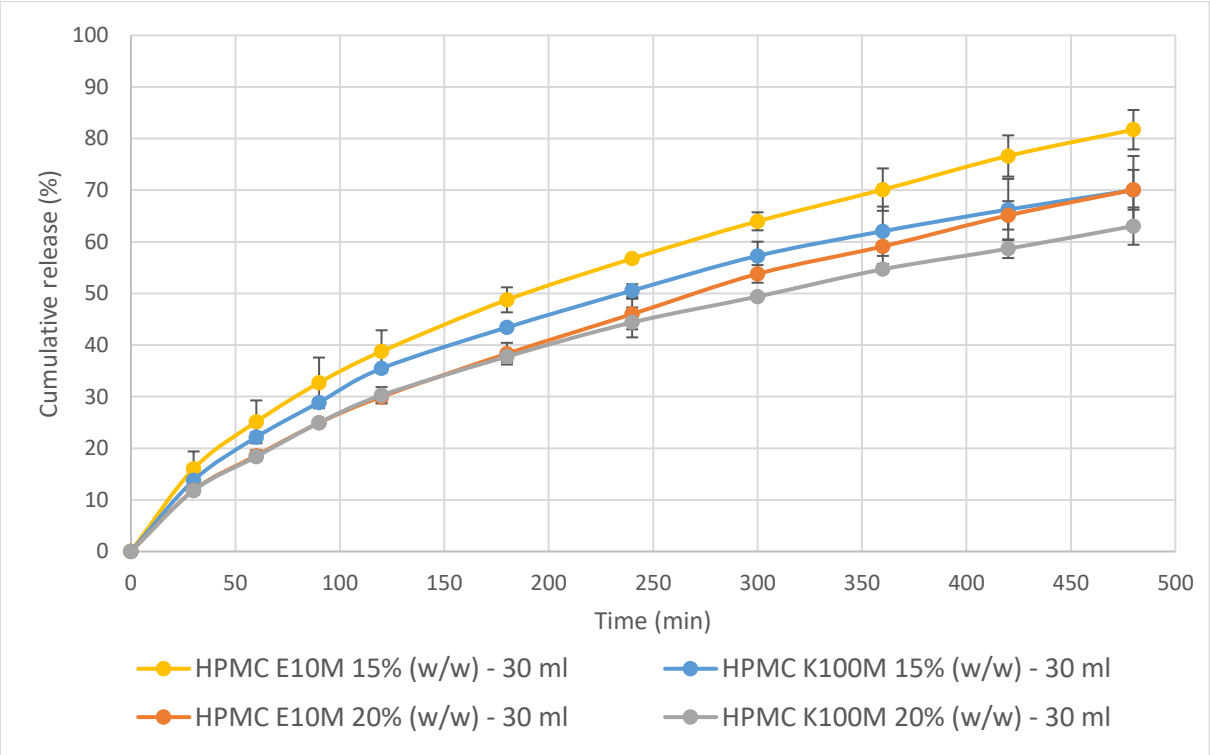

Fig. 7b. Cumulative release profiles of lysozyme loaded inserts prepared in 30 ml barrels (n=8). The drug release is compared to the total amount of drug present after full release of the drug from the matrix.

Erosion of the inserts became visually apparent as the release continued over the course of hours. The differences within the amount of lysozyme released from inserts prepared in a barrel with a volume of 30 ml are statistically significant. In this case, lysozyme molecules exhibit slower release from a K100M matrix than for E10M inserts for the same HPMC percentage. Additionally, the release rate is slower from 20% (w/w) than 15% (w/w) end percentage HPMC inserts. The protein release appears to be influenced by the resistance from the polymer network which is determined by the molecular weight of the drug molecules and the concentration HPMC used to build up the polymer matrix [33]. There seems to be a good correlation between the release profile of inserts prepared in a barrel of 30 ml and the viscosity data obtained. The slower release of drug molecules from the K100M matrix compared to the E10M matrix at the same HPMC percentage correlated with the differences in viscosity measured as shown in figure 6. Furthermore, inserts prepared with K100M 15% (w/w) appear to show similar release profiles and comparable viscosities (at low oscillatory frequencies) as inserts prepared with E10M 20% (w/w).

From a theoretical point of view, inserts loaded in barrels of 20 ml or 30 ml should yield the same end result as the final composition of the drug-polymer mass is the same in both type of barrels. When the polymer cylinder is loaded with the drug solution in 20 ml barrels, the end product has

different physical characteristics. This is because of the unfavourable contact area between the polymer cylinder and the drug solution. The closer the diameter of barrel to the diameter of the polymer cylinder, the less free volume around the polymer cylinder is available for the drug solution. This results in an asymmetrical (radial versus axial) hydration pattern, hence anisotropic swelling, as shown in figure 8. In a 30 ml barrel, the amount of drug solution around the cylinder is more favourable compared to its contact area, enhancing the diffusion pattern of the drug and solvent molecules into the polymer matrix. This results in improved homogenisation between the drug solution and the polymer cylinder. The dimensions of the barrel directly influence the rehydration process of the polymer cylinder.

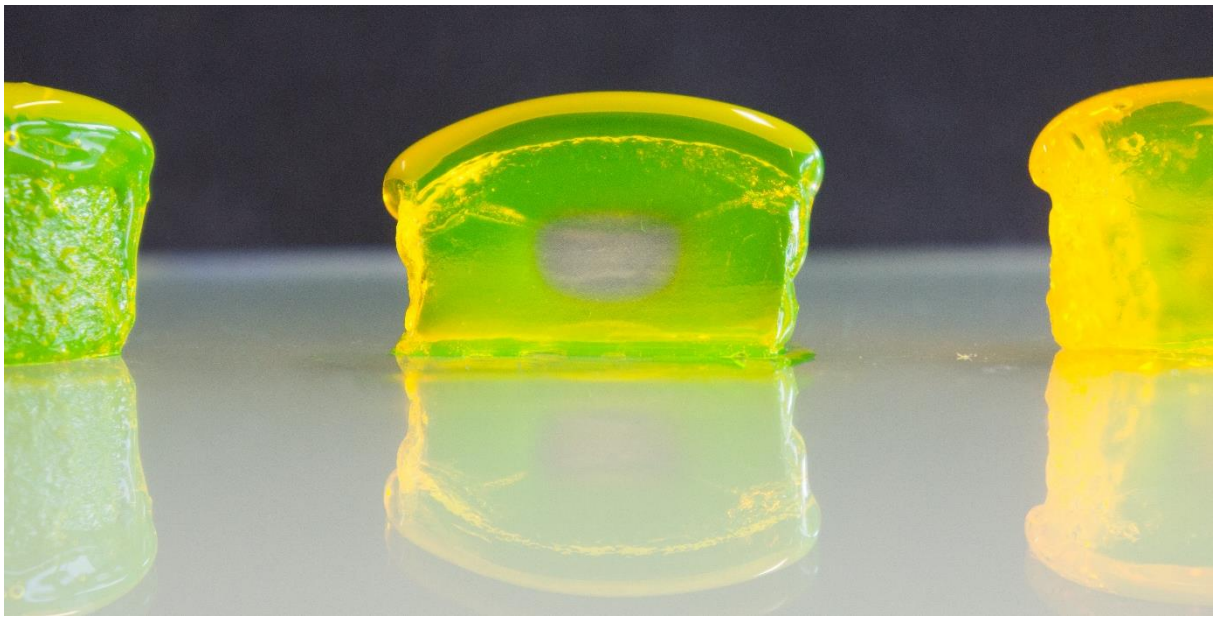

Fig. 8. Cross section of a partially rehydrated polymer cylinder after removing it from the barrel. When a polymer cylinder is submerged in the drug solution, rehydration will occur from all sides. However, a too narrow barrel will limit the swelling of the polymer cylinder radially, leaving only the top side exposed to the drug solution. This in turn will lead to higher hydration levels at the top of the polymer cylinder. Notice how the top side of the polymer cylinder is strongly hydrated and how sodium fluorescein did not reach the central part of the polymer cylinder at the moment of sectioning. *The sample as pictured above was only prepared for better visual understanding of the mechanisms of rehydration. Sodium fluorescein was used for visual purposes and no central perforation was cut.*

Statistical analysis was performed by setting up a first model containing all four variables and their pairwise interactions. This model was successively simplified in a stepwise backward model building approach, removing the least significant term in each step. The final model included a main effect of 'final % HPMC' ($p = 0.001$) and a significant interaction between 'polymer type' and 'volume

barrel' (p = 0.002), indicating that the difference in release between E10M and K100M was dependent on the volume of the barrel used for loading lysozyme in the matrix.

Subsequently, the dataset was split into the measurements of samples prepared in 20 ml volume and the results of samples loaded in 30 ml volume barrels. As shown in figure 9a, when the sample was prepared in a volume of 20 ml, there was a slight but not statistically significant effect of 'final % HPMC' (p = 0.090) and no significant effect of 'polymer type'. On the other hand, when samples were prepared in the 30 ml barrel, both the effect of 'polymer type' (p = 0.004) and 'final % HPMC' (p = 0.004) were statistically significant. The mean release percentage was 9.37% (w/w) lower in the K100M compared to the E10M inserts. For inserts with a final percentage 20% (w/w) HPMC, the release percentage was 9.30% (w/w) lower as opposed to inserts with a final percentage of 15% (w/w) HPMC.

The boxplots in figure 9a and figure 9b show the effects of the parameters 'polymer type', 'volume barrel' and 'final % HPMC'.

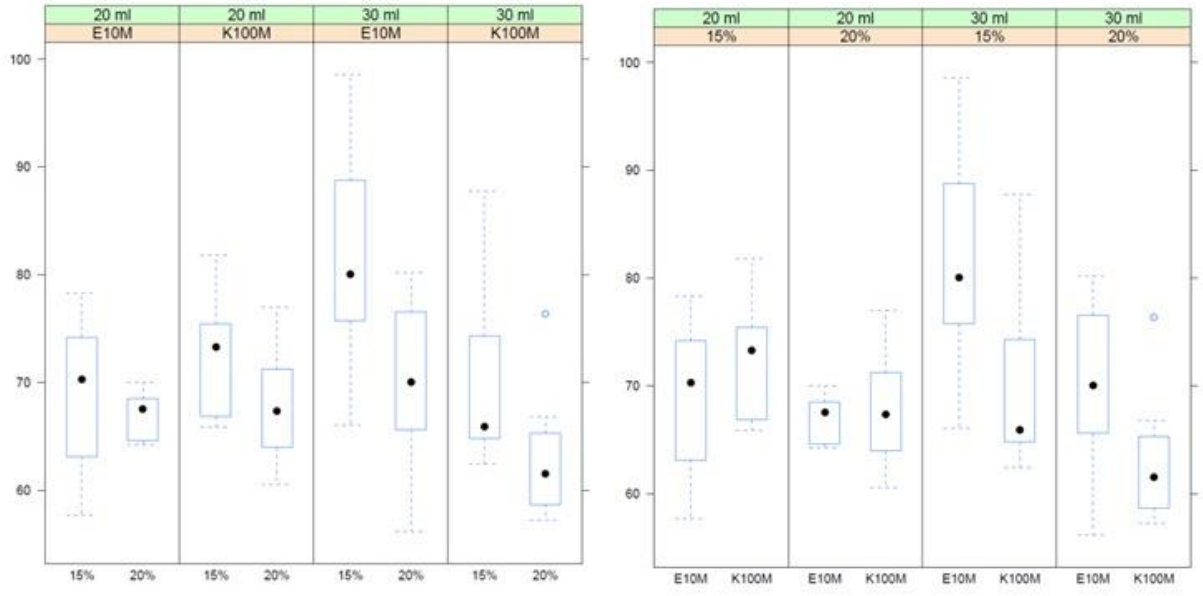

Fig. 9a and 9b. The ordinate is expressed as release percentage. (a) Boxplots comparing the parameters affecting the amount of lysozyme released from the inserts at time point 480 minutes with a final percentage HPMC of 15% (w/w) or 20% (w/w). (b) Boxplots comparing the parameters affecting the amount of lysozyme released from the inserts at time point 480 minutes with different HPMC types E10M or K100M.

As demonstrated in figure 9a, across all volumes and polymers, the 15% (w/w) final percentage HPMC has a higher amount of drug released from the matrix when compared to the 20% (w/w) HPMC. When loaded in 30 ml barrels, the difference is even more pronounced.

The difference between E10M and K100M inserts is marginal as indicated in figure 9b when loaded in the 20 ml volume (two left panels), while prepared in the 30 ml volume barrels the E10M inserts have a considerable larger release percentage.

3.6 Release kinetics

As described above, the release of drug molecules from the polymeric network is both determined by passive diffusion of the drug molecules, as well as the rate of hydration of the polymer matrix. As larger molecules experience more resistance from the polymeric network, drug release will depend less on passive diffusion and more on erosion of the matrix as a result of disentanglement of the unlinked polymer matrix.

The analysis for the release kinetics of the cumulative release profiles is shown in figure 10.

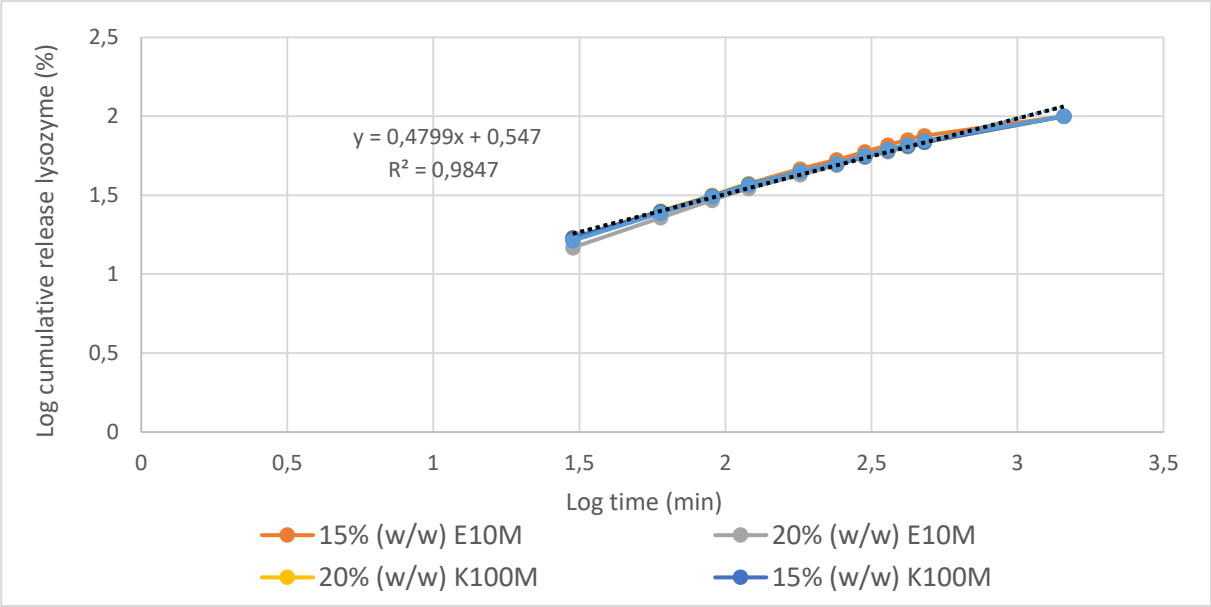

Fig. 10. Release kinetics of lysozyme loaded inserts using the Peppas–Korsmeyer model.

From figure 10, the slope calculated for lysozyme loaded inserts reveals no significant differences in release kinetics for all measured samples. The slope of the linear regression equals a value of 0.4799, thus indicative for mixed zero and first order release kinetics with possibly higher first order kinetics for all formulations. However, it should be pointed out that the application of the power law merely gives a limited insight into the exact release mechanism of the drug due to swelling properties and dissolution of the HPMC insert.

4 CONCLUSION

The newly designed ocular inserts described in this chapter, demonstrate that a water-soluble protein can be loaded into an ocular insert without heat or high shear forces being required and avoiding air bubble entrapment, reducing the risk of oxidation. The amount of drug released from the insert depends on the molecular weight of the drug molecule, due to the entangled polymer network of HPMC used for the development of the inserts. The rehydration period was kept equally lengthy as in the initially developed method described in *chapter 3*, but obtaining homogeneous results with a much larger molecule as lysozyme can be considered an achievement. The release characteristics of these inserts make this drug delivery system suitable for the incorporation of proteins such as lysozyme, although the method or batch size requires optimisation to speed up the drug solution absorption process. The extrusion phase to obtain inserts can be regarded as shear forces, albeit very mild. These shear forces should preferably be avoided or at least reduced as much as possible.

For this reason, the next chapter primarily focusses on shortening the drug loading time and avoiding extrusion forces by preparing the inserts individually. Furthermore, the final HPMC percentage will be increased to 25% (w/w) in an attempt to slow down the release rate even further and bovine serum albumin was added to investigate the effect of even larger proteins on the drug release behaviour.

I would sincerely like to thank prof. dr. Erik Fransen (StatUA, Center for Statistics, University of Antwerp) for his help with the statistical analyses described in this chapter.

References

1. Day L, Zhai J, Xu M, Jones NC, Hoffmann S V., Wooster TJ. Conformational changes of globular proteins adsorbed at oil-in-water emulsion interfaces examined by synchrotron radiation circular dichroism. Food Hydrocoll. 2014;34: 78–87.
2. Bhowal AC, Das K, Kundu S. Fluorescence behavior of globular proteins from their bulk and thin film conformations in presence of mono-, di- and tri-valent ions. Colloids Surfaces B Biointerfaces. 2015;133: 263–269.
3. Brasca M, Morandi S, Silvetti T, Rosi V, Cattaneo S, Pellegrino L. Different analytical approaches in assessing antibacterial activity and the purity of commercial lysozyme preparations for dairy application. Molecules. 2013;18: 6008–6020.
4. Guascito MR, Chirizzi D, Malitesta C, Giotta L, Mastrogiacomo D, Valli L, et al. Development and characterization of a novel bioactive polymer with antibacterial and lysozyme-like activity. Biopolymers. 2014;101: 461–470.
5. Carreira AS, Ferreira P, Ribeiro MP, Correia TR, Coutinho P, Correia IJ, et al. New drug-eluting lenses to be applied as bandages after keratoprosthesis implantation. Int J Pharm. 2014;477: 218–226.
6. Haj-Ahmad RR, Elkordy AA, Chaw CS, Moore A. Compare and contrast the effects of surfactants (Pluronic F-127 and Cremophor EL) and sugars (beta-cyclodextrin and inulin) on properties of spray dried and crystallised lysozyme. Eur J Pharm Sci. 2013;49: 519–534.
7. Dow® METHOCEL Cellulose Ethers Technical Handbook. Journal of the National Cancer Institute. 2012.
8. Vogt W. Oxidation of methionyl residues in proteins: Tools, targets, and reversal. Free Radic Biol Med. 1995;18: 93–105.
9. Torosantucci R, Schöneich C, Jiskoot W. Oxidation of therapeutic proteins and peptides: Structural and biological consequences. Pharm Res. 2014;31: 541–553.
10. Siemann U. Solvent cast technology - A versatile tool for thin film production. Prog Colloid Polym Sci. 2005;130: 1–14.
11. Mahajan HS, Deshmukh SR. Development and evaluation of gel-forming ocular films based on xyloglucan. Carbohydr Polym. 2015;122: 243–247.
12. Aburahma MH, Mahmoud AA. Biodegradable ocular inserts for sustained delivery of brimonidine tartarate: preparation and in vitro/in vivo evaluation. AAPS PharmSciTech. 2011;12: 1335–1347.
13. Mukherjee P, Manvi F V., Sreenivas SA. Sulphacetamide sodium ocular inserts: Design, formulation and evaluation. Indian Drugs. 2006;43: 705–708.
14. Rathore KS, Nema RK, Sisodia SS. Preparation and characterization of timolol maleate ocular films. Int J PharmTech Res. 2010;2: 1995–2000.
15. Kurek M, Brachais CH, Nguimjeu CM, Bonnotte A, Voilley A, Galić K, et al. Structure and thermal properties of a chitosan coated polyethylene bilayer film. Polym Degrad Stab. 2012;97: 1232–1240.
16. Harwood R, Schwartz J. Drug Release from Compression Molded Films: Preliminary Studies with Pilocarpine. Drug Dev Ind Pharm. 1982;8: 663–682.
17. Ghosal K, Chakrabarty S, Nanda A. Hydroxypropyl methylcellulose in drug delivery. Pelagia Res Libr. 2011;2:

152–168.

18. Sundararaj SC, Thomas M V., Dziubla TD, Puleo DA. Bioerodible system for sequential release of multiple drugs. Acta Biomater. 2014;10: 115–125.
19. Hermans K, Van Den Plas D, Everaert A, Weyenberg W, Ludwig A. Full factorial design, physicochemical characterisation and biological assessment of cyclosporine A loaded cationic nanoparticles. Eur J Pharm Biopharm. 2012;82: 27–35.
20. Di Stasio E, De Cristofaro R. The effect of shear stress on protein conformation: Physical forces operating on biochemical systems: The case of von Willebrand factor. Biophys Chem. 2010;153: 1–8.
21. Ashton L, Dusting J, Imomoh E, Balabani S, Blanch EW. Shear-induced unfolding of lysozyme monitored in situ. Biophys J. 2009;96: 4231–4236.
22. Jaspe J, Hagen SJ. Do protein molecules unfold in a simple shear flow? Biophys J. 2006;91: 3415–3424.
23. Charm SE, Wong BL. Shear effects on enzymes. Enzyme Microb Technol. 1981;3: 111–118.
24. Ashton L, Dusting J, Imomoh E, Balabani S, Blanch EW. Susceptibility of different proteins to flow-induced conformational changes monitored with Raman spectroscopy. Biophys J. 2010;98: 707–714.
25. Rowe R, Sheskey P, Quinn M. Handbook of Pharmaceutical Excipients. Handbook of pharmaceutical excipients, Sixth edition. 2009.
26. Ritger PL, Peppas NA. A simple equation for description of solute release II. Fickian and anomalous release from swellable devices. J Control Release. 1987;5: 37–42.
27. Siepmann J, Kranz H, Bodmeier R, Peppas NA. HPMC-matrices for controlled drug delivery: A new model combining diffusion, swelling, and dissolution mechanisms and predicting the release kinetics. Pharmaceutical Research. 1999; 1748–1756.
28. Akbari J, Enayatifard R, Saeedi M, Saghafi M. Influence of hydroxypropyl methylcellulose molecular weight grade on water uptake, erosion and drug release properties of diclofenac sodium matrix tablets. Trop J Pharm Res. 2011;10: 535–541.
29. Abrahamsson B, Alpsten M, Bake B, Larsson A, Sjögren J. In vitro and in vivo erosion of two different hydrophilic gel matrix tablets. Eur J Pharm Biopharm. 1998;46: 69–75.
30. Rajabi-Siahboomi AR, Bowtell RW, Mansfield P, Henderson A, Davies MC, Melia CD. Structure and behaviour in hydrophilic matrix sustained release dosage forms: 2. NMR-imaging studies of dimensional changes in the gel layer and core of HPMC tablets undergoing hydration. J Control Release. 1994;31: 121–128.
31. Bettini R, Catellani PL, Santi P, Massimo G, Peppas NA, Colombo P. Translocation of drug particles in HPMC matrix gel layer: Effect of drug solubility and influence on release rate. J Control Release. 2001;70: 383–391.
32. Ghori MU, Ginting G, Smith AM, Conway BR. Simultaneous quantification of drug release and erosion from hypromellose hydrophilic matrices. Int J Pharm. 2014;465: 406–412.
33. Gao P, Skoug JW, Nixon PR, Ju TR, Stemm NL, Sung KC. Swelling of hydroxypropyl methylcellulose matrix tablets. 2. Mechanistic study of the influence of formulation variables on matrix performance and drug release. J Pharm Sci. 1996;85: 732–740.

Chapter 5: Optimisation of the preparation of ocular inserts loaded with sodium fluorescein, lysozyme and bovine serum albumin

Parts of this chapter have been submitted to:

Everaert A, Wouters Y, Melsbach E, Zakaria N, Ludwig A, Kiekens F, Weyenberg W. Optimisation of HPMC ophthalmic inserts with sustained release properties as a carrier for thermolabile therapeutics. Int J Pharm. 2017

1 INTRODUCTION

In the previous chapters, it has been demonstrated that the newly developed method for preparing drug-loaded ocular inserts is possible without the use of heat, air bubble entrapment or mixing forces. One major drawback that needed to be overcome, was the time-consuming rehydration period of six weeks to obtain a homogeneous HPMC hydrogel loaded with sodium fluorescein and lysozyme.

To achieve a significantly shorter rehydration time without changing the basic principles of the method developed, the inserts were no longer prepared as a batch of multiple inserts per syringe. Instead, the inserts were prepared individually. For practical reasons, the dimensions of the inserts prepared were not as small as the inserts after extrusion.

From a theoretical point of view, preparing inserts individually shortens the rehydration time required, as the diffusion path is reduced [1]. This optimised method allows a rehydration time of days instead of weeks. In contrast to the method described in the previous chapter, shear forces have also been reduced to a minimum. Bovine serum albumin (66.4 kDa) was added as the molecule with the largest molecular weight tested. Polymer HPMC E10M was preferred over previously tested polymers (E4M and K100M) due to its excellent rheological and ophthalmic properties. The HPMC percentage was increased to 25% (w/w) to explore the possibility of slowing down the release rate even further.

2 MATERIALS AND METHODS

2.1 Materials

Sodium fluorescein, lysozyme from chicken egg white, bovine serum albumin and glycerol analytical grade (99.5% (V/V)) were obtained from Sigma-Aldrich (Steinheim, Germany). Hydroxypropylmethyl cellulose type E10M Premium CR was provided by Colorcon (Dartford, UK). By specification, an aqueous 2% (w/w) E10M solution gives an apparent viscosity of 10.000 mPa.s (at 20 °C).

Phosphate-buffered saline solution (PBS, pH 7.4) was prepared using 8.2 g/l sodium chloride (NaCl), 0.300 g/l sodium dihydrogen phosphate dihydrate ($NaH_2PO_4.2H_2O$), 1.540 g/l disodium hydrogen phosphate dihydrate ($Na_2HPO_4.2H_2O$) and purified water. All electrolytes of analytical grade were purchased from Merck (Darmstadt, Germany).

Polyvinyl chloride (PVC)-blisters capsule size 4, used as a mould to produce the ocular inserts, were kindly provided by Janssen Pharmaceutica (Beerse, Belgium).

2.2 Preparation of ocular inserts

In the previous chapters, rod-shaped, ocular inserts were prepared by a method consisting of four phases. Firstly, a polymer solution was prepared using high shear forces and high temperatures, but in the absence of the drug of interest. Subsequently, the resulting polymer solution was dehydrated at a temperature of 150 °C yielding polymer cylinders of high HPMC concentration. These partially dehydrated polymer cylinders were transferred to a closed barrel to which a drug solution was added. The drug solution consisted of drug molecules, glycerol and purified water allowing the polymer cylinder to rehydrate during several weeks. After rehydration, small ocular inserts were extruded from the barrel by means of mild extrusion forces. A major drawback of this method is the extended period required to fully rehydrate and load the polymer cylinder after which extruded inserts could be obtained. Furthermore, shear forces, although they can be considered mild, are still applied in this method during the extrusion step.

To minimise the duration of the production process and to eliminate any shear forces including the mild forces used during extrusion, an alternative method, but based on the same principles as the method described above, was developed. The objective was to shorten the time required for the production process and at the same time to avoid any shear forces by preparing the rod-shaped inserts individually in a PVC-package for capsule size 4. This alternative production method can be

divided into three major phases. The major differences with the previous method are highlighted with an asterisk (*). A schematic overview is given in figure 1.

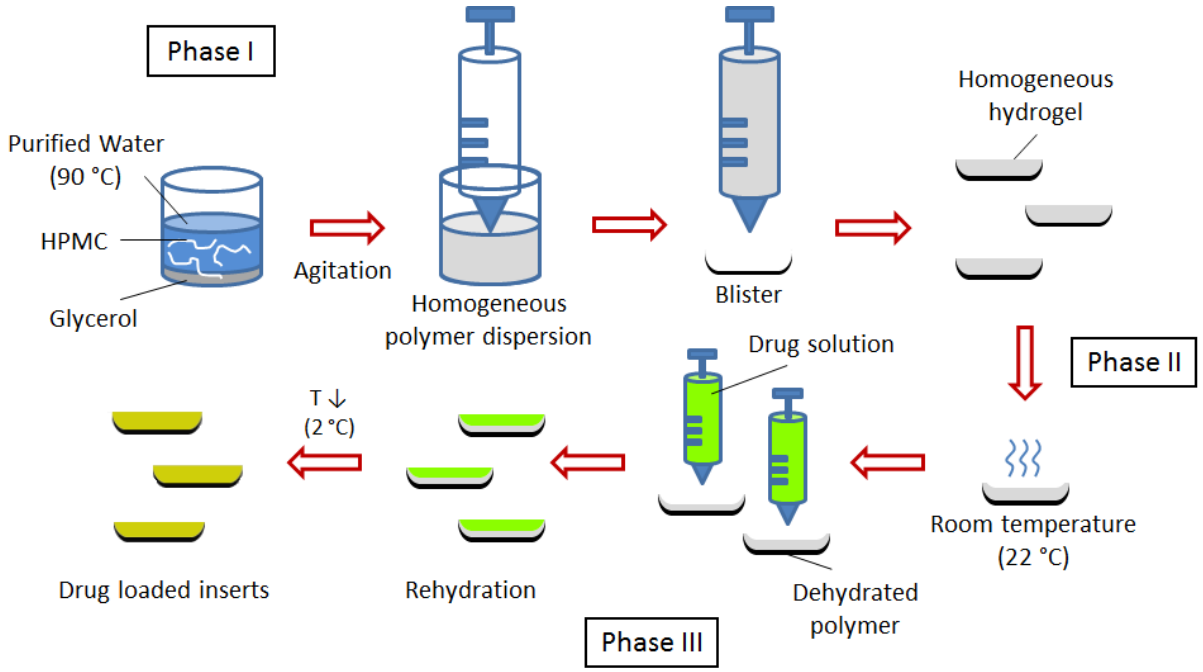

Fig. 1. General overview of the preparation method.

Phase I: Polymer matrix formation

A polymer solution of HPMC 20% (w/w)* was prepared by heating purified water up to 90-100 °C and adding HPMC powder under continuous agitation on a magnetic stirring device (VWR, VMS-C7-2, IKA, Staufen, Germany). A small amount of glycerol was added from the beginning* to obtain a percentage of 0.80% (w/w). The polymer dispersion was continuously stirred and heated. Once a homogeneous HPMC dispersion was obtained, the hot solution was gravimetrically casted into individual PVC-blisters* using an analytical balance (Mettler Toledo AB135-S, Greifensee, Switzerland) and cooled down to room temperature to allow build-up of the polymer matrix. Casting the HPMC dispersion into PVC-blisters causes the inserts to be semi-rod shaped instead of being entirely rod shaped if extruded.

Phase II: Dehydration of the polymer solution

The casted hydrogel was exposed to air to allow evaporation of water from the polymer matrix. The individually filled blisters were dried to the chosen HPMC concentrations. The percentage of HPMC in the matrix was determined by gravimetrical analysis using an analytical balance. The drying time took up several hours at room temperature in order to obtain dry percentages of 50% (w/w) HPMC and 75% (w/w) HPMC. In case of drying to a constant weight yielding a theoretical HPMC percentage of nearly 100% (w/w), the drying period took up to three days. Achieving 100% dehydration is technically not possible when drying to air, due to the presence of bound water. In general, water associated to a polymer can display different types of interaction. In literature, different types of thermodynamic water are recognised. Type I water corresponds to bulk free water. This type of water does not interact with the polymer and behaves as normal water in terms of melting and freezing. If water is loosely bound to the polymer, it is designated as type II water. It displays considerable amounts of supercooling and therefore freezes at temperatures lower than that of type I water. The third type of water is named type III water and is tightly bound to the polymer and is incapable of freezing. The sum of type II and III can be defined as bound water [2,3]. The amount of bound water will most likely not cause any practical implications for the development of the inserts at this level and was therefore not investigated further. In contrary to the previous method, the viscous polymer solution could not be exposed to high temperatures accelerating the evaporation process, due to the deformational nature of the PVC-blister packaging when heat is applied [4]. Therefore, the choice of the packaging material has a significant influence on the choice of drying conditions.

Phase III: Rehydration of the polymer matrix

In this phase, an aqueous drug solution was added to the dried polymer matrix. The percentages of drug and glycerol in the aqueous solution added to the dried polymer matrix was chosen accordingly, to reach final percentages of 3% (w/w) drug, 1% (w/w) glycerol and 25% (w/w) HPMC*.

As opposed to the aforementioned aqueous drug solution, a viscous drug solution* comprising HPMC as a viscosity enhancing agent of the drug solution was additionally tested and evaluated as a secondary experiment. The viscous drug solution consisted of 1% (w/w) HPMC, drug, glycerol and purified water. Because of the viscous character of the drug solution, the migration of water into the dehydrated polymer matrix is slowed down and drug molecules are surrounded by polymer molecules straight from the beginning of the diffusion process.

After adding the drug solution to the dehydrated polymer matrix, blisters containing the different components were stored at a temperature of 2 °C to allow rehydration of the polymer matrix. The rehydration time was either 24 or 72 hours* depending on the design of experiments.

After phase III, the final inserts were carefully removed from the blister package in order to perform dissolution testing. The shape of the blister package is illustrated in figure 2.

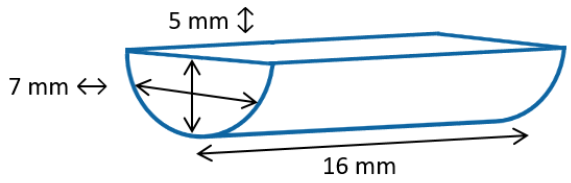

Fig. 2. Graphical representation of semi-rod-shaped inserts.

In figure 3, an overview comparing the previously developed method and the method described in this chapter is schematically laid out. The differences are marked with an asterisk (*).

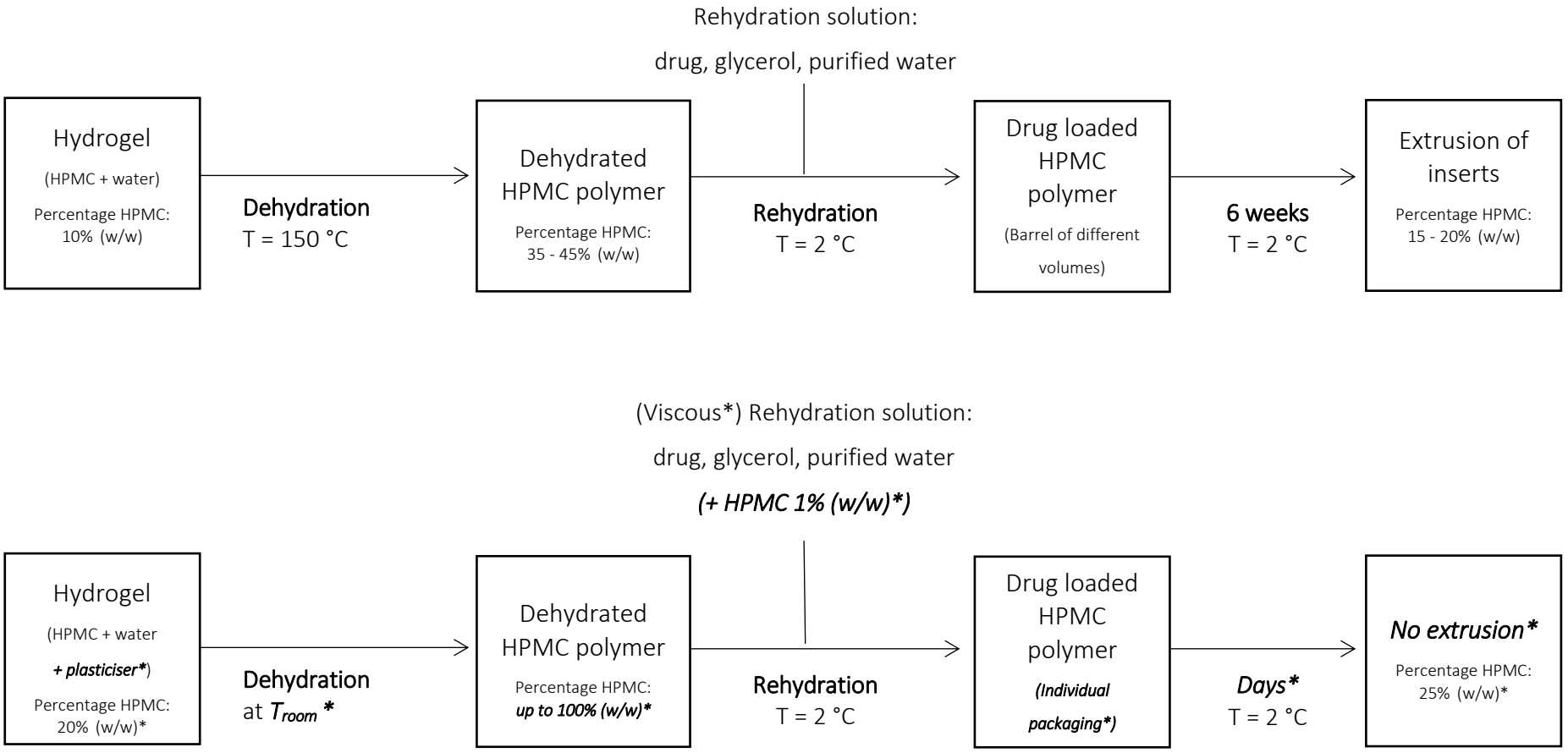

Fig. 3. Overview of the previously developed method compared to the method for preparing insert in individual packaging. The differences are marked with an asterisk (*).

2.3 Factorial design and statistical analysis

Three molecules of different molecular weight, sodium fluorescein 0.376 kDa, lysozyme from chicken egg white 14.3 kDa and bovine serum albumin 66.4 kDa, were used as model molecules to determine the influence of molecular weight on the release profiles of the inserts prepared. The dry percentage of HPMC and the rehydration time were selected as variable parameters based on experience from earlier research. A 2^2 full factorial design was set up for each of these molecules. An overview of the parameters and different levels is given in table 1 and an overview of the different formulations is given in table 2.

Table 1. Overview of the fixed and variable parameters in the factorial design. The upper (+) and lower (-) levels of the chosen parameters are given.

Fixed parameters		
Final % drug	3% (w/w)	
Final % glycerol	1% (w/w)	
Final % HPMC	25% (w/w)	
Variable parameters		
	(+) level	***(-) level***
Dry % HPMC	75% (w/w)	50% (w/w)
Rehydration time	72 h	24 h

Table 2. Overview of the different experiments and the chosen variables. Four inserts per formulation were prepared and analysed. Each formulation was prepared in duplicate.

Formulation	*Dry % HPMC*	*Rehydration time*
1	+	+
2	+	-
3	-	+
4	-	-

The influence of dry percentage HPMC (50% (w/w) and 75% (w/w)) and rehydration time (24 and 72 hours) on the release profiles of different molecules at time point 460 or 480 minutes was tested

using ANOVA with Statistica® 12 (Statsoft, Tulsa, USA). Each experiment was performed in duplicate with four inserts per formulation. An effect is considered statistically significant when $p<0.05$.

2.4 *In vitro* drug release studies

The release patterns of the different formulations were plotted and analysed. Four inserts per formulation (in duplicate) were put into separate test tubes to which 15 g PBS was added at a temperature of 32 °C. The test tubes were placed in a non-oscillating water bath (Julabo 20B, Merck-Belgolabo, Overijse, Belgium) at a temperature of 32.0 ± 0.5 °C. At different time points, samples of 2 g release medium were withdrawn from each test tube and replaced with an equal amount of PBS at 32 °C ensuring sink conditions. Sampling intervals of 10, 30, 60, 90, 120, 180, 240, 300, 360, 420 and 480 minutes were chosen for sodium fluorescein and lysozyme. Sampling intervals of inserts formulated with albumin were chosen at 10, 30, 60, 90, 120, 180, 240, 300, 390 and 460 minutes. Before and after sampling, the content of the test tubes was homogenised by means of gentle stirring.

Samples were analysed spectrophotometrically at a wavelength of 484 nm, 280 nm and 278 nm for the molecules sodium fluorescein, lysozyme and albumin respectively. At the end of every series of measurements, the content of each test tube was intensively vortexed to release the remaining drug from the insert and measured spectrophotometrically.

2.5 Drug release analysis

The *in vitro* drug release curves were analysed for zero order, first order or mixed order kinetics as described under section 2.9 *Drug release analysis* in *chapter 4*.

3 RESULTS AND DISCUSSION

3.1 *In vitro* drug release studies

The objective of the research described in this chapter was to shorten the time required to rehydrate the dehydrated polymer matrix using a (viscous) drug solution. To achieve this goal, smaller single-dose inserts were prepared. Not only is the contact area of the polymer matrix with the surrounding drug solution increased relative to its volume, but the depth to be penetrated by the drug molecules is also reduced thereby shortening the rehydration time required. An additional benefit of this method is that even the mild extrusion process is avoided all together. This method was evaluated using three drug molecules of different molecular weight.

3.1.1 Sodium fluorescein

The inserts contain a certain amount of water, which implicates that the drug molecules can readily be released from the insert by means of diffusion. Upon contact with the release medium, the insert swells due to water uptake and as a result, the polymeric network disentangles. A total disentanglement of the unlinked polymeric network will eventually occur, slowly releasing the drug by means of erosion [5–7]. Because of the dense packing of the polymer network, slower release rates are expected to take place, especially for larger molecules such as lysozyme and albumin [8,9]. The amount of sodium fluorescein released from HPMC inserts is plotted in the cumulative release profiles in figure 4. An overview of the effect of the different parameters on the release of sodium fluorescein loaded inserts is summarised in table 3. Each of the formulations in the design of experiments exhibit slow release with an average cumulative release amount of 68.82% (w/w) of the total amount of drug after an interval of 480 minutes. Statistical analysis revealed no significant differences when the dry percentage HPMC or rehydration time was altered. Sodium fluorescein has a relatively low molecular weight (0.376 kDa) compared to lysozyme and albumin and therefore experiences little resistance from the polymer network upon diffusion.

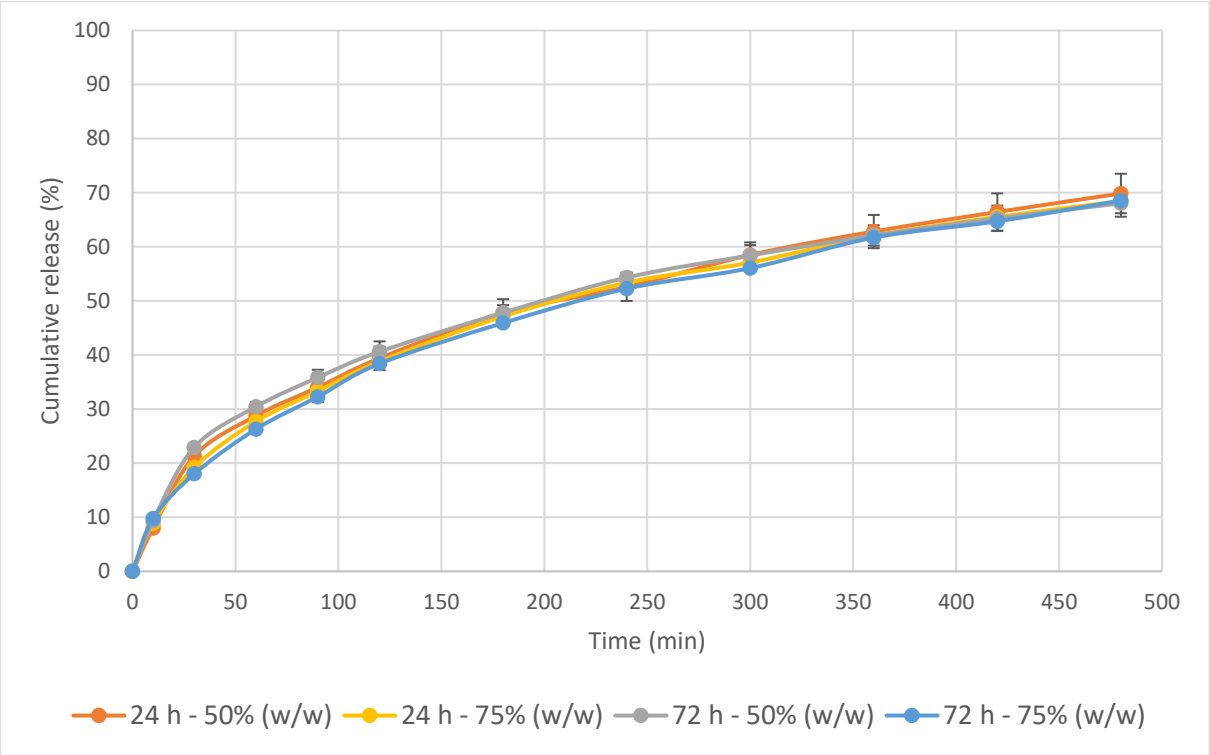

Fig. 4. Cumulative release profiles of sodium fluorescein loaded HPMC inserts. Each graph is a representation of inserts formulated with the parameters as shown in the legend (rehydration period – dry percentage HPMC). The drug release is compared to the total amount of drug present after full release of the drug from the matrix (n=8).

Table 3. An overview of the effect of the different parameters on the release of sodium fluorescein loaded inserts.

Parameter	Effect %	p-value
Dry % HPMC	-0.19	0.145
Rehydration time	0.60	0.643

3.1.2 Lysozyme from chicken egg white

Release profiles of inserts loaded with lysozyme from chicken egg white are shown in figure 5.

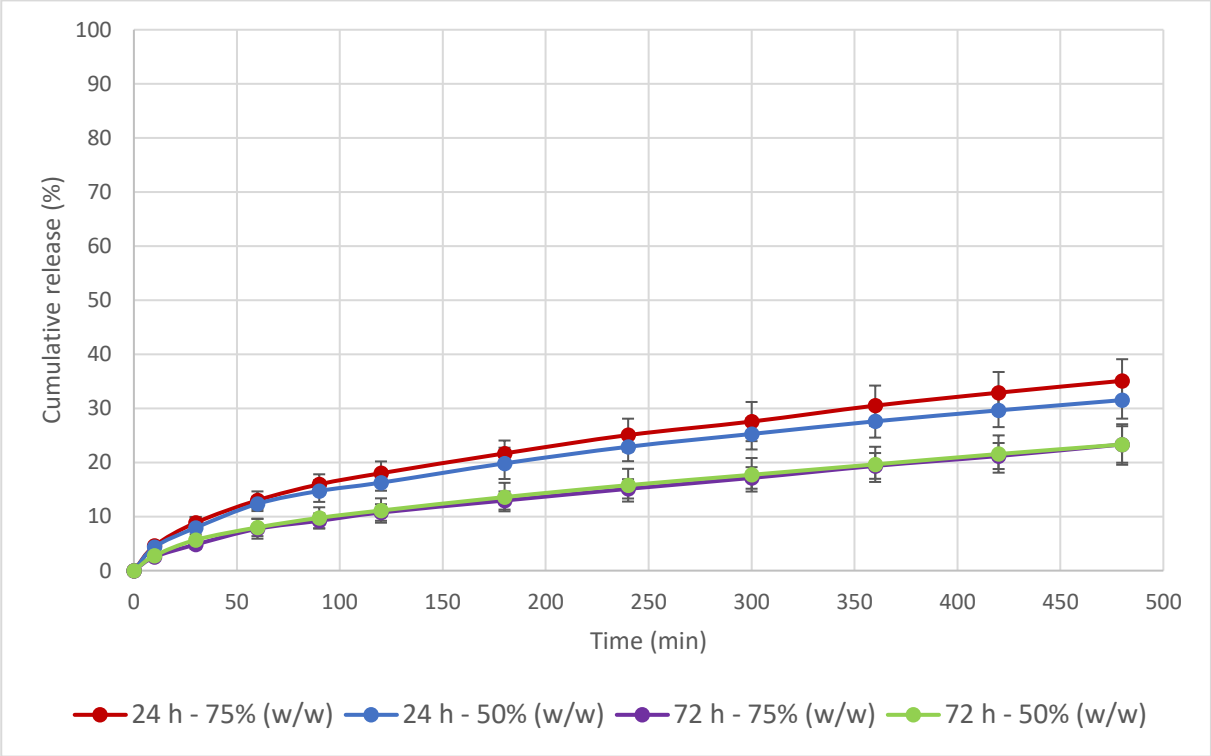

Fig. 5. Cumulative release profiles of inserts loaded with lysozyme. Each graph is a representation of inserts formulated with the parameters as shown in the legend (rehydration period – dry percentage HPMC). The drug release is compared to the total amount of drug present after full release of the drug from the matrix (n=8).

In table 4, an overview of the effect of the different parameters on the release of lysozyme loaded inserts is compiled.

Table 4. An overview of the effect of the different parameters on the release of chicken egg white lysozyme loaded inserts.

Parameter	Effect %	p-value
Dry % HPMC	1.79	0.177
Rehydration time	-9.99	0.000

The dry percentage of HPMC showed no significant influence upon statistical analysis. Contrary to the parameter 'dry % HPMC', increasing the rehydration time from 24 to 72 hours did have a statistical significant impact ($p = 0.000$). Due to the higher molecular weight of lysozyme, the total amount of drug released from the insert for a given time was lower compared to sodium fluorescein and decreased even further by prolonging the rehydration period from 24 to 72 hours. An additional

difference of 9.99% (w/w) over a time interval of 480 minutes was calculated. This could be indicative for the influence of drug loading time on the diffusion process of drug molecules into the polymeric network. The molecular weight of lysozyme is 38 times higher than sodium fluorescein. Therefore the lysozyme molecule experiences more resistance from the polymeric network upon diffusion out of the network as well as upon diffusion into the polymer matrix during preparation [8–10]. After 24 hours, it was visually apparent that the lysozyme molecules did not fully penetrate the core of the insert whereas after 72 hours, the lysozyme molecules appeared to be loaded more deeply in the insert, resulting in slower release rates.

3.1.3 Bovine serum albumin

In figure 6, the release curves of inserts loaded with bovine serum albumin are drawn. Slow release curves of inserts loaded with bovine serum albumin could not be achieved with the chosen parameters. An amount of 45% (w/w) albumin was released rapidly from all formulations tested after a time interval of 10 minutes. After 30 minutes, 80% (w/w) of the total amount of drug present in the insert was released into the surrounding medium. Varying either the parameter 'dry % HPMC' or 'rehydration time' in accordance with the design, did not slow down the release rate of the albumin molecules. A modest but statistically significant reduction ($p = 0.024$) of the total amount of albumin released after 460 minutes could be achieved by extending the rehydration time to 72 hours, but the practical significance of the lower release amount is comparatively low. This effect was minimal with an average decrease of 3.30% (w/w) albumin released after 460 minutes when rehydration time was increased from 24 to 72 hours. The results and their significance are summarised in table 5.

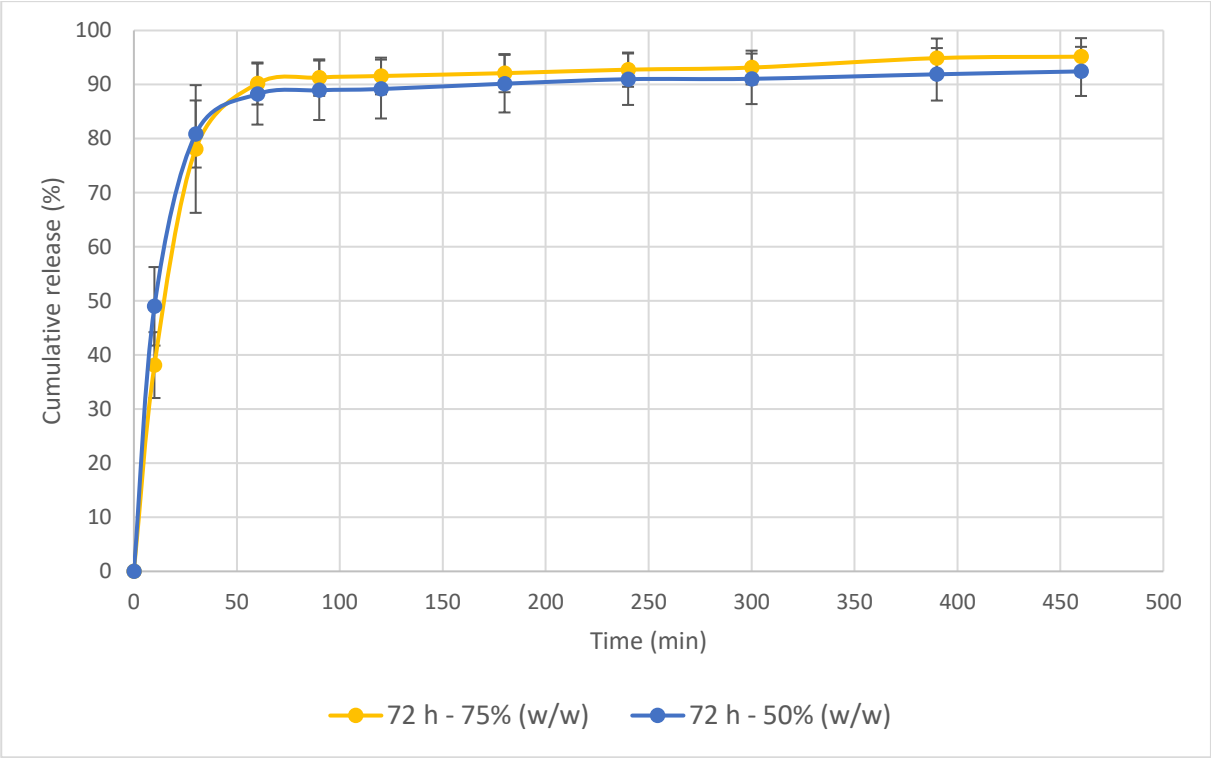

Fig. 6. Cumulative release profiles of inserts loaded with bovine serum albumin. Each graph is a representation of inserts formulated with the parameters as shown in the legend (rehydration period – dry percentage HPMC). The drug release is compared to the total amount of drug present after full release of the drug from the matrix (n=8).

Table 5. An overview of the effect of the different parameters on the release of bovine serum albumin loaded inserts.

Parameter	Effect %	p-value
Dry % HPMC	1.10	0.432
Rehydration time	-3.30	0.024

The molecular weight of the drug molecules influences the release behaviour from the inserts formulated. Bovine serum albumin is a protein with the highest molecular weight (66.4 kDa) of the three molecules tested. Its diffusion into the matrix during preparation is limited due to the entanglement of the polymeric network, especially in case of a final HPMC percentage of 25% (w/w). As larger molecules diffuse at a lower rate compared to smaller molecules, only a small amount of albumin is embedded deeply enough in the matrix. The majority of drug molecules is located at the surface of the insert. The hydrodynamic volume of the drug molecules on one hand and the relatively high diffusional rate of solvent molecules on the other can provide an explanation for this observation. Solvent molecules will diffuse rapidly into the matrix hydrating the surrounding HPMC chains. At the surface of the insert, the diffusion of the solvent molecules into the insert may

result in an oversaturation of the drug solution causing precipitation of albumin molecules. Increasing the dehydration degree of the polymer matrix to e.g. 100% (w/w) means that more rehydration solution is required to obtain the same final HPMC percentage. This also implicates that molecules, especially larger ones such as albumin, will be kept dissolved in the rehydration solution for a longer period of time, theoretically increasing the likelihood of penetrating in the polymer matrix. However, the dehydration degree is directly linked to the water content of the HPMC polymer and therefore influences the density of the polymeric network and hence drug diffusion characteristics. This concept is depicted in figure 7 and is further explored in *chapter 6*.

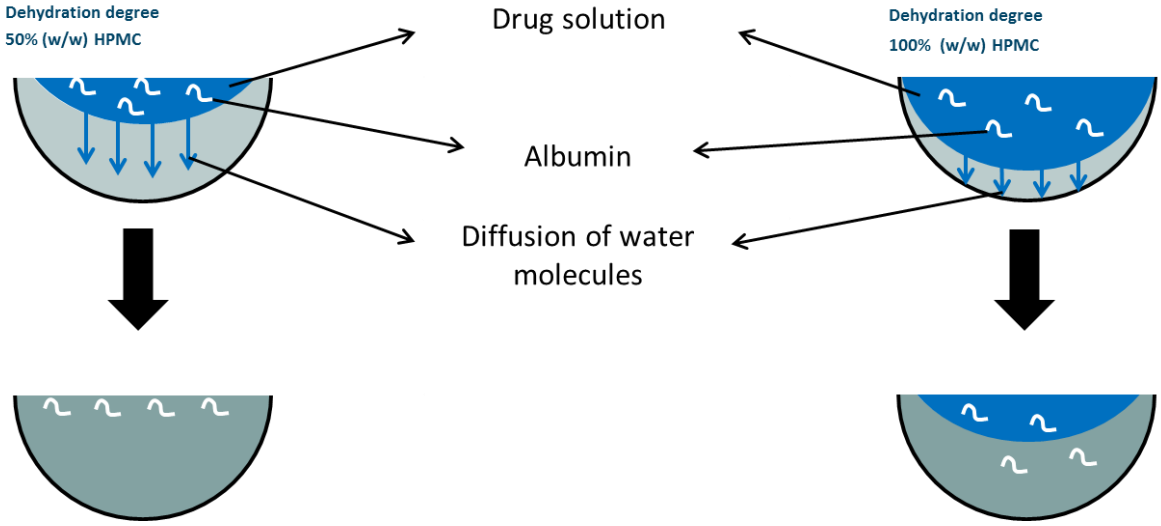

Fig. 7. Theoretical example of how a higher dehydration degree of the polymer matrix might influence the distribution of the drug. Increasing the dehydration degree of the intermediate polymer matrix requires more rehydration solution to be added, giving a dissolved drug substance (in this case albumin) more chance to diffuse in the matrix.

The method of rehydration also highlights a potential problem in case of larger inserts and larger molecules. Rehydration can only occur from one side, meaning that a gradient of the drug solution will come as a result of this process. Although these limitations were known prior to carrying out the experiments, it was kept as described in this chapter in order to reduce manipulations as much as possible. Furthermore, miniaturising the inserts will probably reduce this effect to a great extent but miniaturisation was not the main focus of the current research.

3.1.4 Influence of molecular weight

Comparing the release profiles of sodium fluorescein and chicken egg white lysozyme, an influence of the molecular weight is observed, as mentioned earlier. Closely linked to the molecular weight,

is the hydrodynamic radius of a molecule [11–13]. The larger hydrodynamic radius of a molecule such as lysozyme compared to sodium fluorescein resulted in slower release of lysozyme from the polymeric network [14]. Based on this principle, It was expected that inserts loaded with albumin would yield inserts with an even slower release profile. But due to the high molecular weight and hydrodynamic radius, the resistance upon diffusion into the polymer during loading was too large to overcome in a period of 72 hours. In figure 8, an overview of release profiles of albumin, sodium fluorescein and lysozyme is graphically represented.

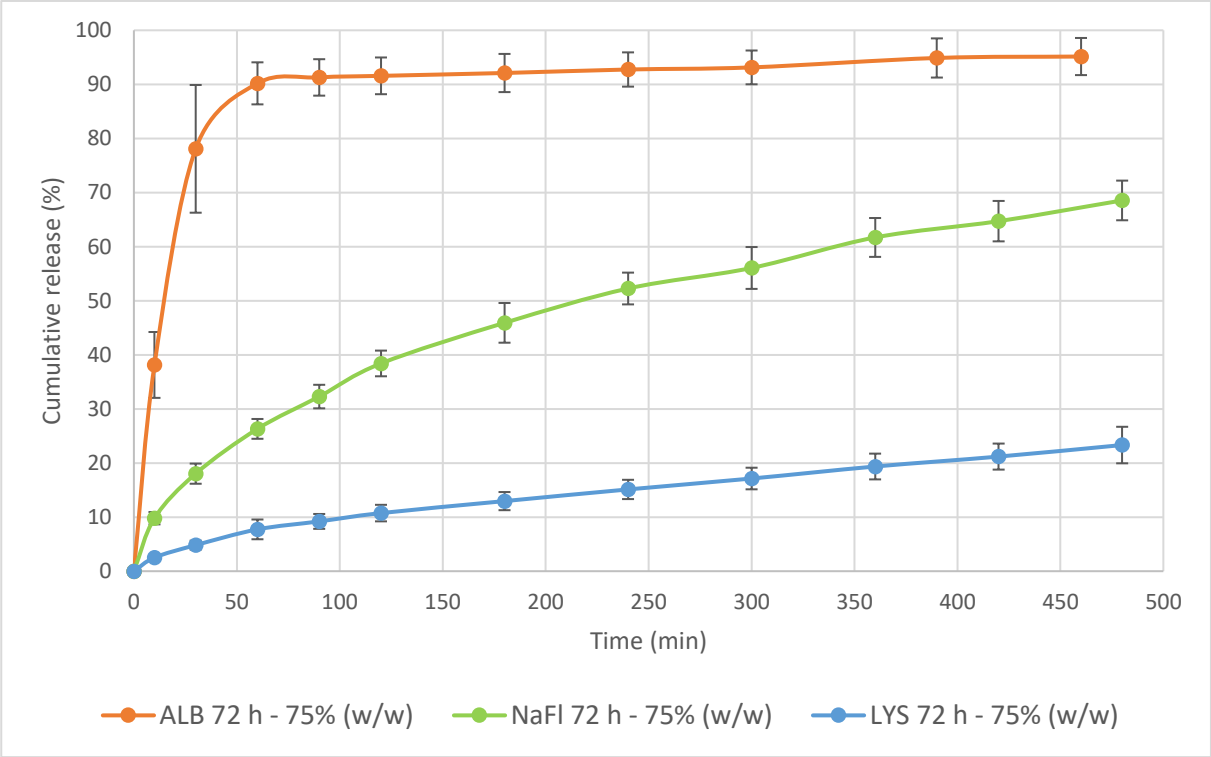

Fig. 8. Cumulative release profiles of inserts loaded with bovine serum albumin (ALB), sodium fluorescein (NaFl) and lysozyme from chicken egg white (LYS). Each graph is a representation of inserts formulated with parameters shown in the legend (molecule type – rehydration period – dry percentage HPMC). The drug release is compared to the total amount of drug present after full release of the drug from the matrix (n=8).

3.1.5 Viscous polymer drug solution

In order to produce slow release ocular inserts of molecules with the largest molecular weight tested, inserts were dehydrated at room temperature to a constant weight giving a theoretical dry percentage of almost 100% (w/w) HPMC. Instead of using an aqueous drug solution in which albumin molecules would precipitate on the surface of the insert as a result of solvent absorption, a viscous polymer drug solution was prepared and added. Because of the viscous character of the drug solution, the migration of water into the dehydrated polymer matrix is slowed down. Additionally, the drug molecules are surrounded by polymer molecules forming a polymeric network from the beginning of the diffusion process. This results in a lower migration speed of water molecules towards the dehydrated polymer matrix which might prevent the occurrence of an oversaturated drug solution, giving solvated drug molecules more time to diffuse into the polymer matrix. This process is depicted in figure 9.

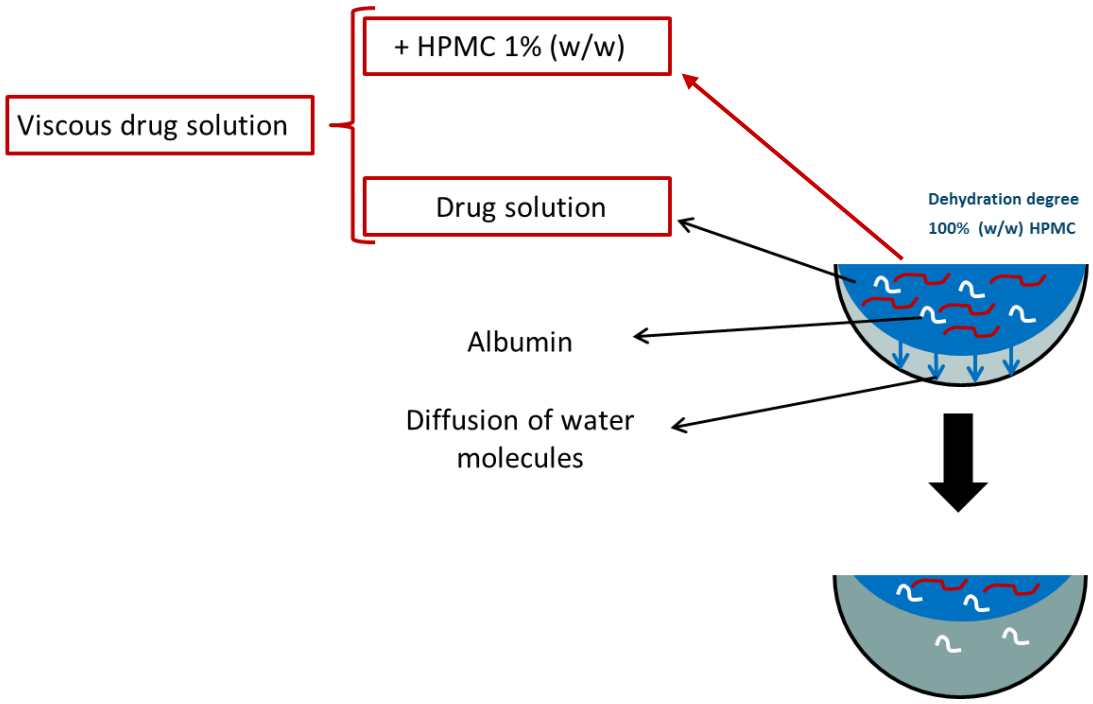

Fig. 9. Theoretical representation of the influence of a viscous drug solution on the embeddedness of albumin molecules in the HPMC matrix. Adding HPMC to the drug solution causes the water molecules to migrate at lower rates into the dehydrated polymer matrix. It also surrounds the albumin molecules with some HPMC molecules, forming a network around the drug substance, slowing down the drug release rate.

Earlier results indicated that time is an important and influential parameter for the drug loading process. For this reason, a rehydration period of 72 hours was chosen instead of 24 hours. The release profiles of inserts loaded with bovine serum albumin with a rehydration time of 72 hours

are shown in figure 10. For the sake of reference, a fully dehydrated polymer matrix rehydrated with an aqueous instead of viscous solution of albumin was added to the comparison.

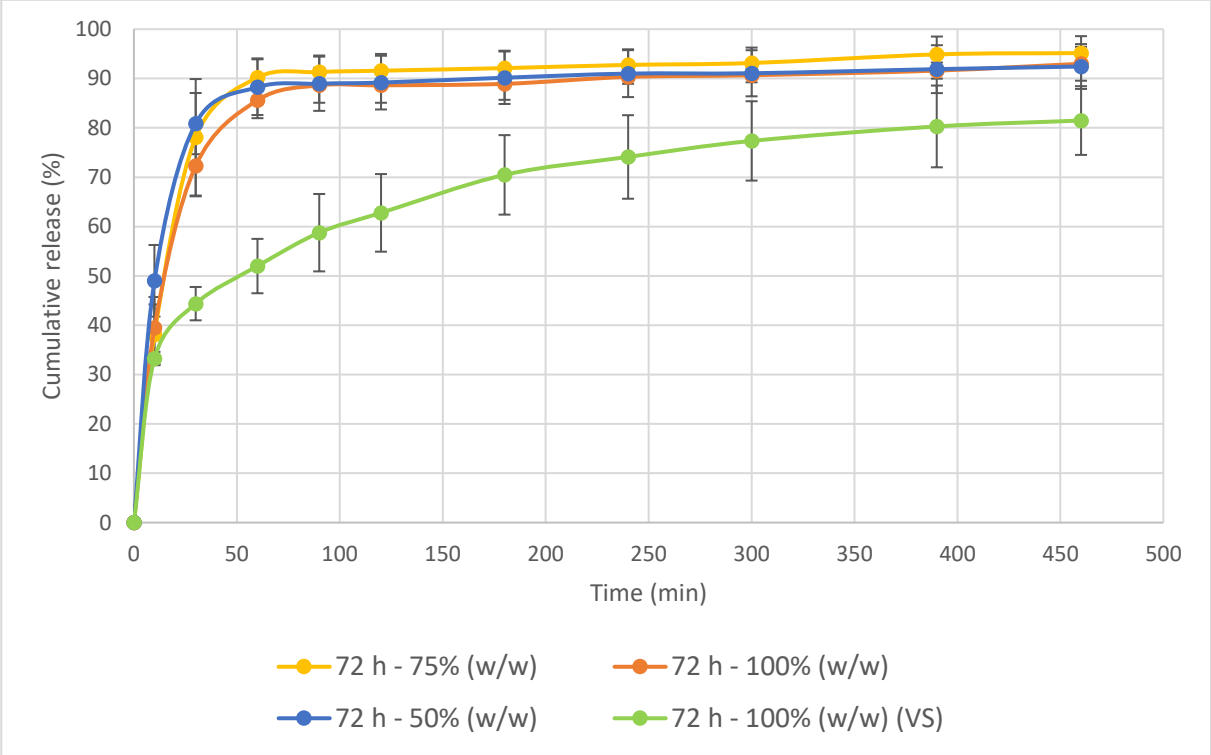

Fig. 10. Cumulative release profiles of inserts loaded with bovine serum albumin. Each graph is a representation of inserts formulated with parameters shown in the legend. The drug release is compared to the total amount of drug present after full release of the drug from the matrix. Inserts are formulated with an aqueous drug solution for dry percentages 50% (w/w), 75% (w/w) (n=8) and 100% (w/w) (n=4), whereas a viscous drug solution (VS) is used for inserts with a theoretical dry percentage of 100% (w/w) (n=4).

The amount of albumin released from the insert is lower at all time points when inserts are formulated with a viscous polymer drug solution. After an interval of 60 minutes, an amount of 44.47% (w/w) albumin was released opposed to 85.18% (w/w) from inserts prepared with an aqueous drug solution. Although a clear improvement was observed, the release profiles are not up to the same level as the release profiles of inserts loaded with lysozyme, as a burst release is still observed.

3.2 Drug release analysis

3.2.1 Sodium fluorescein

The release profiles of ocular inserts formulated with sodium fluorescein and loaded during 24 and 72 hours are presented in figure 11a. The slope of the linear regression of the curve equals a value of 0.5176 and 0.4900 respectively, indicating the release of drug by means of diffusion as well as case-II transport. However, the slope n obtained for the inserts prepared with a loading time of 72 hours, approaches the value of 0.45 which could be indicative for a release of drug molecules predominantly characterised by diffusion.

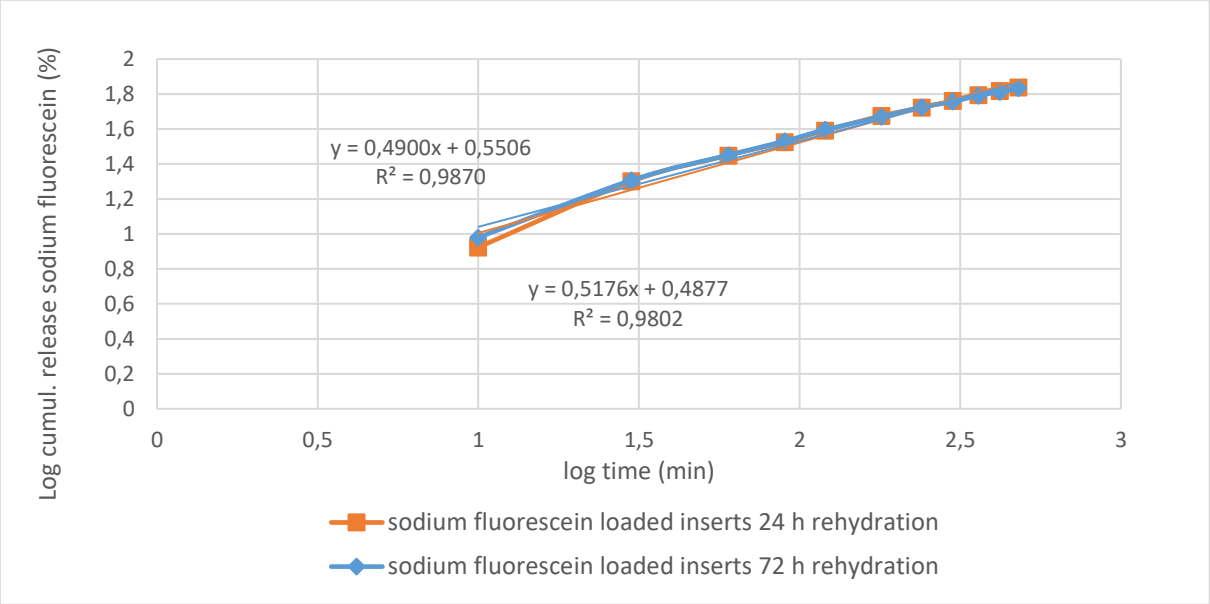

Fig. 11a. Release kinetics of sodium fluorescein loaded inserts using the Peppas–Korsmeyer model.

Upon closer inspection of the release kinetics of sodium fluorescein in figure 11a, it was noticed that the first measuring point is very influential. Therefore, in figure 11b, the same cumulative release profiles are shown after omitting the first measuring point (10 minutes).

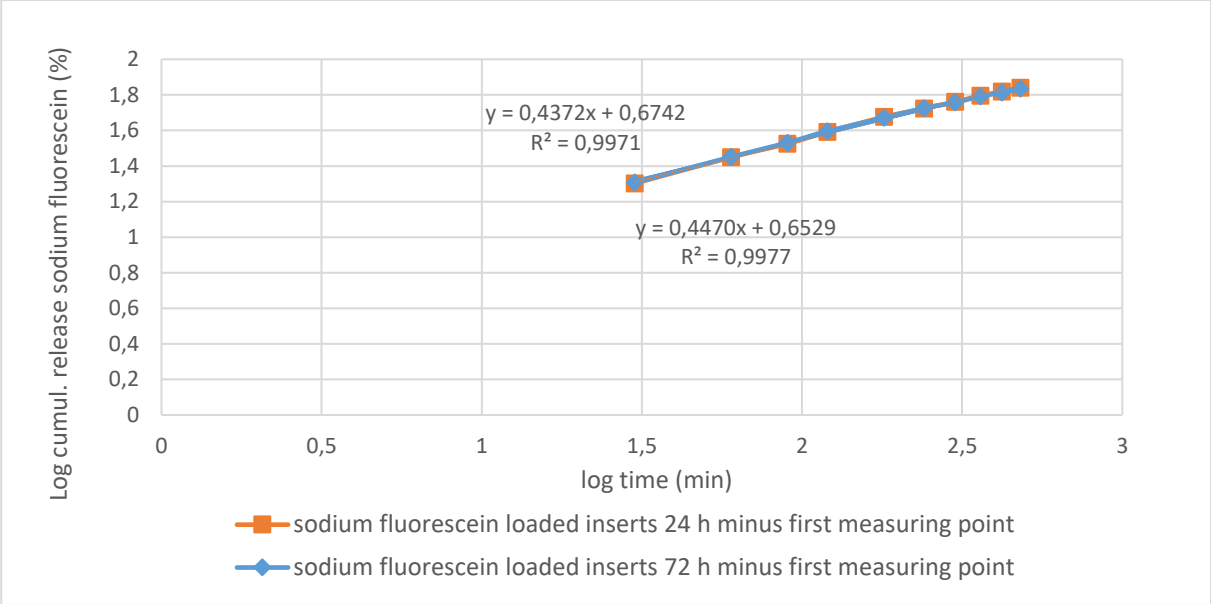

Fig. 11b. Release kinetics of sodium fluorescein loaded inserts using the Peppas–Korsmeyer model after omitting the first measuring point (10 min).

A very small but rapid release of drug molecules within the first 30 minutes of the release process was apparent. Thereafter, the drug molecules were released by diffusion indicated by the slope n being smaller than 0.45 after regression analysis. This observation can be attributed to drug molecules residing on the surface of the insert and being rapidly released in the release medium.

3.2.2 Lysozyme from chicken egg white

Figure 12 shows the release profiles of inserts loaded with chicken egg white lysozyme and represents the release kinetics of inserts which were allowed to rehydrate over a period of 24 hours and the release kinetics of inserts which were measured after a rehydration period of 72 hours. Both profiles indicate the release by means of first and mixed zero order release kinetics due to the value of the slope of their linear regression lines, 0.5086 and 0.5461 respectively. Inserts which were allowed to rehydrate over a period of 72 hours display a value of n closer to 0.89 than inserts rehydrated over a period of 24 hours, indicative of a more prominent role for case-II transport of the drug. This supports the hypothesis that a longer rehydration period allows the protein molecules to penetrate deeper into the polymer matrix. Upon contact with the release medium, resistance from the polymer network and the increased diffusional distance by swelling of the

polymer matrix impairs immediate diffusion of deeply penetrated drug molecules to the surrounding medium. These deeply embedded drug molecules will be released when the unlinked polymeric network disentangles releasing the drug by means of erosion.

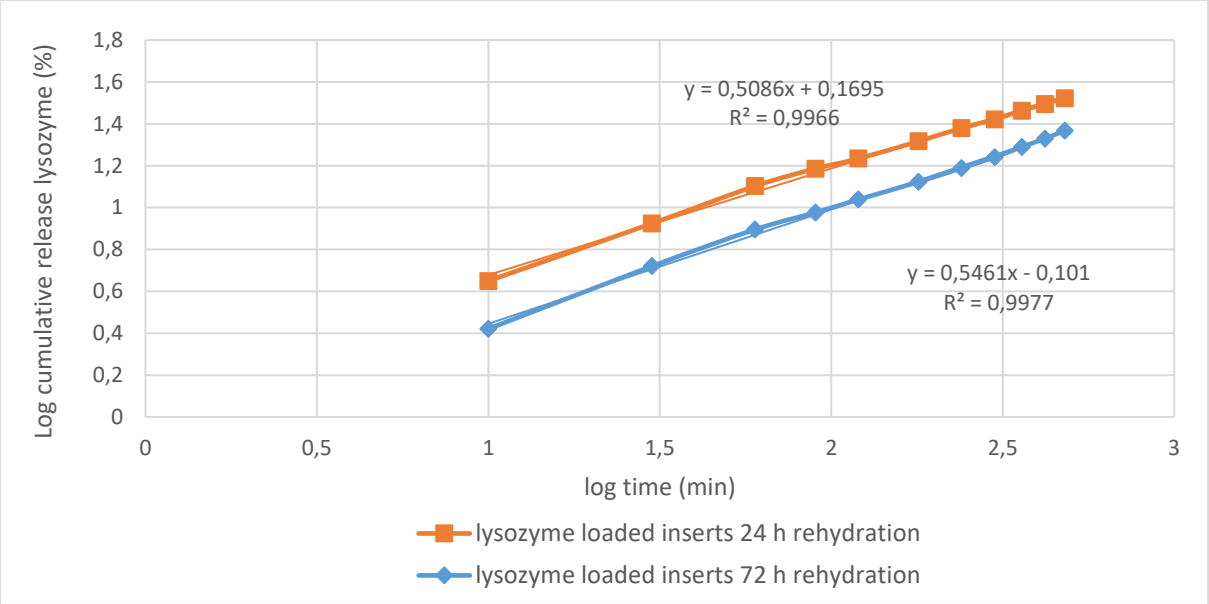

Fig. 12. Cumulative release profiles of inserts loaded with chicken egg white lysozyme.

3.2.3 Bovine serum albumin

Slow release profiles were not obtained for inserts loaded with albumin. Therefore, no release kinetic profiles were generated.

4 CONCLUSION

The ocular inserts prepared by the modified preparation method, as described in the present chapter, shows that the production of inserts with slow release without any extrusion forces is achievable. Furthermore, obtaining inserts with equal amounts of drug is no longer an issue, as the drug solution is added individually for every insert. The method also demonstrates that a drug can be loaded into the insert without exposing the molecules to high temperatures while minimising the risk of oxidation. When large molecules such as lysozyme need to be incorporated, a significant influence of the rehydration time is observed on the release profiles of the inserts.

Another major advantage of the present method compared to the previously developed method is the significant reduction of the rehydration time from several weeks to a few days for sodium fluorescein and lysozyme. However, obtaining slow release was not possible for albumin molecules without further modification. Such a modification involved adding a viscous drug solution which improved the drug release characteristics in case of albumin loaded inserts. Burst release to a certain extent was still observed. However, it should be noted that the increase of the final percentage HPMC to 25% (w/w) and hence resulting in a denser polymeric network can be held partially responsible for the result observed. For this reason, the next chapter will explore the limitations set by the molecular weight of the molecule of interest together with the final HPMC percentage as well as the dimensions of the insert.

Finally, an additional benefit of the method is that rehydration of the polymer matrix with a drug solution is able to occur in the final package of the product, even after being sealed.

References

1. Siepmann J, Siepmann F. Modeling of diffusion controlled drug delivery. J Control Release. 2012;161: 351–362.
2. Ford JL. Thermal analysis of hydroxypropylmethylcellulose and methylcellulose: Powders, gels and matrix tablets. Int J Pharm. 1999;179: 209–228.
3. Almeida N, Rakesh L, Zhao J. Monovalent and divalent salt effects on thermogelation of aqueous hypromellose solutions. Food Hydrocoll. 2014;36: 323–331.
4. Ognedal A. Large-Deformation Behaviour of Thermoplastics at Various Stress States. Norwegian University of Science and Technology. 2012.
5. Barba AA, d'Amore M, Chirico S, Lamberti G, Titomanlio G. Swelling of cellulose derivative (HPMC) matrix systems for drug delivery. Carbohydr Polym. 2009;78: 469–474.
6. Rajabi-Siahboomi AR, Bowtell RW, Mansfield P, Henderson A, Davies MC, Melia CD. Structure and behaviour in hydrophilic matrix sustained release dosage forms: 2. NMR-imaging studies of dimensional changes in the gel layer and core of HPMC tablets undergoing hydration. J Control Release. 1994;31: 121–128.
7. Bettini R, Catellani PL, Santi P, Massimo G, Peppas NA, Colombo P. Translocation of drug particles in HPMC matrix gel layer: Effect of drug solubility and influence on release rate. J Control Release. 2001;70: 383–391.
8. Ghosal K, Chakrabarty S, Nanda A. Hydroxypropyl methylcellulose in drug delivery. Pelagia Res Libr. 2011;2: 152–168.
9. Ghori MU, Ginting G, Smith AM, Conway BR. Simultaneous quantification of drug release and erosion from hypromellose hydrophilic matrices. Int J Pharm. 2014;465: 406–412.
10. Gao P, Skoug JW, Nixon PR, Ju TR, Stemm NL, Sung KC. Swelling of hydroxypropyl methylcellulose matrix tablets. 2. Mechanistic study of the influence of formulation variables on matrix performance and drug release. J Pharm Sci. 1996;85: 732–740.
11. Charalel RA, Engberg K, Noolandi J, Cochran JR, Frank C, Ta CN. Diffusion of protein through the human cornea. Ophthalmic Res. 2012;48: 50–55.
12. Esposito A, Comez L, Cinelli S, Scarponi F, Onori G. Influence of glycerol on the structure and thermal stability of lysozyme: a dynamic light scattering and circular dichroism study. J Phys Chem B. 2009;113: 16420–16424.
13. Fetters LJ, Hadjichristidis N, Lindner JS, Mays JW. Molecular Weight Dependence of Hydrodynamic and Thermodynamic Properties for Well-Defined Linear Polymers in Solution. Journal of Physical and Chemical Reference Data. 1994; 619–640.
14. Mawad D, Anne Boughton E, Boughton P, Lauto A. Advances in Hydrogels Applied to Degenerative Diseases. Curr Pharm Des. 2012;18: 2558–2575.

Chapter 6: Release rate comparison between FITC-dextrans with different molecular weight

1 INTRODUCTION

Chapter 5 pointed out that preparing inserts with small proteins is possible, but a clear limitation in molecular weight was noticed, particularly with a final HPMC percentage of 25% (w/w). In the current chapter, inserts were prepared and loaded with fluorescein isothiocyanate (FITC) dextrans of different molecular weight in order to determine the limitations of the drug loading size for the preparation method developed. These FITC-dextrans are prepared from native Dextran B512F, which was subsequently labelled with fluorescein through stable thiocarbamoyl linkage. The linkage procedure does not lead to depolymerisation [1]. FITC-dextrans are widely used for permeability testing in cells and tissue [2–6], but also for permeability studies of gel matrices [7,8].

Firstly, the inserts were prepared with the same dimensions as described in section *2.2 Preparations of ocular inserts* in *chapter 5*. Thereafter, inserts with smaller dimensions were prepared and loaded with FITC labelled dextrans.

2 MATERIALS AND METHODS

2.1 Materials

FITC labelled dextrans of different molecular weight (10, 20, 40 and 70 kDa) were obtained from Sigma-Aldrich (Steinheim, Germany). Hydroxypropylmethyl cellulose type E10M Premium CR was provided by Colorcon (Dartford, UK). By specification, an aqueous 2% (w/w) E10M solution gives an apparent viscosity of 10.000 mPa.s (at 20 °C).

Phosphate-buffered saline solution (PBS, pH 7.4) was prepared using 8.2 g/l sodium chloride (NaCl), 0.300 g/l sodium dihydrogen phosphate dihydrate ($NaH_2PO_4.2H_2O$), 1.540 g/l disodium hydrogen phosphate dihydrate ($Na_2HPO_4.2H_2O$) and purified water. All electrolytes of analytical grade were purchased from Merck (Darmstadt, Germany).

PVC-blisters capsule size 4, used to produce the ocular inserts, were kindly provided by Janssen Pharmaceutica (Beerse, Belgium). Custom developed Teflon moulds, for the production of smaller inserts, were developed by the technical service of the University of Antwerp (Wilrijk, Belgium).

2.2 Preparation of ocular inserts

The inserts were loaded identically to the method described in section *2.2 Preparation of ocular inserts* in *chapter 5* with a final HPMC percentage of 15% (w/w) or 20% (w/w) and with a rehydration period of three days, ten days and six weeks for all four tested FITC-dextran types. The average mass of the inserts was weighed at approximately 550 mg. Although such a mass is not suited for clinic use in human eyes, the influence of molecular weight during the drug loading process can be demonstrated more clearly in larger inserts. Also, the risk of errors during insert production is reduced. These discriminating conditions help to understand the underlying processes better, but the practical relevance remains to be seen. Therefore, smaller inserts were also produced using custom built Teflon moulds in HPMC percentages of 15% (w/w), 20% (w/w) and 25% (w/w). The average weight of the inserts was set at approximately 82 mg and were loaded over a period of six weeks for all four tested FITC-dextrans (10, 20, 40 and 70 kDa). The method of preparation was identical to the method mentioned above. The dimensions of the inserts are compared in figure 1.

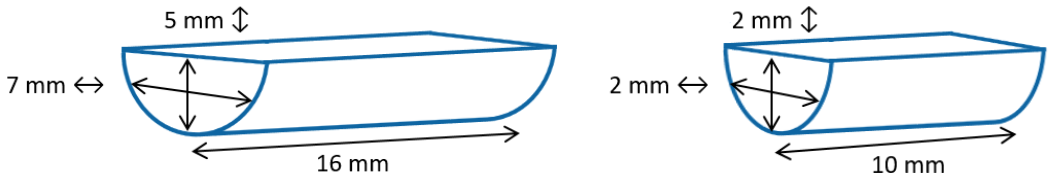

Fig. 1. Dimensions and shape of the inserts weighing approximately 550 mg (L) and 82 mg (R), casted in PVC-blisters and Teflon moulds respectively.

An alteration to this method was also made by directly adding dry FITC-powder to the dehydrated HPMC matrix on which the 1% (w/w) viscous HPMC solution was casted. Basically, this means that the FITC-dextrans were dissolved *in situ* instead of a drug solution being prepared in advance. This alternative method was assessed in order to examine whether there was an influence of the way the drug was added to the dehydrated polymer. For every individual blister package, the calculated amount of drug was weighed and added, resulting in no waste of drug compound. The final HPMC percentage was kept at 15% (w/w) and 20% (w/w). The drug loading time was set to three days and compared to the results obtained with inserts prepared with a viscous drug solution. This experiment, in which FITC-dextrans are dissolved *in situ,* was only performed on the large-sized inserts prepared in the PVC-blister package. A summary of the experiments is laid out in figure 2.

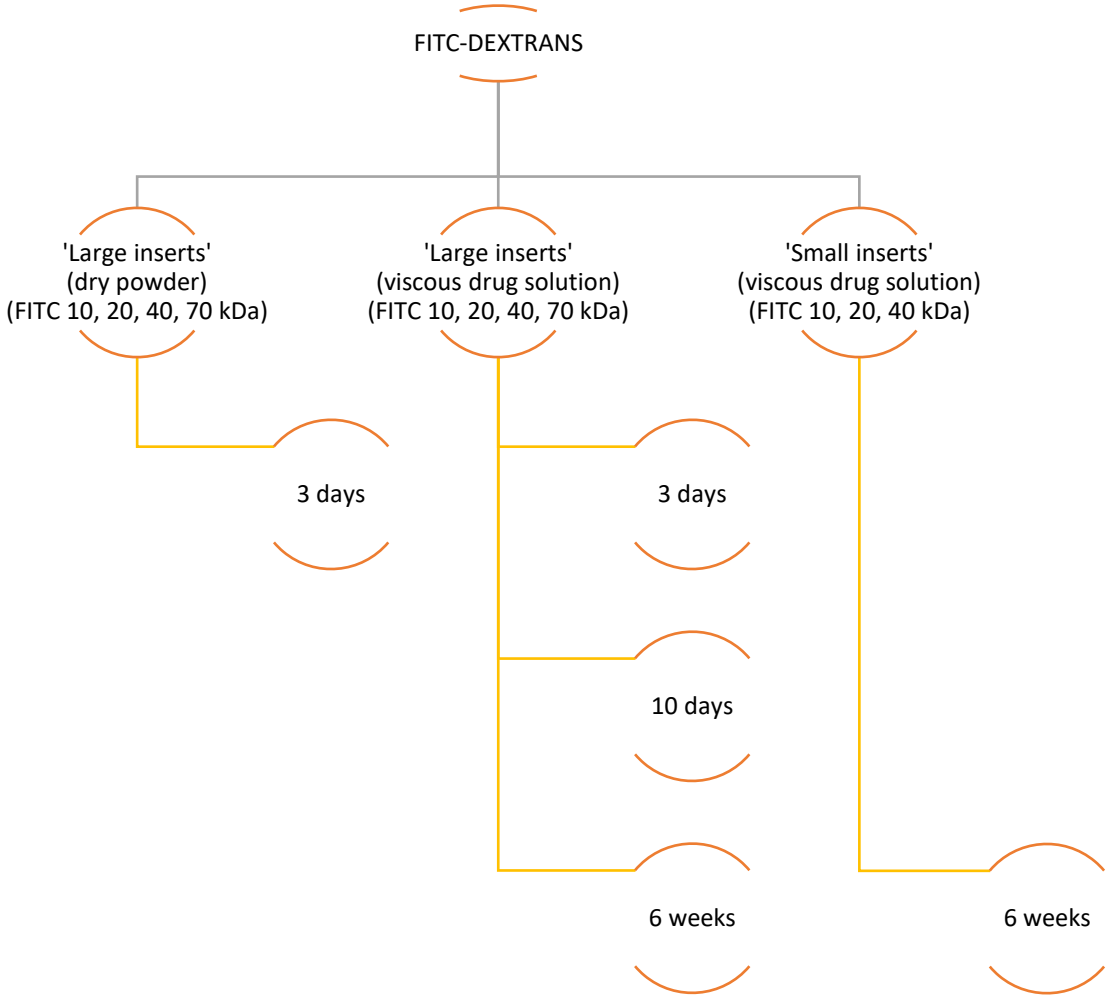

Fig. 2. Overview of the experiments carried out on inserts loaded with FITC-dextrans of different molecular weight. The label 'small inserts' refers to inserts with a total weight of 82 mg while 'large inserts' refers to inserts weighing approximately 550 mg.

2.3 *In vitro* drug release studies

The release patterns of the different formulations were plotted and analysed. For inserts prepared in the PVC-blister package, four inserts per formulation were put into separate test tubes to which 15 g PBS was added at a temperature of 32 °C. The test tubes were placed in a non-oscillating hot water bath (Julabo 20B, Merck-Belgolabo, Overijse, Belgium) at a temperature of 32.0 ± 0.5 °C. At different time points, samples of 2 g release medium were withdrawn from each test tube and replaced with an equal amount of PBS at 32 °C. Sampling intervals of 10, 30, 60, 90, 120, 180, 240, 300, 360, 420 and 480 minutes were chosen. For the smaller inserts prepared in Teflon moulds, four inserts per formulation were put into separate test tubes to which 10 g PBS was added and sampled at different intervals of 20, 60, 90, 120, 180, 240, 300, 360, 420 and 480 minutes. Before and after sampling, the content of the test tubes was homogenised by means of gentle stirring.

All samples were analysed spectrophotometrically at a wavelength of 484 nm. At the end of every series of measurements, the content of each test tube was intensively vortexed to release all of the remaining drug from the insert and measured spectrophotometrically.

3 RESULTS AND DISCUSSION

3.1 Inserts with large dimensions

3.1.1 Rehydration period: three days

Firstly, the results obtained from inserts prepared with dry FITC powder and the viscous FITC solution were compared after a drug loading time of three days. The results are respectively given in figure 3 and in figure 4.

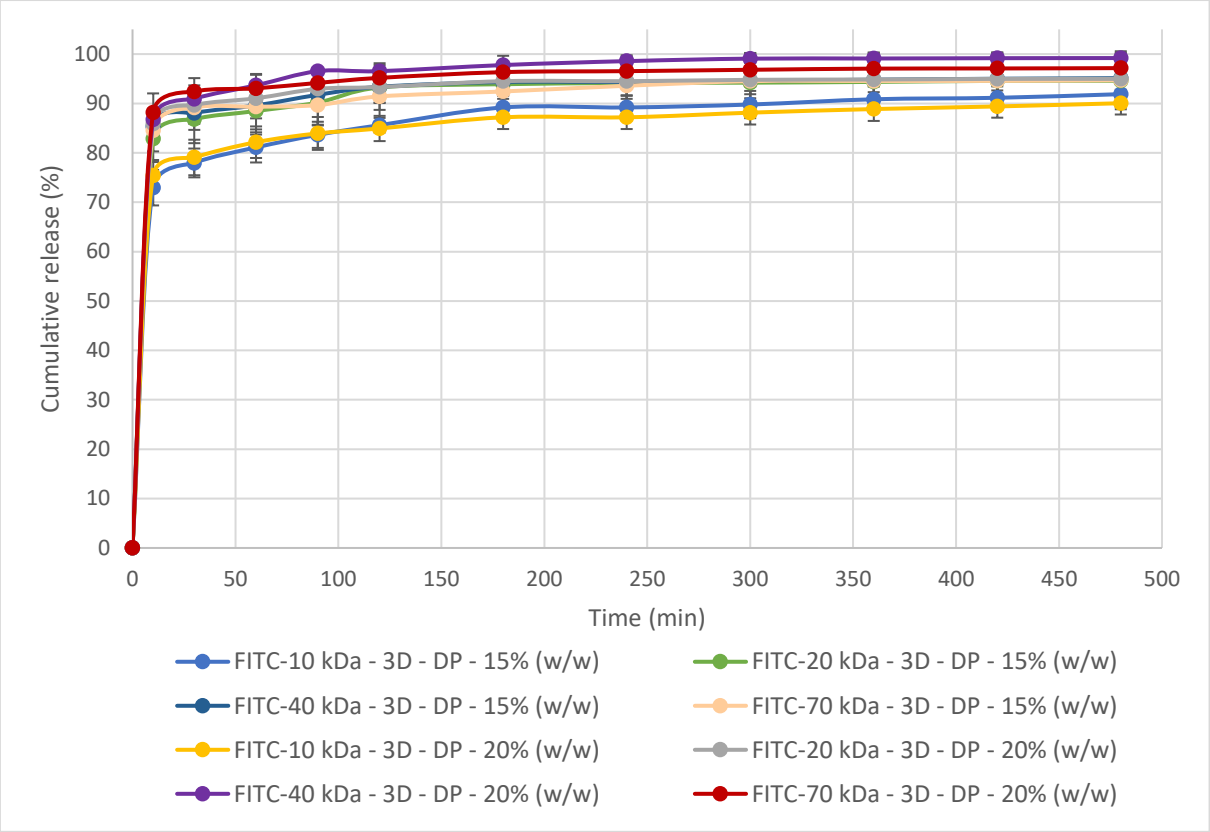

Fig. 3. Cumulative release profiles of inserts loaded with FITC-dextrans of different molecular weight and a rehydration period of three days using dry FITC-dextran powder for *in situ* dissolution. In the legend, the molecular weight is given, followed by the rehydration period, while DP stands for Dry Powder and the final HPMC percentage is given at the end (n=4).

All release profiles in figure 3 demonstrate a rapid release of the FITC-dextrans for all molecular weight tested. Inserts prepared with 10 kDa FITC seem to release the FITC molecules a little slower, as 10 kDa is the smallest molecule of the FITC-dextrans examined [9].

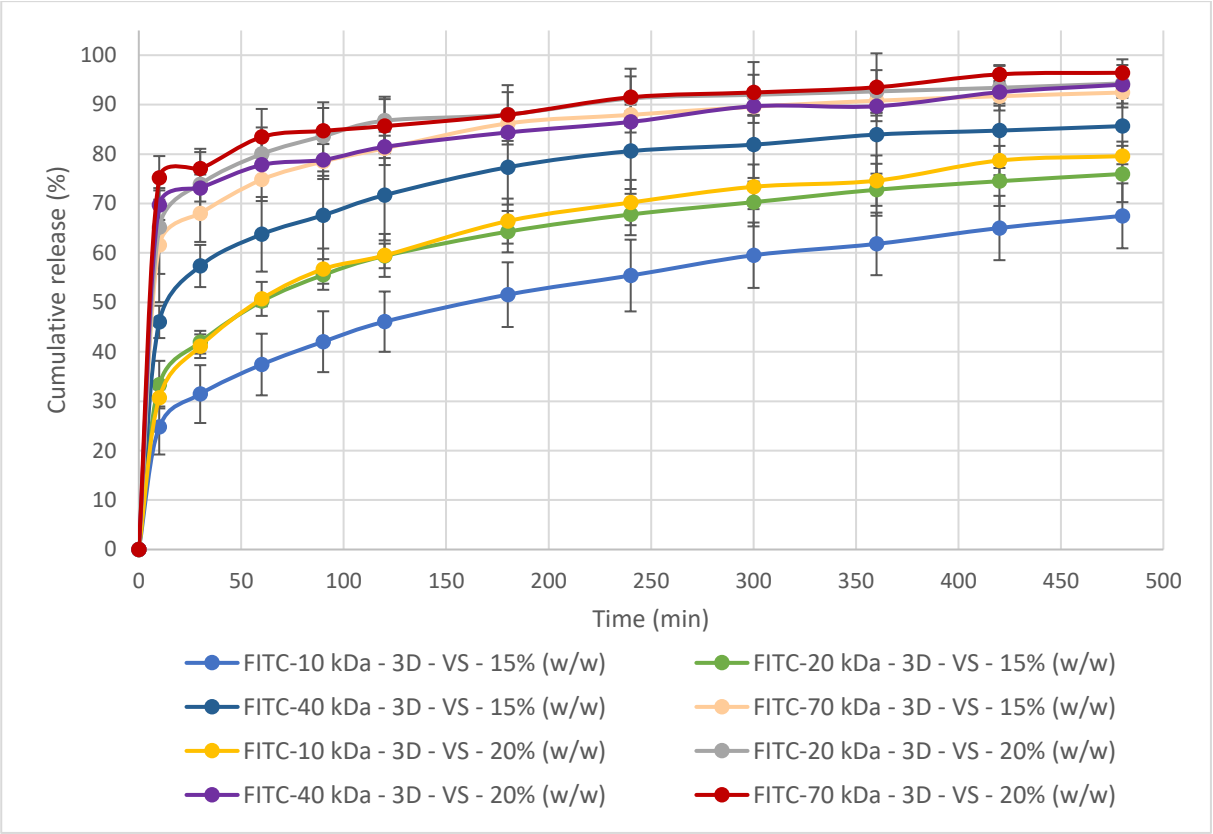

Fig. 4. Cumulative release profiles of inserts loaded with FITC-dextrans of different molecular weight and a rehydration period of three days using a viscous FITC-dextran solution. In the legend, the molecular weight is given, followed by the rehydration period, while VS stands for Viscous Solution and the final HPMC percentage is given at the end (n=4).

When comparing the releases profiles from figures 3 and 4, it is immediately clear that preparing a viscous drug solution instead of an *in situ* solution, slows down the release rate of the molecules. Preparing the drug solution *in situ* might lead to an absorption of water from the drug vehicle (viscous HPMC solution) into the dehydrated matrix before a homogeneous drug solution can be formed *in situ*. In case of preparing the drug solution in advance, the dextran molecules are more likely to trail the solvent molecules during the rehydration process.

Still, for all FITC-dextrans released, a burst release can be seen at time point 10 minutes, suggesting that a full penetration of the FITC-dextrans into the core of the insert is not possible in three days for the given method. It should be noted that some degree of fast release will always occur, as a homogeneous distribution of molecules implicates molecules residing at the surface as well as in the entire volume of the insert. The lower viscosity of the 15% (w/w) insert and loaded with the smallest FITC molecule (10 kDa), revealed quite unsurprisingly the lowest burst release and hence the lowest amount of FITC-dextran released. As mentioned in the previous chapters, the largest

molecule should theoretically be released the slowest if a homogeneous distribution of the FITC-dextrans in the inserts is obtained. But the less compact structure of the 15% (w/w) polymeric matrix allows the molecules to be more deeply embedded, improving the drug release profile, especially when the drug loading time is relatively short. The release profile of 10 kDa at an HPMC percentage of 20% (w/w) seems very similar to the higher molecular weight FITC-dextran of 20 kDa but from an insert with a lower final HPMC percentage of 15% (w/w). The largest FITC-dextrans (40 kDa and especially 70 kDa) exhibit high burst release amounts, confirming the difficulty large molecules face when penetrating into the polymer matrix at the given rehydration period. The influence of the molecular weight and the viscosity of the matrix are major determining factors for the drug loading process.

3.1.2 Rehydration period: ten days

Although using the viscous drug solution did improve the release profile dramatically for smaller proteins (*see chapter 5, 3.1.5 Viscous polymer drug solution)*, burst release occurs for all formulations tested in this research with a drug loading period of three days. In order to improve the distribution of the FITC-dextrans in the polymeric matrix, the rehydration period was increased to ten days and the inserts were prepared using a viscous drug solution. The result for the drug release after ten days of rehydration is given in figure 5.

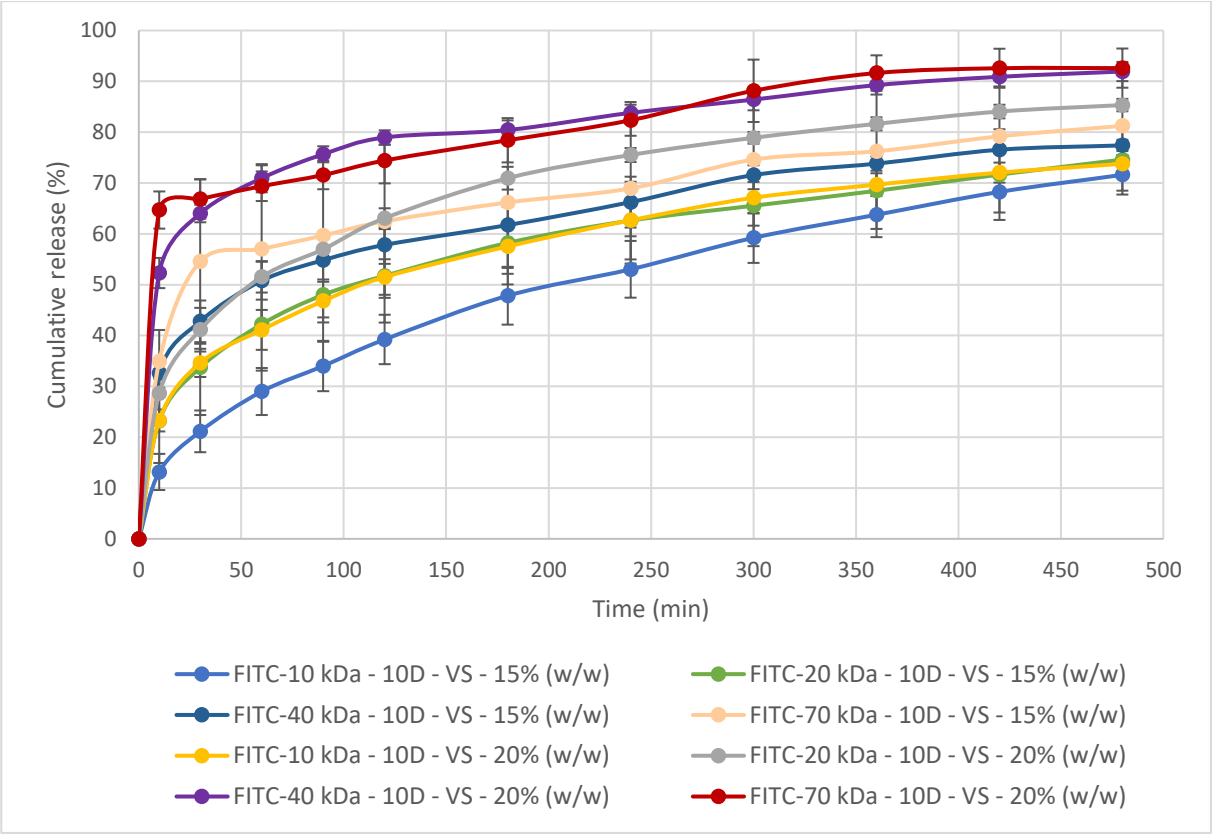

Fig. 5. Cumulative release profiles of inserts loaded with FITC-dextrans of different molecular weight and a rehydration period of ten days using a viscous FITC-dextran solution. In the legend, the molecular weight is given, followed by the rehydration period, while VS stands for Viscous Solution and the final HPMC percentage is given at the end (n=4).

Lengthening the rehydration period to ten days, improves the drug loading in the insert for all formulations. The amount of FITC-dextrans released after ten minutes is much lower compared to the three days loading time. But the looser packing of the polymer chains of the matrix helps the penetration process of the molecules during loading as the FITC-molecules for all formulations prepared with a final HPMC percentage of 15% (w/w) are released slower than their equivalent counterpart with an HPMC percentage of 20% (w/w). There seems to be only a small improvement for the largest FITC-molecules (70 kDa) for both 15% (w/w) and 20% (w/w) HPMC inserts, suggesting that the pore size of the HPMC matrix is too narrow for FITC-70 kDa to pass through. Nevertheless, for inserts prepared with a final percentage of 20% (w/w) HPMC, a loading time of ten days remains insufficient. Therefore, the rehydration period was increased to six weeks.

3.1.3 Rehydration period: six weeks

To evaluate the effect of longer periods of time, the drug loading period was increased to six weeks for all formulations. These results are plotted in figure 6.

Extending the rehydration period from ten days to six weeks improved the release profiles of FITC-dextrans with lower molecular weight (10 and 20 kDa) and 15% (w/w) HPMC percentages. These release profiles barely exhibit rapid release after ten minutes of release. But for all FITC-dextran loaded inserts with a final HPMC percentage of 20% (w/w), no significant improvement was realised compared to a rehydration period of ten days.

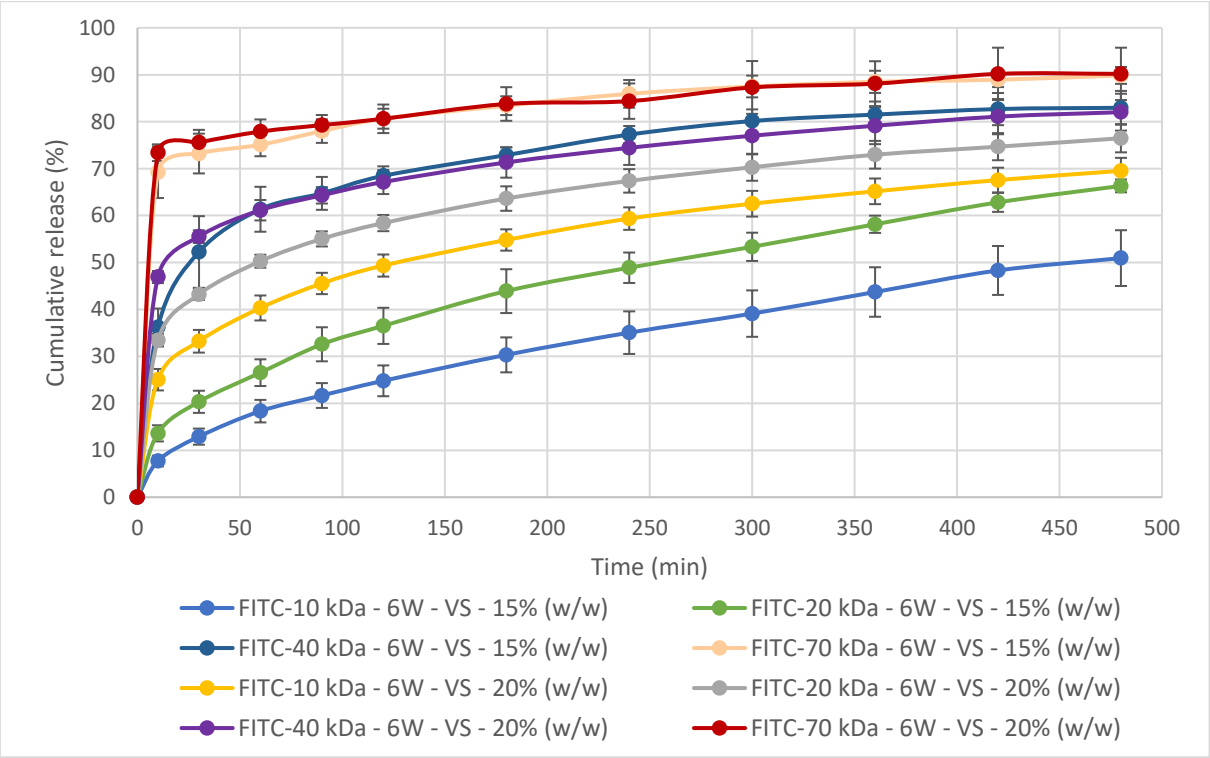

Fig. 6. Cumulative release profiles of inserts loaded with FITC-dextrans of different molecular weight and a rehydration period of six weeks using a viscous FITC-dextran solution. In the legend, the molecular weight is given, followed by the rehydration period, while VS stands for Viscous Solution and the final HPMC percentage is given at the end (n=4).

For the molecules examined, the polymeric network of inserts with an HPMC percentage of 20% (w/w) seems too dense to obtain a homogeneous drug loading of large molecules in the matrix, regardless of the rehydration period. When comparing a rehydration period of ten days to six weeks, the drug loading rates seem to be low to such an extent that further improvements of the drug penetration in the matrix and hence slower release rates fail to be achieved. FITC-dextrans with a molecular weight of 40 and 70 kDa require new strategies to enable homogeneous drug

loading for this polymer type and percentages used. This might implicit the need of facilitated diffusion forces such as pressure differences or oscillatory techniques to temporarily increase the pore size of the polymeric network. Although the relationship between the physical principles of polymeric density versus molecular weight are generally true, the molecular weight of the molecules is only indirectly indicative for the molecular shape. In literature, some researchers have described the influence of the molecular shape and deformability of the molecule having a significant impact on drug diffusion properties [10–12]. FITC-dextrans with a molecular weight greater than 5 kDa, behave as flexible, extended coils in solution [13]. This is markedly different compared to globular proteins such as lysozyme [14,15]. These properties were not within the scope of this research work and therefore not examined.

3.2 Inserts with small dimensions

3.2.1 Rehydration period: six weeks

The results of inserts with an HPMC percentage of 15% (w/w) and 20% (w/w) loaded with 10, 20 and 40 kDa dextrans and a rehydration period of six weeks are presented in figure 7.

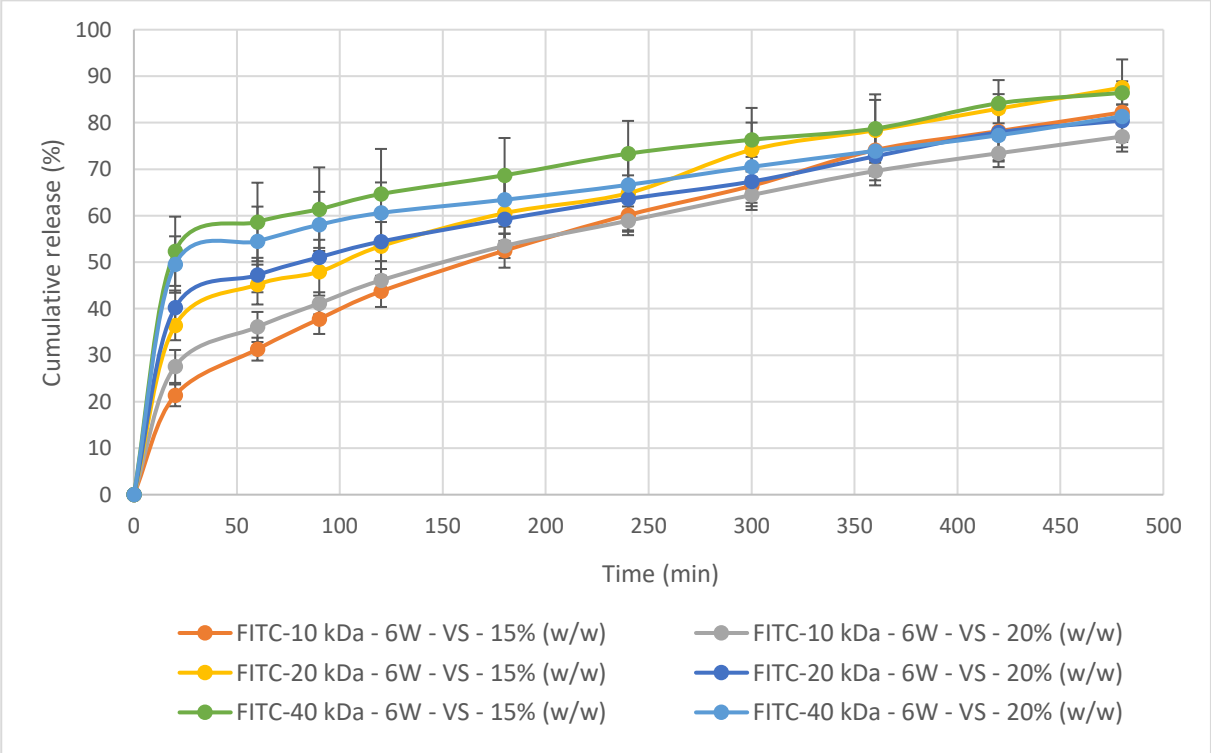

Fig. 7. Cumulative release profiles of inserts loaded with FITC-dextrans of different molecular weight and a rehydration period of six weeks using a viscous FITC-dextran solution. In the legend, the molecular weight is given, followed by the rehydration period, while VS stands for Viscous Solution and the final HPMC percentage is given at the end (n=4).

It is important to note that the results discussed in this section cannot be directly compared to results previously obtained. The smaller dimensions and therefore different surface-to-volume ratio make direct comparison of release rates difficult. This means that high initial release amounts cannot strictly be attributed to an insufficient penetration depth of the drug molecules, while for larger inserts, a rapid release of molecules residing on the surface can be held responsible for this effect.

In these smaller inserts, the trend of smaller molecules being able to penetrate more easily in the polymeric matrix is still visible. While lower HPMC percentages and hence a less compact polymeric network are still beneficial for the drug loading, the differences between 15% (w/w) and 20% (w/w) HPMC are less pronounced and the release amount is similar for a given molecular weight after 20 minutes.

Interestingly, there is a substantial difference in the amount of drug released after 20 minutes between all formulations. The drug release amounts for all formulations are situated between 20% and 55% after 20 minutes, while after 480 minutes, the drug is released between 75% and 90%, a much smaller difference. Furthermore, inserts loaded with FITC 10 kDa show good drug loading, but as this molecule has the lowest molecular weight, it is released relatively faster than the other molecules, especially when 15% (w/w) HPMC is used. The slope of the plot has unsurprisingly the highest inclination, indicative for faster release due to lower polymeric resistance of the network, resulting in a total amount of FITC released after 480 minutes being situated amongst all other release profiles at just over 80%.

Out of curiosity, the HPMC percentage of the inserts was increased to 25% (w/w). After evaluating the results obtained for 15% (w/w) and 20% (w/w), it was expected that the release profiles of 25% (w/w) would be higher as a result of a too dense polymeric network. This additional experiment might shed some light on the importance of the polymeric network for both drug loading as well as drug release. The results are presented in figure 8.

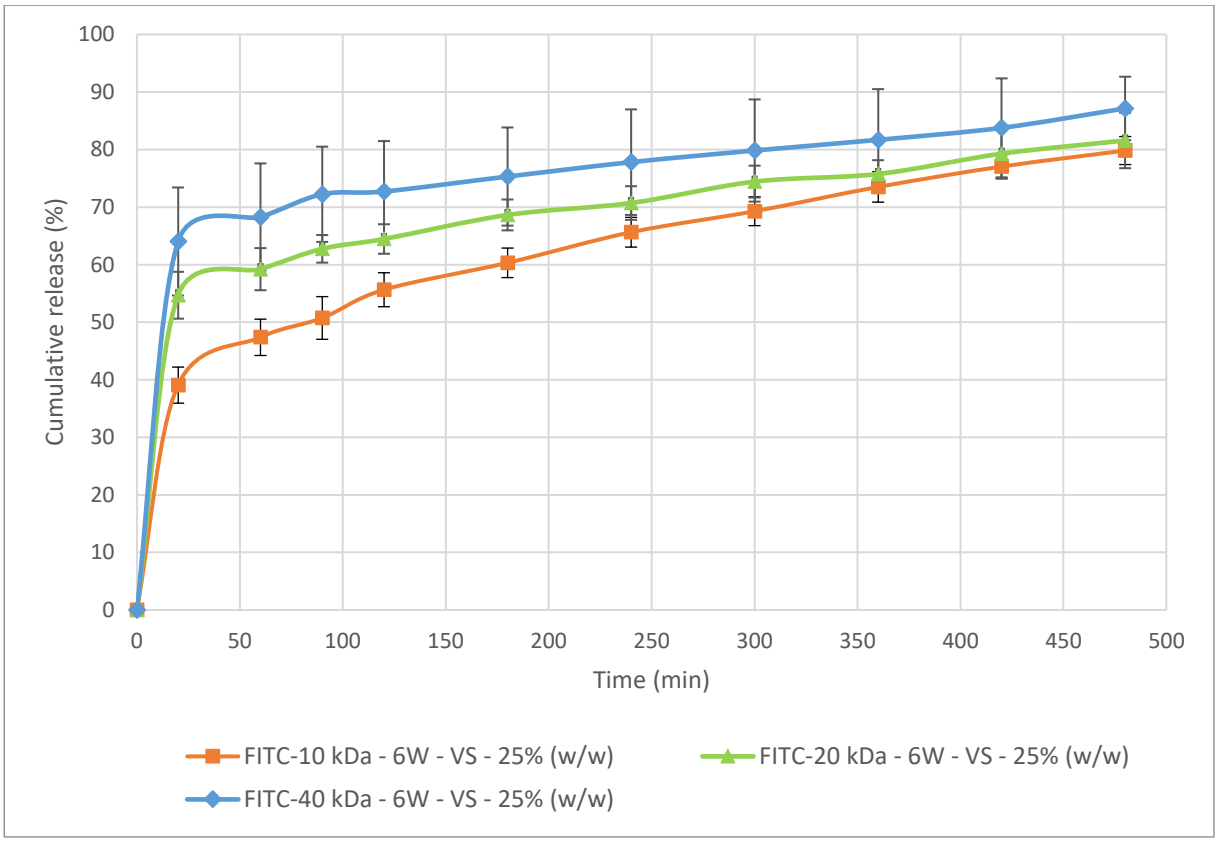

Fig. 8. Cumulative release profiles of inserts loaded with FITC-dextrans of different molecular weight and a rehydration period of six weeks using a viscous FITC-dextran solution. In the legend, the molecular weight is given, followed by the rehydration period, while VS stands for Viscous Solution and the final HPMC percentage is given at the end (n=4).

Increasing the final HPMC percentage and hence viscosity and polymeric density has a negative impact on the amount of drug loaded in the inserts as anticipated. The amount of FITC 10 kDa released from the insert has almost doubled to nearly 40% (w/w) after 20 minutes compared to an insert with the same dimensions, but with an HPMC percentage of 15% (w/w). Comparable results were recorded for 20 kDa and 40 kDa. But similar to inserts with an HPMC percentage of 15% (w/w) and 20% (w/w), the large difference between inserts loaded with FITC-dextran 10 kDa and FITC-dextran 40 kDa after 20 minutes of release decreases, as the drug release progresses. After 480 minutes, the difference between all FITC molecules tested is much smaller.

These findings could lead to improved development of ocular inserts when different polymeric compounds are mixed for different drug release behaviour. An initial drug release burst can even be regarded as beneficial if certain minimum peptide or protein levels are required for biological activity.

4 CONCLUSION

This chapter describes the loading characteristics of FITC-dextran loaded inserts. Both for large and smaller inserts, the same trends in drug release were registered. Increasing the final HPMC percentage, which enhances the viscosity and polymeric density, resulted in higher initial drug release amounts suggesting poorer drug loading capacities. The dense polymeric network hinders the diffusion of molecules particularly affecting the larger molecules such as FITC-dextrans 40 kDa and 70 kDa. However, it is important to understand that the molecular shape might have a significant influence on the diffusion behaviour into the polymeric matrix. This complicates a precise prediction on how a given drug substance will behave.

The final HPMC percentage also allows researchers to control the release rate to a certain degree. A mixture of different polymer blends could alter the release rate in a desired manner. The experiments performed in this chapter also indicate a limitation in molecular weight for FITC-dextrans. For the method used to develop these inserts, incorporating FITC molecules over 20 kDa can be very challenging and new strategies involving facilitated diffusion are required to homogeneous distribute the drug in the polymeric network.

References

1. De Belder AN, Granath K. Preparation and properties of fluorescein-labelled dextrans. Carbohydr Res. 1973;30: 375–378.
2. Hämäläinen KM, Kananen K, Auriola S, Kontturi K, Urtti A. Characterization of Paracellular and Aqueous Penetration Routes in Cornea , Conjunctiva , and Sclera. Invest Ophthalmol Vis Sci. 1997;38: 627–634.
3. Järvinen K, Järvinen T, Urtti A. Ocular absorption following topical delivery. Adv Drug Deliv Rev. 1995;16: 3–19.
4. Braeckmans K, Peeters L, Sanders NN, De Smedt SC, Demeester J. Three-dimensional fluorescence recovery after photobleaching with the confocal scanning laser microscope. Biophys J. 2003;85: 2240–2252.
5. Tratta E, Pescina S, Padula C, Santi P, Nicoli S. In vitro permeability of a model protein across ocular tissues and effect of iontophoresis on the transscleral delivery. Eur J Pharm Biopharm. 2014;88: 116–122.
6. Rai UDJP, Young SA, Thrimawithana TR, Abdelkader H, Alani AWG, Pierscionek B, et al. The suprachoroidal pathway: A new drug delivery route to the back of the eye. Drug Discov Today. 2015;20: 491–495.
7. Balakrishnan G, Nicolai T, Durand D. Relation between the gel structure and the mobility of tracers in globular protein gels. J Colloid Interface Sci. 2012;388: 293–299.
8. Mains J, Wilson CG. The Vitreous Humor As a Barrier to Nanoparticle Distribution. J Ocul Pharmacol Ther. 2013;29: 143–150.
9. Fetters LJ, Hadjichristidis N, Lindner JS, Mays JW. Molecular Weight Dependence of Hydrodynamic and Thermodynamic Properties for Well-Defined Linear Polymers in Solution. Journal of Physical and Chemical Reference Data. 1994; 619–640.
10. Silva JVC, Peixoto PDS, Lortal S, Floury J. Transport phenomena in a model cheese: The influence of the charge and shape of solutes on diffusion. J Dairy Sci. 2013;96: 6186–6198.
11. Venturoli D. Ficoll and dextran vs. globular proteins as probes for testing glomerular permselectivity: effects of molecular size, shape, charge, and deformability. AJP Ren Physiol. 2004;288: 605–613.
12. Srikantha N, Mourad F, Suhling K, Elsaid N, Levitt J, Chung PH, et al. Influence of molecular shape, conformability, net surface charge, and tissue interaction on transscleral macromolecular diffusion. Exp Eye Res. 2012;102: 85–92.
13. TdB Consultancy. FITC-Dextran. Tech sheet. 2010; 1–5.
14. Bhowal AC, Das K, Kundu S. Fluorescence behavior of globular proteins from their bulk and thin film conformations in presence of mono-, di- and tri-valent ions. Colloids Surfaces B Biointerfaces. 2015;133: 263–269.
15. Day L, Zhai J, Xu M, Jones NC, Hoffmann S V., Wooster TJ. Conformational changes of globular proteins adsorbed at oil-in-water emulsion interfaces examined by synchrotron radiation circular dichroism. Food Hydrocoll. 2014;34: 78–87.

Chapter 7: Evaluation of cytotoxicity and viability of SV40-HCEC in the presence of blank ocular inserts

Parts of this chapter have been submitted to:

Everaert A, Wouters Y, Melsbach E, Zakaria N, Ludwig A, Kiekens F, Weyenberg W. Optimisation of HPMC ophthalmic inserts with sustained release properties as a carrier for thermolabile therapeutics. Int J Pharm. 2017

1 INTRODUCTION

The developed ocular inserts should be suited for precorneal use. Not only is the drug released from the insert, but also the various excipients dissolve over time into the tear film. Therefore, to determine the cytotoxicity and biocompatibility of the excipients used for the development of the ophthalmic inserts, SV40-immortalised human corneal epithelial cells (SV40-HCEC) were used [1]. The human corneal epithelial cells were treated by adding two different dilutions of a blank insert based on HPMC. These results were assessed and compared to two different dilutions of a reference polymer (HPC). The polymer HPC was chosen based on the commercially available insert Lacrisert®, a precorneal rod-shaped device to treat dry eye disease [2,3].

The cell viability was measured using PrestoBlue® reagent, which is a resazurin-based cell viability reagent. Resazurin, a blue compound with no intrinsic fluorescent value, is irreversibly reduced to resorufin, a red in colour and highly fluorescent substance. This conversion is proportional to the number of metabolically active cells making quantitative measurements possible [4].

The present chapter evaluates the cytotoxicity and biocompatibility of blank HPMC inserts on SV40-HCEC both in a quantitative and qualitative manner.

2 MATERIALS AND METHODS

2.1 Materials

SV40-immortalised human corneal epithelium cells were kindly gifted by the Integrative Regenerative Medicine Centre, (Linköping University, Linköping, Sweden). Keratinocyte-Serum-Free Medium (K-SFM) enriched with bovine pituitary extract (BPE) and human recombinant epidermal growth factor type B 1-53 (EGF 1-53) nutrients were obtained from Gibco® by Life Technologies (Paisley, UK). PrestoBlue® cell viability reagent and trypan blue stain (0.4% (w/V)) were purchased from Life Technologies (Frederick, USA).

Glycerol analytical grade (99.5% (V/V)) was obtained from Sigma-Aldrich (Steinheim, Germany). Hydroxypropylmethyl cellulose type E10M Premium CR was provided by Colorcon (Dartford, UK) and hydroxypropyl cellulose was purchased from ABC Chemicals (Wauthier-Braine, Belgium). By specification, an aqueous 2% (w/w) HPMC E10M solution gives an apparent viscosity of 10.000 mPa.s (at 20 °C), while the apparent viscosity of an aqueous 2% (w/w) HPC solution is 304 mPa.s.

2.2 Preparation of inserts

Blank inserts were prepared following the principles described in *phase I* of the method in section *2.2 Preparation of ocular inserts* in *chapter 5*.

2.3 Cytotoxicity and biocompatibility

Two different dilutions of 0.555% (w/w) and 1.11% (w/w) HPMC E10M were prepared by dissolving an adequate amount of HPMC insert (containing 20% (w/w) HPMC and 1% (w/w) glycerol in purified water) in K-SFM. These percentages, determining the viscosity of the dilutions, were chosen to allow pipetting in 96-well plates. For the sake of reference, two different dilutions of 1.22% (w/w) and 2.44% (w/w) HPC were prepared by dissolving HPC powder in medium, also comprising glycerol in a 1% (w/w) percentage. The amount of HPC polymer was chosen based on comparable viscosities between the HPMC solution and the HPC solution. The viscosity was measured using rotational viscosimetry (flow) (Anton Paar MCR-102, Graz, Austria). A parallel plate measuring device with a diameter of 50 mm was used, set at 1 mm gap and at a temperature of 32.0 ± 0.1 °C. The shear rate was set between 0.01 s^{-1} to 100 s^{-1}. To prevent the polymer from drying out during the measurements, a solvent trap was used to cover the sample. All measurements were performed in triplicate. Figure 1 shows the rheological profiles for HPMC in a percentage of 0.555% (w/w) and 1.11% (w/w) and for HPC in a percentage of 1.22% (w/w) and 2.44% (w/w).

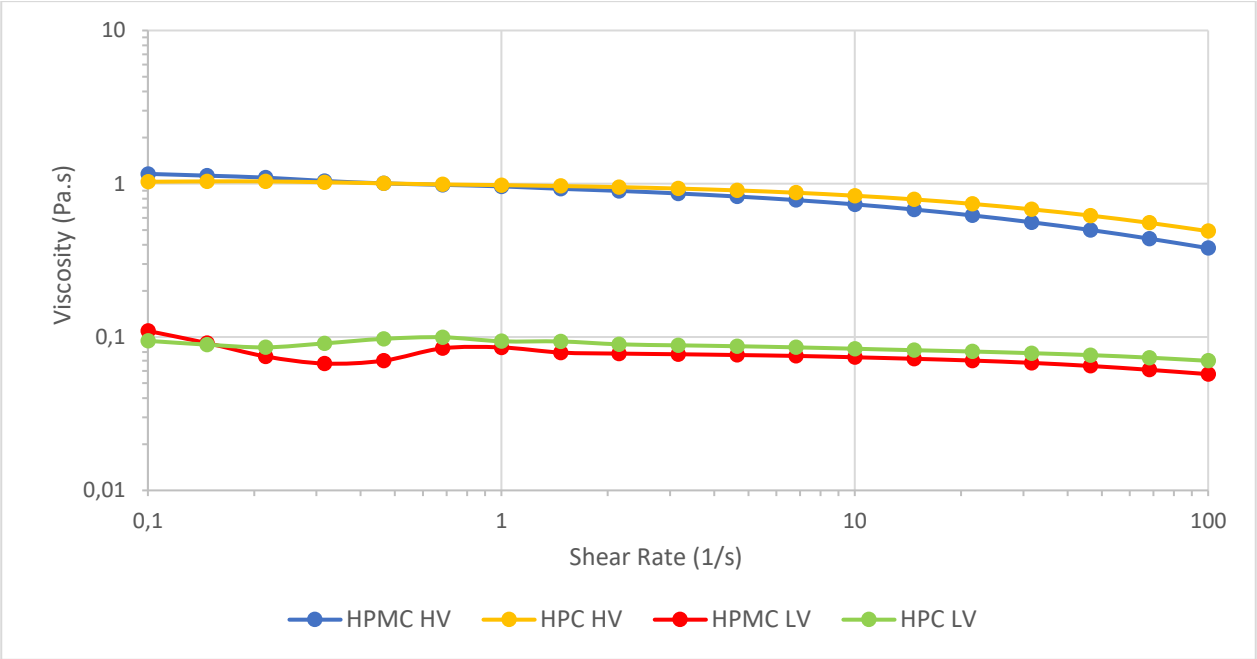

Fig. 1. Rheological profiles for HPMC in a percentage of 0.555% (w/w) (HPMC LV) and 1.11% (w/w) (HPMC HV) and for HPC in a percentage of 1.22% (w/w) (HPC LV) and 2.44% (w/w) (HPC HV).

The stock cell cultures were maintained in T-75 flasks in Keratinocyte-SFM (K-SFM) medium enriched with bovine pituitary extract (BPE) and human recombinant epidermal growth factor type B 1-53 (EGF 1-53) at 37 °C in a 95% air and 5% CO_2 incubator (Galaxy R, Eppendorf, Hamburg, Germany). The human corneal epithelial cells were plated into 96-well plates with K-SFM at 37 °C in a 5% CO_2 incubator overnight. During this time period, cells were allowed to attach. The amount of cells was determined at an average of 30.000 cells per well using an automated cell counter (ABX Micros 60 OT, Horiba, Montpellier, France). Both hydrogel types (HPMC and HPC) and both groups of dilutions (high and low viscosities) were added to different wells on the same plate. The properties of benzalkonium chloride are well understood and it is often used in commercial eye drops as a preservative. It is mainly active against Gram-positive bacteria (e.g. *Staphylococcus spp.*) even at very low concentrations (0.004% (w/V)). Furthermore, adding EDTA in a concentration of 0.1% (w/V) increases its activity against Gram-negative bacteria (e.g. *Pseudomonas aeruginosa*). In general, quaternary ammonium compounds are also active against fungi and particularly active against *Candida albicans* and *Aspergillus fumigatus* [5]. Benzalkonium chloride is also known to be cytotoxic [5–8] and was used in three different percentages, 1% (w/V), 0.01% (w/V) and 0.004% (w/V) as a positive control group [5]. Untreated cells in medium and plain medium without cells were added as negative and blank control groups respectively.

All experiments were performed in triplicate and on different time points: 0, 2, 8, 24, 48 and 72 hours. For each time point, a separate 96-well plate was used. At every time point, all wells were rinsed four times with medium to remove the compound of interest. The wells with the highest percentage HPMC or HPC were rinsed up to seven times to remove the viscous polymer solution as much as possible. The viability of the cells was measured at every time point by adding 100 µl PrestoBlue® solution for exactly 30 minutes to all wells after rinsing. The PrestoBlue® solution was prepared by adding one part of pure PrestoBlue® reagent to nine parts of K-SFM. The fluorescence was measured using a microplate reader (Victor 3 1420 Multilabel Counter, Perkin Elmer, Shelton, USA) at a wavelength of 531/590 nm for excitation/emission respectively.

As it was not practically possible to assess the influence of the insert in its true shape and composition, a qualitative analysis of the HPMC inserts was set up and performed using microscopic visualisation. Inserts weighing approximately 150 mg of a 10% (w/w) and 20% (w/w) final percentage of HPMC were prepared and added to three wells of a six-well plate for each polymer percentage type in the centre of the well. These inserts were allowed to settle during 24 hours at 37 °C and 5% CO_2 in a humidified atmosphere. An amount of 400.000 cells per well was seeded and incubated using the same conditions. After seeding the cells (time point 0 hours (T0)) and after 5, 24, 29, 48, 53 and 72 hours, pictures were taken with a Sony ILCE-7Rm2 camera (Tokyo, Japan) using a Leica DM IL microscope (Leica Microsystems, Wetzlar, Germany) with 40x magnification as depicted in figure 2. All measurements were carried out in triplicate. Additionally, at the 72 hours time point, a trypan blue staining was performed. Trypan blue stain is an aqueous solution which is not absorbed by healthy viable cells but can readily enter damaged or dead cells. Visibly blue cells are therefore indicative for damaged or dead cells.

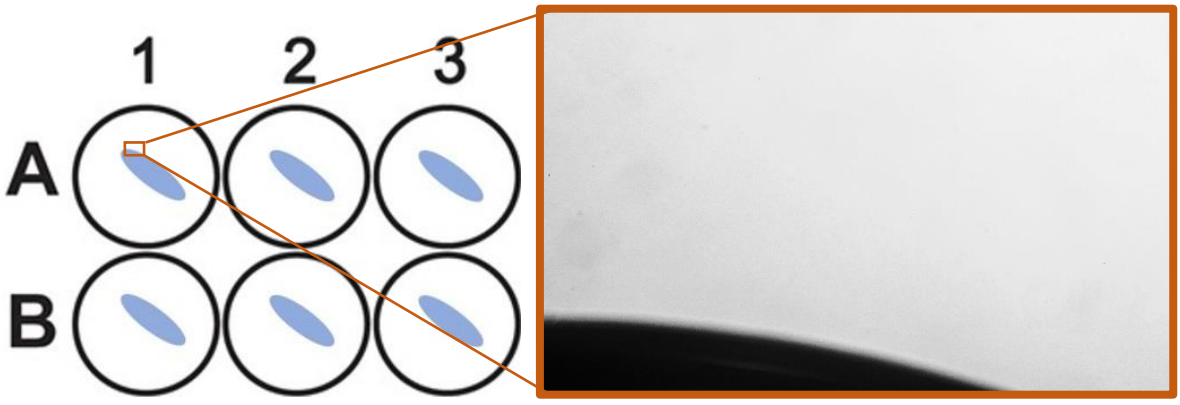

Fig. 2. Overview and crop of the section of the insert that has been visually determined. Six wells are drawn with an insert (in blue) placed in each well (time point T0).

3 RESULTS AND DISCUSSION

3.1 Cytotoxicity and biocompatibility

The viability of SV40-HCEC was evaluated by adding the chosen hydrogel solutions to these cells in a 96-well plate and was compared to cells in plain medium. Three different concentrations of benzalkonium chloride were added to wells containing cells as a cytotoxic reference. PrestoBlue® was subsequently added and the resulting fluorescence was measured. The results are shown in figure 3.

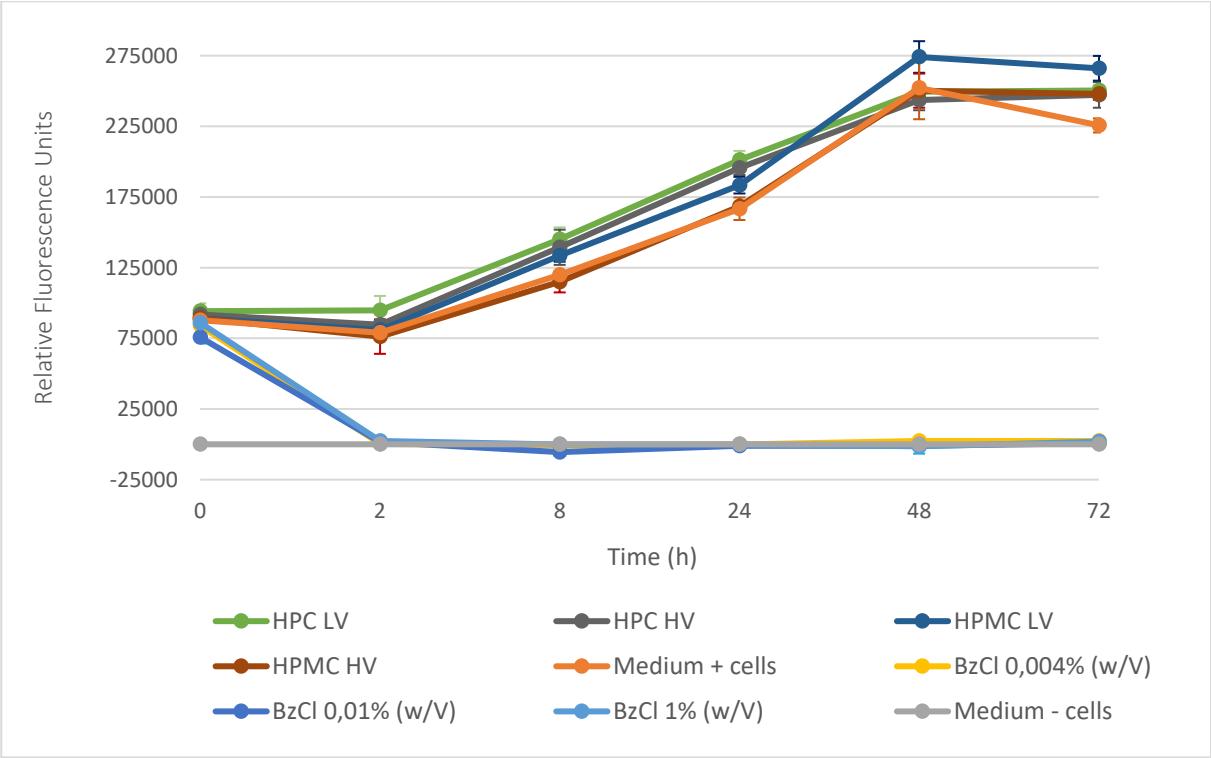

Fig. 3. Effect on cell viability by adding a solution of 2.44% (w/w) HPC (HPC HV) and 1.44% (w/w) HPC (HPC LV), 1.11% (w/w) HPMC (HPMC HV) and 0.555% (w/w) HPMC (HPMC LV) in medium. Benzalkonium chloride in concentrations of 1% (w/V), 0.01% (w/V) and 0.004% (w/V) dissolved in medium was added as a known cytotoxic reference. A negative control (medium + cells) and a blank group (medium – cells) were also added (n=3).

The results, as presented in figure 3, indicate that for all percentages tested (1% (w/V), 0.01% (w/V) and 0.004% (w/V)) benzalkonium chloride has a cytotoxic effect. The fall of relative fluorescence reflects complete absence of viable cells, as present in the blank control samples by the second measurement at two hours. All polymer solution treated cells, both HPC and HPMC in a high and low viscosity solution, yield excellent results with relative fluorescence values at least as high as the negative reference. After two hours, the relative fluorescence of the polymer solution treated cells

increases progressively, indicating increasing cellular proliferation and metabolic activity reaching a plateau after 48 hours, indicative for confluency of the cells.

To evaluate the ability of SV40-HCEC to grow in the presence of an insert with a final HPMC E10M percentage of 10% (w/w) and 20% (w/w), an insert of approximately 150 mg was added to a 6-well plate and incubated overnight to allow the insert to spread out. Thereafter, 400.000 cells were added in medium to each well. Each experiment was performed in triplicate. The growth of the cells was visually evaluated and is presented in figure 4a and 4b (40x magnification) for inserts prepared with 10% (w/w) HPMC. An overview of the growth of these cells over different time points is given as a reference in figure 4c.

The photographs obtained of 20% (w/w) HPMC inserts revealed visually identical results.

Fig. 4a. Visual evaluation of the growth of SV40-HCEC in the presence of a 10% (w/w) HPMC insert after 5 hours incubation. On the bottom left hand side of the picture, a small part of the area where the insert was placed, is visible.

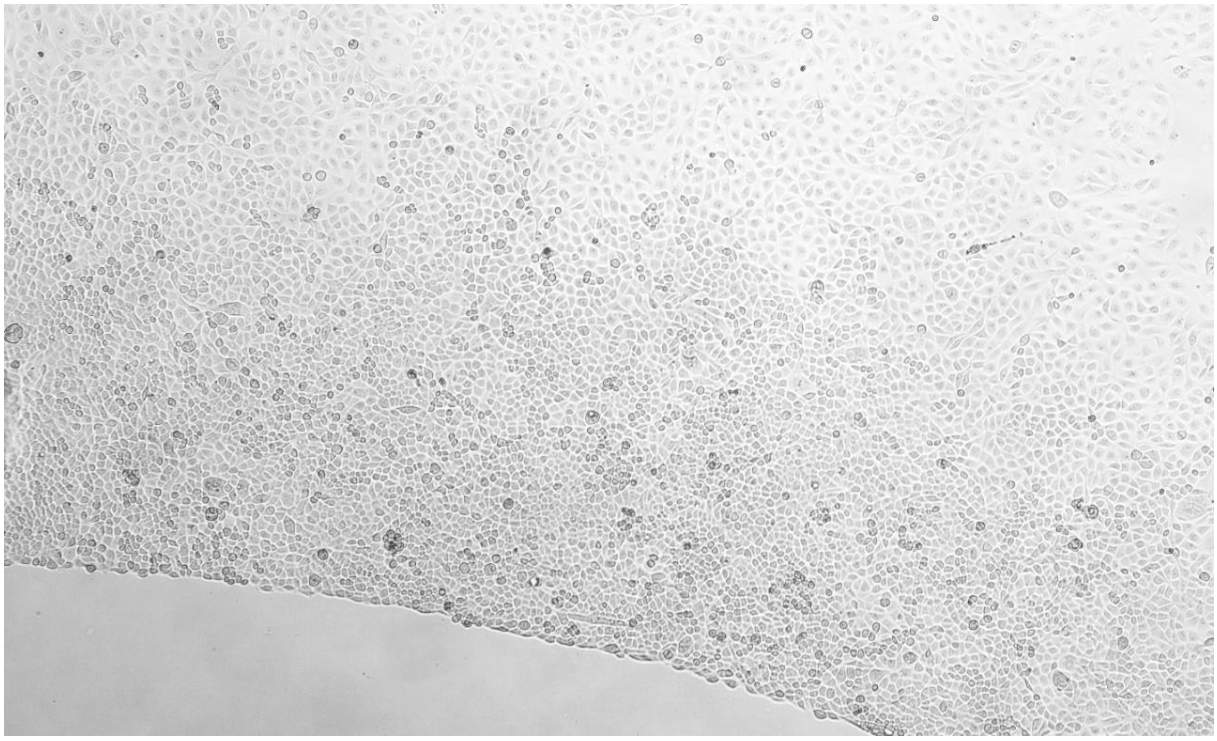

Fig. 4b. Visual evaluation of the growth of SV40-HCEC in the presence of a 10% (w/w) HPMC insert after 72 hours incubation.

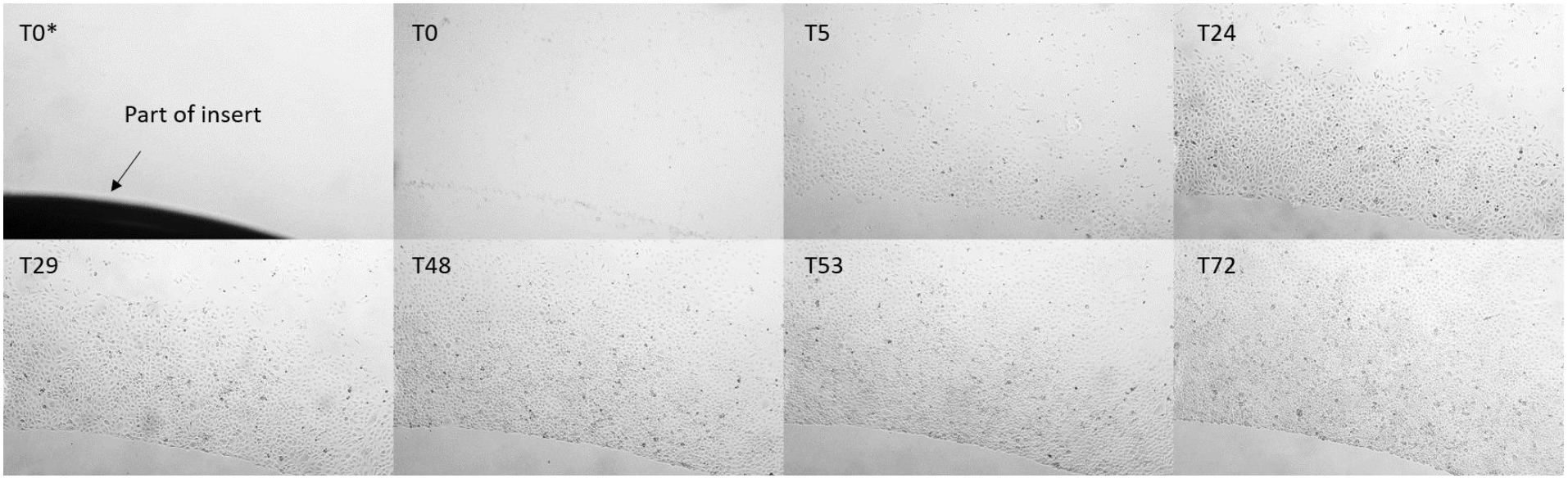

Fig. 4c. Overview of the growth of SV40-HCEC cells in the presence of 10% (w/w) HPMC inserts. At T0* no cells are added to the well, the black area is a small part of the entire insert. At T0, the cells are seeded but have not attached to the bottom of the well or on the insert. From T5 to T72, attachment to the well and growth of SV40-HCEC can be seen. The high viscosity of the insert acts as an effective mechanical barrier against the cells. The growth of the cells does not appear to be limited by the ocular insert, even after T72.

After an incubation period of five hours, the cells show attachment to the surface of the well. The cells observed at the periphery appear somewhat flattened as the viscous mass of the insert forms a mechanical barrier for the growth of cells on the insert as the cells cannot grow where the insert is located. After an incubation period of 72 hours, the cells were near confluent over the surface of the well. At this time point, the insert had dissolved entirely. The cells still did not appear to attach to the bottom of the well where the insert was originally located which suggests a continued presence of HPMC film on the bottom of the well. This observation does not come as a surprise as some researchers have suggested the possibility of using cellulose-derivatives as anti-adhesive substrates for cells [9]. Following trypan blue staining, the number of dead cells can be visually evaluated as only dead cells stain blue. The photograph taken after trypan blue treatment is pictured in figure 5.

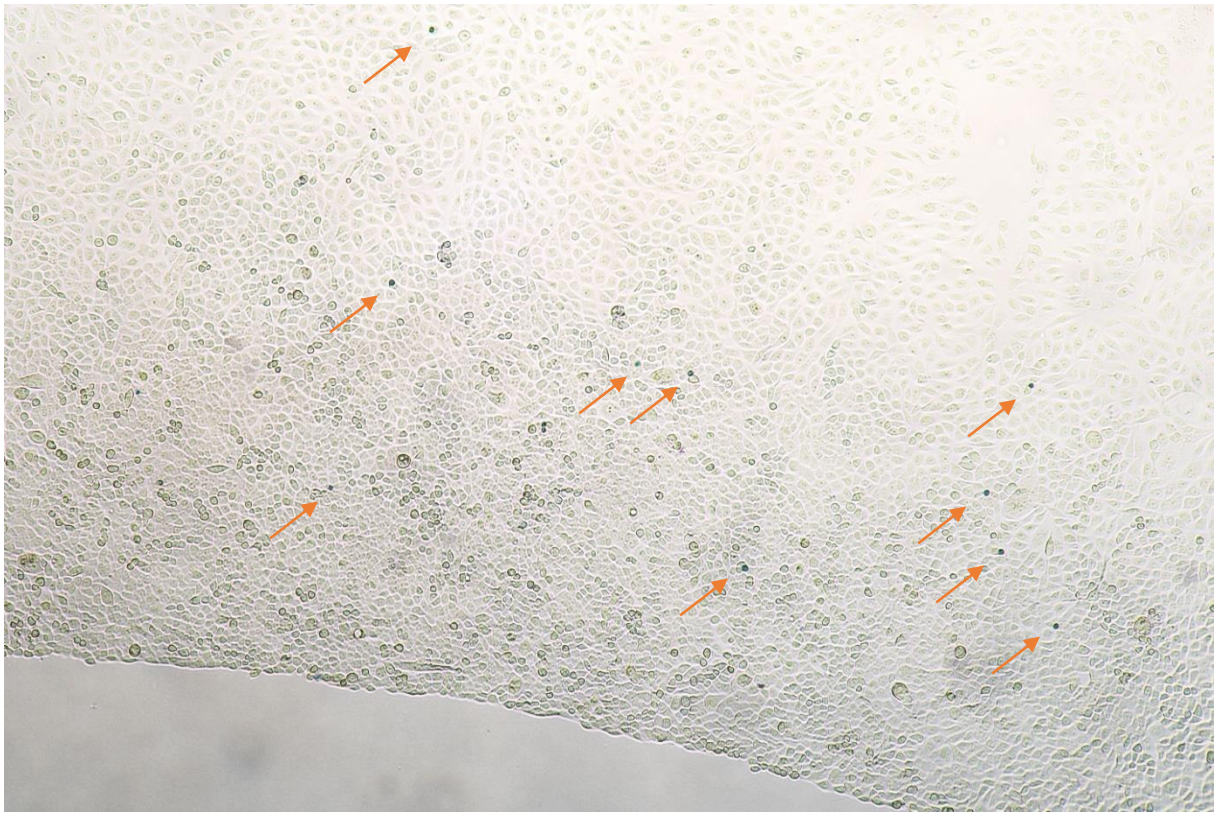

Fig. 5. Visual evaluation of the growth of SV40-HCEC in the presence of a 10% (w/w) HPMC insert after 72 hours incubation and trypan blue staining.

Very few dead cells are observed sparsely dispersed throughout the culture (indicated with arrows in orange). The edge of the HPMC insert is populated with viable cells indicating the biocompatibility of the HPMC inserts.

4 CONCLUSION

The HPMC inserts described in this research work have no negative influence on the growth of the SV40-HCEC. Viability measurements show high cytotoxicity levels for benzalkonium chloride treated cells, as expected. No difference was noted in cell viability between HPC and HPMC (E10M) polymers, irrespective of the percentage polymer used. All polymer treated cells were able to grow in the presence of HPC or HPMC. Visual evaluation confirmed the ability of the cells to grow close to the insert, only being mechanically hindered. After trypan blue staining (at T72), very few blue cells could be visually detected, indicative for healthy cells. Therefore, it can be concluded that the HPMC inserts tested are not harmful to SV40-immortalised human corneal epithelial cells.

Acknowledgements

I would like to express my utmost appreciation to Eline Melsbach and prof. dr. Nadia Zakaria (Department of Ophthalmology, Antwerp University Hospital) for their help with cytotoxicity testing.

References

1. Kang S, Choi H, Rho CR. Differential Effects of Bevacizumab, Ranibizumab, and Aflibercept on the Viability and Wound Healing of Corneal Epithelial Cells. J Ocul Pharmacol Ther. 2016;32: 671–676.
2. Nguyen T, Latkany R. Review of hydroxypropyl cellulose ophthalmic inserts for treatment of dry eye. Clin Ophthalmol. 2011;5: 587–591.
3. Saettone MF, Salminen L. Ocular inserts for topical delivery. Adv Drug Deliv Rev. 1995;16: 95–106.
4. Invitrogen. PrestoBlue ™ reagent Product Overview. Technical information. 2012.
5. Baudouin C, Labbé A, Liang H, Pauly A, Brignole-Baudouin F. Preservatives in eyedrops: The good, the bad and the ugly. Prog Retin Eye Res. 2010;29: 312–334.
6. Paimela T, Ryhänen T, Kauppinen A, Marttila L, Salminen A, Kaarniranta K. The preservative polyquaternium-1 increases cytoxicity and NF-kappaB linked inflammation in human corneal epithelial cells. Mol Vis. 2012;18: 1189–1196.
7. Durand-cavagna G, Delort P, Duprat P, Bailly Y, Plazonnet B, Gordon LR. Corneal toxicity studies in rabbits and dogs with hydroxyethyl Cellulose and benzalkonium chloride. Toxicol Sci. 1989;13: 500–508.
8. Noecker R. Effects of common ophthalmic preservatives on ocular health. Adv Ther. 2001;18: 205–215.
9. Velzenberger E, Vayssade M, Legeay G, Nagel MD. Study of cell behaviour on a cellulose anti-adhesive substratum. Cellulose. 2008;15: 347–357.

Chapter 8: Stability testing of inserts containing lysozyme

1 INTRODUCTION

The purpose of stability testing is to examine how drug loaded inserts behave after longer periods of storage. The quality of the drug substance or product can vary with time and under given circumstances such as changing temperature, humidity and light. Therefore, stability studies are important to understand and ensure that the properties of the product do not alter during storage, particularly when peptides and proteins are involved [1]. This chapter investigates the behaviour of the inserts prepared and loaded with lysozyme over time at a constant temperature of 2 °C. Stability testing was assessed by performing activity measurements on lysozyme loaded inserts, on rheological data and through release profile analysis.

Release profiles describe the behaviour when an incorporated drug substance is released from its carrier, but it gives no information whether the drug substance remains active. Activity assays can give a valuable insight on the physicochemical behaviour of lysozyme after storage. Rheological measurements can provide a useful understanding of the stability of the hydrogel and whether the loaded drug substance influences the viscosity of the carrier over time.

The factors limiting the stability of these inserts are likely to be determined by the drug substance (peptide or protein), rather that the excipients used to build up the insert. For this reason, stability testing at this stage of product development is non-classical and relatively limited, as the final specifications of the insert, as well as the drug of interest and packaging material are not yet specified.

2 MATERIALS AND METHODS

2.1 Materials

Lysozyme from chicken egg white and glycerol analytical grade (99.5% (V/V)) were obtained from Sigma-Aldrich (Steinheim, Germany). Hydroxypropylmethyl cellulose type E10M Premium CR was provided by Colorcon (Dartford, UK). By specification, an aqueous 2% (w/w) E10M solution gives an apparent viscosity of 10.000 mPa.s (at 20 °C).

Phosphate-buffered saline solution (PBS, pH 7.4) was prepared using 8.2 g/l sodium chloride (NaCl), 0.300 g/l sodium dihydrogen phosphate dihydrate ($NaH_2PO_4.2H_2O$), 1.540 g/l disodium hydrogen phosphate dihydrate ($Na_2HPO_4.2H_2O$) and purified water. All electrolytes of analytical grade were purchased from Merck (Darmstadt, Germany).

EnzChek® Lysozyme Assay Kit was purchased from Life Technologies (Erembodegem, Belgium) and used to perform activity testing.

PVC-blisters capsule size 4, used as a mould to produce the ocular inserts, were kindly provided by Janssen Pharmaceutica (Beerse, Belgium).

2.2 Method

The inserts were prepared following the method as described in section *2.2 Preparation of ocular inserts* in *chapter 5*. The inserts were loaded with 3% (w/w) lysozyme with a final HPMC percentage of 25% (w/w). The average weight of the inserts was chosen at approximately 400 mg and stored at a temperature of 2 °C up to 12 months.

2.2.1 Activity

The lysozyme activity was measured using a lysozyme assay kit. The lysozyme activity assay is a fluorescence-based assay to measure lysozyme activity on *Micrococcus lysodeikticus* cell walls. These cell walls are labelled to such a degree that the fluorescence is quenched. Lysozyme activity on the cell wall of *Micrococcus lysodeikticus* relieves this quenching, resulting in a measurable fluorescence amount, proportional to lysozyme activity [2].

The lysozyme activity measurement was performed at day 0 in PBS solution to determine the maximum activity after preparation of the inserts. This value was used as a reference and compared to lysozyme activity measurements (both in the insert as in solution) performed after 1, 3, 6 and 12 months. At day 0, the lysozyme activity was measured for newly prepared lysozyme loaded inserts.

Obviously, the activity at day 0 for these inserts is expected to be similar if not identical to the activity level of a lysozyme-PBS solution.

All inserts were prepared in quadruplicate and dissolved while stirring in 15 g PBS overnight at room temperature (22 ± 2 °C). All quadruplicates were serially diluted in a white 96-well plate starting from 1/50 up to 1/1600. Two additional lysozyme solutions were also prepared at day 0 in a concentration of 0.084% (w/w) in PBS solution (pH 7.4) and purified water. This percentage corresponds to the amount of lysozyme present in the insert after dissolution in 15 g PBS. These solutions make a direct comparison between lysozyme dissolved in purified water and in PBS possible, as well as a comparison between lysozyme loaded in the insert and both lysozyme solutions. Comparing these solutions mutually gives an idea on whether the excipients of the insert have a potentially stabilising effect on the denaturation of lysozyme during storage over 12 months, retaining its initial activity as much as possible. The enzyme is active over a broad pH range (6-9) [3].

Fluorescence measurements were performed using a fluorescence microplate reader (Tecan Infinite 200, Männedorf, Switzerland) using excitation/emission wavelengths of 485/530 nm respectively. The data obtained was converted to percentages and compared to the activity of 0.084% (w/w) lysozyme dissolved in PBS at day 0, which was set as the reference activity level.

2.2.2 Release profiles

Different inserts stored during 1, 3, 6 and 12 months at 2 °C were analysed. The inserts were put into separate test tubes to which 15 g PBS was added at a temperature of 32 °C. All experiments were carried out in quadruplicate. The test tubes were placed in a non-oscillating water bath (Julabo 20B, Merck-Belgolabo, Overijse, Belgium) at a temperature of 32.0 ± 0.5 °C. At different time points, samples of 2 g release medium were taken from each test tube and replaced with an equal amount of PBS at 32 °C. Sampling intervals of 10, 30, 60, 90, 120, 180, 240, 300, 360, 420 and 480 minutes were chosen. Before and after sampling, the content of the test tubes was homogenised by means of gentle stirring.

Samples were analysed spectrophotometrically at a wavelength of 280 nm. At the end of every series of measurements, the content of each test tube was intensively vortexed to release the remaining drug from the insert and measured spectrophotometrically.

2.2.3 Rheological measurement

The viscosity of the inserts was measured using an Anton Paar rheometer (MCR-102, Graz, Austria) with a parallel plate measuring device. The measurement was performed through oscillation at a constant amplitude of 1% and a varying angular frequency of 100 to 0.1 rad/s. A parallel plate with a diameter of 8 mm was chosen. The gap was set at 1.5 mm and a temperature of 32.0 ± 0.1 °C was configured. To prevent the polymer from drying out during the measurements, a solvent trap was used to cover the sample. Every formulation was measured in quadruplicate and two separate measurements were taken per replicate.

3 RESULTS AND DISCUSSION

3.1 Activity

In figure 1, the activity levels compared to the reference lysozyme solution is given.

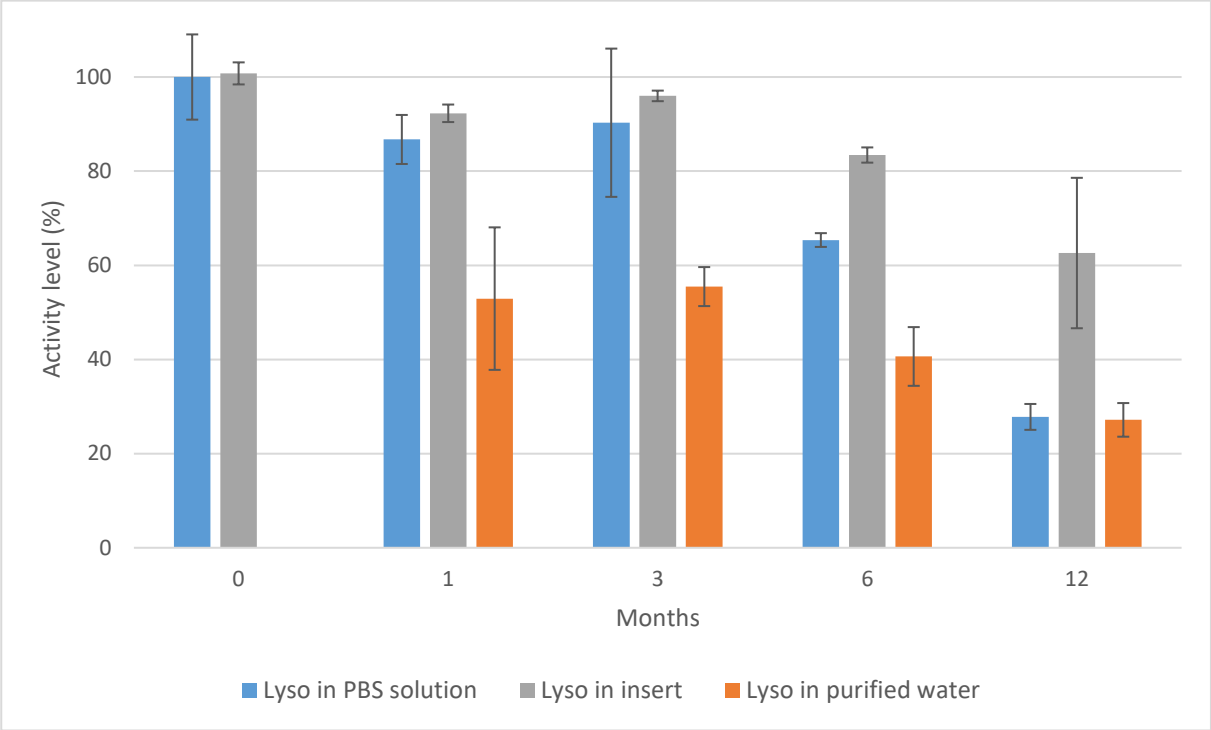

Fig. 1. Evolution of activity over time for a lysozyme (lyso) solution in PBS, lysozyme loaded inserts in PBS and a solution of lysozyme in purified water.

The activity of lysozyme in PBS at day 0 was set as the reference activity level. Unsurprisingly, the PBS solution of lysozyme and the insert showed near identical activity levels at day 0. After one month, interesting data was collected. The activity level of a lysozyme solution in purified water seems to drop dramatically, compared to lysozyme in PBS solution. The buffered environment of PBS keeps the pH within a stable range for lysozyme. The result of the activity level of lysozyme after one month loaded in the insert seems to be at least equal if not slightly better than the activity levels in PBS. After three months, the results obtained are similar. A very small increase is observed for all three solutions, which might be the result of small errors during pipetting in the 96-well plate.

A sharp drop in activity levels is seen for all solutions after six months. Still, a solution of lysozyme in PBS seems to retain the activity of lysozyme better compared to lysozyme in an aqueous solution, while the excipients of the inserts seem to improve the stability of lysozyme even more. Even after 12 months, the activity level of lysozyme loaded in inserts is still over 60% of its initial activity. The activity of lysozyme in PBS and purified water have dropped to the same level (respectively 28%

and 27% of the initial activity) which is less than half the lysozyme activity in inserts. The viscosity of the insert likely contributes to improve the stability of the protein, but also sugars, as present in the backbone of HPMC, and the presence of glycerol in the insert are known for stabilising proteins [4–7]. Proteins are stabilised because sugars and polyols are preferentially excluded from the surface of the protein as a result of repulsion between the protein backbone and the stabilising molecule. As a result, the native structure of the protein is therefore shifted into a more stable and compact tertiary structure with a reduced surface area, preventing protein aggregation, thus improving the stability of the substance [1,4,8–10].

3.2 Release profiles

The release profiles for the different lysozyme loaded inserts stored at various time points are given in figure 2.

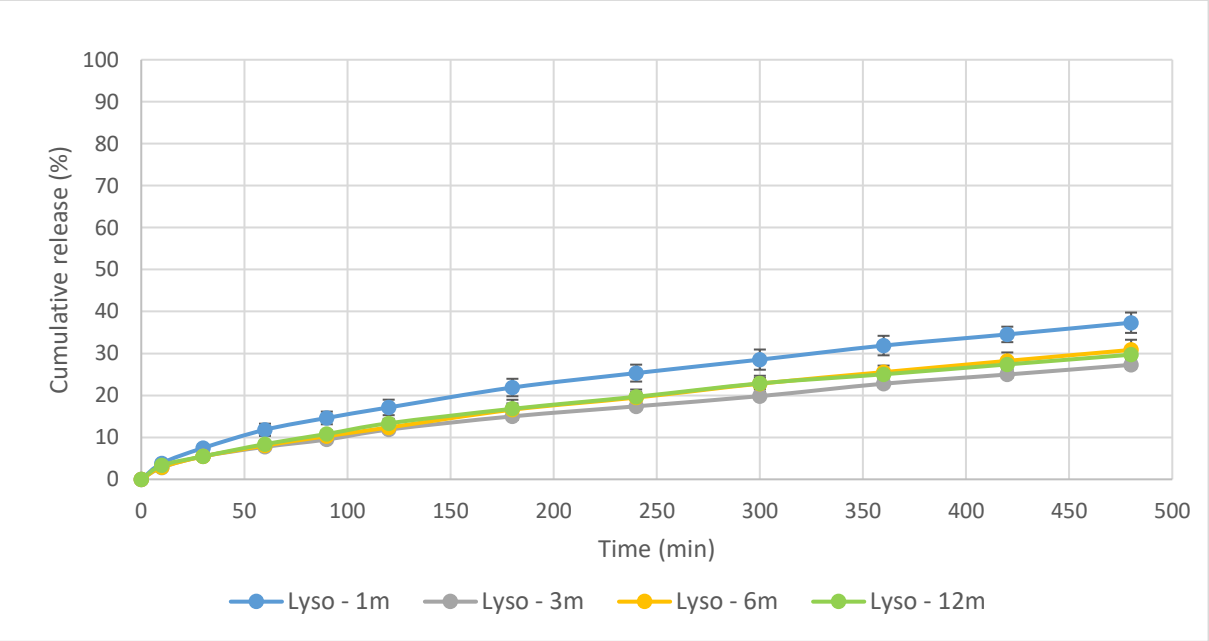

Fig. 2. Cumulative release profiles for lysozyme released from the insert after 1, 3, 6 and 12 months, respectively indicated by Lyso - 1m, Lyso - 3m, Lyso - 6m and Lyso - 12m (n=4).

Similar to previously developed inserts with lysozyme, no burst release is noted for any of the release curves. However, the release profile of inserts after one month of storage reveal slightly higher release amounts of lysozyme starting from 30 minutes which might be indicative for not obtaining a perfectly homogeneous distribution of the rehydration solution containing lysozyme. There is no apparent difference in the release profiles after three months. Such a result is not surprising, as a storage time of one month for inserts of this size and weight is quite optimistic,

based on experience and results from earlier experiments as described in the previous chapters. It is important to understand that obtaining a homogeneous distribution of both drug and rehydration solution will highly be influenced by the characteristics of the drug, but also influenced by the temperature and not the least the dimensions of the insert. Stability-wise, the release profiles show no evidence of altered release profiles between three and twelve months of storage.

3.3 Rheological measurement

The results of viscosity measurements of different inserts loaded with lysozyme and stored during various time periods, are graphically presented in figure 3.

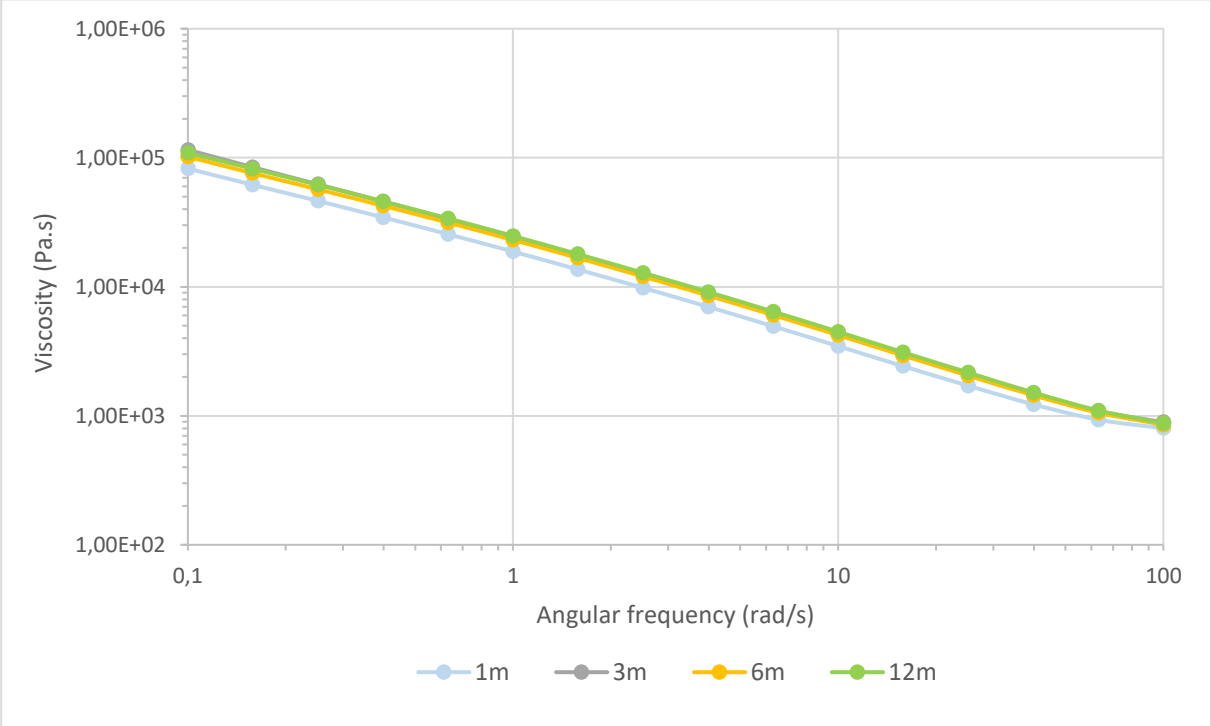

Fig. 3. Viscosity profiles for inserts loaded with lysozyme and measured after 1, 3, 6 and 12 months, respectively indicated by 1m, 3m, 6m and 12m (n=8).

Similar to the results of release profiles in figure 2, the inserts stored during one month show a slightly deviating viscosity profile compared to inserts stored during three or more months. The lower viscosity could be explained by the insufficiently homogeneous distribution of the drug and particularly in this case, a nonhomogeneous distribution of the rehydration solution. This causes one side of the insert to be slightly less hydrated than the opposing side, based on the mechanism of rehydration of the method developed. As a drug solution is added from one side of the dehydrated polymeric matrix, the top part of the matrix will be hydrated sooner than the bottom part of the insert. An incomplete hydration of the polymer matrix will lead to a viscosity gradient.

This in turn alters rheological measurements or in the case of a relatively 'wet' surface to *wall slip*. Wall slip is a phenomenon where one of the plates of the viscosimeter cannot sufficiently grip the entire sample resulting in an underestimation of the true viscosity of the sample. In this case, only a part of the sample would be brought into movement which affects the rheological profile [11–13]. Nonetheless, the rheological results indicate excellent stability of the properties of the HPMC inserts.

4 CONCLUSION

From the activity measurements, a stabilising effect of the drug carrier on lysozyme is seen over time. Especially after 12 months of storage, the activity of lysozyme loaded in inserts is more than double the activity of lysozyme in both PBS and purified water. The stabilising effect of the excipients glycerol and HPMC can most likely be held responsible for this observation. Both release profiles and rheological measurements show signs of evidence that full rehydration of the drug solution in the dehydrated polymer matrix have not fully occurred after one month. Storage of the inserts between three and twelve months show no difference in both release profiles as well as in the rheological data which indicated excellent stability of the inserts over the time period investigated.

Acknowledgements

I would like to express my gratitude to drs. Gwendolyn Vliegen and prof. dr. Anne-Marie Lambeir (Laboratory of Medical Biochemistry, Department of Pharmaceutical Sciences, University of Antwerp) for their help with the stability measurements.

References

1. Manning MC, Chou DK, Murphy BM, Payne RW, Katayama DS. Stability of protein pharmaceuticals: An update. Pharm Res. 2010;27: 544–575.
2. Molecular Probes. EnzChek® Lysozyme Assay Kit (E-22013). Technical information. 2001.
3. Davies RC, Neuberger A, Wilson BM. The dependence of lysozyme activity on pH and ionic strength. Biochim Biophys Acta - Enzymol. 1969;178: 294–305.
4. Avanti C, Saluja V, Van Streun ELP, Frijlink HW, Hinrichs WLJ. Stability of lysozyme in aqueous extremolyte solutions during heat shock and accelerated thermal conditions. PLoS One. 2014;9: 2–7.
5. Sedgwick H, Cameron JE, Poon WCK, Egelhaaf SU. Protein phase behavior and crystallization: Effect of glycerol. J Chem Phys. 2007;127: 1–6.
6. Vagenende V, Yap MGS, Trout BL. Mechanisms of protein stabilization and prevention of protein aggregation by glycerol. Biochemistry. 2009;48: 11084–11096.
7. Esposito A, Comez L, Cinelli S, Scarponi F, Onori G. Influence of glycerol on the structure and thermal stability of lysozyme: a dynamic light scattering and circular dichroism study. J Phys Chem B. 2009;113: 16420–16424.
8. Edelman R, Kusner I, Kisiliak R, Srebnik S, Livney YD. Sugar stereochemistry effects on water structure and on protein stability: The templating concept. Food Hydrocoll. 2015;48: 27–37.
9. Tonnis WF, Mensink MA, De Jager A, Van Der Voort Maarschalk K, Frijlink HW, Hinrichs WLJ. Size and molecular flexibility of sugars determine the storage stability of freeze-dried proteins. Mol Pharm. 2015;12: 684–694.
10. Honig B. Protein Folding: From the Levinthal Paradox to Structure Prediction. J Mol Biol. 1999;293: 283–293.
11. Durairaj R, Man LW, Ekere NN, Mallik S. The effect of wall-slip formation on the rheological behaviour of lead-free solder pastes. Mater Des. 2010;31: 1056–1062.
12. Walls HJ, Caines SB, Sanchez AM, Khan SA. Yield stress and wall slip phenomena in colloidal silica gels. J Rheol. 2003;47: 847–868.
13. Ozkan S, Gillece TW, Senak L, Moore DJ. Characterization of yield stress and slip behaviour of skin/hair care gels using steady flow and LAOS measurements and their correlation with sensorial attributes. Int J Cosmet Sci. 2012;34: 193–201.

Chapter 9: *In vivo* evaluation

1 INTRODUCTION

In the previous chapters, it has been demonstrated that the inserts developed have slow release characteristics *in vitro* and do not reveal any cytotoxic effects on human corneal epithelial cells *ex vivo*. The main aim of the *in vivo* study is to analyse the behaviour of the ocular inserts when administered in living animals.

For this experiment, a dry eye rat model has been developed by researchers of the Laboratory of Microbiology, Parasitology and Hygiene at the University of Antwerp, Belgium. This method includes the surgical removal of the exorbital gland of the rat, responsible for tear fluid production. Dry eye disease is characterised by a series of inflammatory events, releasing cytokines such as interleukin-1α (IL-1α) and tumour necrosis factor-α (TNF-α) [1,2]. Therefore, to treat the dry eye pathology, dexamethasone sodium phosphate was used as a reference drug in an aqueous eye drop solution to suppress the inflammatory cycle [1,3,4]. Experimentally, inserts with different concentrations of dexamethasone sodium phosphate were administered and compared to the reference group.

Measurements were performed on the ocular tissue damage through fluorescein scoring, tear volumes were measured and an analysis was performed on the cytokine levels of IL-1α and TNF-α, linked to dry eye disease.

Although the treatment of dry eye disease is not necessarily within the scope of this research work, the data obtained from such animal model could provide valuable information on the strengths and weaknesses of ocular inserts *in vivo.*

2 MATERIALS AND METHODS

2.1 Materials

Twenty female Wistar rats with a body mass between 200 g and 300 g were purchased from Janvier (Saint-Berthevin Cedex, France) and kept under controlled, pathogen-free conditions. The female Wistar rats were kept in the following husbandry conditions: at a temperature of 20-25 °C and a humidity level of 45%. The day-night cycle was set at 12 h/12 h. Food and water were available *ad libitum*. Dexamethasone sodium phosphate was purchased from Sigma-Aldrich (Steinheim, Germany). Isoflurane (Halocarbon®, New-Jersey, USA), ketamine (Anesketin®, Eurovet, Bladel, Netherlands) and xylazine (Rompun®, Bayer, Leverkusen, Germany) were used as anaesthetics. Isobetadine® (Meda, Brussels, Belgium), Astrexine® (Pierre-Fabre Médicament, Boulogne, France) and Temgesic® (Reckitt Benckiser Healthcare, Hull, UK) were used to perform surgery. Baytrill® (Bayer, Leverkusen, Germany) was given to the rats post-surgically as an antibiotic.

Glycerol analytical grade (99.5% (V/V)) was obtained from Sigma-Aldrich (Steinheim, Germany). Hydroxypropylmethyl cellulose type E10M Premium CR was provided by Colorcon (Dartford, UK). By specification, an aqueous 2% (w/w) E10M solution gives an apparent viscosity of 10.000 mPa.s (at 20 °C).

2.2 Method

All *in vivo* experiments were approved by the Animal Ethical Committee of the University of Antwerp (2013-67).

2.2.1 Surgical induction of dry eye disease

All rats were anaesthetised prior to surgery with an intraperitoneal injection of 25 mg/kg bodyweight ketamine and 2.5 mg/kg xylazine after a three-fold dilution in PBS solution. The right exorbital lachrymal gland of the rat was surgically removed by an incision of approximately 10 mm in front of and inferior to the tragus below the right ear. The left eye remained untreated and served as a control eye.

Prior to surgery, Isobetadine® was used to disinfect the skin of the rat. After surgery, the wound was disinfected with Astrexine®. To relieve pain, Temgesic® was given as a post-operative analgesic. In order to reduce the risk of post-operative complications, an antibiotic (Baytrill®) was administered orally for five consecutive days (1 ml Baytrill® per drinking bottle).

2.2.2 Evaluation of ocular tissue damage

A volume of 1 µl sodium fluorescein solution (1% (w/V) in PBS) was topically administered on the eye surface using a micropipette. After two minutes, the excess sodium fluorescein solution was removed by rinsing the eye with 4 µl PBS. The eye was photographed using a Canon digital camera with a microscopic lens attached to it. The photographs were taken in a darkened room under cobalt blue light. In case of tissue damage, yellow fluorescent stains are visible.

The photographs were analysed using the Oxford fluorescein grading scale for evaluation of the ocular surface. Scores were given from 0 to 5 for each eye to indicate the severity of tissue damage. A score of 0 implies no noticeable harm done to the eye, while 5 indicates severe ocular surface deterioration [5].

2.2.3 Tear volume measurement

The tear volume was measured once a week using a phenol red thread tear test (Zone-Quick™, Menicon, Nagoya, Japan) which was placed centrally under the lower conjunctival fornix during 15 seconds. The tear volume can be estimated by measuring the discolouration of the phenol red thread from yellow to red and is expressed in the length of discolouration of the cotton thread in mm.

2.2.4 Tear collection

Tear fluid was collected with a glass capillary, connected to a flexible tube and a syringe. A partial vacuum was induced using the syringe, in order to increase the amount of tear fluid collected. The capillaries were subsequently stored at -80 °C for flow cytometric analysis. The tear collection was carried out twice every week.

2.2.5 Flow cytometric analysis of tear fluid

The cytokine levels of IL-1α and TNF-α in tear fluid were measured using a Cytometric Bead Array (CBA) kit according to the manufacturers protocol (Rat IL-1α and TNF-α CBA flex sets, BD Biosciences, Erembodegem, Belgium). The data was collected through flow cytometric techniques (FACS calibur, BD Biosciences, San Jose, USA). Tear fluid samples were taken as much as possible, given the available amount. Tear fluid of all animals (n=4) of the same treatment group were pooled per animal prior to the analysis. The collected samples were diluted to 15 µl with assay diluent. The same protocol was followed for the untreated left eye of the rat.

2.2.6 Preparation of eye drops

The eye drops were prepared in a laminar flow cabinet (Safemate 1.8, Euroclone, Pero, Italy) by dissolving dexamethasone sodium phosphate in PBS solution in a concentration of 1 mg/ml. The rats were given four eye drops per day, with a single drop measuring 2.5 µl.

2.2.7 Preparation of insert

The inserts loaded with dexamethasone sodium phosphate were prepared in custom made Teflon moulds with a diameter of 2 mm and a length of 10 mm. The method described in section *2.2 Preparation of ocular inserts* in *chapter 5* was followed using an aqueous solution of dexamethasone sodium phosphate. The mass of the inserts was set at 70 mg, but to accommodate the dimensions of the rats fornix, smaller samples weighing 4 mg were taken and inserted in the lower conjunctival fornix of the right eye.

Two series of inserts were prepared with different concentrations of dexamethasone sodium phosphate. The dosage of the inserts was calculated for twice a day application in case an insert would get expelled from the conjunctival fornix and set at a dose twice the daily dose of the eye drops (20 µg dexamethasone sodium phosphate) and a dose equivalent to five times the daily dose (50 µg dexamethasone sodium phosphate). These groups are hereafter indicated by ‘dexa-2x’ and ‘dexa-5x’ respectively. An additional series of blank inserts were also produced.

2.2.8 Experimental setup

Within the same day of surgical removal of the exorbital lachrymal gland, all rats were treated during 12 days. For the inserts, both loaded with dexamethasone sodium phosphate and blank inserts, the experiment was executed in a double blind manner. All inserts were administered to the rats within one hour, between 8h30 – 9h30 and a second dose between 15h30 – 16h30. Tear samples were taken on every Monday, Wednesday and Friday morning. An overview of the experimental groups is given in table 1.

Table 1. Overview of the experimental groups.

Group	Treatment	# Animals	Treatment frequency
Negative control (dry eye)	No treatment	4	-
Positive control (eye drops)	Eye drops (1 mg/ml)	4	4x 1 drop/day
Test group A (insert) 'dexa-2x'	Inserts with 2-fold of daily eye drop dosage	4	2x/day
Test group B (insert) 'dexa-5x'	Inserts with 5-fold of daily eye drop dosage	4	2x/day
Blank insert	Inserts without drug	4	2x/day

3 RESULTS AND DISCUSSION

3.1 Evaluation of ocular tissue damage

The results for the evaluation of ocular tissue damage using the Oxford fluorescein grading scale are graphically presented in figure 1.

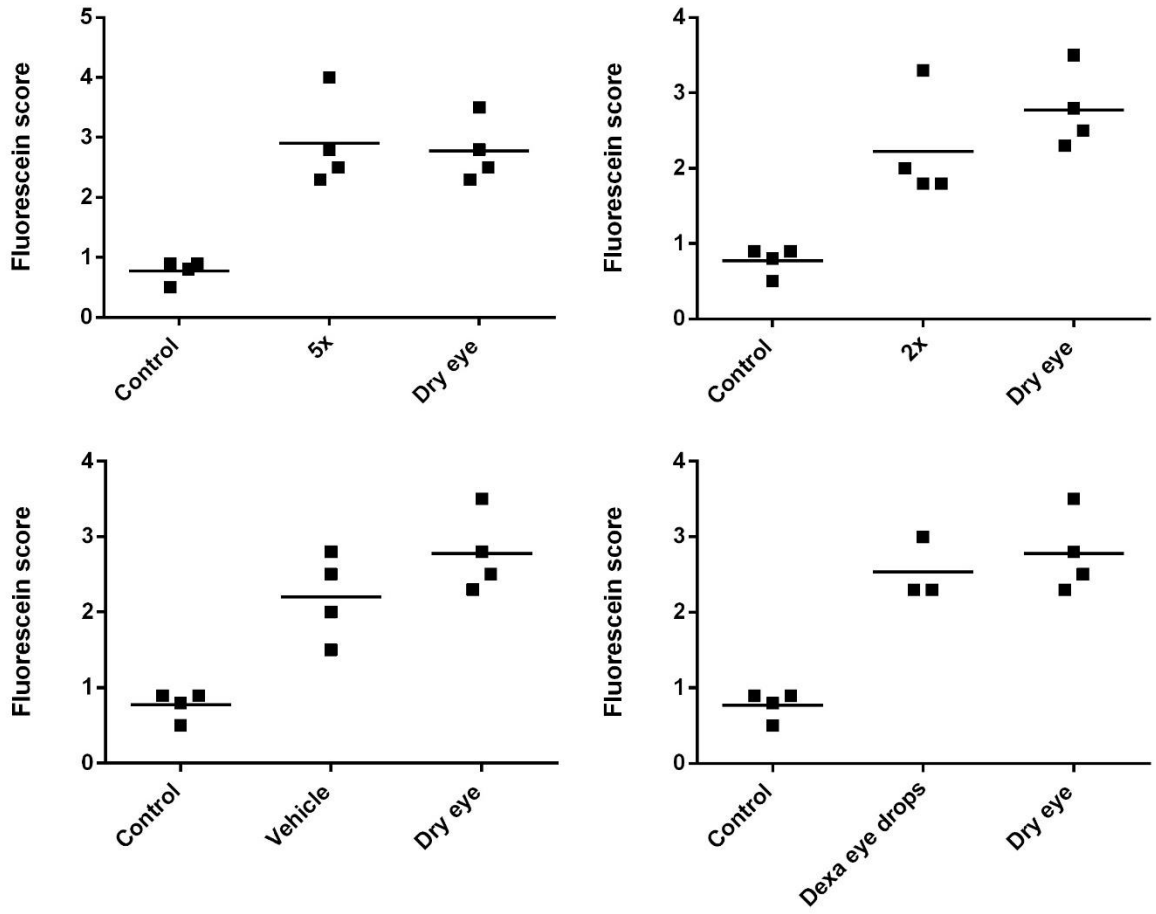

Fig. 1. Overview of the individual fluorescein scores for each group compared to the left eye (control group) and the untreated group, indicated by 'Dry eye'. The labels '5x', '2x' and 'Vehicle' correspond to the groups 'dexa-5x', 'dexa-2x' and blank inserts respectively. The label 'dexa eye drops' represents rats treated with dexamethasone sodium phosphate in PBS eye drops.

Treatment of the right eye with 'dexa-5x' did not show any decrease in tissue damage compared to the untreated dry eye group or rats treated with dexamethasone sodium phosphate eye drops. From the treated animals, the lowest fluorescein scores indicating less tissue damage are obtained for animals treated with 'dexa-2x' and blank inserts. Although some improvement was observed for blank inserts and the 'dexa-2x' group, these results still indicate a relatively high degree of tissue damage from all groups compared to the left control eye. This can be explained by the potentially harmful effects of corticosteroids on the ocular surface, disregarding the carrier in which

dexamethasone sodium phosphate is administered [6,7]. It should be noted that *in vivo* experiments on a relatively small number of animals make interpretation of the results difficult.

3.2 Tear volume measurement

The results for the tear volume measurement are presented in figure 2.

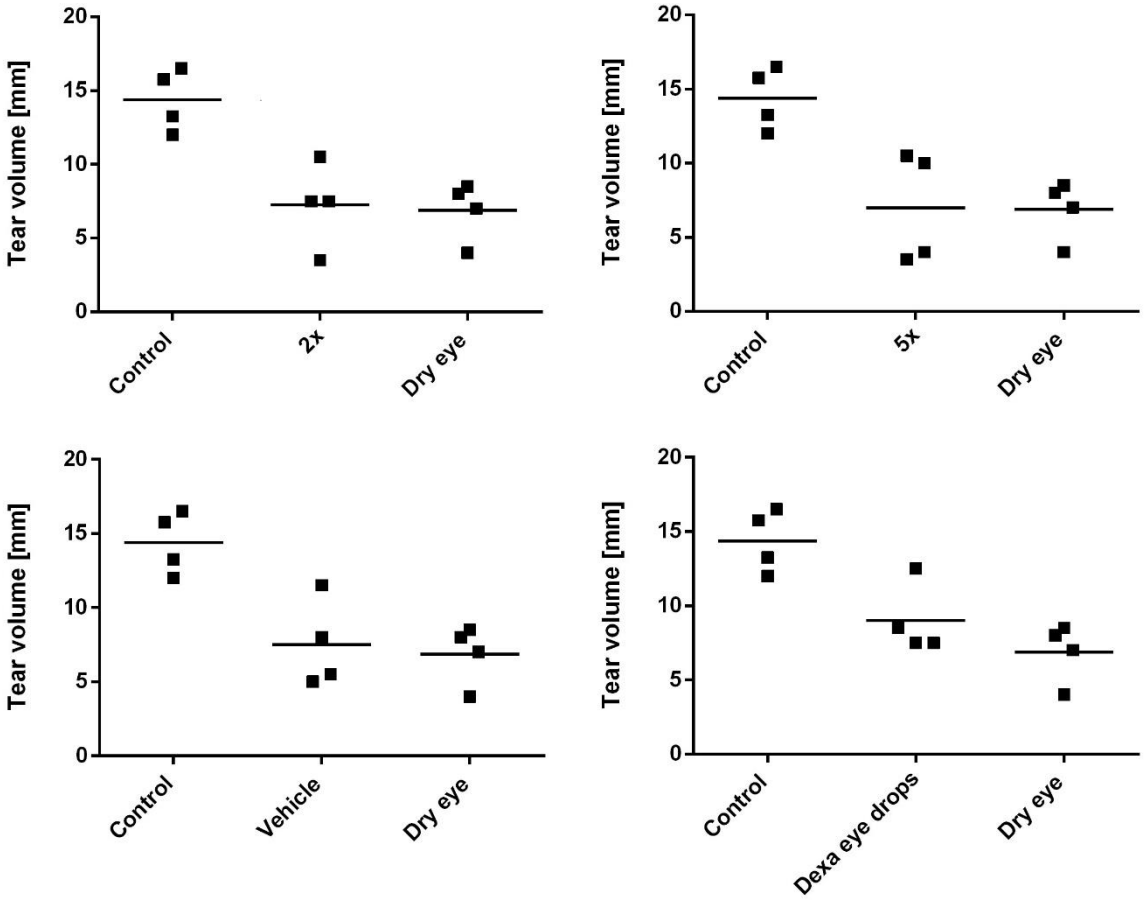

Fig. 2. Overview of the individual tear volumes for each group compared to the left eye (control group) and the untreated group, indicated by 'Dry eye'. The labels '5x', '2x' and 'Vehicle' represent the groups 'dexa-5x', 'dexa-2x' and blank inserts respectively. The label 'dexa eye drops' represents rats treated with dexamethasone sodium phosphate in PBS eye drops.

There were no differences detected between inserts loaded with and without dexamethasone sodium phosphate compared to the dry eye group. Only a modest increase in tear volume for animals treated with dexamethasone loaded eye drops can be reported, but still below control group levels. The mechanism of treating dry eyes with corticosteroids does not rely on increasing tear fluid volumes, but on suppressing the inflammatory cascade linked to dry eye disease.

Furthermore, this dry eye rat model is based on the surgical removal of the exorbital lachrymal gland. Therefore, tear volumes as high as the control group were not expected.

3.3 Measurement of cytokine levels

After flow cytometric analysis, the results for IL-1α and TNF-α concentrations were plotted in the following figure 3 and figure 4.

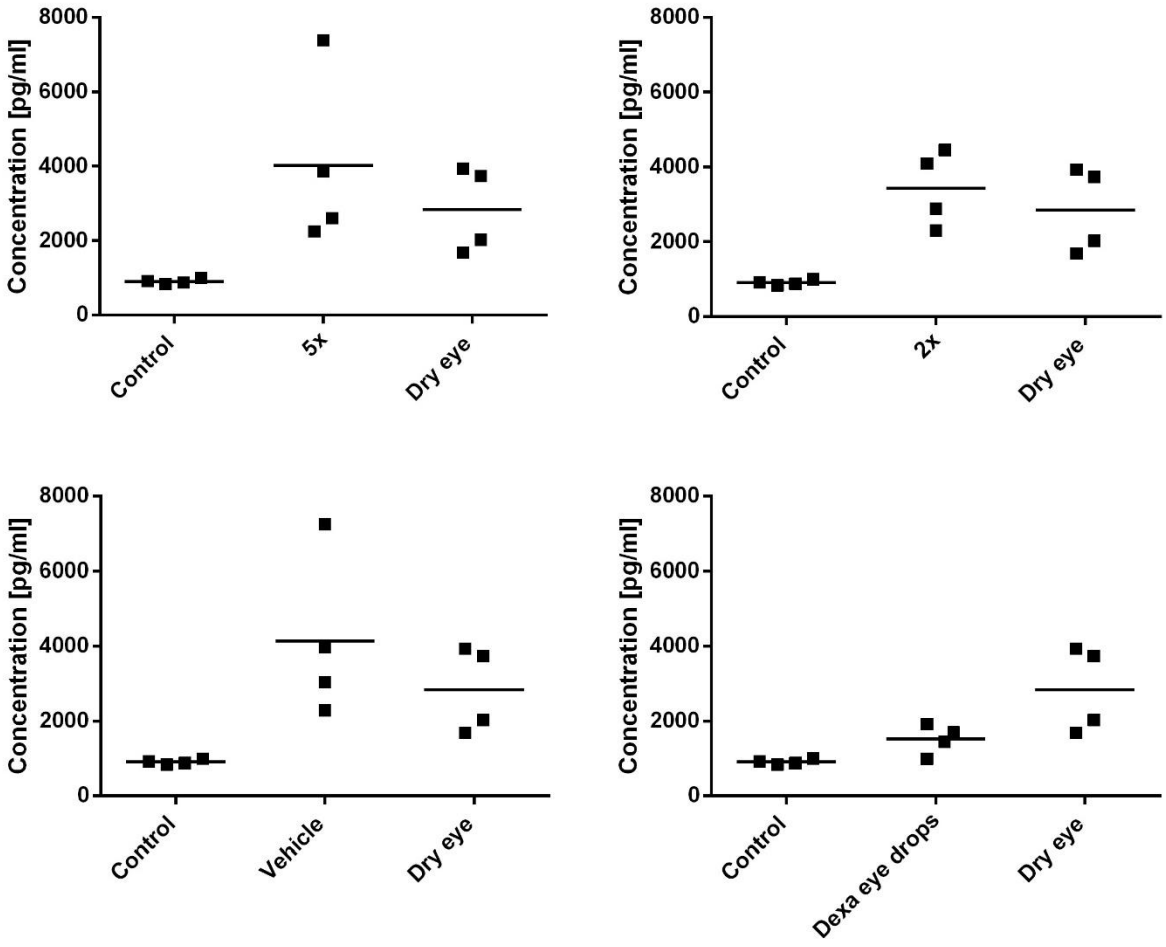

Fig. 3. Overview of the individual cytokine concentrations of IL-1α for each group compared to the left eye (control group) and the untreated group, indicated by 'Dry eye'. The labels '5x', '2x' and 'Vehicle' represent the groups 'dexa-5x', 'dexa-2x' and blank inserts respectively. The label 'dexa eye drops' represents rats treated with dexamethasone sodium phosphate in PBS eye drops.

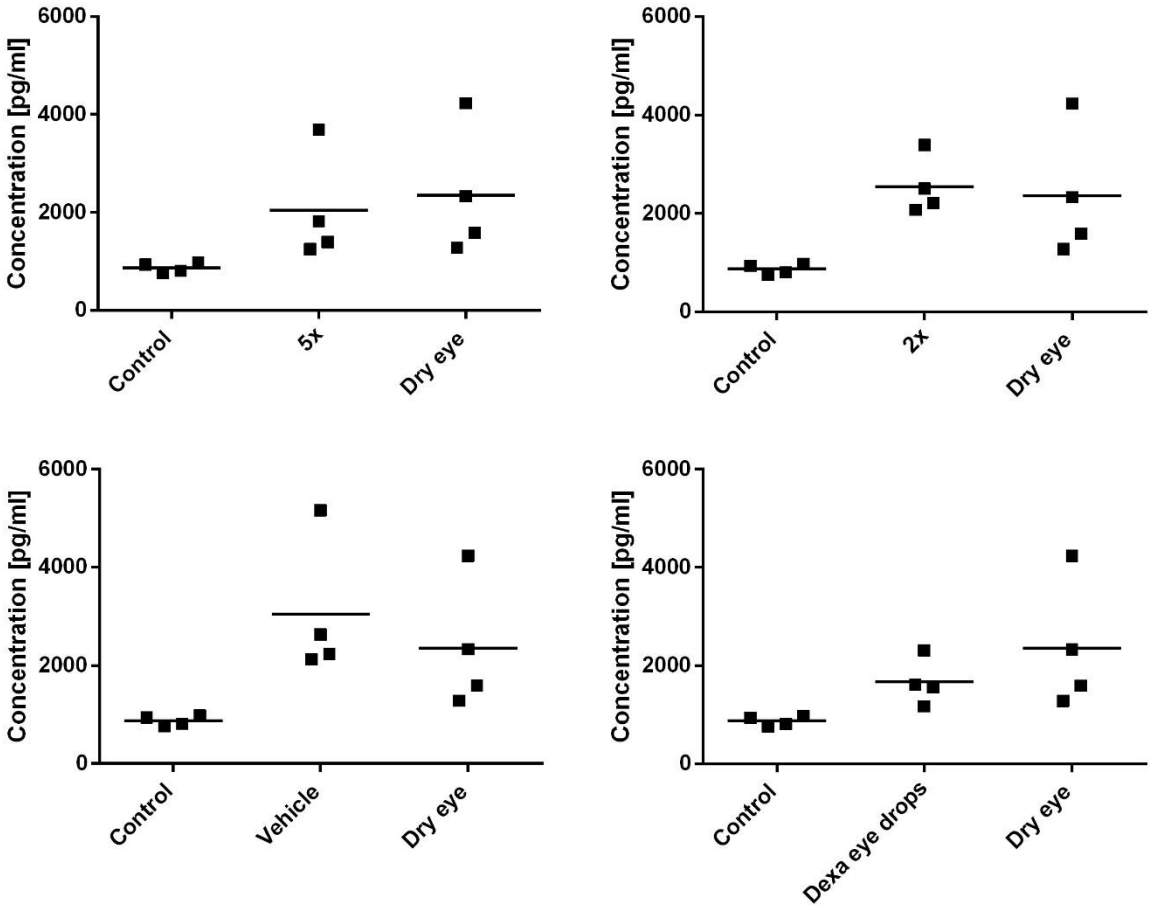

Fig. 4. Overview of the individual cytokine concentrations of TNF-α for each group compared to the left eye (control group) and the untreated group, indicated by 'Dry eye'. The labels '5x', '2x' and 'Vehicle' represent the groups 'dexa-5x', 'dexa-2x' and blank inserts respectively. The label 'dexa eye drops' represents rats treated with dexamethasone sodium phosphate in PBS eye drops.

Rather unexpectedly, the average concentrations of cytokines in the insert treated groups are comparable or higher than the cytokine levels of the dry eye group. This indicates that the inserts loaded with dexamethasone sodium phosphate were unable to suppress the inflammatory events compared to dexamethasone eye drops. A modest suppression of cytokine levels is noticed for rats treated with dexamethasone eye drops, but not to the same level as the control group. In almost every insert treated group, there is one animal with diverging results, compared to the other three animals stressing the importance of a larger number of animals for a solid interpretation of the results. The same variability is seen for the untreated dry eye group.

There are several reasons that argument for these results.

Firstly, the inserts are given twice daily, but whether the inserts remained at the site of application is unknown. From preliminary studies, it was noticed that in case of hydrated eyes, the inserts got expelled from the fornix more easily due to the movement of the eyelids and the inability of the inserts to absorb tear fluid and attach to the ocular surface. The small size and transparency of the inserts make it hard to detect such an event. Experience and practice improved the insertion techniques, minimising the apparent frequency of expulsion.

Secondly, it is possible that the viscosity of the inserts was too high for the amount of tear fluid available in the eye of the rats. In some cases, when the second insert was applied, the first insert was found in a partially dissolved state on the surface of the eye. This could mean that therapeutic levels of the drug might not have been reached or only for a short period of time, insufficient to trigger an anti-inflammatory response. Such an observation implicates the need to make the dimensions of the insert even smaller for drug unloading to occur or the development of inserts with lower viscosities and hence faster dissolution and drug release rates for the treatment of dry eye disease in rats, but not necessarily in humans.

Thirdly, hydrogels are known to absorb aqueous fluid from their surroundings and swell [8–10]. Application of a hydrogel on the ocular surface might lead to reduced free tear fluid, which in case of dry eye disease is not desirable. However, hydrogels are already commercially used for treatment of dry eye disease as the polymer chains of hydrogels disentangle in tear fluid and spread over the surface of the eye in a thin film, retaining water at the ocular surface. A well-known example of such a device is Lacrisert®, based on the polymer hydroxypropyl cellulose (HPC) [11]. High concentrations of HPMC in the insert or inserts with large dimensions might reduce or even annihilate the lubricating effect of polymers entirely in case of severe dry eye disease, certainly in the case where certain lachrymal glands are lacking. Additionally, it was noticed that collecting sufficient amounts of tear fluid was more difficult to achieve for insert treated eyes. In case of insert treated eyes, smaller amounts of tear fluid were available for cytokine analysis compared to non-insert treated eyes, potentially causing erroneous results and misinterpretation.

The property of inserts to absorb tear fluid could also lead to higher levels of cytokines measured in free tear fluid. From earlier studies, it has been proven that small molecules are more easily embedded in hydrogels through passive diffusion. For instance water is a very small molecule compared to larger molecules such as IL-1α and TNF-α and is therefore absorbed easily by an insert. Absorption of tear fluid might shift the ratio cytokines/tear fluid to higher levels due to less free

tear volume being available for tear collection, increasing the measured cytokine concentrations. However, the time period between application of an insert and the collection of tear fluid is approximately 17 hours. Although it was impossible to determine whether the insert was able to exert its effect, it is less likely that the insert was still present at the site of application. No cases as such were reported, although the presence of a thin layer of polymer over the surface might be enough to reduce the amount of tear fluid available for tear collection.

4 CONCLUSION

The inserts loaded with a dexamethasone sodium phosphate brought no clear improvements for the treatment of dry eyes in rats. No difference was measured between blank, 'dexa-2x' and 'dexa-5x' inserts which suggest that other mechanisms prohibit the action of dexamethasone sodium phosphate. The slow dissolution rate of the insert and hence slow release rate of the drug incorporated seems to play an important role in the outcome of the conducted experiments. The viscosity and absorbing capacity of the insert increasing the local cytokine concentration in tear fluid might also contribute to this observation.

Acknowledgements

I am very grateful to drs. Cedric Joossen and prof. dr. Paul Cos (Laboratory for Parasitology, Microbiology and Hygiene, Department of Pharmaceutical Sciences, University of Antwerp) for conducting the animal studies.

References

1. De Paiva CS, Corrales RM, Villarreal AL, Farley WJ, Li DQ, Stern ME, et al. Corticosteroid and doxycycline suppress MMP-9 and inflammatory cytokine expression, MAPK activation in the corneal epithelium in experimental dry eye. Exp Eye Res. 2006;83: 526–535.
2. Enríquez-de-Salamanca A, Castellanos E, Stern ME, Fernández I, Carreño E, García-Vázquez C, et al. Tear cytokine and chemokine analysis and clinical correlations in evaporative-type dry eye disease. Mol Vis. 2010;16: 862–873.
3. Sadrai Z, Stevenson W, Okanobo A, Chen Y, Dohlman TH, Hua J, et al. PDE4 inhibition suppresses IL-17-associated immunity in dry eye disease. Investig Ophthalmol Vis Sci. 2012;53: 3584–3591.
4. Narayanan S, Redfern RL, Miller WL, Nichols KK, Mcdermott AM. Dry eye disease and microbial keratitis: Is there a connection? Ocul Surf. 2013;11: 75–92.
5. Bron AJ, Evans VE, Smith JA. Grading of corneal and conjunctival staining in the context of other dry eye tests. Cornea. 2003;22: 640–650.
6. Bourcier T, Forgez P, Borderie V, Scheer S, Rostène W, Laroche L. Regulation of human corneal epithelial cell proliferation and apoptosis by dexamethasone. Invest Ophthalmol Vis Sci. 2000;41: 4133–4141.
7. Petersen A, Carlsson T, Karlsson J, Jonhede S, Zetterberg M. Effects of dexamethasone on human lens epithelial cells in culture. Mol Vis. 2008;14: 1344–1352.
8. Barba AA, d'Amore M, Chirico S, Lamberti G, Titomanlio G. Swelling of cellulose derivative (HPMC) matrix systems for drug delivery. Carbohydr Polym. 2009;78: 469–474.
9. Joshi SC. Sol-gel behavior of hydroxypropyl methylcellulose (HPMC) in ionic media including drug release. Materials. 2011;4: 1861–1905.
10. Siepmann J, Kranz H, Bodmeier R, Peppas NA. HPMC-matrices for controlled drug delivery: A new model combining diffusion, swelling, and dissolution mechanisms and predicting the release kinetics. Pharmaceutical Research. 1999; 1748–1756.
11. Nguyen T, Latkany R. Review of hydroxypropyl cellulose ophthalmic inserts for treatment of dry eye. Clin Ophthalmol. 2011;5: 587–591.

GENERAL CONCLUSIONS AND FUTURE PERSPECTIVES

One of the most prominent challenges for researchers in the ophthalmic field is the development of a drug delivery device that replaces eye drops for sustained delivery of ocular drugs. Despite many efforts over several decades, the popularity of eye drops has remained high. However, in recent years, peptide and protein therapeutics have emerged as a new field of ocular therapeutics with specific requirements during formulation.

In this regard, a novel method for preparing ocular inserts was developed, particularly focussing on the incorporation of peptides and proteins. Generally, these molecules have to be treated with necessary care and require specific attention, as they tend to be temperature sensitive, prone to oxidation and can lose their conformation and activity as the result of external forces applied. However, many drug carriers based on polymers require heat or shear forces, therefore not appearing to be suitable for drug carrier development when peptides or proteins are involved. The objective of the present work was to develop a novel method exploring the possibilities of a protein loaded polymeric insert.

Is was demonstrated that it is possible to produce ocular inserts loaded with a peptide or protein without the need for shear forces, air bubble entrapment (which is common when using polymers in high concentrations) or elevated temperatures. The drug loading occurs through a passive diffusion process, which was made possible by an initial pre-treatment of the HPMC hydrogel serving as the drug carrier. Using passive diffusion implies that the drug loading is a temperature dependent process where mainly the viscosity of the carrier as well as the molecular weight of the drug play an important role. Due to the nature of the molecules envisioned, the temperature was fixed at 2 °C.

The dissolution tests showed interesting results. Slow release profiles were measured for most molecules tested such as sodium fluorescein, lysozyme or FITC-dextrans 10 – 20 kDa. For slow release to occur, full penetration of the drug in the core of the matrix is a basic requirement as the slow release profiles are closely linked to the drug loading process. Unsurprisingly, small molecules, such as sodium fluorescein, can easily be loaded through passive diffusion in the inserts, even in a single day loading period. Reducing the dimension of the polymeric matrix had a beneficial effect on the drug loading process. As expected, an increase in molecular weight reduced the level of success by which molecules can penetrate into the matrix. Loading FITC-dextrans with a molecular weight of 40 kDa or larger showed high initial drug release amount where slow release was

expected. The large size of these molecules caused impregnation of the surface of the insert rather than reaching the core of the insert matrix due to the high polymeric density. Lowering the final percentage of HPMC in the drug carrier improved the drug loading and hence release characteristics to some extent, but passive diffusion clearly poses limitations on the drug loading behaviour of large molecules. The final percentage HPMC also depends on the characteristics imposed by researchers for a semisolid ocular device.

The excipients used to build up the insert did not show any harmful effect on SV40-immortalised human corneal epithelial cells (SV40-HCEC). The results obtained through cell viability measurements showed no difference between HPMC or HPC hydrogels, which was used as a reference polymer. The latter is commercially available as a solid insert for the treatment of dry eye disease in humans. This data was also compared to cell viability measurements performed with benzalkonium chloride in different concentrations, which is a known cytotoxic compound. Even at concentrations as low as 0.004% (w/V), benzalkonium chloride appeared lethal to SV40-HCEC.

Excellent stability results were reported for lysozyme loaded inserts. Both rheological and release measurements yielded good results with no noticeable difference between profiles of inserts stored between three and twelve months. Inserts stored during one month showed slightly differing results compared to three or more months of storage. An insufficient completion of the drug loading process can be held responsible for this observation. Activity measurements showed a stabilising effect of HPMC and/or glycerol on the stability of lysozyme. After a storage period of twelve months at a temperature of 2 °C, the activity of lysozyme was measured to be twice as high as lysozyme stored under the same conditions in purified water or PBS solution.

In vivo studies on rats with dry eye disease did not reveal any improvement over untreated eyes. However, the low number of animals and the tear collection difficulty associated with the viscous nature of the inserts, might have had a significant influence on the outcome of the experiment. Therefore, the true *in vivo* potential of the inserts remains to be seen.

The ocular inserts described in the work were developed to meet the increasing need of slow release preparations loaded with peptide or protein therapeutics. Further studies could provide insights on the diffusion behaviour of drug molecules both during loading and release when different polymer blends in varying concentrations are used. For instance, the use of thermogelling systems such as poloxamer polymers in combination with HPMC hydrogels can be useful for lower

viscosities during drug loading, hence better penetration of the drug in the core of the insert. But after placing the insert in the lower fornix, the higher temperature of the conjunctival sac will trigger a sharp viscosity increase of poloxamer, thereby slowing down drug release.

The influence of pressure or vibration might increase the chance of successfully incorporating large molecules. By using low pressure chambers or vibration during drug loading, the polymeric density of the matrix might be temporarily lowered, making passive diffusion of the large molecules more likely to occur or speed up the drug loading process in case of small molecules, provided that denaturation of these molecules under the given forces does not occur.

Optimisation of rehydration can also be achieved by altering the shape of the dehydrated polymer matrix and increasing the contact area with the rehydration solution. Very thin sheets of dehydrated polymer sandwiched between drug solution can accelerate and improve drug penetration.

Furthermore, miniaturisation of the insert is absolutely required for patient compliance as well as from a technological point of view. Inserts weighing approximately 5 mg instead or 82 mg (for the smallest inserts examined in this research) can be proposed bringing such inserts in the same league as commercially available products such as Lacrisert®.

If technologically feasible, drug loading could be done by injecting the drug of interest directly in a laser-burnt cavity in the core of insert. The drug could homogeneously distribute radially starting from the core of the insert or in case of large molecular weight molecules be trapped in the centre of the insert, only being released by means of erosion. Even water insoluble drugs might benefit from this method.

The emergence of 3D-printing might open new technological doors in drug delivery sciences. Obtaining homogeneous inserts could be made possible by printing the polymer of choice onto and around the drug of interest, thereby avoiding unnecessary manipulations on the thermolabile drug.

SUMMARY

In chapter 1, the major biopharmaceutical aspects related to the anatomical structures and physiological barriers of the eye are discussed, followed by an overview of possible strategies to overcome the issues of low ocular availability, typically associated with eye drops. Moreover, the importance of inserts and the technological role in the treatment of eye diseases with peptides and proteins it can play, are explored. A number of (eye) diseases that are currently treated with proteins is summarised. As sterility of ocular inserts is legally required, a brief summary of the most common sterilisation methods is given.

The main purpose of this research is described in chapter 2. The development of a method to produce slow release ocular inserts without the need for heat, air bubble entrapment or shear forces was set as the primary objective in order to incorporate thermolabile molecules.

A proof-of-concept method is described in chapter 3. The inserts were prepared in four phases. Phase I involved preparation of a highly viscous hydrogel with heat while stirring but devoid of air bubbles. In phase II, the hydrogel was dehydrated by increasing the temperature to 100 °C. At this temperature, the polymer chains cannot retain water and the polymer matrix shrinks as water is lost. Rehydration with a drug solution occurs in phase III. Both drug solution and the partially dehydrated polymer matrix (cylindrically shaped) are placed in a syringe and stored for six weeks at a temperature of 2 °C. After this period, the resulting mass is extruded from the syringe in phase IV after which it can be evaluated for e.g. homogeneity, release kinetics, etc. Factorial design was used, in order to efficiently conduct different experiments determining the influence of various parameters. The resulting inserts were soft and mouldable to prevent the eye from tissue damage. Slow release was obtained, even with a small molecule such as sodium fluorescein. The initial percentage HPMC was the main influencing factor for a homogeneous distribution of sodium fluorescein molecules during rehydration, followed by the polymer type (HPMC E10M or E4M) to a lesser extent.

In chapter 4, the ocular inserts were developed further using a model protein, lysozyme. The same basic methodology described in chapter 3 was applied with some modifications to the polymer cylinder geometry and the dehydration temperature. In order to increase the viscosity of the insert and hence slow down the release rate, HPMC types E10M and K100M were selected. A factorial design was set up and additionally, the influence of the geometry of the dehydrated polymer

cylinder was also taken into account. To accelerate the drug loading process, a hashtag geometry was cut in the polymer cylinder. This has led to homogeneous results for some formulations of the experimental design over the course of six weeks. Considering the relative size of lysozyme over sodium fluorescein, obtaining homogeneous results can be considered an interesting achievement.

In Chapter 5, three molecules with different molecular weight (sodium fluorescein (0.376 kDa), lysozyme (14.3 kDa) and albumin (66.4 kDa)) were compared. Significant alterations to the method were made to reduce the time required for rehydration of the polymer matrix. This was achieved by decreasing the diffusion depth. The modified method is based on preparing the inserts individually, although the dimensions of a single insert were sized up for practical reasons. Instead of a drug loading period of six weeks, the inserts were only rehydrated during one or three days. In case of inserts loaded with sodium fluorescein, no difference concerning release rate was observed between one or three days of loading. For lysozyme and albumin, the rehydration time did have a significant effect on the release rate. Incorporating molecules as large as albumin did pose issues that were hard to overcome. The dense polymeric network of HPMC in the percentages used, caused an insufficient penetration into the core of the insert, thereby releasing albumin molecules rapidly as they resided on the surface of the insert. Adding a viscous drug solution instead of a merely aqueous drug solution did slow down the release rate of albumin from the insert.

In the previous chapter, it became apparent that the molecular weight played an important role in the penetration of the drug molecule and the drug release profiles. In chapter 6, four FITC-dextrans were used as model molecules to compare the release rate of molecules with different molecular weight. Changing the dimensions of the insert did influence the release behaviour of FITC-dextrans, but the general conclusions remained the same. For FITC-dextrans with a molecular weight over 40 kDa, obtaining sufficient penetration in the core of the insert and slow release profiles, continues to be a challenge.

In chapter 7, the cytotoxicity and biocompatibility of blank inserts was studied on human corneal epithelial cells. Cell viability was tested using hydroxypropyl cellulose (HPC) as the reference polymer along with cells to which no compound was added. Benzalkonium chloride, often used in commercial eye drops as a preservative, was added as a known cytotoxic compound. Expectedly, adding benzalkonium chloride immediately led to cell death, even in percentages as low as 0.004% (w/V). There was no difference observed between HPC and HPMC viscous solutions on cell viability and in comparison to cells to which no compound was added.

Chapter 8 describes the effect of storage, which was evaluated on viscosity, release profiles and the activity of lysozyme. Storage of inserts loaded with lysozyme during twelve months at a temperature of 2 °C did not reveal any negative impact both on rheological behaviour nor on release patterns. However, activity measurements were surprisingly positive: the activity levels decreased over time but after twelve months, the activity level of lysozyme loaded in the insert was twice as high compared to lysozyme stored in solution. Protective mechanisms of HPMC and/or glycerol have been suggested.

In vivo studies on rats with dry eye disease were performed in chapter 9. Treatment of these rats with inserts loaded with dexamethasone sodium phosphate did not show any improvement over untreated eyes. The low number of animals and the tear collection difficulty associated with the viscosity of the inserts, limits the insights this experiment might provide on truly understanding the potential of the inserts developed.

SAMENVATTING

De biofarmaceutische aspecten van het oog worden in hoofdstuk 1 besproken. Deze biofarmaceutische aspecten worden beïnvloed door de anatomische structuren en fysiologische barrières van het oog. Verder komen in dit hoofdstuk de mogelijke strategieën aan bod die een oplossing kunnen bieden voor de lage oculaire beschikbaarheid van oogdruppels. De potentiële rol die oculaire inserten in de strijd tegen oogziekten kunnen spelen, wordt besproken, voornamelijk dankzij de toenemende interesse en ontwikkeling van peptiden en proteïnen als therapeutica. Steriliteit is een wettelijke bepaling voor oogpreparaten; een kort overzicht van de voornaamste sterilisatietechnieken wordt gegeven.

Het algemene doel van het onderzoek wordt aangegeven in hoofdstuk 2. De ontwikkeling van een methode die het mogelijk maakt om thermolabiele moleculen zoals peptiden en proteïnen te verwerken in oculaire inserten met vertraagde afgifte maar zonder het gebruik van hoge temperaturen, luchtbelvorming of scheerkrachten, werd als primair doel voorop gesteld.

Een eerste voorstel van dergelijke methode wordt uitgebreid beschreven in hoofdstuk 3. De initiële bereidingsmethode van de inserten kan opgedeeld worden in vier fasen. In de eerste fase wordt een hoog viskeuze hydrogel bereid, gebruik makend van hitte en mengkrachten ten einde een homogene, luchtbelvrije hydrogel te bekomen. Deze hydrogel wordt dan in fase II bij een temperatuur van 100 °C gedehydrateerd tot het gewenste niveau en is cilindervormig. In fase III wordt de bekomen matrix vervolgens opnieuw gerehydrateerd in een spuit met een waterige oplossing waarin het gewenste geneesmiddel is opgelost, in dit geval natrium fluoresceïne als *tracer*. Dit rehydratatieproces voltrekt zich bij een temperatuur van 2 °C. Na een oplaadperiode van zes weken, wordt de massa geëxtrudeerd. *Factorial design* werd toegepast om op efficiënte wijze een groot aantal experimenten uit te voeren waarbij de invloed van verschillende parameters werd nagegaan. De geëxtrudeerde inserten waren zacht en flexibel zodat het oogoppervlak niet beschadigd zou worden. Het vooropgestelde doel van vertraagde afgifte van natrium fluoresceïne werd gehaald. Voorts bleek het startpercentage HPMC een significante parameter om een homogene verdeling van natrium fluoresceïne te bekomen, gevolgd door het type polymeer (HPMC E10M of E4M) hetzij in veel geringere mate.

De initieel ontwikkelde methode wordt in hoofdstuk 4 verder onderzocht. Hierbij werd gebruik gemaakt van lysozyme als model proteïne. Er werden wijzigingen doorgevoerd aan het bereidingsproces, waaronder een gewijzigde geometrie van de gedehydrateerde polymeercilinder,

alsook een dehydratatie bij hogere temperatuur. De mogelijkheden van vertraagde afgifte werden eveneens onderzocht door gebruik te maken van intrinsiek viskeuze polymeertypes (E10M en K100M). Door gebruik te maken van *factorial design*, werd de invloed van de vorm van de gedehydrateerde polymeercilinder onderzocht. Hoewel het oplaadproces nog steeds op zes weken werd gesteld, heeft de wijziging van een kleine molecule als natrium fluoresceïne naar een grotere molecule zoals lysozyme een belangrijke invloed op het oplaadproces. Om deze oplading mogelijk te maken, werd de polymeercilinder als een *hashtag* vorm uitgesneden. Het bekomen van een homogene massa met lysozyme in plaats van natrium fluoresceïne over eenzelfde tijdspanne, kan als een gunstig resultaat beschouwd worden.

Vervolgens werden formulaties, opgeladen met drie moleculen met een verschillend moleculair gewicht (natrium fluoresceïne (0.376 kDa), lysozyme (14.3 kDa) en albumine (66.4 kDa)) bereid en onderling vergeleken. Het voornaamste doel van het onderzoek dat uitgevoerd werd in hoofdstuk 5, is het verkorten van de oplaadtijd. Door gebruik te maken van drie verschillende moleculen werd een eerste inzicht verkregen in de beperking van het oplaadproces in verhouding tot het moleculaire gewicht. Het oplaadproces werd verkort van zes weken tot één of drie dagen. In geval van inserten opgeladen met natrium fluoresceïne, bleek er geen statistisch significant verschil te bestaan wat betreft een oplaadtijd van één of drie dagen. Lysozyme daarentegen, ondervond wel een invloed van deze parameter, waarbij drie dagen oplaadtijd voor een vertraagde afgifte zorgde als gevolg van een betere penetratie van lysozyme in de kern van het insert. Op het eerste gezicht bleek het niet mogelijk albumine op te laden in de inserten, wat werd afgeleid uit de afgifteprofielen. Deze profielen werden gekenmerkt door een snelle afgifte van albumine bij het eerste meetpunt (10 minuten). Een wijziging van de waterige oplossing met albumine naar een viskeuze oplossing met deze molecule had een significante invloed op het afgifteprofiel. Toch kan ook in dit geval niet gesproken worden van vertraagde afgifte op het niveau als deze van natrium fluoresceïne of lysozyme.

In het vorige hoofdstuk bleek duidelijk dat het moleculair gewicht van de doelwitmolecule een belangrijke invloed heeft op het oplaadproces en daarmee ook op de wijze van afgifte van de molecule. In hoofdstuk 6 worden vier FITC-dextranen met een verschillend moleculair gewicht gebruikt om het gedrag van HPMC inserten opgeladen met deze moleculen te onderzoeken. Er konden telkens vergelijkbare trends worden waargenomen, ongeacht de dimensies van de geproduceerde inserten. Echter, om FITC-dextranen op te laden met een moleculair gewicht van

meer dan 40 kDa dienen nieuwe technieken ontwikkeld te worden om een voldoende penetratie in de kern van het insert te bewerkstelligen.

Hoofdstuk 7 beschrijft de cytotoxische eigenschappen en biocompatibiliteit van blanco HPMC inserten. Dit onderzoek werd uitgevoerd op humane corneale epitheelcellen. Het polymeer hydroxypropylcellulose (HPC) werd als referentiepolymeer aangewend alsook cellen in groeimedium zonder toevoeging van een substantie. Benzalkonium chloride werd als gekend cytotoxisch product gebruikt. De celoverleving in aanwezigheid van blanco HPMC inserten werd onderling vergeleken. De resultaten voor celoverleving bleken vergelijkbaar voor zowel HPMC als HPC viskeuze oplossingen tegenover cellen in groeimedium. Dit resultaat was ongeacht de geteste concentraties aan polymeer. Benzalkonium gaf, geheel in lijn met de verwachting, aanleiding tot onmiddellijke celdood, zelfs in een zeer lage concentratie van 0,004% (m/V).

De invloed van langdurige bewaring bij 2 °C wordt beschreven in hoofdstuk 8. Deze invloed werd onderzocht door de evolutie in viscositeit van het insert, de afgifteprofielen en activiteit van lysozyme over een periode van 12 maanden na te gaan. Er werd geen negatieve invloed waargenomen wat de viscositeit en het afgifteprofiel betreft voor inserten die bewaard werden gedurende 12 maanden bij een temperatuur van 2 °C. Wel werd opgemerkt dat, zoals bleek uit de vorige hoofdstukken, een periode van één maand wellicht niet resulteert in een volledige penetratie van lysozyme in het insert met de gegeven afmetingen. Vanaf drie maanden werden geen verschillen gedetecteerd. Daarentegen bleken de activiteitsmetingen wel verrassend positief: de activiteit van lysozyme daalde in functie van de tijd, maar wanneer lysozyme werd opgeladen in het insert, werd na 12 maanden een dubbel zo hoge activiteit vastgesteld in vergelijking met lysozyme in oplossing. In de literatuur worden beschermende mechanismen van HPMC en/of glycerol ten aanzien van proteïnen beschreven.

In vivo onderzoek uitgevoerd op ratten, lijdend aan droge ogen, wordt behandeld in hoofdstuk 9. De behandeling van deze ratten met inserten opgeladen met dexamethason natrium fosfaat gaf geen beduidend verschil in resultaat met ratten die geen behandeling ontvingen. Het kleine aantal proefdieren, alsook de moeilijkheden van traanstaalname die gepaard gaan met de viskeuze massa eigen aan een insert, kunnen bijgedragen hebben tot dit resultaat. Het werkelijke potentieel van de ontwikkelde inserten blijft daarmee grotendeels onverkend.

APPENDIX

In the following part, the linear regression analyses of sodium fluorescein, lysozyme from chicken egg white and bovine serum albumin are discussed.

1 REGRESSION ANALYSES

The regression analyses were performed using Microsoft Excel® 2010 (Microsoft®, Redmond, USA).

1.1 Sodium fluorescein

A stock solution of sodium fluorescein was prepared in PBS and serially diluted in five-fold and measured at an experimentally determined wavelength of 484 nm. Every measurement was performed in duplicate using a UV/VIS spectrophotometer (Genesys 10 UV, Thermo Electron Corporation, Madison, USA). The linear regression is shown in figure A1.

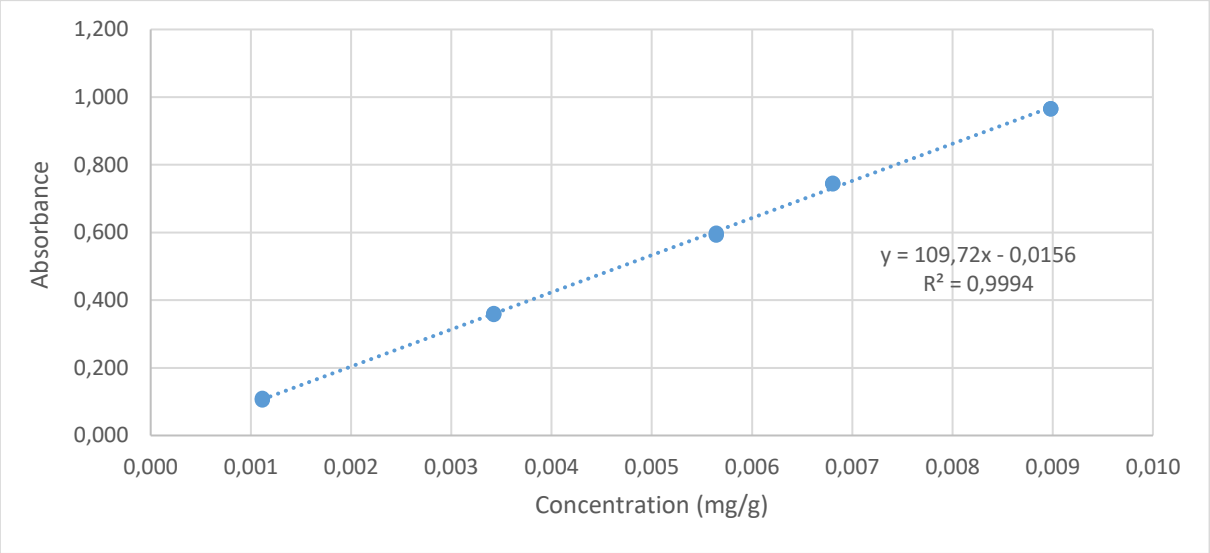

Fig. A1. Linear regression of sodium fluorescein.

No trend was seen using residual analysis. The residual plot, as shown in figure A2, is considered to be homoscedastic, which means that the deviations are scattered at random. There is no correlation between the deviations and the concentration of sodium fluorescein measured.

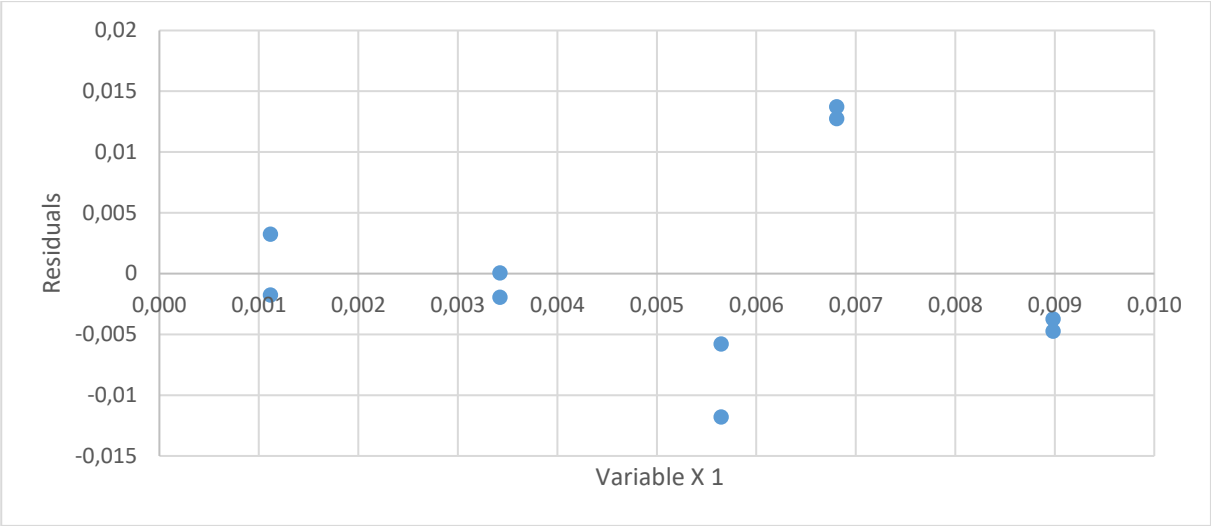

Fig. A2. Residual analysis of sodium fluorescein.

An overview of all regression statistics is given in table A1.

To statistically prove that the slope of the linear regression is not equal to zero, a t-test was performed. The t-value should exceed the value of the calculated critical t-value. The critical t-value in this case was calculated as 2.306. The t-value (111.023) is larger than 2.306, which means that there is a linear relationship between X and Y.

The 95% confidence interval (CI) for analysis of the intercept was calculated. If this CI encloses the value 0, the linear plot is considered intersecting with the origin (0,0). In this case the value 0 is not enclosed between the lower and upper 95% CI (-0.029 and -0.002) which implicates that one-point calibration is not possible.

The correlation coefficient (multiple R) represents the degree of correlation between X and Y. The closer this number is to 1, the higher the correlation. R square (R^2) is a statistical measure which expresses the percentage of the response variable variation that is explained by the linear model. Values higher than 0.99 are considered excellent.

Table A1. Overview of regression statistics.

Regression Statistics	
Multiple R	0,99968
R Square	0,99935
Adjusted R Square	0,99927
Standard Error	0,00849
Observations	10

ANOVA

	df	*SS*	*MS*	*F*	*P-value*
Regression	1	0,88883	0,88883	12326,19	4,840E-14
Residual	8	0,00057	7,21097E-05		
Total	9	0,88941			

	Coeff.	*Standard Error*	*t Stat*	*P-value*	*Lower 95%*	*Upper 95%*	*Lower 95,0%*	*Upper 95,0%*
Intercept	-0,016	0,006	-2,698	0,027	-0,029	-0,002	-0,029	-0,002
Var X 1	109,723	0,988	111,023	0,000	107,444	112,002	107,444	112,002

1.2 Lysozyme from chicken egg white

A stock solution of lysozyme from chicken egg white was prepared in PBS and serially diluted in five-fold and measured at an experimentally determined wavelength of 280 nm. Every measurement was performed in duplicate using a UV/VIS spectrophotometer (Genesys 10 UV, Thermo Electron Corporation, Madison, USA). The linear regression is shown in figure A3.

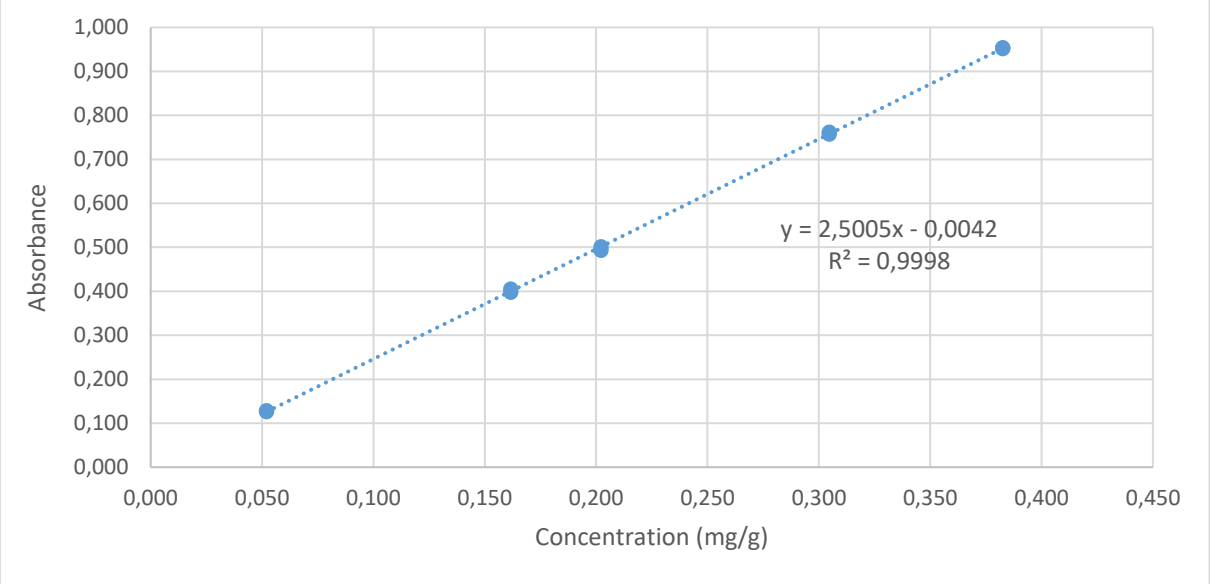

Fig. A3. Linear regression of lysozyme.

No trend was observed using residual analysis. The residual plot, as shown in figure A4, is considered to be homoscedastic, which means that the deviations are scattered at random. There is no correlation between the deviations and the concentration of lysozyme measured.

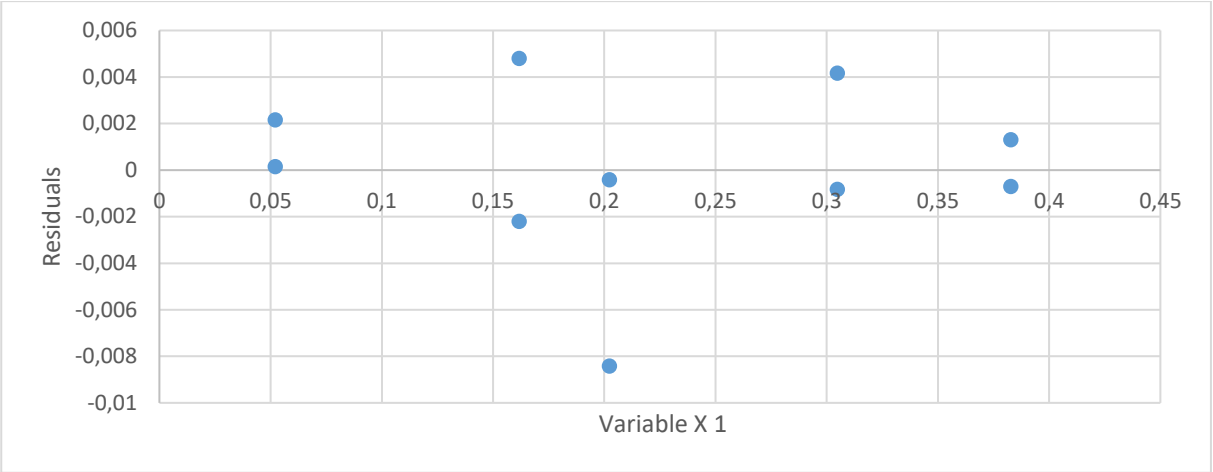

Fig. A4. Residual analysis of lysozyme.

An overview of all regression statistics is given in table A2.

To statistically prove that the slope of the linear regression is not equal to zero, a t-test was performed. The t-value should exceed the value of the calculated critical t-value. The critical t-value in this case was calculated as 2.306. The t-value (230.134) is larger than 2.306, which means that there is a linear relationship between X and Y.

The 95% CI for analysis of the intercept was calculated. If this CI encloses the value 0, the linear plot is considered intersecting with the origin (0,0). In this case the value 0 is enclosed between the lower and upper 95% CI (-0.010 and 0.002) which implicates that one-point calibration is possible.

The correlation coefficient (multiple R) represents the degree of correlation between X and Y. The closer this number is to 1, the higher the correlation. R square (R^2) is a statistical measure which expresses the percentage of the response variable variation that is explained by the linear model. Values higher than 0.99 are considered excellent.

Table A2. Overview of regression statistics.

Regression Statistics	
Multiple R	0,99992
R Square	0,99985
Adjusted R Square	0,99983
Standard Error	0,00393
Observations	10

ANOVA

	df	SS	MS	F	P-value
Regression	1	0,82007	0,82007	52961,83968	1,42275E-16
Residual	8	0,00012	1,54842E-05		
Total	9	0,82019			

	Coeff.	Standard Error	t Stat	P-value	Lower 95%	Upper 95%	Lower 95,0%	Upper 95,0%
Intercept	-0,004	0,003	-1,557	0,158	-0,010	0,002	-0,010	0,002
Var X 1	2,501	0,011	230,134	0,000	2,475	2,526	2,475	2,526

1.3 Bovine serum albumin

A stock solution of bovine serum albumin was prepared in PBS and serially diluted in five-fold and measured at an experimentally determined wavelength of 278 nm. Every measurement was performed in duplicate using a UV/VIS spectrophotometer (Genesys 10 UV, Thermo Electron Corporation, Madison, USA). The linear regression is shown in figure A5.

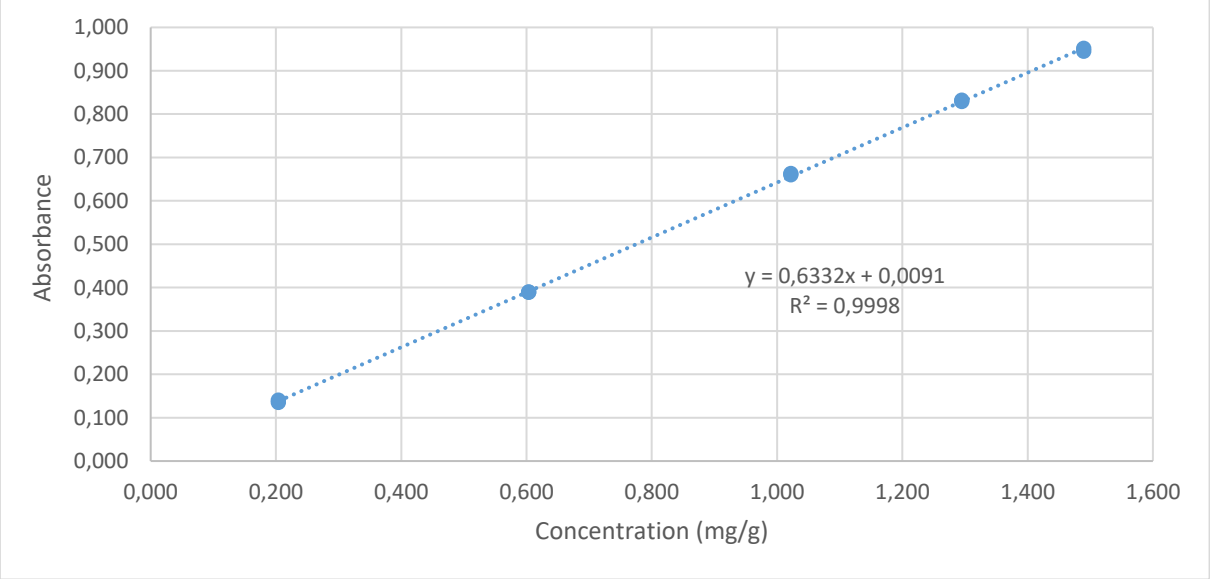

Fig. A5. Linear regression of bovine serum albumin.

No trend was noticed using residual analysis. The residual plot, as shown in figure A6, is considered to be homoscedastic, which means that the deviations are scattered at random. There is no correlation between the deviations and the concentration of lysozyme measured.

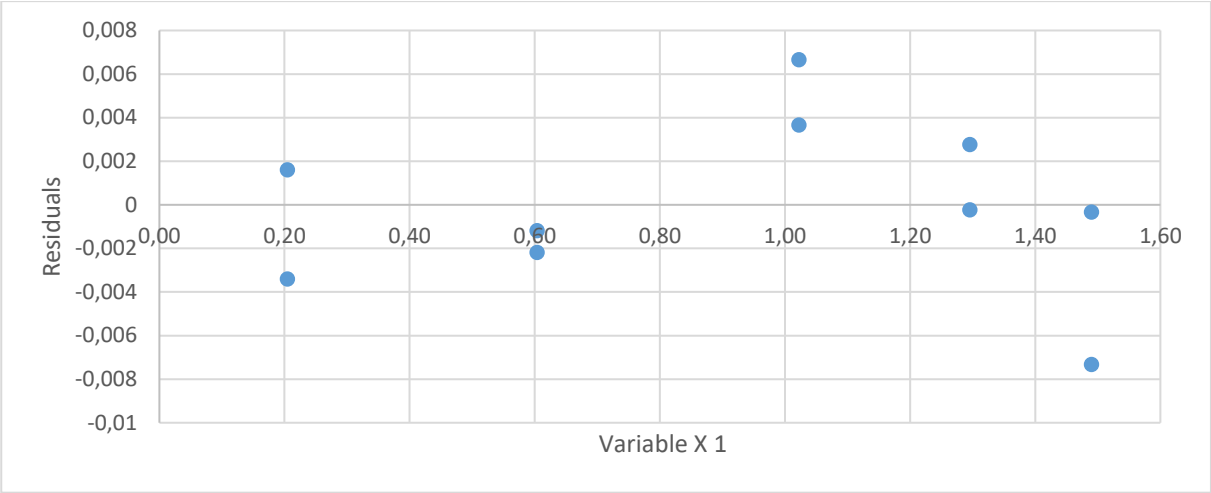

Fig. A6. Residual analysis of bovine serum albumin.

An overview of all regression statistics is given in table A3.

To statistically prove that the slope of the linear regression is not equal to zero, a t-test was performed. The t-value should exceed the value of the calculated critical t-value. The critical t-value in this case was calculated as 2.306. The t-value (223.536) is larger than 2.306, which means that there is a linear relationship between X and Y.

The 95% CI for analysis of the intercept was calculated. If this CI encloses the value 0, the linear plot is considered intersecting with the origin (0,0). In this case the value 0 is not enclosed between the lower and upper 95% CI (0.002 and 0.016) which implicates that one-point calibration is not possible.

The correlation coefficient (multiple R) represents the degree of correlation between X and Y. The closer this number is to 1, the higher the correlation. R square (R^2) is a statistical measure which expresses the percentage of the response variable variation that is explained by the linear model. Values higher than 0.99 are considered excellent.

Table A3. Overview of regression statistics.

Regression Statistics	
Multiple R	0,99992
R Square	0,99984
Adjusted R Square	0,99982
Standard Error	0,00418
Observations	10

ANOVA

	df	*SS*	*MS*	*F*	*P-value*
Regression	1	0,87264	0,872647	49968,38	1,8E-16
Residual	8	0,00014	1,75E-05		
Total	9	0,87278			

	Coeff.	*Standard Error*	*t Stat*	*P-value*	*Lower 95%*	*Upper 95%*	*Lower 95,0%*	*Upper 95,0%*
Intercept	0,009	0,003	3,107	0,015	0,002	0,016	0,002	0,016
Var X 1	0,633	0,003	223,536	0,000	0,627	0,640	0,627	0,640